Journal of Structural Chemistry

Vol. 2 No. 4

THE CENTENARY OF THE STRUCTURAL THEORY

G. B. Bykov

Translated from Zhurnal Strukturnoi Khimii, Vol. 2, No. 4,
pp. 395-401, July-August 1961

It was only when thought penetrated to the mutual relationships of individual atoms in the molecule, i.e., when the structural hypothesis came into being, that reality became visible and clear – and then only gradually.

A. M. Butlerov

The rapid development of organic chemistry during the last third of the last century, the successful study and artificial production of natural substances, the preparation of new substances with predetermined properties, the establishment of the organic synthesis industry – all this is due to the fact that in the 1860's organic chemistry was provided with a sound theoretical basis – the theory of chemical structure. Subsequently this theory exerted a most fruitful influence on the development of inorganic chemistry and biochemistry.

The modern theory of structure, otherwise the structural theory, comprises the sum of our knowledge of the molecular structure of organic and inorganic compounds and of the relationship between their structure and properties. Structure now implies the sequence of interatomic bonds, chemical structure itself, the spatial configuration of atoms or bonds and, finally, the distribution of electron density in molecules; when we speak of properties, we imply both the chemical and the physical properties of substances in bulk, of individual molecules, and of their structural elements. However, this form of the structural theory has arisen only as the result of prolonged development. Initially it was known as the theory of chemical structure. Its subject comprised merely chemical structure and the relationship between the latter and the chemical properties of organic compounds only.

The theory of chemical structure was enunciated for the first time by A. M. Butlerov in an address entitled "The Chemical Structure of Matter," presented September 19, 1861 at a congress of German naturalists and doctors in Speyer. In this address he gave the first definition of the concept of chemical structure, put forward the main point of the theory, namely that the chemical properties of molecules are primarily determined by their composition and chemical structure, drew attention to the possible application of various chemical reactions to determination of the chemical structure of the substances involved in them, and explained the meaning and significance of structural formulas. Here Butlerov opposed the conviction, held by the enormous majority of chemists, that the properties of molecules depend primarily on their mechanical structure (positions of the atoms)*, and called upon chemists to reject the type theory which was predominant at that time and which rejected all attempts to develop concepts of the structure ("constitution") of molecules.

The theory of chemical structure could arise only at a definite stage in the development of theoretical chemistry: in particular, after formulation of the concept of the valence of elements, including the quadrivalence of carbon, and of the concept of the chemical bond, and primarily of interatomic carbon – carbon bonding. These concepts were introduced by A. Kekule and A. S. Couper. Because of this the prerequisites for the origin of the theory of chemical structure are often, especially in the West, identified with the theory itself and the honor of its creation is attributed not to A. M. Butlerov but to Kekule or to Kekule and Couper jointly. The erroneous character of this view, first pointed out by V. V. Markovnikov, has now been adequately demonstrated by Soviet chemical historians and need not be considered further.

*Of course, at that time this concept did not imply, as it does at the present time, geometrical bond directions and the relatively stable relative positions of the atoms in space which result from this, but rather a molecular structure in which atoms have the role, in the opinion of some chemists, analogous to bricks in the wall of a building, and according to others, to the sun, planets, and their satellites in the solar system.

Since the theory of chemical structure, even in its original form, gave a deep and accurate reflection of reality, it was able to develop further with great success. Let us consider the principal stages in this development. In 1863, A. M. Butlerov used this theory to give the first satisfactory interpretation of isomerism. He was also the first to predict the existence of a number of theoretically possible compounds, including branched-chain hydrocarbons -- isobutane and isobutylene. Butlerov, and his pupils and close associates V. V. Markovnikov and A. N. Popov, obtained the compounds predicted by the theory, and thus obtained brilliant experimental confirmation for it. In 1865 the theory of chemical structure was extended by Kekulé to benzene and its derivatives, and in the same year E. Erlenmeyer proposed the formulas which are now accepted for compounds with double and triple bonds. During these years Butlerov and his associates worked out the principles of the theory of the mutual influence of atoms. The most important work in this field was V. V. Markovnikov' doctorate dissertation (1869). Markovnikov formulated a series of rules on the dependence of the directions of various reactions on the chemical structure of the reacting substances, and was the first to examine isomerization reactions, distinguishing between mono- and bimolecular mechanisms of such reactions. In 1876 Butlerov quite definitely referred to the possibility of reversible isomerization, for which Laar proposed the term "tautomerism" in 1885. However, Butlerov referred to the possibility of reactions of this type in various particular cases even earlier, starting from 1862.

Later, when the chemical structure of the most important organic compounds had been established by chemical methods, it became possible to study the dependence of physical and physicochemical properties on structure also. Extensive systematic studies were conducted in this field by J. Thomsen and J. Bruhl in the 1870's and later.

The discovery of isomerism in organic compounds, which could not be explained in the light of the theory of chemical structure, led to the hypothesis of the tetrahedral carbon atom. By this hypothesis, optical isomerism occurs in compounds containing asymmetric carbon atoms, while isomerism of the type found in maleic and fumaric acids is associated with cis and trans positions of substituents attached to carbon atoms joined by double bonds. This hypothesis was put forward in 1874 simultaneously by van't Hoff in Holland and, with far less bold conclusions, by Le Bel in France. This was the origin of stereochemistry.

The transition from the theory of chemical structure to stereochemistry was so natural and logical that the fundamental idea of the latter was indicated even in 1865 by Markovnikov, who noted that "the physical grouping of atoms may differ while the chemical structure is the same." Van't Hoff wrote in 1887 that "there is but a single step between the concept of the manner in which atoms are linked together in a molecule and the problem of the relative positions of the atoms."

Stereochemistry had the same fruitful influence as the classic theory of chemical structure on the development of organic chemistry. For example, in 1885 A. Baeyer put forward his stereochemical interpretation, which has retained its significance to the present day, of the instability of small alicycles -- the so-called strain theory. The ideas of stereochemistry were later extended to compounds of nitrogen and other elements. At the same time stereochemistry prepared the ground for the future theory of the structure of complex compounds.

After several failures in the application of the ideas of the theory of chemical structure in inorganic chemistry -- failures due to a reluctance to recognize variable valence in elements such as nitrogen and chlorine -- by the end of the 8170's chemists were using formulas for inorganic compounds which do not differ essentially from those used in modern books on inorganic chemistry. Only complex compounds gave rise to difficulties. In 1893 A. Werner put forward his coordination theory, which was a further development of the ideas of the theory of chemical structure and stereochemistry, and which supplemented them by the fundamental concepts of coordination numbers and subsidiary valences of complex-forming atoms.

However, by that time (the end of the 19th century) it became acutely clear that further progress in the development of structural chemistry could not be made before the physical meaning of the fundamental concepts of the classic theory of chemical structure and stereochemistry -- the concepts of valence and the chemical bond -- had been revealed. This accounts for the failure, for example, of numerous attempts to explain the structure of benzene, conjugated compounds, and triarylmethane radicals with the aid of supplementary hypotheses, to elucidate the mechanism of chemical reactions, and thereby to provide a physical interpretation of the concept of the mutual influence of atoms. One such attempt, which might seem to have been among the most promising, was the hypothesis of J. Thiele (1899) about the existence and role of "partial" valences in unsaturated organic compounds.

Structural chemistry could no longer be expected to make further substantial progress without aid from physics. The remarkable discoveries made by physicists at the end of the 19th and the beginning of the 20th century led to a

new advance in the study of molecular structure. The most important of these discoveries was the experimental demonstration of the existence of the electron, carried out almost simultaneously by E. Wichert and J. J. Thomson. At the turn of the century there arose the first electronic theories of the structure and properties of chemical compounds. It was natural that at that time they should first have been applied to explanations of the phenomena of electrolytic dissociation. However, this led logically to the hypothesis that molecules of chemical compounds contain ionic (electrostatic) bonds formed by complete transfer of electrons from one atom to another. This picture was to some extent consistent with reality in the case of inorganic compounds, but electrostatic theories of the structure of organic compounds met serious difficulties right from the start and supplementary hypotheses had to be put forward. Success was achieved only after introduction of the concept of covalent bonds formed by one, two, or three pairs of electrons. In this respect the well-known 1916 paper by G. N. Lewis and the subsequent work by Lewis and I. Langmuir were of the most significance in chemistry. However, it must be pointed out that Lewis had his predecessors: N. A. Morozov (1907), J. Stark (1912), J. Thomson (1914), N. Bohr (1913), and A. L. Parson (1915).

However, the work of Lewis included another idea which was later developed considerably – the idea that a pair of electrons forming a covalent bond may be displaced toward one of the two atoms, so that the bond becomes polar. On the basis of the general principle that the direction and mechanism of an organic reaction are determined by a definite electron concentration at a given region of a molecule, chemists have postulated the existence of different types of electron displacements, which may be subdivided into two main groups: static displacements, taking place in molecules in the ground state, and dynamic displacements, arising under the influence of a reagent, solvent, or catalyst. For a clear representation of the electronic structure of such molecules there was introduced the concept of the mesomeric or intermediate state of compounds with multiple bonds, in comparison with conceivable structures in which electron displacement does not occur and which are represented by the usual structural formulas. Concepts of the various postulated electron displacements, electron interactions, and their influence on the properties of organic compounds comprise the theory of electron displacements, developed mainly by R. Robinson, C. K. Ingold, and other English chemists. This theory finally emerged by the middle of the 1930's and has since been systematically extended to new classes of compounds and new reaction types, and supplemented by new ideas.

These ideas include the concepts of conjugation of single with multiple bonds and of single bonds with each other. J. W. Baker and W. S. Nathan (1935) concluded that alkyl groups are capable of furnishing electrons if these groups are directly adjacent to a benzene nucleus or to double or triple bonds. It was found that the methyl group is especially susceptible to such electron displacement, which differs in its mechanism from inductive displacement. This new type of electron displacement was given the name of "hyperconjugation" by R. S. Mulliken (1939), and the peculiar behavior of the methyl group was attributed to the fact that the σ electrons of C–H bonds are less localized than the σ electrons of C–C bonds. In 1950 A. N. Nesmeyanov gave a generalized interpretation of these effects of σπ conjugation, which include hyperconjugation involving methyl groups. In addition, he introduced the concept of σσ conjugation, or conjugation of single bonds, and demonstrated the existence of an analogy between σσ and ππ conjugation.

However, it is now becoming increasingly clear that the qualitative theory of electron displacements is insufficient for interpretation of the enormous amount of quantitative data now provided by physical, physicochemical, and even chemical methods. It is becoming evident that the theory of electron displacements cannot be the principle direction in the theory of the electronic structure of molecules. A new trend in structural chemistry, also associated with progress in physics – theoretical in this case – is much more promising in this respect.

The greatest impetus to the development of the electronic theory in chemistry was provided at the beginning of the 1930's by quantum mechanics. In 1926 Schrodinger put forward his famous equation, which has since then been repeatedly used for quantum-mechanical calculations in structural physics and chemistry. However, it became clear even after the first calculations, performed in 1927 for H_2^+ and H_2, that a precise solution of the problem cannot be obtained for more complex molecules, and the subsequent development of the theory of molecular structure and the chemical bond involved the derivation of theoretical concepts in which ideas and methods adopted from quantum mechanics were closely interwoven with empirical conclusions. The concept of hybridization of the electron orbitals of a saturated carbon atom (L. Pauling, 1928) is such a theoretical concept of a "mixed" character.

The first computations of the hydrogen molecule served as the prototypes of the two most useful approaches to computation of more complex molecules. The Heitler–London method was the starting point for the development of the valence bond method, whereas the Condon method together with F. Bloch's interpretation of electronic conductance in metals (1928) led to the method of molecular orbitals. Both these methods were applied since the beginning

of the 1930's mainly to calculations of π-electron systems (the terms π and σ electrons were themselves introduced in 1931 by F. Hund). The most important work in this field at the beginning of the 1930's was done by E. Huckel; this work was mainly concerned with energy characteristics of unsaturated and aromatic molecules, and to a lesser degree with electron density distribution in these molecules. Of the two methods named above, Huckel definitely gave preference to the method of molecular orbitals.

In 1933 L. Pauling began to develop the resonance theory based, on the one hand, on the quantum-mechanical valence bond method, and on the other, on the qualitative theory of mesomerism. The resonance theory was widely used by Pauling, G. W. Wheland, and many others for explaining the energy characteristics of molecules, for establishing the relationship between the "percentage double-bond character," interatomic distances and certain other characteristics of bonds and molecules, and also for interpreting the reactivity of organic compounds. However, the resonance theory has made no contribution to calculations of electron density distribution in molecules, which are undoubtedly among the main problems of the most recent electronic structure theories. Most promising in this respect was the "mesomerism method" developed in France (R. Daudel, A. Pullman, 1945); this was a modification of the valence bond method. Initially the mesomerism method was applied to calculations for the "electronic charges of bonds and atoms" which were subsequently renamed the "indices of bonds and atoms", when the dependence of the numerical results on the assumptions made had been established. This method was used for working out the "molecular diagrams" of numerous organic compounds, mainly consisting of condensed aromatic systems, and the calculated results were correlated with various properties of the molecules, including their physiological activity.

In the 1930's J. E. Lennard-Jones and subsequently C. A. Coulson developed the molecular orbital method considerably and used it for calculation of "bond orders" and "free valences of atoms." Numerous comparisons of molecular orbital method showed that a definite correlation exists between them. Nevertheless, these comparisons indicate that the molecular orbital method is preferable: it is simpler, especially in relation to polar molecules and molecules containing heteroatoms; finally, this method can be used for calculation, perhaps approximate as yet, of the distribution of σ electrons in saturated molecules (C. Sandorfy, 1955). There is now a quite definite tendency for the molecular orbital method to replace calculations of the electronic structure and properties of organic molecules by different variants of the valence bond method. One version of the molecular orbital method, with the use of what is known as the free-electron model, has been especially developed during the past decade.

About ten years ago the resonance theory was subjected to severe and, in the main, valid criticism by Soviet chemists, primarily because it is defective from the methodological aspect. This theory allows arbitrary selection of the resonating structures, this arbitrary character was freely admitted both by Pauling and by Wheland, but was at the same time pragmatically justified by alleged convenience and usefulness. Moreover, certain prominent adherents of this theory, both abroad and in our country, slipped to the path of objectivization of resonating structures, i. e., to purely idealistic positions from the philosophical viewpoint. The universality of this theory was also exaggerated, because the language of the theory was used for formulating principles which could have been expressed better in terms of other theories. It is not surprising that, despite the publication of new editions of Pauling's and Wheland's monographs, the resonance theory is passing from the scene.

The modern electronic structural theory of chemical compounds is now confronted with a very large and serious task: it is necessary to develop a concept of the electronic structure of molecules and the electronic mechanism of reactions which would serve chemists in their daily research work in the same way as the classic theory of chemical structure did in its time.

It is appropriate in this connection to recollect the basic principle of the class theory — study of the chemical structure of molecules based on their properties. It is now being asserted that the electronic structure of molecules can be calculated only by the methods of quantum mechanics. However, these methods are extremely laborious and are in effect beyond the scope of the average research chemist. Moreover, after calculation of the electronic characteristics of molecules it becomes necessary to establish the relationship between these characteristics and the properties of the molecules. If such relationships exist, they can evidently be used for calculating, with the precision necessary for practical purposes, of the electronic structure of molecules from their properties. Therefore in the development of a modern structural electronic theory we must turn to the principle first introduced by A. M. Butlerov 100 years ago. The fact that this approach is still possible is demonstrated, for instance, by calculations of electronic bond charges. For example, the π-electron charges of bonds in a number of hydrocarbons were first calculated by the classic method, and only after that were analogous results obtained by the methods of quantum mechanics. Calculations of the σ-electron charges of propane by the quantum-mechanical and classic methods gave very similar results, but calculations

by the former method involved lengthy work by a computer whereas calculations by the latter method can be performed in a few minutes without the need for any computer techniques.

We refer to calculations throughout, because the structural theory is now undergoing a quite logical evolution characteristic of physical and chemical theories – initially entirely qualitative, it is becoming quantitative and evidently the transformation will be complete after one or two more generations of chemists.

In order that the theory should become more definite and concrete it is also necessary that a transition should be made from calculations of "indices" and similar quantities, often without strictly definite physical meaning, to calculations of electron density distribution in molecules and establishment of relationships between this distribution and the properties of individual groups, and combinations of these. This tendency is also becoming apparent in the modern structural electronic theory.

The second (stereochemical) aspect of the modern structural theory was also greatly developed during the 20th century. After the first Laue diffraction pattern had been obtained in 1912, during the next 30 years the x-ray method for investigation of the structure of organic compounds was developed; this method made it possible to determine interatomic distances and valence angles in molecules of very complex structure, even if their chemical structure had not been reliably established. Since the beginning of the 1930's the electron-diffraction method has been used for the same purpose, but only with the simplest molecules, and in the 1950's neutron diffraction has also come into use. During the last 20-25 years various spectroscopic methods have also been extensively used for determination of spatial structure parameters of molecules.

In the great majority of cases the qualitative results of classic stereochemistry have been confirmed by these methods. However, the reverse was the case in one important respect. According to van't Hoff, substituents can rotate freely about a single bond. However, "rotational isomers" or "conformations" have been discovered; these are due to hindered rotation about single bonds as the result of steric (nonvalent) interaction between atoms and groups. The somewhat peculiar conformations of cyclohexane ("chair" and "boat" forms) and other alicyclic hydrocarbons and their derivatives have also been discovered. A new branch of stereochemistry has arisen – "conformational analysis," which deals with the energy relationships between different conformations and with their characteristic physical and chemical properties.

In the modern science of chemical reaction mechanisms almost as much attention is devoted to the spatial as to the electronic structure of the reacting molecules. However, each of these concepts is merely a refinement and deepening of the concept of the chemical structure of the same molecules in the original Butlerov sense of the term.

Moreover, instances could be cited in which even now the chemist confines himself to the concept of chemical structure only; for example, in most syntheses he is guided by the usual structural formula as the plan to which the given chemical compounds must be built up; when meeting a natural substance or an unexpected reaction product his first aim is to establish its chemical structure. The modern nomenclature and classification of organic compounds are based on the Butlerov concept of chemical structure. Thus, the classic theory of chemical structure enters, partly as an independent entity and partly in conjunction with other ideas, into the modern structural theory. Therefore at this time, 100 years after its creation, we can still speak of the classic structural theory in the words of its founder: ". . . it is still valuable in a certain sense and, in becoming obsolete, it enters in more or less modified form as a component part of a more extensive new theory. The relationship between facts which was indicated by the earlier theory is confirmed, extended, and explained even better by the new theory, and the discoveries to which the old theory led remain as durable memorials to its merits."

THE ELECTRONIC STRUCTURE OF THE WATER MOLECULE IN THE CONDENSED PHASE

Yu. V. Gurikov

V. G. Khlopin Radium Institute, Academy of Sciences USSR
Translated from Zhurnal Strukturnoi Khimii, Vol. 2, No. 4,
pp. 402–407, July-August 1961
Original article submitted December 30, 1960

The effective charge qe of the proton of a water molecule involved in hydrogen bonding with the neighboring water molecules is estimated from data on the shift of the deformational vibration frequencies in condensation of steam. The observed shift toward higher frequencies is correlated with Coulomb repulsion of protons which arises during the redistribution of electron density owing to hydrogen bond formation. The value of 0.16 e found for the effective charge of the proton is in agreement with data of other authors.

The formation of hydrogen bonds through directed orbitals of unshared electron pairs of the oxygen atom leads to the appearance of a new vibrational degree of freedom, associated with independent changes of the angle between the orbitals of the unshared pairs and the O–H bonds in the same molecule. The second deformational frequency is shifted toward lower values because of interaction of the effective proton charges with the excess electron density of the orbitals of the unshared pairs. The second deformational frequency is in fact observed in the infrared spectrum of ice. The observed shift (95 cm^{-1}) is in good agreement with the calculated value (90 cm^{-1}) if the value q = 0.16 is used and the asymmetry of the water molecule is taken into account.

The estimated value is used for calculation of the "coherent dipole moment of the hydrogen bond." Good agreement was found with the value of 0.33 D found earlier; this provides further confirmation of the concepts put forward earlier [9] on the role of hydrogen bonds in the formation of the structure of water and aqueous electrolyte solutions.

In addition to the action of the specific hydrogen bond, which has sharply pronounced directional character, the electronic structure of the water molecule is the cause of the peculiar crystal structure of water, with tetrahedral coordination of neighboring molecules [1], and of other unusual properties [2] of water.

Quantum-mechanical calculations show that the electron density distribution in the water molecule is determined to a considerable extent by the influence of two pairs of unshared electrons of the oxygen atom. In consequence of sp^3 hybridization in the ground electronic state of the molecule the directions of the orbitals of the unshared pairs and of the O–H bonds form approximately tetrahedral angles with each other [3]. Recent calculations of the molecular orbitals of H_2O by the self-consistent field method [4] lead to the conclusion that the polarity of the O–H bond is very low [5]; the contribution of each bond to the total dipole moment of the molecule is smaller by an order of magnitude than the value of 1.51 D assigned to it earlier [13].

Aleksandrov and Sokolov [7], took into account, first, that in order to explain the observed shift of the valence vibration frequencies in the infrared spectrum of water and ice into the long-wave region it is necessary to assume the existence of donor-acceptor interaction between a hydrogen atom and an oxygen atom of a neighboring molecule [6] and second, that for donor-acceptor bonding to occur the proton effecting the bonding must have a sufficiently large positive charge; accordingly, they postulated that O–H polarization occurs during the actual process of hydrogen bond formation.

Since the electron density distribution in the free molecule has almost tetrahedral symmetry, it is to be expected that in the condensed phase the final charge distribution also has this type of symmetry. Bjerrum [8] was the first to propose a tetrahedral model of the H_2O molecule, and he found that this model makes it possible to describe quantitatively the thermodynamic properties of ice. In the Bjerrum model four point charges of $\frac{1}{2}$.17 e are at the vertices

of an equilateral tetrahedron at distances of 0.99 A from the nucleus of the oxygen atom. Two vertices of the tetrahedron are at protons and the other two are at the centers of gravity of the electron clouds of the unshared pairs. In liquid water some of the bonds are broken as the result of thermal fluctuations [2]. The charge distribution which occurs after condensation may be approximately represented by placing, between neighboring linked molecules, dipoles the positive ends of which, each carrying the charge +qe, are situated at protons, while the negative ends each with charge -qe are at the centers of gravity of the electron clouds of the unshared pairs. It was shown recently [9] that breakdown of water structure in ionic solutions can be explained by correlation of each hydrogen bond with its "intrinsic dipole moment" $\mu_H = qed$, where $d = 1.98$ A is the distance between neighboring oxygen atoms. In these calculations the value $q = 0.17$ was used; this was the value estimated by Bjerrum on the assumption that the dipole moment of the free H_2O molecule, 1.87 D, is retained in the condensed phase. However, it would be interesting to estimate q independently. For this purpose we shall use data on the frequency shift of the deformational vibrations ν_δ of the H_2O molecules on condensation.

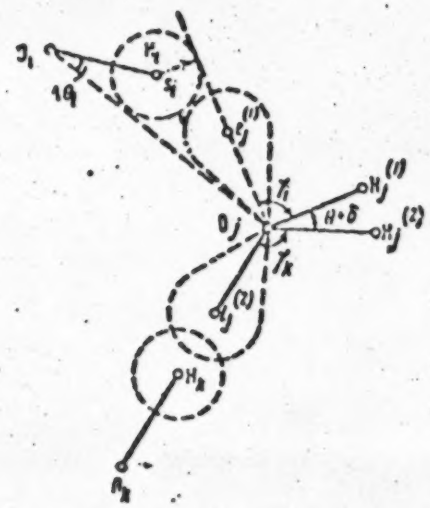

Fig. 1.

It is known that the H_2O molecule has three characteristic frequencies, which correspond to symmetrical and antisymmetrical vibrations of two O–H bonds and deformational vibrations of these bonds about the equilibrium angle $\theta = 105°$. In the vapor state $\nu_\delta = 1595$ cm^{-1}. When condensation occurs, ν_δ increases on the average by 55 cm^{-1}. The following specific points must be taken into account: 1) shift of ν_δ is almost independent of temperature; 2) ν_δ does not change on fusion; 3) the deformational frequency in the vapor state and in ice is revealed only in the infrared spectrum; ν_δ is absent from the Raman spectrum; in liquid water ν_δ is found in both spectra:

Spectrum	ν_δ, cm^{-1}	t°, C	Literature
IR	1650	−170	[10]
» »	1650	−55	[10]
» »	1644	−9	[11]
» »	1649	+3	[11]
Raman	1659	+12	[12]
IR	1646	+19	[11]
Raman	1656	+60	[11]
IR	1642	+70	[11]

The intensity of the Raman spectra is $\sim(\partial\alpha/\partial\theta)^2$, where α is the polarizability of the molecule. If the interaction between O–H bonds in free H_2O molecules is not large $\partial\alpha/\partial\theta$ differs from zero with sharp electrical asymmetry between the O–H bonds of the same molecule. It is easy to see that ν_δ may appear in the Raman spectrum of pure water under the following conditions: 1) the protons of a given molecule bear the same charge in the vapor state as in ice; 2) the charge of the proton changes when a hydrogen bond is formed; 3) hydrogen bonds formed by the H_2O molecule in the liquid phase are broken independently of each other. These conclusions are consistent with the views of Aleksandrov and Sokolov (7) concerning the polarization of the electron cloud in the hydrogen bridge.

To explain the shift of ν_δ toward higher frequencies, it was taken into account in [13,14] that when a proton is displaced from the line of the O–O bond (the length of the O–H bond is fixed) the hydrogen bond is weakened. If the orientation of the neighboring H_2O molecule is fixed, the corresponding increase of energy leads to restriction of the rotational freedom of the molecule under consideration. In the general case the proton moves simultaneously in the potential field restricting the rotational freedom of the molecule and in the potential field preventing deformation of the angle between the O–H bonds. The corresponding force constants are added, and the new frequency of deformational vibrations is

$$\tilde{\nu}_\delta = (2\pi)^{-1} [2 (k_\delta + k_H) / m_H r_{HH}^2]^{1/2} > \nu_\delta,$$

where K_R is the force constant of restricted rotation, m_H is the mass of the proton, and r_H is its distance from the nucleus of the oxygen atom. However, this explanation is not consistent with the existing experimental data on the frequency ν_R of restricted rotation.

Despite the considerable variations of data on liquid water and ice, it can be definitely stated that during fusion of ice ν_R decreases by approximately 100 cm^{-1} [10,15]. Giguere and Harvey [10] made a special study of the effect of temperature on ν_R for ice. Their results and the values calculated by the method of Fox and Martin [11] for $\widetilde{\nu}_\delta$ are given below.

T°,C	$\nu_R cm^{-1}$	$\widetilde{\nu}_\delta, cm^{-1}$
-170	850	1803
-55	820	1790
-15	800	1780
+10	710	1740

It is evident that the calculated $\widetilde{\nu}_\delta$ are considerably greater than the observed $\widetilde{\nu}_\delta = 1650\ cm^{-1}$ and are clearly dependent on the temperature; on fusion the calculated changes by approximately 40 cm^{-1}. We consider that the cause of these discrepancies lies in the fact that in the derivations of Cross [13] and Fox and Martin [11] the electronic structure of the H_2O molecule is assumed rigid and independent of the positions of neighboring molecules.

By the theory of equivalent orbitals [3,16] localized near certain directions in space, the electron energy of the water molecule can be represented as a function of $r_H^{(1)}$, $r_H^{(2)}$ and two angles: θ, between the directions of the OH bonds, and γ between the direction of either of the unshared electron orbitals $e^{(1)}$ or $e^{(2)}$ and the direction of one of the O–H bonds. The final distribution of electron density is determined by the condition of minimum electron energy for a given configuration of the nuclei. As we are concerned with the angular dependence of the energy of the water molecule, we assign their equilibrium values to the distances $r_H^{(1)}$ and $r_H^{(2)}$, neglecting interaction of deformational and valence vibrations. Then in the ground electronic state of the free water molecule the angle γ is determined uniquely by the magnitude of the angle θ. In the condensed phase, where the orbitals of unshared electrons are involved in hydrogen bonds, the electron density distribution is determined, as before, by the condition of minimum electron energy of the molecule for an arbitrary fixed configuration of the oxygen nucleus and the two protons of the water molecule in question, and also of two protons of neighboring molecules.

When a hydrogen bond is formed between molecules i and j, the minimum electron energy of the molecule in the equilibrium position of the nuclei is attained with maximum overlapping of the electron clouds of the H_i atom and the pair of unshared electrons $e_j^{(1)}$ (Fig. 1). In a nonequilibrium configuration of the nuclei the minimum electron density of molecule j cannot be attained with complete overlapping of the electron clouds of the H_i atom and the $e_j^{(1)}$ orbital, because as the angle γ_i deviates from its equilibrium value in the free H_2O molecule repulsion between the $e_j^{(1)}$ orbital and the $e_j^{(2)}$ orbital, and between the former and the electron clouds of the $H_j^{(1)}$ and $H_j^{(2)}$ atoms, increases owing to breakdown of the condition of orthogonality of the hybrid wave functions of the j molecule. In the new equilibrium electronic state the proton is displaced somewhat from the direction $e_j^{(1)}$ by the quantity s_i. In the first approximation the energy required for a change in the degree of overlapping of the wave functions depends only on the displacement s_i and, for small displacements, can be represented as $k_s s_i^2/2$. At the same time, displacement of the proton H_i by the angle $\Delta\theta_i$ results in a deviation of the angle γ_i from the value $\gamma_e(0)$ in the free molecule; the corresponding change of potential energy in the "valence force" scheme [17] may be represented as $k_\gamma(\gamma_i-\gamma_e)^2/2$. The potential energy of the molecule j as a whole is given by the expression:

$$\Delta U = k_\delta \delta^2/2 + k_\gamma(\gamma_i - \gamma_e)^2/2 + k_\gamma(\gamma_k - \gamma_e)^2/2 + k_s s_i^2 + k_s s_k^2/2. \qquad (1)$$

where $\delta, \gamma_i, \gamma_k, s_i$ and s_k are independent vibrational coordinates. In fact, in the system of five nuclei under consideration, in addition to deformational vibrations of the $H_j^{(1)}$ and $H_j^{(2)}$ protons about the angle θ, independent vibrations are also possible, associated with movement of the H_i and H_k protons, leading to changes of the angles γ_i and γ_k between the directions of the O–H bonds and the orbitals of the unshared electron pairs of the j molecule. Since each of the protons H_i and H_k have two degrees of freedom (the distances H_iO_i and H_kO_k are fixed), there appear in the condensed phase, in addition to the usual deformational vibrations of the $H_j^{(1)}$ and $H_j^{(2)}$ protons with frequency ν_δ four pairs of degenerate independent vibrations. The frequency ν_R which is ascribed to rotational oscillations of the H_2O molecule should probably be associated with changes in the degree of overlapping of the wave functions of the electrons taking part in the hydrogen bond rather than with stretching of the H_i-O_j and H_k-O_j distances with changes in the angles $\Delta\theta_i$ and $\Delta\theta_k$. Equation (1) contains two degenerate proper vibrations of frequency $\nu_s = (2\pi)^{-1}\cdot(2k_s/m_H r_H^2)^{1/2}$ corresponding to changes of the angle γ with deformational vibrations of two protons of neighboring molecules about

the common nucleus of the oxygen atom. In absence of hydrogen bonds (in the vapor phase) this frequency, like ν_R, cannot appear. Calculation of k_γ requires a knowledge of the exact wave functions, which is at present impossible. However, if the interaction of O–H bonds within the molecule is not great, and there are no effective charges on the protons in the free molecule, it is likely that the equilibrium values of the angles ζ and γ are determined primarily by mutual repulsion of the four hybrid orbitals about the oxygen atom [10]. Then $k_\gamma \approx k_\delta$.

An extremely interesting fact is that the second deformational frequency ν_γ is in fact found in the infrared spectrum of ice [10,11]. It is displaced toward low frequencies by 95 cm^{-1}. The intensity of this band diminishes sharply with rise of temperature. It is almost nonexistent in the spectrum of liquid water. This behavior is in good agreement with the interpretation given above, because the perturbation due to the hydrogen bond gradually weakens and diminishes sharply on fusion. Giguere and Harvey [10] regarded ν_γ as an overtone of $2\nu_R$. However, as the temperature falls ν_R increases, whereas ν_γ, if it changes at all, decreases from 1515±15 cm^{-1} at -9° [11] to 1500 cm^{-1} at 55° [10]. The splitting of the deformational vibration frequency may be attributed to the anisotropy of ice. This would also account for the sharp decrease in the intensity of the second deformational frequency on fusion. In presence of appreciable anisotropy displacement of the proton from the O–O line in two mutually perpendicular directions occurs at different frequencies. If we accept the explanation given in [11] and [14] for the shift of deformational frequency, splitting of the rotational oscillation frequency should lead to splitting of the deformational frequency $\tilde{\nu}\delta^2 = \nu\delta^2 + \nu_R^2$. However, it is impossible in this way to explain the shift of ν_γ in the direction of lower frequencies. Moreover, there is no definite indication in the literature that two different frequencies ν_R exist for ice. On the contrary, in a number of publications [12, 20-22] there are reports of two absorption bands (~700 and ~550 cm^{-1}) for liquid water, where the anisotropy characteristic of the solid state is virtually nonexistent.

Equation (1) is not complete. If the formation of a hydrogen bond leads to the appearance of charge qe on the protons, and the orbitals of the unshared electrons acquire additional electron density qe with its center of gravity at a distance r_H from the nucleus (the Bjerrum model), the total potential energy of the molecule should be written as

$$\Delta\tilde{U} = \Delta U + (q^2e^2/r_0) - 2(q^2e^2/r_{\gamma_1}) - 2(q^2e^2/r_{\gamma_2}), \qquad (2)$$

where $r_0 = 2r_H \cos \theta/2$ and $r_\gamma = 2r_H \cos \gamma/2$.

It is easy to find from (2) the new values of the force constants of the deformational vibrations of the H_2O molecule in the condensed phase:

$$\tilde{k}_\delta = k_\delta + \frac{1}{4} q^2e^2r_H^2 \tan^2\frac{\theta}{2} \sec\frac{\theta}{2},$$
$$\tilde{k}_\gamma = k_\gamma - \frac{1}{2} q^2e^2r_H^2 \tan^2\frac{\theta}{2} \sec\frac{\theta}{2}. \qquad (3)$$

According to (3), the decrease $\tilde{\nu}_\gamma - \nu\delta$ of the second deformational frequency (observed shift 95 cm^{-1}) is approximately double the increase of the fundamental frequency $\tilde{\nu}\delta - \nu\delta$ of the deformational vibrations (observed shift 55 cm^{-1}).

Equations (3) can be used for estimating the charge qe which appears on protons in the condensed phase. With $r_H = 0.99$ A, $\theta = 109°$ and $\tilde{\nu}\delta = 1650$ cm^{-1} we have $q = 0.16$. This value is close to the value of 0.17 given by Bjerrum [8]. Aleksandrov and Sokolov [7] showed that data on proton resonance spectra are in agreement with the estimated value $q = 0.15$.

In reality, the water molecule does not have strictly tetrahedral symmetry. Using Pople's theoretical estimates of the dipole moment of the water molecule, we can assign the value of 0.88 A to the distance between the center of gravity of the electron cloud of the unshared pair and the nucleus of the oxygen atom. We then have $\Delta\nu_\gamma \sim 90$ cm^{-1} for the shift of the second deformational frequency.

It is of interest to obtain an independent estimate of the "intrinsic dipole moment of the hydrogen bond".

$$\mu_H = qe(d - 0{,}99 - 0{,}88).$$

At 20°, d = 2.95 A, and $q = 0.16$, this gives $\mu_H = 0.33$, which agrees exactly with the value found earlier [9] for μ_H required for quantitative prediction of the salting-out coefficients of benzene and of the energy barriers between the equilibrium positions of H_2O molecules near an ion and in pure water.

LITERATURE CITED

1. J. D. Bernal, R. H. Fowler, J. Chem. Phys., 1, 515 (1933).
2. O. Ya. Samoilov, Structure of Aqueous Electrolyte Solutions and Ion Hydration [in Russian] (Izd. AN SSSR, Moscow, 1957).
3. J. A. Pople, Proc. Roy. Soc., A202, 323 (1950).
4. E. O. Ellison, H. Shull, J. Chem. Phys., 23, 2348 (1955).
5. Z. Burnell, C. Coulson, Trans. Faraday Soc., 53, 403 (1957).
6. N. D. Sokolov, Zh. eksperim. i teor. fiziki, 23, 392 (1952); Uspekhi fiz.n., 107, 205 (1955).
7. L. V. Aleksandrov, N. D. Sokolov, Dokl. AN SSSR, 124, 115 (1959).
8. N. Bjerrum, Dan. Mat. Fys. Medd., 27, 1 (1951).
9. Yu. V. Gurikov, Zh. Strukt. khimii, 1, 3, 286 (1960).
10. P. A. Giguere, K. B. Harvey, Canad. J. Chem. 34, 798 (1956).
11. J. J. Fox, E. Martin, Proc. Roy. Soc., A174, 234 (1940).
12. M. Magat, Ann. Phys., 6, 108 (1936).
13. J. H. Van Vleck, P. C. Cross, J. Chem. Phys., 1, 357 (1933).
14. P. C. Cross, S. Burnham, P. A. Leighton, J. Amer. Chem. Soc., 59, 1134 (1937).
15. L. H. Hibben, J. Chem. Phys., 5, 166 (1937).
16. J. Lennard-Jones, J. A. Pople, Proc. Roy. Soc., A202, 166 (1950).
17. G. Herzberg, Infrared and Raman Spectra of Polyatomic molecules [Russian translation] (Izd. inostr. lit., Moscow 1949).
18. L. Pauling, Nature of the Chemical Bond [Russian translation] (Goskhimizdat, Moscow–Leningrad, 1947).
19. D. F. Heath, J. W. Zinnett, Trans. Faraday Soc., 44, 556 (1948).
20. G. Bolla, Nuovo cimento, 10, 101 (1933).
21. J. Cabannes, J. de Riols, Compt. rend., 198, 30 (1934).
22. P. Narayanaswamy, Proc. Ind. Acad. Sic., A27, 311 (1948).

All abbreviations of periodicals in the above bibliography are letter-by-letter transliterations of the abbreviations as given in the original Russian journal. *Some or all of this periodical literature may will be available in English translation.* A complete list of the cover-to-cover English translations appears at the back of this issue.

SOLUBILITY OF NONPOLAR GASES IN WATER

A. Yu. Namiot

All-Union Petroleum Gas Scientific Research Institute
Translated from Zhurnal Strukturnoi Khimii, Vol. 2, No. 4,
pp. 408-417, July-August 1961
Original article submitted April 12, 1961

The structure of aqueous solutions of nonpolar gases is discussed on the basis of the two-structure model of water. Explanations are offered for the low solubility of gases in water, peculiarities of the changes in the volume of water when gases dissolve in it, and the influence of the sizes of the molecules of dissolved gases on the decrease of their solubility when salts are added to water.

Solutions of gases in water have a number of peculiarities which distinguish them from solutions of gases in other liquids. First, we must note the very low solubility of nonpolar gases in water. Table 1 gives values of the Henry coefficient K_i' for a number of gases in aqueous solutions and the vapor pressures of the same gases when in the liquid state. The ratio of the Henry coefficient to the vapor pressure (more accurately, the volatility) is equal to the ratio of the ideal to the actual solubility. The values of RTln (K_i'/P_i^0), given in the same table represent the changes of chemical potential when a mole of dissolved gas passes form a real solution into an ideal solution of the same concentration. It is evident from Table 1 that the ideal solubilities of gases in water are hundreds and even thousands of times as high as the actual solubilities.

TABLE 1. Henry Coefficients K_i' of Gases Dissolved in Water and Vapor Pressures of P_i^0 of the Liquefied Gases at 10°

Gas	K_i', atm/mole fraction	P_i^0, atm	K_i'/P_i^0	RTln (K_i'/P_i^0), kcal/mole
Nitrogen	64 000	725*	880	3,82
Methane	29 000	225*	129	2,74
Ethane	21 200	29,8	710	3,7
Propane	21 400	6,3	3 400	4,6
n-Butane	27 400	1,46	18 800	5,55

*For gases with critical temperatures above 10° these values were found by linear extrapolation of log P_i^0 – 1/T plots.

A distinguishing feature of the solubility of gases in water is the low solubility in conjunction with considerable liberation of heat during the dissolution. An appreciable heat of solution usually indicates that the energy of interaction between the solvent molecules and the molecules of the dissolved gas is greater than the energy of interaction between the solvent molecules. In the case of water, which is strongly associated, and nonpolar gases this contradicts the accepted ideas.

Another characteristic feature of aqueous solutions of nonpolar gases is the appreciable difference between the partial volumes of gases in water and in other solvents (Table 2).

Explanations of some peculiarities in the behavior of aqueous solutions of gases have been given by Eley [3] and by Frank and Evans [3]. Eley used the concepts developed by Korosy and Uhlig, according to whom the process of dissolution of a gas may be considered as consisting of two stages: formation of cavities in the solvent and transfer of gas molecules from the gas phase into these cavities. The change of internal energy ΔU during dissolution of a gas can be represented as the sum of the internal energy change ΔU_C due to cavity formation and the internal energy change ΔU_A associated with entry of the molecules into the cavities. Calculations of the energy of cavity formation in water, based on the heat of evaporation of water or on the value of the surface tension, gives very high values. Complete separation of water molecules from each other involves the expenditure of a considerable amount of energy for rup-

ture of the hydrogen bonds which confer comparatively high strength to the structure of water. If the formation of cavities in water is not accompanied by rupture of hydrogen bonds, then evidently the energy required for cavity formation in water should be very small.

TABLE 2. Partial Molar Volumes of Gases in Various Solvents at 25°

Solvents	Partial molar volumes, cc/mole			
	gases			
	H_2	N_2	CH_4	C_2H_6
Benzene	34.6 [1]	52.6 [3]	52 [1]	67 [1]
Ethyl ether	50 [1]	66 [1]	58 [1]	—
Acetone	38 [1]	55 [1]	55 [1]	64 [1]
Methyl acetate	38 [1]	54 [1]	53 [1]	69 [1]
Carbon tetrachloride	36 [1]	53 [1]	52 [1]	67 [1]
Methanol	32 [1]	49 [6]	52 [1]	—
Ammonia	75 [4]	53 [4]	58 [5]	—
Water	28 [2]	40 [2]	37 [2]	51 [7]

According to Eley, the heat of solution of nonpolar gases in water at room temperature is large because the energy requirements for cavity formation in water are small. In his explanation of the magnitude of the heat effect Eley, unlike earlier workers, did not have to make improbable assumptions concerning the existence of very large van der Waals forces between the molecules of nonpolar gases and water, or of specific interaction when nonpolar gases are dissolved in water.

Calculations of the heat of solution of gases in water on the basis of Eley's views can explain only the variations of solubility with temperature. The absolute magnitude of the solubility cannot be found from the heat of solution.

For determination of solubility, Eley used the methods of statistical mechanics to calculate the entropy changes when gases are dissolved in water. In order to obtain agreement between the calculated and experimental values Eley was forced to assume that the gas molecules can occupy only a very small proportion (about 2%) of the sites in the quasicrystalline lattice composed of water molecules and molecules of the dissolved gas.

Frank and Evans [9] use a different approach for explaining the solubility of nonpolar substances in water. They consider that when nonpolar substances dissolve in water the structure of water changes toward higher "crystallinity". In the words of Frank and Evans, "microscopic icebergs" form in the waters around the solute molecules. The equilibrium between the various structures existing in water is shifted toward crystal structures with relatively low entropy values. The considerable decrease of entropy when nonpolar substances are dissolved in water are attributed to this fact by Frank and Evans.

Theoretical and experimental studies of the structure of crystalline hydrates of various gases and liquids [10-18] have been of great importance in subsequent development of the theory of structure of aqueous nonelectrolyte solutions.

The structure of crystal hydrates of gases and liquids has been established as the result of x-ray structural determinations by Stackelberg [10,11,15] and of the theoretical work of Claussen [16,17]. The latter showed that water molecules can form structures which, while retaining the intermolecular distances and angles characteristic of ice, are looser than ice and contain relatively large cavities. Despite the great "looseness" of these structures they are energetically stable because, like ice, they contain hydrogen bonds. The x-ray structural investigations of Stackelberg and his associates confirmed that in hydrates of nonelectrolytes the distances and angles between the water molecules differ little from the corresponding values for ordinary ice. According to Stackelberg, the crystalline hydrate structures consist of various polyhedrons the faces of which are pentagons and hexagons.

At the present time the hydrates of gases are regarded as representatives of the "clathrate" compounds, which are essentially solid solutions [16]. In these solutions the solute molecules are contained in the interstices between the solvent molecules.

After the structure of the crystal hydrates of nonelectrolytes had been elucidated, certain investigators studying the solubility of nonpolar substances in water began to assume that in aqueous solutions the molecules of nonpolar substances

are also contained in cavities analogous to those in crystal hydrates [19,20]. The relatively high energetic strength of crystal hydrate structures provided a physical explanation for the liberation of heat when gases are dissolved in water.

Comparison of the experimental data with the explanations put forward for the various peculiarities of aqueous solutions of gases leads to the conclusion that the magnitude of the heat effect when gases dissolve in water can be explained satisfactorily by means of Eley's views on the nature of aqueous solutions of nonpolar gases.

The special explanation given by Eley for the considerable decrease of entropy when gases dissolve and, consequently, for the low solubility of gases in water is not confirmed by experiment. In fact, from Eley's hypothesis that the gas molecules can occupy only about 2% of the sites in the quasicrystalline lattice it follows that the solubility isotherm should be analogous in form to the Langmuir isotherm, the curvature of which is due to the fact that the number of points at which adsorption can occur is limited. It follows from our experimental determinations and calculations [21] that the solubility isotherm of nitrogen and methane in water is linear (the activity coefficient is constant). If we accept Eley's hypothesis, the activity coefficient in our aqueous solutions of methane and nitrogen (the mole fraction of the dissolved gases reached the value of 0.005) should alter by more than 30%.

The views put forward by Frank and Evans on the increase of the "crystallinity" of water when nonpolar substances are dissolved in it are very significant for interpretation of the nature of aqueous solutions, but difficulties arise in using these views to explain the low solubility of gases in water. These difficulties are due to the fact that as the crystallinity of the structures increases the decrease of solubility caused by the entropy change is completely compensated by the increase of solubility caused by the change of enthalpy on "freezing."

The analogy between aqueous solutions of gases and crystal hydrates of these gases, assumed by a number of authors is also very important but, if we assume a fairly considerable similarity between crystal hydrates and solutions, it is difficult to explain the low solubility of gases in water. The consequence of a similarity between crystal hydrates and solutions of gases should be that the formation of a solution from a gas and water should be analogous to the formation of a crystal hydrate from a gas and ice.

Table 3 contains comparisons of the changes of enthalpy, entropy, and free energy in formation of aqueous solutions of methane and ethane with the corresponding changes in formation of crystal hydrates of the same gases from gas and ice (experimental data for calculation of these values are available only for methane and ethane [10]).

TABLE 3. Changes of Enthalpy, Entropy, and Free Energy in Formation of Crystal Hydrates and Aqueous Solutions of Methane and Ethane at 0°

Gas	Formation of crystal hydrate from gas (1 atm) and ice.			Formation of hypothetical solution, (N_2=1) from gas (1 atm) and water		
	ΔH kcal/mole	ΔS, cal/°C.mole	Δμ kcal/mole	ΔH, kcal/mole	ΔS, cal/°C.mole	Δμ kcal/mole
Methane	−4.8	−23	1.8	−4.5	−37	5.6
Ethane	−6.0	−27.4	0.9	−5.5	−40	5.4

It may be seen in Table 3 that the changes of enthalpy in the two processes are almost the same. However, the changes of entropy and therefore of free energy differ sharply for the two processes. Since the change of free energy when a gas goes into aqueous solution characterizes the solubility of the gas in water, the considerable discrepancy between the changes of free energy indicate that the assumption of a relatively far-reaching analogy between crystal hydrates and aqueous solutions does not provide an explanation of the low solubility of gases in water. Thus, although there is a similarity between aqueous solutions and crystal hydrates of gases, indicated by the agreement of the enthalpy changes in their formation, there is also a significant difference between them which must be taken into account for explanation of the low solubility of gases in water.

An attempt is made in this paper to use the two-structure model of water [22-24] for explaining the low solubility of gases in water, the peculiarities in the volume changes of water when gases are dissolved in it, and the influence of salts on the solubility of gases in water.

The two-structure model is based on modern concepts of the structure of water. According to these concepts [25], the arrangement of molecules in liquid water (restricted to the short-range order characteristic of liquids) gen-

erally reproduces the structure of ice. The structure of ice is characterized by fourfold coordination and a very "open" arrangement of the molecules, which alternate with numerous relatively large cavities. In contrast to ice, in liquid water some of these cavities are occupied by water molecules, so that the density of water is higher than that of ice. In the two-structure model of water a distinction is made between two types of molecules: the first type forms an ice-like structure which reproduces, within the limits of short-range order, the structure of ice with cavities not occupied by water molecules; the second type forms a close-packed structure, corresponding to that of ice with the cavities filled with water molecules. Although the molecules of the close-packed structure are of two kinds (at the ice lattice sites and within the cavities), all the molecules of this structure may formally be regarded as equivalent, with thermodynamic properties which may be considered as averaged out.

The transition of molecules of the ice-like structure into the close-packed structure is represented by the equation

$$[H_2O]_i \rightleftarrows [H_2O]_c. \qquad (1)$$

The equilibrium between the structures may be represented as follows:

$$RT \ln \frac{a_i}{a_c} = \mu_c^0 - \mu_i^0 = RT \ln K^*, \qquad (2)$$

where a_i and a_c are the activities of the ice-like and close-packed structures; μ_i^0 and μ_c^0 are the chemical potentials of the "pure" structures, and K^* is the equilibrium constant of process (1). Here and subsequently the activity values in (2) are replaced by mole fractions; it is assumed that this simplification is justifiable for the model under consideration:

$$RT \ln K^* = RT \ln \frac{a_i}{a_c} \approx RT \ln \frac{N_i}{N_c}. \qquad (3)$$

The value of $\mu_c^0 - \mu_i^0 = RT \ln K^*$ at 0° is estimated at 500 [illegible]. Using this value, we find from Eq. (3) the mole fraction of the ice-like structure; this is found to be 0.7[illegible]. The difference between the molar volumes of the two structures is assumed to be ~6 cm³ [2].

When nonpolar gases dissolve in water, if the size of their molecules permits they are apparently incorporated directly in the cavities of the ice-like structure, but if the gas molecules are large the molecules of the ice-like structure probably become arranged so as to form larger cavities, as in crystal hydrate structures.

After a gas molecule has entered a cavity in the ice-like structure (or a cavity analogous to those in crystal hydrates), water molecules cannot enter there. The water molecules surrounding this cavity are eliminated from equilibrium (1). An equilibrium should then be established between the dissolved gas and the water molecules of the ice-like structure:

$$n(H_2O)_i + M \rightleftarrows M \cdot n H_2O, \qquad (4)$$

where n is the number of water molecules combined with one molecule of the dissolved gas M.

The equilibrium of process (4) is determined by the condition

$$RT \ln \frac{N^*}{N_{M \cdot n H_2O}} = \mu^0_{M \cdot n H_2O} - n\mu^0 - \mu^0_M. \qquad (5)$$

Gas solubilities are usually studied at constant gas pressure (for example, at 1 atm). Condition (5) can then be written in the form

$$RT \ln K' N_i^n - \mu^0_{M \cdot n H_2O} - n\mu_i^0 - \mu^0_M\ (1\ \text{atm}) = RT \ln K^*, \qquad (6)$$

where $K' = 1/N_{M \cdot n H_2O}$ is the Henry coefficient of the gas dissolved in water, and K^* is the equilibrium constant of process (4). The quantity $RT \ln K^*$ is the change of free energy of the gas when it passes from the standard state at 1 atm pressure into the dissolved state in the pure ice-like structure.

For gases the molecules of which are not larger than the cavities in the ice structure this quantity is probably close to the corresponding change of free energy when the gas is dissolved in ice, since incorporation of the gas in the ice-like structure should differ little from incorporation of the gas in the ice lattice.

When gases with large molecules are incorporated in structures in the liquid which are analogous to the structures of solid crystal hydrates of the gases it may be assumed that the water molecules forming the elements of the crystal hydrate structures are indistinguishable from the water molecules of the ice-like structure*. With this assumption the value of $\mu^0_M \cdot n\mu^0_{H_2O} - n\mu^0_i - \mu^0_M + RT\ln K''$ may be assumed to be approximately equal to the change of chemical potential in the formation of solid crystal hydrates from gas and ice. This last quantity is determined by the pressure of the gas over the crystal hydrate at 0°.

$$RT \ln K'' = \mu^0_{M \cdot n H_2O} - n\mu^0_i - \mu^0_M (1 \text{ atm}) = RT \ln P_K. \quad (7)$$

where P_K is the pressure of the gas over its crystal hydrate.

From (7) we can find the expression for the Henry coefficient K' of a gas dissolved in water:

$$K' = K''/N^n_i = K''/(0,71)^n. \quad (8)$$

To explain the anomalously high value of the Henry coefficient and the corresponding anomalously low solubility we may assume that the number n of water molecules of the ice-like structure bound to one gas molecule is large. Indeed, since

$$1/(0,71)^7 \approx 10; \quad 1/(0,71)^{20} \approx 1000 \text{ and } 1/(0,71)^{27} \approx 10000,$$

we find that for values of n of 20-30 the Henry coefficients of gases dissolved in water should differ by factors of thousands or tens of thousands from the pressures of the corresponding gases over solid crystal hydrates.

Thus, the explanation of the low solubility of gases in water may be that the dissolving gas does not interact with all the water molecules but only with the molecules of the ice-like structure, and that when a gas molecule goes into solution it binds a large number of water molecules.

Equations (7) and (8) for gases forming crystal hydrates can be used for finding the number n of water molecules bound by one molecule of the dissolved gas

$$n = \log \frac{P_K}{K'} \Big/ \log N_e = \frac{P_K}{K'} \Big/ \log 0,71. \quad (9)$$

Table 4 contains values of n calculated from (9); they range from 15.7 to 17.6.

TABLE 4. Number of Water Molecules Bound by One Molecule of Dissolved Gas, and Number Δn_i of Water Molecules of the Close-Packed Structure Passing into the Ice-Like Structure when One Gas Molecule Dissolves in Water at 0°

Gas	K', atm/mole fraction	P_K, atm	Calculated from eqs. (2) and (14)		Calculated from eqs. (15) and (14)	
			n	Δn_i	n	Δn_i
He	127000	—	—	—	7,4	2,1
H_2	58000	—	—	—	10,5	3
A	23700	105	15,7	4,4	14,0	4
CH_4	22500	26	19,6	5,7	16,1	4,6
Kr	12395	11,5	19,6	5,7	—	—
C_2H_6	12500	5,2	22,5	6,4	21	6,0
Xe	6145	1,5	24,1	6,8	—	—
C_3H_8	13800	1,0	27,6	7,9	27,6	7,9

In connection with these results it is important to note that the calculated values of n ... close to the number of water molecules enclosing the cavities in crystal hydrates of gases. Thus all the gases from argon through ethane

*Solid crystals hydrate structures approximately retain the distances and angles characteristic of the ice lattice. Since the complex configuration of crystal hydrate structures, the unit cells of which contain many tens of molecules, is manifested in long-range order, within the limits of short-range order we can probably assume that the molecules belonging to the ice-like structure (which is the liquid analog of solid crystal hydrate structures) are indistinguishable from each other in water.

in Table 4 form crystal hydrates the cavities in which are polyhedrons containing 20 and 21 water molecules at their vertices. Propane forms a hydrate the cavities in which are enclosed by 28 water molecules. It is shown below that approximately the same values of n are found by calculation from data on the volume changes of water when gases are dissolved in it.

It was stated earlier that Eley's assumption concerning the presence of a small number of cavities (2% of the number of water molecules) in water is not consistent with the experimentally established constancy of the activity coefficient at different concentrations of the dissolved gas. Let us consider the relationship between the activity coefficient and concentration with this mechanism of dissolution of a gas in water. Expressing the chemical potential of the gas in terms of its volatility f_M in (5) and (6), we derive the equation

$$RT \ln \frac{f_M}{N_{M \cdot n H_2O}} = RT \ln K' - RT \ln N_1^n. \qquad (10)$$

In these equations the mole fractions N_1 and $N_{M \cdot nH_2O}$ are the true values, and when they are calculated it must be taken into account that when one molecule of gas is dissolved the number of free water molecules diminishes by n.

When activity coefficients of gases dissolved in water are calculated, the mole fraction of the gas is usually calculated formally with the assumption that the number of free water molecules does not alter when the gas dissolves. Introducing into (10) the formally calculated mole fraction $\tilde{N}_M$ of the gas dissolved in water, we have

$$RT \ln \frac{f_M}{\tilde{N}_M} = RT \ln K' + RT \ln \frac{1}{N_1^n} + RT \ln \frac{n_W + 1}{n_W + 1 - n}. \qquad (11)$$

Here n_W is the number of water molecules (both free and bound) per molecule of dissolved gas. The quantity $f_M/\tilde{N}_M$ in the left-hand side of (11) is the activity coefficient of the dissolved gas accurate to the constant factor.

Using the condition (3) we can show that the mole fraction N_1 of the water molecule of the ice-like structure is $0.71\,(n_W - n)/(n_W + 1 - n)$. Substituting this value into (11), we have

$$RT \ln \frac{f_M}{\tilde{N}_M} \approx RT \ln K' + RT \ln \frac{1}{(0.71)^n} \frac{(n_W + 1)(n_W - 2n)}{(n_W + 1 - n)(n_W - n)}. \qquad (12)$$

Assuming in (12) the value $n_W = 200$ (this corresponds to $\tilde{N}_M = 0.005$) and $n = 20$, we calculated that the activity coefficient at the given concentration of the dissolved gas has almost the same value as at an extremely low content of the dissolved gas.

It follows from the foregoing that the views advanced in this paper on the dissolution of gases in water are consistent with experimental data on the solubility of gases in water at high pressures [21].

Let us now consider the volume changes which should occur in water when a gas dissolves in it, in order to explain the peculiarities in the partial molar volumes of gases dissolved in water. When one mole of gas is dissolved, n moles of water of the ice-like structure become bound. In accordance with condition (3) for equilibrium between the ice-like and close-packed structures, a certain number Δn_c of moles of the close-packed structure must then pass into the ice-like structure. The total change of the number of moles Δn_c of the ice-like structure is then $n - \Delta n_c$. Taking condition (3) into account, we can write:

$$\frac{\Delta n_1}{\Delta n_c} = \frac{n - \Delta n_c}{\Delta n_c} = K', \qquad (13)$$

and hence

$$\Delta n_c = \frac{n}{K' + 1}. \qquad (14)$$

When small gas molecules enter the cavities of the ice-like structure the water should not expand. The volume change when the gas dissolves is in this case due only to transition of water molecules of the close-packed structure into the ice-like structure, which occurs in order to restore equilibrium (1).

It was noted earlier that the volume change Δv_W when a mole of water of the ice-like structure is converted into a mole of water of the close-packed structure is taken to be approximately 3 cm^3. Since the dissolution of one mole of gas is accompanied by conversion of n_c moles of water from the close-packed into the ice-like structure, the change of volume when one mole of gas is dissolved in water or, which is the same thing, the partial molar volume v of the dissolved gas, is given by the equation:

$$\bar{v} \approx \Delta v_w \Delta n_c \approx 8 \Delta n_c. \quad (15)$$

The partial molar volume of hydrogen dissolved in water at 0° was determined experimentally [2] and was found to be 24 cm³. The partial molar volume of helium dissolved in water is approximately 17 cm³*.

Using the partial molar volumes of hydrogen and helium dissolved in water, we have, from (15) and (14), n=10.5 for hydrogen and n=7.4 for helium.

It is important to emphasize the peculiar character of the partial volume of a dissolved gas the molecules of which can fit into the cavities of the ice lattice. In such cases when a gas dissolves special formation of cavities into which the gas enters is not required, because such cavities are present in the water in very large numbers. The volume increase in this case is due to the existence of an equilibrium between the two water structures and is determined by the equilibrium constant of process (1) and not by the molecular size of the dissolving gas.

When a gas with large molecules dissolves in water there must undoubtedly be a change in the volume of the water, associated with conversion of the close-packed structure into the ice-like form. However, the total volume change when the gas dissolves may be determined not only by this conversion but also by conversion of the ice-like structure into a structure of the gas crystal hydrate type. In order to estimate the volume change due to conversion of the close-packed structure into the ice-like structure when gas molecules capable of forming crystal hydrates dissolve in water the value of Δn_c must be found by another and independent method, and not from (15) as was done above for helium and hydrogen. We used values of Δn_c calculated from (9) and (14) for this purpose (Table 4). (15) was then used to calculate the partial molar volumes of these gases from the values so found for Δn_c (Table 5). The data in Table 5 lead to the conclusion that with the exception of the partial molar volume of methane, the calculated and experimental values are in good agreement. This agreement indicates that when relatively large gas molecules are dissolved in water the volume change is primarily determined only by the conversion of Δn_c molecules of the close-packed structure into the ice-like structure. There is no significant volume increase due to expansion of the ice-like structure by incorporation of the gas molecules in it. This result was unexpected, because the conversion of ice into a solid crystal hydrate is accompanied by an appreciable increase in volume [11].

TABLE 5. Comparison of Calculated and Experimental Partial Volumes of Gases Dissolved in Water

Gas	Partial molar volume, cm³		Literature
	expt.	calculated	
A	32	35	[28]
CH_4	36	46	[2]
C_2H_6	48	51	[7]
C_3H_8	63	63	[7]

It is of interest to determine the relationship between the volume change when a gas dissolves in water, due, as we have shown, to process (1), and the true volume of the gas dissolved in water.

For a gas with molecules of moderate size (ethane), the partial molar volume is 46 cm³, and the volume of the cavity in the crystal hydrate structure containing a mole of ethane in the solid hydrate is 65 cm³ [11]. In this case the partial molar volume is about 75% of the volume which the gas apparently occupies in solution. The anomalous partial molar volumes of gases dissolved in water are associated with the peculiar nature of such volumes. The attempt to attribute the anomalous volume changes of gases when dissolved in water to the high internal pressure of water seems unconvincing [7].

With the aid of (15) it is possible to assess the influence of pressure and of the contents of dissolved salts on the partial molar volumes of gases dissolved in water. The partial molar volume of a dissolved gas is determined by the product of Δv_w and Δn_c [see Eq. 15]. The difference Δv_w between the volumes of water in the two structures apparently diminishes with pressure, as the more open ice-like structure should be more compressible than the close-packed structure. In accordance with (14), the value of Δn_c depends on the equilibrium constant of process (1). It is known that pressure favors the conversion of the ice-like structure into the close-packed structure; therefore the equilibrium constant K* diminishes with increase of pressure while Δn_c increases. The consequence of this may be that the partial molar volume of the gas dissolved in water would have low compressibility, and it is even possible that its value would increase with increasing pressure. Salts dissolved in water also decrease the constant K* [14]; in accordance with (15) and (11) this should lead to an increase of the partial molar volumes of gases dissolved in water with increasing contents of dissolved salts.

This mechanism of the dissolution of nonpolar gases in water makes it possible to explain why a salt added to water influences the solubilities of different gases to different extents.

*Calculated by us from experimental data [27] by means of the Krichevskii-Kazarnovskii equation [2].

The salting-out action of salts is usually characterized by the coefficient x of the Sechenov equation

$$x = \frac{1}{c} \log \frac{K^0}{K^{0'}}, \qquad (16)$$

where K'^0 is the Henry coefficient of the substance in an aqueous salt solution of concentration c; K^0 is the Henry coefficient in pure water.

It is reasonable to assume that when a gas dissolves in an aqueous salt solution the number n of water molecules surrounding a gas molecule is the same in pure water as in the salt solution. According to Mikhailov and Syrnikov [24]

TABLE 6. Comparison of The Coefficients x of the Sechenov Equation and the Number n

Gas	x	n	Gas	x	n
H_2	0.097	10.5	C_2H_6	0.184	22.5
CH_4	0.153	19.6	C_3H_8	0.216	27.6

the influence of a salt on the properties of water is manifested by a decrease of the constant for process (1) and correspondingly by the concentration of the ice-like structure. Writing (8) for water containing a dissolved salt and for pure water, dividing one equation by the other, taking logarithms of the result and dividing by the concentration c, we have:

$$x = n \frac{1}{c} \log \frac{N_i}{N'_i}, \qquad (17)$$

where N_i and N'_i are the concentrations of water molecules of the ice-like structure in pure water and in a salt solution of concentration c respectively. The ratio of the Sechenov coefficients of different gases dissolved in water containing the same concentration of a dissolved salt is determined by the values of n for the respective gases.

Table 6 gives the values of n and Sechenov coefficients of certain gases dissolved in water [29]. It is clear from Table 6 that the coefficients of the Sechenov equation are roughly proportional to n.

On the whole it may be claimed that the very rough ideas advanced in this paper make it possible to explain many peculiarities in the behavior of aqueous solutions of nonpolar gases.

In conclusion, the author is deeply grateful to O. Ya. Samoilov for valuable advice.

LITERATURE CITED

1. J. H. Hildebrand, R. L. Scott, The Solubility of Nonelectrolytes, New York, 1950.
2. I. R. Krichevskii, Phase Equilibria in Solutions at High Pressures [in Russian] (Goskhimizdat, Moscow, 1952).
3. I. R. Krichevskii, G. D. Efremova, Zh. fiz. khimii, 22, 1216 (1948).
4. I. R. Krichevskii, G. D. Efremova, Zh. fiz. khimii, 26, 1117 (1952).
5. I. R. Krichevskii, G. D. Efremova, Zh. fiz. Khimii, 27, 1682 (1953).
6. I. R. Krichevskii, G. D. Efremova, Zh. fiz. khimii, 24, 277 (1950).
7. W. L. Masterton, J. Chem. Phys., 22, 1830 (1954).
8. D. D. Eley, Trans. Faraday Soc., 35, 1281 (1939).
9. H. Frank, M. Evans, J. Chem. Phys., 13, 507 (1945).
10. M. Stackelberg, NaturwLs., 36, 327, 359 (1949).
11. M. Stackelberg, H. Muller, Z. Elektrochem., 48, 25 (1954).
12. M. Stackelberg, W. Meinhold, Z. Elektrochem., 58, 40 (1954).
13. M. Stackelberg, H. Frubuss, Z. Elektrochem., 58, 99 (1954).
14. M. Stackelberg, Z. Elektrochem, 58, 104 (1954).
15. M. Stackelberg, W. Jahns, Z. Elektrochem., 58, 162 (1954).
16. W. F. Claussen, J. Chem. Phys., 19, 1425 (1951).

17. W. F. Claussen, J. Chem. Phys., 19, 259 (1951).
18. L. Pauling, R. Marsh, Proc. Nat. Acad. Sci. Wash., 38, 112 (1952).
19. W. F. Claussen, M. F. Polglas, J. Amer. Chem. Soc., 74, 4817 (1952).
20. D. W. Glew, R. E. Robertson, J. Phys. Chem., 60, 332 (1956).
21. A. Yu. Namiot, Zh. fiz. khimii, 31, 1593 (1960).
22. L. Hall, Phys. Rev. 73, 7, 775 (1948).
23. K. Grjotheim, J. Krogh-Moe, Acta Chem. Scand., 8, 7, 1193 (1954).
24. I. G. Mikhailov, Yu. P. Syrnikov, Zh. struk. khimii, 1, 12 (1960).
25. O. Ya. Samoilov, Structure of Aqueous Electrolyte Solutions and Ion Hydration [in Russian] (Izd. AN SSSR, Moscow, 1957).
26. L. C. Platteew, J. H. van der Waals, Mol. Phys., 1, 91 (1958).
27. R. Wiebe, V. Gaddy, J. Amer. Chem. Soc., 57, 817 (1935).
28. A. Yu. Namiot, M. M. Bondareva, Tr. Vses. neftegaz. n.-i. inst. (VNII), No. 34, Gostoptekhizdat (in the press).
29. T. L. Morrison, F. Billet, J. Chem. Soc., 3819 (1952).

All abbreviations of periodicals in the above bibliography are letter-by-letter transliterations of the abbreviations as given in the original Russian journal. *Some or all of this periodical literature may well be available in English translation.* A complete list of the cover-to-cover English translations appears at the back of this issue.

POSSIBLE SUPERSTRUCTURES OF n-LAYERED CLOSE PACKINGS WITH n ≥ 3

N. L. Smirnova

M. V. Lomonosov Moscow State University
Translated from Zhurnal Strukturnoi Khimii, Vol. 2, No. 4,
pp. 413–423, July–August 1961
Original article submitted May 10, 1960

The distribution has been determined of two kinds of atoms, A and B, jointly distributed at sites of an n-layered close packing (n≥3) when all the centers of the octahedrons are occupied by X atoms and "the composition of the octahedron" A_pB_{6-p} remains unchanged. When p = 2 or 3 the A and B atoms can be arranged in two different ways in the octahedron. Only superstructures with all the octahedrons constructed in either one way or the other were found. The distributions so found were compared with experimentally determined structure types.

Our determinations of possible superstructures of n-layered close packings [1] were based on the general principle that superstructure formation is the result of a tendency for atoms of one kind to surround themselves with atoms of another kind. We considered the possible distributions of two kinds of atoms, A and B, distributed jointly at the sites of an n-layered close packing if each A atom is surrounded by B atoms only, while each B atom contains in its 4, 3, 2, 1 coordination sphere a neighboring A atom. Investigation of this problem is equivalent to determinations of the possible distribution of cube-octahedrons consisting of B atoms with A atoms at the centers if each vertex of a cube-octahedron belongs to four, three, two, or one cube-octahedron.

Below [2] showed that every n-layered close packing can also be regarded as a packing of octahedrons and tetrahedrons. If all the centers of the octahedrons are occupied by X atoms of the same kind and the vertices are occupied by A and B atoms, then the most common case will be such that the "composition of the octahedron" A_pB_{6-p} remains unchanged. Let us consider the possible distribution of A and B atoms in such cases. This investigation is equivalent to determinations of the possible distribution of octahedrons and prisms of X atoms with A and B atoms at the centers.

In solving this problem, as in the preceding instance [1], we considered only the centers of the atoms, and therefore the superstructures found are possible, in general, with any ratios of the radii of A and B atoms; therefore the atoms must be at the close-packing sites but they need not be close-packed.

The preceding investigation showed that similar superstructures based on the simplest motifs may occur in chemical compounds of entirely different properties. Here the A and B atoms may be both cations or both anions, one may be a cation and the other an anion, etc. Moreover, the positions of the A atoms and also of the B atoms need not be filled. X atoms may be absent, or additional T, C, D atoms may be present in the tetrahedral cavities and other positions.

In the geometrical investigation (not detailed here) and in the presentation of the results below the X atoms are omitted. These results are as follows.

1. Each octahedron is formed by one A atom and five B atoms (composition AB_5, Fig. 1a). When n = 3 (the cubic close packing), two series of superstructures are possible. In the first of these (I) the close-packed layers of B atoms alternate with AB_2 layers (the B atoms form graphite networks with A atoms in the centers of the rings). All the diversity of superstructures of this series is due to the various types of relative displacement of the AB_2 layers. Figure 2 shows one of the superstructures of this series and two of its projections in the directions of the other former threefold axes.

In the second series (II) the close-packed layer is formed from parallel bands consisting of hexagons joined along their parallel edges (Fig. 3). In some bands the hexagons of B atoms have A atoms at centers; in others, B atoms. The bands may be single, double, or wider still. In successive layers above bands with A(B) atoms at the centers are bands with B(A) atoms at the centers. The distribution of atoms in one layer determined the whole structure. All the diver-

sity of superstructures of this series is due to differences in the width and alternation sequence of the bands in the first layer. It should be noted that all the possible distributions of the second series can be obtained from one type of the first series (Fig. 2a) as the result of displacement of the layers (to avoid confusion with the close-packed layers, we shall refer to these layers as "packets"). The packets may have widths corresponding to one, two, or more bands. The bands must be parallel to the direction indicated by the arrow in Fig. 2a. In a single case alternation of packets one band wide gives the projection of one of the superstructures of the first series (Fig. 2b).

When n>3 both series of superstructures described for n=3 are possible. It must be pointed out, however, that when n>3 may also depend on the type (c or h) to which the close-packed so formed belongs (for example, a type composed of B atoms only). When n>3 there is only one direction perpendicular to the course of the close-packed layers and therefore the arrangement of the bands shown in Fig. 2b leads to the formation of a new type of superstructure, which belongs to the second series. Two new series (III and IV) are also possible when n>3. In the first of these (III) the close-packed layer is formed from single parallel bands, but in these bands the hexagons can join also by their vertices (Fig. 4a). The distribution of A and B atoms in the whole superstructure is determined rigidly (i.e., without alternatives) by the arrangement of the bands in one close-packed layer and the type of layer packing. All the close-packed layers of each superstructure of this type are constructed similarly, but are shifted relatively to each other. Superstructures of this series for each given n-layered close packing can also be derived from a superstructure with a distribution of A and B atoms similar to that shown for the cubic close packing in Fig. 2b. For this, the layers (packets) must be shifted in a direction perpendicular to the bands and shown in Fig. 4a by arrows. The band must not "tear," i.e., the shift should lead to junctions at vertices or edges. The last series (IV) is possible if all the bands are formed from hexagons joined at opposite vertices. In this case we assume a shift of the layers (packets) in the direction of the bands (shown by an arrow in Fig. 4b) extending the length of the hexagon edge. Superstructures of this type for each given n-layered close packing are also derived from a type constructed similarly to the distribution shown in Fig. 2c for cubic close packing. The superstructure of series III and IV with n=3 are projections of superstructures of series I and II in the direction of the former threefold axes and when n>3 they are independent types.

These arrangements can also be considered from another viewpoint. In these arrangements each A atom is contained in a cube-octahedron consisting of 8 atoms. Six B atoms of each cube-octahedron have three neighboring A atoms, and six others, two neighboring A atoms. Only one representative of this group, the W_2Al_7 structure type (see table), has been found among existing compounds.

2. Each octahedron is formed by two A atoms and four B atoms (composition AB_2). The A and B atoms in the octahedron can be arranged in two different ways (Fig. 1b,c). By one of Pauling's rules [3] the number of essentially different components in a crystal tends to be small; therefore only the superstructures with octahedrons constructed either only in the one way or only in the other were considered first. It was found that in the second case no distribution is possible. In the first case there are two series of superstructures when n=3. In one of these (I) a close-packed layer of B atoms alternates with an A_2B layer (the A atoms form graphite networks with B atoms at the centers of the rings). The diversity of superstructure types in the series is determined by different displacements of the A_2B layers relative to each other. One such type and two of its projections in the direction of other former threefold axes are shown in Fig. 5. This arrangement occurs in $Al_{\square}Cl_3$ (A = Al, B = □ = unoccupied places in the close packing). This series also includes $Cr_{\square}Cl_3$, but here the Cr atoms in the sixth layer are not at the points 6, but at other points.

The only difference between the superstructures shown in Fig. 5a and Fig. 2a is that in the former the graphite layers are formed by A atoms with B atoms at the ring centers, and in the latter by B atoms with A atoms at the ring centers. We have just shown that when n>3 three more series of possible superstructures can be derived from superstructures built similarly to the arrangement shown for n=3 in Fig. 2. Three such series are also found in the present instance. To obtain the arrangements of the second series, we must take all the superstructure types of the second series discussed in the previous section, replace A atoms by B atoms, and replace B atoms by A atoms at all the shared vertices of the hexagons (compare Figs. 6 and 3, 5b and 2b). To obtain all the superstructure types of series III and IV we must take all the superstructure types of series III and IV of the previous section, replace A atoms by B atoms, and have A atoms at the opposite vertices of each hexagon, so that the lines joining these vertices are parallel to the double-headed arrow in Figs. 2c and 4 (compare Figs. 6C and 2c, 7a and 4a, 7b and 4b). As in the first section, when n=3 the superstructures of the last two series are projections of superstructures of the first two series in the directions of the other former threefold axes.

3. Each octahedron is formed by three A atoms and three B atoms (composition AB). The A and B atoms in the octahedron can be arranged in two ways (Fig. 1d, e).

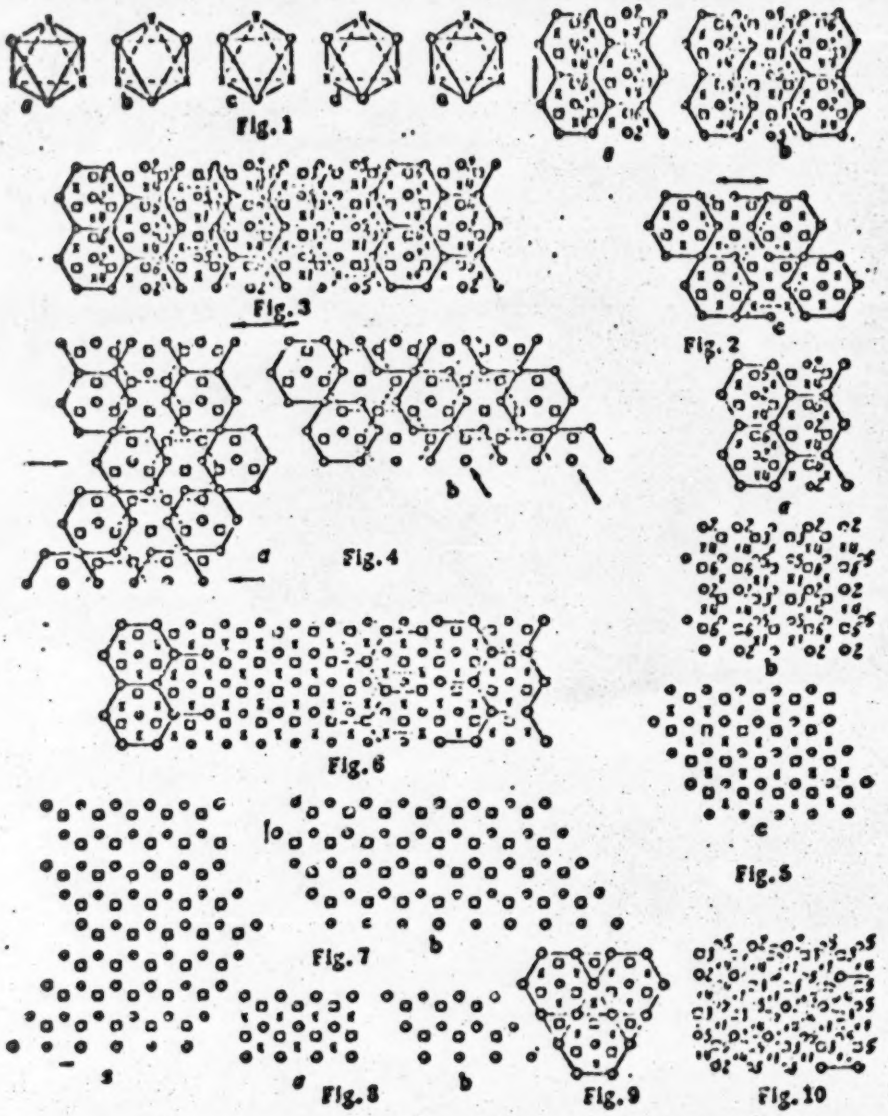

Fig. 1. Fig. 2. Layer sequence ×, O, □, etc. The A atoms are indicated in bold type in three layers only. Numbers indicate A atoms at the height of the corresponding layer (in Fig. 2c the positions of the A atoms in the fourth and higher layers are not shown). Fig. 3. Layer sequence ×, O, □, etc. The A atoms are indicated in bold type in three layers. Numbers indicate A atoms at the height of the corresponding layer. Fig. 4. Only two layers are shown; A atoms indicated in bold type. Fig. 5. See caption to Fig. 2. Fig. 6. Layer sequence ×, O, □, etc. The A atoms are indicated in bold type in three layers only. Fig. 7. See caption to Fig. 4. Fig. 8. Fig. 9. See caption to Fig. 6. Fig. 10. See caption to Fig. 6.

Let us consider the cases when all the octahedrons are constructed in each one of these ways only. In the first case, when n = 3, only two types of superstructure were found. In the first type (I) close-packed layers of A atoms alternate with close-packed layers of B atoms (Fig. 8a). The table shows that this type of arrangement is fairly common. In the second type (II) layers of the composition AB_3, formed from hexagons of B atoms with shared vertices and with A atoms at the centers of the rings alternate with A_3B layers formed from hexagons of A atoms with shared vertices and with B atoms at the centers of the rings. The A atoms are between pairs of triangles of A atoms and within hexagons of B atoms. The A and B atoms form the same motif. Such superstructures are found in a number of structure types (see table), in particular in $MgAl_3[]_2O_4$ (A = Al; B = [] = unoccupied positions of the close packing, Fig. 9a).

When n>3 there are also two such superstructures, but the motif of A atoms is not the same as that of B atoms. The reason is that, as already stated, it is significant here whether the close-packed layer is of the h or the c type.

TABLE*

A : B	Number of series	Close-packing type	Structure type	A	B	O	T
1 : 3	I	abcb	WAl_3	W	Al_3		
1 : 2	I	[illegible]	$AlCl_3$	Al	Π_3	Cl_3	$Si\Pi_2$
			[illegible]	Cr	Π_3	Cl_3	
			$K_4[SiO_4][K, OH)_2$	(F, OH)$_2$	O_4	$Al_3\Pi_4$	
			Ta_2FeN_4	Fe	Ta_2	N_4	
1 : 1	I	abc	$CdCl_2$	Cd	Π	Cl_2	
		abc	$CuCl_2$	Cu	Π	Cl_2	
		abc	CuPt	Cu	Pt		
		abc	$NaFeO_2$	Na	Fe	O_2	
		abc	$CuFeO_2$	Cu	Fe	O_2	
		ab	Cd(ON)Cl	OH	Cl	CdΠ	
		ab	MoS_2	Mo	Π	S_2	
		abac	Ta_2MnN_4	Ta_2	(Ta, Mn)	N_4	
	II	abc	$MgAl_2O_4$	Al_2	Π_2	O_4	$Mg\Pi_2$
		abc	$MgCu_2$	Cu_2	Π_2		$Mg\Pi_2$
		abc	SiO_2 — cristobalite	O_2	Π_2		$Si\Pi_2$
		abc	$Cu_2(OH)_3Cl$ — atacamite	Cu_2	Π_2	$(OH)_2Cl$	
		abc	$Co_2(OH)_3Cl$	Co_2	Π_2	$(OH)_2Cl$	
		abcb	SiO_2 — tridymite	O_2	Π_2		$Si\Pi_2$
		abac	$MgZn_2$	Zn_2	Π_2		$Mg\Pi_2$
		abcbacbc	$MgNi_2$	Ni_2	Π_2		$Mg\Pi_2$
	III	abc	TiO_2 — anatase	Ti	Π	O_2	
		abc	$CuFeS_2$ — chalcopyrite	Cu	Fe		Π_2S_2
		abc	$CaWO_4$	Ca	W		O_4

*A and B are distributed together at the positions of an n-layered close packing; O and T are the positions of the octahedral and tetrahedral interstices; π = positions not occupied by atoms.

Let us illustrate this by the examples of $Mg\Pi Zn_2$ and $Si\Pi O_2$ (tridymite). In both cases the Zn and O atoms and the unoccupied positions Π of the close packing form a close-packed structure of the abac type. In both cases the layers have the composition: $O_2\Pi(Zn_2\Pi)$ and $O\Pi_2(Zn\Pi_2)$. However, in tridymite the $O_2\Pi$ layers are of the c type, and in $MgZn_2$ the $Zn_2\Pi$ layers are of the h type. Therefore in SiO_2 the tetrahedrons are joined only by their vertices, while in $MgZn_2$ they are joined by their vertices and triangular faces.

In addition to the two main types of superstructure described above when n>3 there is a further type, III (Fig. 8b). The layers are formed from alternating chains of A and B atoms. A single type of arrangement corresponds to each type of close packing. When n=3 this type is a projection of the superstructure of type I (Fig. 8a) in the direction of one of the three other former threefold axes. Finally, when the octahedrons are formed in the second way (Fig. 1e), one type of superstructure (Fig. 10) is possible when n=3. This is the arrangement of Cu and Fe atoms in $CuFeS_2$ (chalcopyrite) and of Ti and Π in $Ti\Pi O_2$ (anatase); see table. When n>3 there is only one arrangement for each type. The close-packed layers are formed as for n=3, but the type of close packing in their superposition should be taken into account.

When n=2 (hexagonal close packing) all the superstructure types described above for n=3 are possible, but there are probably others. Analysis of these superstructures is beyond the scope of this paper.

Thus, our earlier conclusions [1] are confirmed once again.

1. Investigations of possible superstructure explain why particular atomic arrangements and not others are found, and make it possible to predict possible new arrangements.

2. Superstructure is a more general concept than structure type.

3. Many complex structure types can be represented as combinations of simple arrangements with particular superstructures.

In conclusion, I am deeply grateful to Corresponding Member G. B. Bokii and Academician N. V. Belov for valuable advice and guidance.

LITERATURE CITED

1. N. L. Smirnova, Kristallografiya, 4, 1, 13 (1959).
2. N. V. Belov, Structure of Ionic Crystals and Metallic Phases [in Russian] (Izd. AN SSSR, Moscow, 1947).
3. L. Pauling, Nature of the Chemical Bond [Russian translation] (Goskhimizdat, Moscow – Leningrad, 1947).

All abbreviations of periodicals in the above bibliography are letter-by-letter transliterations of the abbreviations as given in the original Russian journal. *Some or all of this periodical literature may well be available in English translation.* A complete list of the cover-to-cover English translations appears at the back of this issue.

CRYSTAL STRUCTURES AND CERTAIN PROPERTIES OF HAFNIUM – BERYLLIUM COMPOUNDS

P. I. Kripyakevich, M. A. Tylkina, and E. M. Savitskii

Iv. Franko L'vov State University
A. A. Baikov Institute of [illegible] Academy of Sciences USSR
Translated from Zhurnal Strukturnoi Khimii, Vol. 2, No. 4
pp. 421–433, July-August 1961
Original article submitted July 5, 1960.

The existence of four compounds of hafnium with b[illegible]blished; their crystal structures and certain properties were determined.

The system hafnium – beryllium has not been studied previously. In view of the resemblance between hafnium and zirconium systems (for example, Zr–B [1] and Hf–B [2]) and of the existence of four compounds in the Zr–Be system [3] it is to be expected that several compounds are formed in the Hf–Be system. The purpose of the present investigation was to find whether compounds of Hf with Be exist, and if so, to determine their structures and certain properties.

Starting Materials; Methods of Preparing and Investigating the Alloys

The starting materials for the alloys were hafnium obtained from the iodide (impurities: 0.43% Zr; 0.0022% Si; 0.006% Ti; 0.0012% Al; 0.003% Mg; 0.13% Mo) and beryllium (99.3% Be). For additional purification the original beryllium was twice melted in a high-frequency vacuum furnace in argon at 50 mm pressure in BeO crucibles.

Beryllium-based alloys containing (by synthesis) 0.0025; 0.005; 0.013; 0.025; 0.10; 0.56; 1.24; 2.44 at. % Hf (0.05; 0.1; 0.25; 0.5; 2.0; 10.0; 20.0; 33.0 wt. %) were also prepared in the high-frequency vacuum furnace in argon, but the pressure was increased to 100–200 mm. Alloys rich in hafnium, containing (by synthesis): 7.74; 10.50; 16.80; 20.90; 33.73 and 51.64 at. % Hf (62.5; 70.0; 80.0; 31.0; 91.0 and 95.5 wt. %) were [illegible] in an arc furnace with a copper water-cooled floor and an inexpendable tungsten electrode, in an argon atmosphere (pressure 300–400 mm). When BeO crucibles were used for fusion of hafnium-rich alloys the hafnium reacted with the crucible material.

The alloys were not subjected to heat treatment.

The x-ray structural investigation was carried out by the powder method [illegible]bye cameras (diameter 57.3 mm) and Preston cameras with chromium radiation. The following properties were determined for some of the alloys: melting point, hardness, microstructure, and microhardness of the structural constituents. The melting point was determined in argon (100 mm pressure) by the "drop" method* based on filling a hole drilled in the specimen with liquid metal, with the aid of an optical pyrometer calibrated against the pure metals under the same conditions. Hardness was determined on the B scale with the Rockwell instrument (ball 2.5 mm diameter, load 100 kg), and the PMT-3 instrument (load 100 g) was used for microhardness determinations.

Results of the Investigation

a) Alloys with 0–2.44% at. % Hf

The melting points and hardness values of alloys of low Hf contents are given in Table 1.

These alloys have a two-phase structure (Fig. 1, a,b). They consist of a main phase – a solid solution of Hf in Be, or beryllium (microhardness H_μ = 200 kg/mm^2) with segregations of the second phase (H_μ = 1200 kg/mm^2). The amount of the second phase increases with the hafnium content.

*The apparatus and method are described in a paper by E. M. Savitskii and M. A. Tylkina, Zh. neorg. khimii, 3, 815 (1958).

The x-ray structural investigation confirmed the results of microstructure analysis. The x-ray patterns of the alloys contain lines of two phases. One has hexagonal structure with $c/a = 2.28$, $c = 3.63$ kX, $c/a = 1.57$, i. e., almost equal to the constants of pure beryllium; this shows that beryllium is almost or entirely insoluble in hafnium. The intensity of the beryllium lines decreases with increasing Hf content. The lines of the second phase are indexed on

TABLE 1. Melting points and Hardness of Hf–Be Alloys

Hf content		Melting point, °C	Hardness, R_B	Hf content		Melting point, °C	Hardness, R_B
at. %	wt. %			at. %	wt. %		
0	0	1283	65	0,10	2,0	1275	68
0,0025	0,05	1283	60	0,56	10,0	1273	77
0,005	0,10	1280	—	1,24	20,0	1270	87
0,013	0,25	1277	65	2,44	33,0	1463	98
0,025	0,50	1275	65				

the basis of a cubic primitive lattice with $a = 4.992 \pm 0.01$ kX or a cubic face-centered lattice with $a = 9.985 \pm 0.002$ kX (Table 2). A lattice constant close to the latter is found for the compound $ZrBe_{13}$ ($NaZn_{13}$ type, face-centered lattice, $a = 10.047$ A [4]); we therefore assumed that the cubic phase is the compound $HfBe_{13}$ with a structure of the $NaZn_{13}$ type.

TABLE 2. X-ray Powder Pattern of the Alloy $Hf_{2.4}Be_{97.6}$ ($HfBe_{13}$ + Be). Cr–K radiation.

$h^2+k^2+l^2$	hkl	$\sin^2\Theta$ mea.	$\sin^2\Theta$ calc.	Intensity*** mea.	Intensity*** calc.	$h^2+k^2+l^2$	hkl	$\sin^2\Theta$ mea.	$\sin^2\Theta$ calc.	Intensity*** mea.	Intensity*** calc.
4	200	0,052	0,052	40	53,7	44	622	0,575	0,577	40	37,2
8	220	0,103	0,105	50	75,5	48	444	0,625	0,620	25	18,7
12	222	0,155	0,157	40	35,8	52	640	0,680	0,682	45	45,5
16	400	0,210	0,210	20	22,5	56	642	0,733	0,734	80	90,2
20	420	0,262	0,262	70	77,0	59	721	—	0,771	0	0,03
24	422	0,314	0,315	60	70,0	64	800	0,839	0,839	20	21,7
32	440	0,419	0,420	25	17,3	68	820	0,892	0,890	90 / 90	94,2 / 80,0	170,2
35	531	—	0,458	0	0,2		644					
36	600	0,471	0,472	40	5,4 / 29,6	72	822	0,943	0,943	100 / 100	92,5 / 67,5	160,0
	442				35,0		660					
40	620	0,524	0,524	45	41,2	75	752	—	0,992	0		0,8

*** The apparatus and method are described in a paper by E. M. Savitskii and M. A. Tylkina, Zh. neorg. khimii, 3, 815 (1958).

Intensities were calculated from the formula $I = S^2 p \varphi \cdot 10^{-5}$ (where S is the structure factor, p is the multiplicity factor, and φ is the product of the Lorentz and the polarization factors) for the following atomic arrangements (space group $Fm3c - O_h^6$) [5]: 8Hf in 8 (a); $8Be^{(1)}$ in 8 (b); $96\,Be^{(2)}$ in 96 (i), $y = 0.178$, $z = 0.122$. Table 2 shows that the calculated and visually observed intensities are in good agreement, which confirms our hypothesis concerning the composition and structure of the compound in equilibrium with beryllium.

The interatomic distances in the $HfBe_{13}$ structure are given in Table 3.

b) Alloys with 7.74-51.64 at. % Hf

The x-ray pattern of the microstructurally heterogeneous alloy with 51.64 at. % (95.5 wt. %) of Hf (Fig. 1, e) contains lines corresponding to hafnium or a solid solution based on it (structure type Mg, $a = 3.183$, $c = 5.052$ kX, $c/a = 1.585$) and to a second phase. The lines of this phase appear in the pure state in the x-ray pattern of the almost homogeneous alloy with 33.33 at. % (91 wt. %) of Hf (Fig. 1, d). In view of the composition of this last alloy it may be assumed that it mainly contains the compound $HfBe_2$ (33.33 at. % Hf). The microhardness H_μ of $HfBe_2$ is 980 kg/mm^2. All the lines in the x-ray pattern of $HfBe_2$ (Table 4) are indexed on the basis of a hexagonal lattice with $a = 3.775 \pm 0.002$, $c = 3.157 \pm 0.001$ kX, $c/a = 0.836$). Similar values of the lattice constants ($a = 3.82$, $c = 3.24$ A, $c/a = 0.847$) are found for the compound $ZrBe_2$, which has a structure of the AlF_2 type [6]. Comparison of the visually observed intensities with the values calculated from the formula $I = S^2 p \varphi \cdot 10^{-5}$ for the AlF_2 type [space group $C6/mmm - D_{6h}^1$, 1 Hf in 1(a), 2 Be in 2 (d)] shows (Table 4) that the $HfBe_2$ structure belongs to this type.

The interatomic distances in the $HfBe_2$ structure are given in Table 8.

The question of the coordination numbers of the atoms in the $HfBe_2$ structure arises in connection with the consideration of interatomic distances. Compounds assigned to the AlB_2 structure type are divided into two groups: in one (borides, gallides, and silicides with atomic radius ratio $k>1.3$ and $c/a=1.00$) the coordination numbers (c.n.) are 20 and 9, and in the other (intermetallic compounds with $k=1.0-1.2$ and $c/a \approx 0.60-0.65$) the c.n. are 14 and 11 [7a].

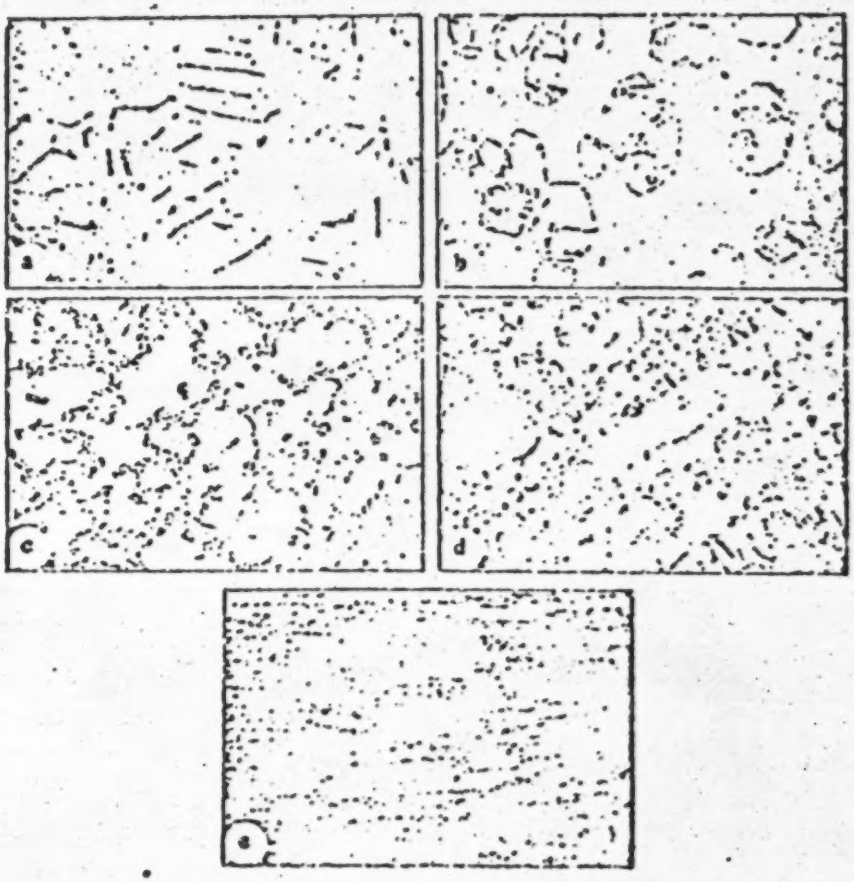

Fig. 1. Microstructures of cast alloys in the system Hf–Be: a) $Hf_{3.1}Be_{93.9}$ (2 wt. % Hf); × 270; Be + $HfBe_{13}$ (small rounded and elongated inclusions). b) $Hf_{2.45}Be_{97.55}$ (33 wt. % Hf); × 270; Be + $HfBe_{13}$ (polyhedrons). c) $Hf_{20.9}Be_{79.1}$ (91 wt. % Hf); × 600; $HfBe_5$ (light phase) + $HfBe_2$ (dark phase). d) $Hf_{22.72}Be_{77.27}$ (91 wt. % Hf); × 600; $HfBe_2$ (light background) + small inclusions of hafnium (or solid solution of Be in Hf); e) $Hf_{21.64}Be_{78.36}$ (95.5 wt. % Hf); × 400 $HfBe_2$ + Hf.

One representative of the second group, In_2Bi, was recently found to have a structure of the Ni_2In type [8]; it is possible that other compounds of this group may have structures of the same type. The compound $HfBe_2$, like $ZrBe_2$, occupies an intermediate position between the compounds of the above-mentioned groups, and it is difficult to determine the coordination number for it from the interatomic distances only. We used A. V. Shubnikov's method, described by Bokii [7b], to determine the coordination number. By drawing the face perpendicular to the lines joining the atoms in the $HfBe_2$ structure (at distances proportional to the radii of the connected atoms) we obtained an icosahedron (a combination of a hexagonal bipyramid, a hexagonal prism, and a pinacoid) around the Hf atom, and a nonahedron (a combination of a trigonal bipyramid and a trigonal prism) around the Be atom. Therefore the coordination numbers of Hf and Be are 20 and 9 respectively, and the structure of $HfBe_2$ belongs to the first group of structures, i.e., to the AlB_2 type itself.

The two-phase alloy with 20.90 at. % (31.0 wt. %) of Hf (Fig. 1) contains, in addition to $HfBe_2$, a second compound of higher beryllium content. The microhardness of the second compound is H_μ = 1340 kg/mm². Its lines in the x-ray pattern (Table 6) are indexed on the basis of a hexagonal lattice with $ca = 4.525 \pm 0.010$, $c = 3.461 \pm 0.010$ kX, $c/a = 0.765$. The values of the constants ($a \approx 4a_{Be}$, $c \approx a\sqrt{3}$) indicate the $CaZn_5$ type [9]. The observed intensities agree with the calculated values ($I = S^2_{\varphi} \cdot 10^{-4}$) for a structure of the $CaZn_5$ type with following arrangement of atoms [space group $P6/mmm - D^1_{6h}$]: 1Hf in 1 (a), 2 $Be^{(1)}$ in 2 (c), 3 $Be^{(2)}$ in 3 (g). Therefore the composition $HfBe_5$ should be assigned to this compound. The interatomic distances in the $HfBe_5$ structure are given in Table 7.

TABLE 3. Interatomic Distances d in the Structure of $HfBe_{12}$

Atoms	d, kX	Coordination numbers
Hf — 24 $Be^{(2)}$	2,90	24
$Be^{(1)}$ — 12 $Be^{(2)}$	2,16	12
$Be^{(2)}$ — 2 $Be^{(2)}$	2,07	
1 $Be^{(1)}$	2,10	
4 $Be^{(2)}$	2,22	12
2 $Be^{(2)}$	2,24	
1 $Be^{(2)}$	2,44	
2 Hf	2,90	

The x-ray pattern of the alloy with 7.74 at. % (62.5 wt. %) of Hf contains about 50 lines, which do not include $HfBe_5$ or $HfBe_{12}$ lines (Table 8). The microhardness of H_μ of the principal component of the alloy with (1035 kg/mm²) differs from H_μ of the other compounds. The composition of the alloy, close to $HfBe_{12}$, indicates the possible existence of a compound of the $ThMn_{12}$ type [10]. However, only the strongest lines are also indexed on the basis of the hexagonal unit cell characteristic of the $CaZn_5$ type, with $ca = 4.321$, $c = 3.643$ kX, $c/a = 0.843$. The higher value of c/a in comparison with structures of the $CaZn_5$ type indicates the possible existence of R_2X_{17} structure types (Th_2Ni_{17} [11], Th_2Zn_{17} [12], V_2Zn_{17} [12]), allied to the $ThMn_{12}$ and $CaZn_5$ types. Most of the lines can be indexed if structures of the Th_2Ni_{17} and Th_2Zn_{17} types are assumed. All the lines are indexed on the basis of the U_2Zn_{17} types only (Table 8). The lattice constants corresponding to it have the following values: $a = 4.321\sqrt{3} = 7.484(\pm 0.002)$ kX, $c = 3.643 \cdot 6 = 21.861(\pm 0.006)$ kX, $c/a = 2.921$. The observed line intensities

TABLE 4. X-ray Powder Pattern of the Compound $HfBe_2$. Cr—K radiation*

hkl	$\sin^2\vartheta$ meas	$\sin^2\vartheta$ calc**	Intensity meas	Intensity calc.	hkl	$\sin^2\vartheta$ meas	$\sin^2\vartheta$ calc**	Intensity meas	Intensity calc.
100	0,123	0,122	20	50,4	002	0,524	0,525	5	5,8
001	0,131	0,131	5	14,7	201	0,629	0,629	30	33,4
101	0,256	0,254	35	59,4	102	0,648	0,647	30	31,0
110	0,367	0,367	15	19,8	210	0,855	0,855	40	45,4
200	0,488	0,489	10	14,6	112	0,890	0,891	50	64,5
111	0,498	0,498	25	26,8	211 α_1	0,993	0,990	100	308,0

*Only the α (or α_1) lines are given.
**$\sin^2\vartheta = C[\frac{1}{3}(h^2 + k^2 + hk) + 1.430\, l^2]$, where $Q = 0.03175$ (α line) or 0.03159 (α_1).

TABLE 5. Interatomic Distances d in the Structure of $HfBe_2$

Atoms	d, kX	Coordination numbers
Hf — 12 Be	2,689	20
2 Hf	3,157	
6 Hf	3,775	
Be — 3 Be	2,179	9
6 Hf	2,689	
2 Be	3,157	

The interatomic distances in the $HfBe_{12}$ structure are given in Table 7.

The x-ray pattern of the alloy with 7.74 at. % (62.5 wt. %) of Hf contains about 50 lines, which do not include $HfBe_5$ or $HfBe_{12}$ lines (Table 8). The microhardness of H_μ of the principal component of the alloy with (1035 kg/mm²) differs from H_μ of the other compounds. The composition of the alloy, close to $HfBe_{12}$, indicates the possible existence of a compound of the $ThMn_{12}$ type [10]. However, only the strongest lines are also indexed on the basis of the hexagonal unit cell characteristic of the $CaZn_5$ type, with $ca = 4.321$, $c = 3.643$ kX, $c/a = 0.843$. The higher value of c/a in comparison with structures of the $CaZn_5$ type indicates the possible existence of R_2X_{17} structure types (Th_2Ni_{17} [11], Th_2Zn_{17} [12], V_2Zn_{17} [12]), allied to the $ThMn_{12}$ and $CaZn_5$ types. Most of the lines can be indexed if structures of the Th_2Ni_{17} and Th_2Zn_{17} types are assumed. All the lines are indexed on the basis of the U_2Zn_{17} types only (Table 8). The lattice constants corresponding to it have the following values: $a = 4.321\sqrt{3} = 7.484(\pm 0.002)$ kX, $c = 3.643 \cdot 6 = 21.861(\pm 0.006)$ kX, $c/a = 2.921$. The observed line intensities are in good agreement with the calculated values ($I = S^2_{\varphi} \cdot 10^{-5}$) for a structure of the U_2Zn_{17} type (space group $C6m_3 - D^1_{3h}$; constants taken the same as for U_2Zn_{17} [12]):

2 $Hf^{(1)}$ in 1 (*d*), 1 (*c*);
2 $Hf^{(2)}$ in 1 (*c*), 1 (*f*);
8 $Hf^{(3)}$ in 2 (*g*) $z = 1/8$, 2 (*g*) $z = 1/3$, 2 (*h*) $z = 1/3$, 2 (*i*) $z = 1/8$;
36 $Be^{(1)}$ 6 (*l*) $x = 1/2$, $y = 0$; 6 (*m*) $x = 1/2$, $y = 0$;
12 (*o*) $x = 1/2$, $y = 0$, $z = 1/8$; 12 (*o*) $x = 1/2$, $y = 0$, $z = 1/3$;
36 $Be^{(2)}$ in 6 (*n*) $x = 1/2$, $z = 1/12$; 6 (*n*) $x = 1/2$, $z = 5/12$;
6 (*n*) $x = 1/6$, $z = 1/4$; 6 (*n*) $x = 1/6$, $z = 5/24$;
6 (*n*) $x = 5/6$, $z = 1/12$; 6 (*n*) $x = 5/6$, $z = 7/24$;
18 $Be^{(3)}$ in 6 (*n*) $x = 1/2$, $z = 1/4$; 6 (*n*) $x = 1/6$, $z = 1/12$;
6 (*n*) $x = 5/6$, $z = 5/12$;
12 $Be^{(4)}$ in 2 (*g*) $z = 0.049$; 2 (*g*) $z = 0.451$; 2 (*h*) $z = 0.118$;
2 (*h*) $z = 0.784$; 2 (*i*) $z = 0.284$; 2 (*i*) $z = 0.618$

Therefore the compound in the alloy with 7.74 at. % Hf has a structure of the U_3Zn_{17} type, and its composition is represented by the formula Hf_3Be_{17}.

The interatomic distances in the Hf_3Be_{17} structure are given in Table 9.

Alloys with 16.80 and 10.50 at. % (80.0 and 70.0 wt. %) of Hf consist of $HfBe_5$ and Hf_3Be_{17}.

TABLE 6. X-ray Powder Pattern of the Alloy $Hf_{2.9}Be_{14.1}$ ($HfBe_5$ + $HfBe_2$). Cr–radiation.

hkl	$\sin^2\vartheta$ meas	$\sin^2\vartheta$ calc**	Intensity meas***	Intensity calc.	hkl	$\sin^2\vartheta$ meas	$\sin^2\vartheta$ calc**	Intensity meas***	Intensity calc.
100	0,087	0,085	5	43,0	102	0,520	0,521	3	7,1
001	0,100	0,100	2	11,3	210	0,596	0,595	4	6,6
101	0,185	0,184	5	20,4	112	0,699	0,692	5	8,0
110	0,255	0,255	4	10,6	211	0,707	0,705	7	15,4
200	0,340	0,340	3	7,9	300	0,766	0,766	2	4,3
111	0,265	0,265	4	13,5	202	0,775	0,776	6	9,5
002	0,434	0,435	1	2,1	301	0,874	0,876	6	14,3
201	0,450	0,449	3	6,9					

*Only the α lines of $HfBe_5$ are given.

** $\sin^2\vartheta = 0{,}0\,\left[\frac{4}{3}(h^2+k^2+hk) + 1{,}762\,l^2\right]$.

***The intensities are assessed on a seven-point scale; from the intensities of the 110, 111, and 211 lines the intensities of the 101, 110, and 210 α lines of the compound $HfBe_2$, which coincide with them, have been substracted.

TABLE 7. Interatomic Distances (d, kX) and Coordination Numbers (c.n.) in the $HfBe_5$ structure.

	Hf		Be(1)		Be(2)		Total c.n.
	c.n.	d	c.n.	d	c.n.	d	
Hf	2	3,46	6	2,61	12	2,85	20
Be(1)	3	2,61	3	2,61	6	2,17	12
Be(2)	4	2,85	4	2,17	4	2,26	12

DISCUSSION OF RESULTS

The results of these determinations of the crystal structures of hafnium–beryllium compounds indicate that the Hf–Be system is very close in the crystal-chemical sense to the Zr–Be system. In the latter system four compounds were known, and the structure type has been determined for two of them: $ZrBe_2$ (AlF_2 type) [6] and $ZrBe_{13}$ ($NaZn_{13}$ type) [4]. During the preparation of this paper we became acquainted with a new investigation [13] in which the compositions and structures of the remaining compounds were determined; these were $ZrBe_5$ ($CaZn_5$ type) and Zr_2Be_{17} (Nb_2Be_{17} type*). Therefore the compounds of the Hf–Be system do not differ in composition from the corresponding compounds of the Zr–Be system. Three of the hafnium compounds are isostructural with the zirconium compounds, and one (Hf_2Be_{17}) is structurally related to the zirconium compound. It is interesting to compare the lattice constants of the compounds of the two systems (Table 10). It is found that the lattice constants of hafnium–beryllium compounds are in every case less than the constants of the zirconium compounds. The decrease of the constant when Zr is replaced by Hf, due to the decrease of the atomic radius ($r_{Zr} = 1{,}60$, $r_{Hf} = 1{,}59$ [7c]), is found in compounds of these elements with cV, Cr, Mo, W, Co[15], Si[16], B, C, N, [2] and F [7d]; it is not found only in compounds of Zr and Hf with Ge [17] and O [7e].

There is also a crystal-chemical analogy between the Hf–Be and Th–Ni systems; the latter includes compounds of the types AlB_2 ($ThNi_2$), $CaZn_5$ ($ThNi_5$) and Th_2Ni_{17} (Th_2Ni_{17}) [11]. The existence of a compound of the $NaZn_{13}$ type in the Hf–Be system brings it close to the systems Ce–Be, Th–Be, U–Be [4].

*The Nb_2Be_{17} structure type [14] is identical to the Th_2Zn_{17} type [12]; by adding 00½ to the coordinates of the Nb_2Be_{17} atoms and altering the constants slightly we obtain the coordinates of the atoms in the Th_2Zn_{17} structures.

TABLE 8. X-ray Powder Pattern of the Compound Hf_2Be_{17} (in alloy $Hf_{7.71}Be_{92.29}$). Cr–K radiation*

hkl			$\sin^2\Theta$		Intensity	
type U_2Zn_{17}	type Th_2Zn_{17}	type $CaZn_5$	meas.	calc.**	meas.	calc.
101	—	—	—	0,035	0	1,4
102	011	—	0,042	0,042	20	4,3
103	—	—	0,056	0,056	20	5,7
104	102	—	0,077	0,075	20	4,3
110	110	100	0,003	0,003	70	30,2
006	003	001	} 0,096	0,008	} 30	11,8 } 13,2
105	—	—		0,099		1,4
201	—	—	—	0,127	0	1,2
202	201	—	0,136	0,136	10	3,7
203	—	—	0,148	0,149	5	4,9
107	—	—	—	0,165	0	1,4
204	022	—	0,166	0,168	10	3,8
116	113	101	0,191	0,190	100	60,0
205	—	—	—	0,193	0	1,3
108	014	—	0,204	0,206	15	8,3
211	—	—	—	0,221	0	2,2
212	121	—	0,228	0,229	10	6,5
213	—	—	0,244	0,242	15	8,6
109	—	—	0,249	0,253	5	5,3
207	—	—	—	0,258	0	1,3
21·	212	—	0,262	0,262	10	6,6
3	300	110	0,278	0,280	50	32,2
2 ·	—	—	—	0,286	0	2,3
208	204	—		0,309		3,7 } 7,5
1, 0, 10	105	—	} 0,301	0,304	} 5	3,8
209	—	—	0,348	0,346	5	4,8
217	—	—	—	0,352	0	2,3
1, 0, 11	—	—	—	0,362	0	0,9
220	220	200	0,375	0,374	20	31,7
306	303	111	0,377	0,379	80	63,9
218	124	—		0,393		6,7 } 18,7
0, 0, 12	006	002	} 0,393	0,394	} 20	12,0
2, 0, 10	025	—	—	0,396	0	1,0
311	—	—	—	0,407	0	1,8
312	311	—	0,414	0,415	5	5,3
313	—	—		0,429		7,3 } 16,1
219	—	—	} 0,434****	0,430	} 15	8,8
314	132	—	0,446	0,449	5	5,6
2, 0, 11	—	—	—	0,455	0	0,8
226	223	201	0,471	0,473	30	28,5
315	—	—	0,475	0,474	5	1,9
1, 1, 12	116	102	} 0,486	0,487	} 30	34,2 } 40,6
2, 1, 10	215	—		0,491		6,4
1, 0, 13	—	—	—	0,493	0	1,0
401	—	—	—	0,501	0	0,8
402	041	—	—	0,509	0	2,5
403	—	—	—	0,522	0	3,4
317	—	—		0,539		1,9 } 4,5
404	402	—	} 0,540	0,541	} 3	2,6
2, 1, 11	—	—	—	0,548	0	1,6
405	—	—		0,566		0,9 } 1,9
1, 0, 14	017	—	} 0,566	0,567	} 3	1,0
318	314	—	0,580	0,580	5	5,8
2, 0, 13	—	—	—	0,586	0	0,9
321	—	—	—	0,594	0	1,5
322	231	—	0,602	0,602	5	4,5
323	—	—		0,615		0,2 } 13,7
319	—	—	} 0,620***	0,626	} 30 ***	7,5

*Only the α lines are given.

**$\sin^2\Theta = 0{,}02335\,[\frac{4}{3}(h^2+k^2+hk)+0{,}11780\,l^2]$.

***The high intensity is due to the presence of a β line at the given angle Θ.

****Band.

TABLE 8 (continued)

hkl			$\sin^2\vartheta$		Intensity	
type U_3Zn_{22}	type Th_2Zn_{17}	type Ca_2Zn_{11}	meas.	calc.**	meas.	calc.
407	—	—	0,635	0,632	30 ***	0,9 5,7
324	322	—		0,635		4,8
1, 0, 15	—	—	—	0,646	0	3,3
410	410	210	0,652	0,654	40	34,1
325	—	—	0,661	0,660	10	1,6 2,5
2, 0, 14	207	—		0,660		0,9
403	0.4	—		0,673	10	2,7 43,1
3, 0, 12	306	112		0,675		40,4
315	—	—	—	0,679	0	1,6 3,4
2, 1, 13	—	—		0,680		1,8
409	—	—	—	0,720	0	3,5
327	—	—	—	0,725	0	1,7
1, 0, 16	108	—	—	0,730	0	2,2
3, 1, 11	—	—	—	0,735	0	1,3
2, 0, 15	—	—	—	0,740	0	3,1
416	413	211		0,752	100	72,0 76,8
2, 1, 14	127	—		0,[illegible]		4,8
328	234	—		[illegible]	80	46,3
2, 2, 12	226	203		[illegible]		42,0
4, 0, 10	405	—	—	0,771	0	0,7
501	—	—	—	0,781	0	0,6
502	501	—	—	0,789	0	2,0
503	—	—	—	0,801	0	2,7
329	—	—	0,815	0,813	10	6,7
1, 0, 17	—	—	—	0,821	0	0,7
504	052	—	0,821	0,822	10	2,1 4,2
2, 0, 16	028	—		0,824		2,1
4, 0, 11	—	—	—	0,830	0	0,6
2, 1, 15	—	—	0,838	0,[illegible]	30	5,8 26,2
330	330	300		0,840		20,4
505	—	—	—	0,846	5***	0,7
3, 2, 10	325	—	0,866	0,[illegible]	60***	4,9 6,4
3, 1, 13	—	—		0,867		1,5
421	—	—	—	0,874	0	1,2
422	421	—	0,885	0,882	20	3,7 14,0
0, 0, 0, 18	009	003	—0,892****	0,885		5,3
423	—	—		0,895		5,0
507	—	—		0,910		0,7
2, 0, 17	—	—	0,910—	0,915	20	0,6 9,2
424	242	—	—0,918****	0,916		3,9
2, 11, 16	218	—		0,918		4,0
3, 2, 11	—	—	—	0,922	0	1,2
336	333	301	0,930	0,938	100	13,0 48,6
425	—	—		0,940		1,3
3, 11, 14	317	—		0,941		4,3
508	504	—	0,951	0,953	10	1,8
4, 0, 13	—	—	—	0,960	0	0,7
511	—	—	—	0,966	0	1,2
512	151	—	0,975	0,975	15	3,5
1, 1, 18	119	103	0,980	0,980	80	33,4

*Only the α lines are given.

**$\sin^2\vartheta = 0.02335[\frac{4}{3}(h^2 + k^2 + hk) + 0.117801^2]$.

***The high intensity is due to the presence of a β line at the given angle θ.

****Band.

TABLE 9. Interatomic Distances (d, kX) and Coordination numbers (c.n.) in the Hf_2Be_{17} Structure

	Hf		$Be^{(1)}$		$Be^{(2,3)}$		$Be^{(4)}$		Total c.n.
	c.n.	d	c.n.	d	c.n.	d	c.n.	d	
$Hf^{(1)}$	2	3,67	3	2,50	12	2,82	—	—	20
$Hf^{(2)}$	—	—	6	2,50	12	2,82	2	2,58	20
$Hf^{(3)}$	1	3,67	6	2,50	12	2,82	1	2,58	20
$Be^{(1)}$	2	2,50	3	2,50	6	2,21	2	2,71	13
$Be^{(2)}$	3	2,82	4	2,21	4	2,16	1	2,29	12
$Be^{(3)}$	2	2,82	4	2,21	4	2,16	2	2,29	12
$Be^{(4)}$	1	2,58	6	2,71	6	2,29	1	2,14	14

The compounds $HfBe_5$, Hf_2Be_{17} and $HfBe_{13}$ belong to the class of intermetallic compounds with close packing of atoms of unequal sizes and with high coordination numbers [18, 19]. The formation of compounds of this class in the Hf–Be system is due to the metallic character of the components, while their composition (high contents of the component with the smaller atomic radius) is the consequence of the relatively high ratio of the atomic radii ($k = 1.41$).

TABLE 10. Lattice Constants of Compounds in the System Zr–Be and Hf–Be (in A)

R	RBe_2	RBe_5	R_2Be_{17}	RBe_{13}
Zr	a 3,82 c 3,24 c/a 0,847	4,564 3,485 0,764	7,548 10,997 1,457	10,047 — —
Hf	a 3,783 c 3,163 c/a 0,836	4,534 3,471 0,765	2.10,952 7,499 2.1,460	10,005 — —

Comparison of interatomic distances in the structures of Hf–Be compounds shows that with increasing beryllium content the distance between the beryllium atom decreases (the minimum distance is 2.179 in $HfBe_2$, 2.17 in $HfBe_5$, 2.14 in Hf_2Be_{17}, and 2.07 in $HfBe_{13}$), while the distance between the Hf atoms increases.

The work was carried out with the assistance of V. P. Vinokurov.

SUMMARY

The system Hf–Be was investigated by x-ray structural and microstructural analysis and by determinations of microhardness. The existence of four compounds was established:

$HfBe_2$, type AlB_2, $a = 3.775 \pm 0.002$, $c = 3.157 \pm 0.001$ kX, $c/a = 0.836$; $H\mu = 980$ kg/mm²;
$HfBe_5$, type $CaZn_5$, $a = 4.525 \pm 0.010$, $c = 3.464 \pm 0.010$ kX, $c/a = 0.765$; $H\mu = 1340$ kg/mm²;
Hf_2Be_{17}, type U_2Zn_{17}, $a = 7.484 \pm 0.002$, $c = 21.361 \pm 0.006$ kX, $c/a = 2.921$; $H\mu = 1085$ kg/mm²;
$HfBe_{13}$, type $NaZn_{13}$, $a = 9.935 \pm 0.002$ kX; $H\mu = 1200$ kg/mm².

LITERATURE CITED

1. F. W. Glaser, B. Post, J. Metals, 5, 9, Sect. 1, 1117 (1953).
2. F. W. Glaser, D. Moskowitz, B. Post, J. Metals, 5, 9, Sect. 1, 1119 (1953).
3. H. H. Hausner, H. S. Kalish, J. Metals, 2, 1, 59 (1950).
4. N. C. Baenzinger, R. W. Rundle, Acta crystallogr., 2, 258 (1949).
5. E. Zintl, W. Haucke, Z. Elektrokem 44, 104 (1938).

6. J. W. Nielsen, N. C. Baenziger, Acta crystallogr., 7, 132 (1954).
7. G. B. Bokii, Introduction to Crystal Chemistry (in Russian) (Izd. MGU, 1954), a) p. 323; b) p. 109; c) P. 258; d) p. 400; e) P. 367.
8. E. S. Makarov, Kristallografiya, 3, 1, 5 (1958).
9. W. Haucke, Z. anorgan. und allgem. Chem., 244, 17 (1940).
10. J. V. Florio, R. E. Rundle, A. I. Snow, Acta crystallogr., 5, 449 (1952).
11. J. V. Florio, N. C. Baenziger, R. E. Rundle, Acta crystallogr., 9, 367 (1956).
12. E. S. Makarov, S. I. Vinogradov, Kristallografiya, 1, 6, 631 (1956).
13. A. Zalkin, R. G. Bedford, D. E. Sands, Acta crystallogr., 12, 9 700 (1959).
14. A. Zalkin, D. E. Sands, O. H. Krikorian, Acta Crystallogr., 12, 9, 713 (1959).
15 R. P. Elliott, W. Rostoker, Trans. Amer. Soc., Metals 50 617 (1958).
16. P. G. Cotter, J. A. Kohn, R. A. Potter, J. Amer. Ceram. Soc., 39, 1, 11 (1956), cited through Met. Abstr., 24, 569 (1956/57).
17. J. F. Smith, D. M. Bailey, Acta crystallogr., 10, 4, 341 (1957).
18. P. I. Kripyakevich, Kristallografiya, 5, 1, 79 (1960).
19. P. I. Kripyakevich, Dokl. AN SSSR, 85, 2, 321 (1952).

All abbreviations of periodicals in the above bibliography are letter-by-letter transliterations of the abbreviations as given in the original Russian journal. *Some or all of this periodical literature may well be available in English translation.* A complete list of the cover-to-cover English translations appears at the back of this issue.

ELECTRON DIFFRACTION STUDY OF THE CRYSTAL STRUCTURES OF INTERNAL COMPLEX NICKEL AND COPPER COMPOUNDS OF SALICYLALIMINE AND ITS DERIVATIVES

G. N. Tishchenko, P. M. Zorkii, and M. A. Poraĭ-Koshits

M. V. Lomonosov Moscow State University

Translated from Zhurnal Strukturnoĭ Khimii, Vol. 2, No. 4,
pp. 434-441, July-August 1961
Original article submitted March 5, 1960

The crystal structure of copper and diamagnetic nickel internal complex compounds of salicylaliimine, 5-bromosalicylalimine, and 4-methylsalicylalimine has been studied by the electron diffraction method. The cell constants and space groups have been determined. All the pairs of corresponding copper and nickel compounds were isostructural. Structure models have been derived by geometrical analysis and confirmed by Patterson projections. The structure found for the salicylaliminates is in good agreement with the results obtained by Stewart and Lingafelter by complete x-ray structural investigations of these crystals. The structures of salicylaliminate and 5-bromosalicylaliminate exhibit anomalous closeness of the molecules in layers (especially in the latter case). A possible cause of this is formation of intermolecular metal–oxygen bonds with augmentation of the coordination polyhedron of the metal atom to an extremely elongated octahedron. The Ni–O distance is 3.85 A in salicylaliminate, and 3.5$_4$ in 5-bromosalicylaliminate. The molecules of all six substances studied have planar trans structure.

INTRODUCTION

In studies of the stereochemistry of metal complex formers in internal complex compounds, many workers consider the molecule of such a compound in isolation, without any connection with other molecules. Directed intermolecular bonds may be formed in solution and even in the gas phase, to say nothing of solids. This may lead to an increase in the coordination number of the metal atom. Therefore we must distinguish between the molecular coordination number, i.e., the number of bonds formed by a metal atom in an isolated molecule, and the complete coordination number, which may be greater than the molecular number owing to augmentation of the coordination sphere of the metal by atoms of neighboring molecules.

The crystal structure of internal complex compounds in which the molecular coordination number is six or in which the bonds of the metal atom have tetrahedral direction do not exhibit any anomalies. They obey the principles of closest molecular packing, usual for all organic crystals. On the other hand, internal complex compounds, in which the metal bonds are directed along the diagonals of a square, often form structures in which insufficient shielding of the metal by the ligands gives rise to special forms of intermolecular interaction. Because of this, it is necessary to distinguish the crystal chemistry of such compounds as a separate group in organic crystal chemistry, in the same way as crystals with intermolecular hydrogen bonds form a separate group.

Specific intermolecular contacts in crystals of internal complex compounds may be of two kinds. First, they may be metal–metal bonds. Examples of this type of interaction are nickel dimethylglyoximate [1, 2] and copper salicylaliminate [3], in whose crystals the distance between the metal atoms is 3.25 and 3.33 A respectively*. In both cases the metal atoms form infinite chains (perpendicular to the plane layers of molecules), so that the environment of each metal atom is made up to an octahedron by intermolecular interaction. These octahedrons are very elongated, and yet the distances of 3.25 and 3.33 A appear shortened if it is taken into account that the thickness of layers of organic molecules is usually less.

Determination of the positions of metal atoms in nickel acetylacetonate [4] showed that crystals of this compound contain trimers with fairly short Ni–Ni distances (2.72 and 2.98 A) A similar situation is found in nickel salicylaldehydate [5] (the number of molecules in the unit cell is $12 = 3 \times 4$). It is quite possible that in these two cases the dis-

*Stackelberg [3] gives 3.35 for the Cu-Cu distance. However, our refinement based on electron-diffraction data gives the value 3.33 ± 0.01 A.

tances between the metal atoms are so short owing to formation of chemical bonds; however, the possibility of a structure in which one ligand is linked to two different nickel atoms is not excluded.

A second type of known specific intermolecular interaction in crystals of internal complex compounds involves bonding between metal atoms and oxygen atoms of neighboring molecules. A good example of this is the structure of copper dimethylglyoximate [6,7] in which the copper atom leaves the plane of the molecule and forms a bond 2.43 Å long with oxygen of a neighboring molecule; as a result the coordination polyhedron of the metal atom is in the form of a tetragonal pyramid.

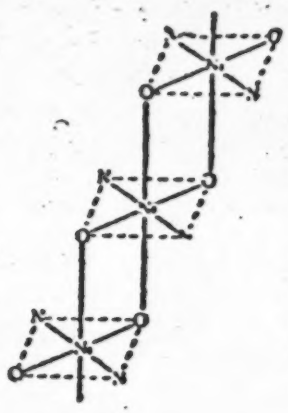

Fig. 1. Diagram representing intermolecular interaction as an explanation of the paramagnetism of one modification of salicylalmethyliminate.

The paramagnetism of one of the modifications of nickel salicylalmethyliminate was recently explained [8] by intermolecular interaction of the metal–oxygen type. The authors of [8] assumed that the coordination sphere of the nickel atom is made up to an octahedron owing to the formation of infinite chains as shown in Fig. 1. It must be pointed out, however, that with such a structure the octahedrons must be very elongated; since the molecules have definite thickness, the length of the intermolecular nickel–oxygen bond must be considerably greater than 3 Å. Such an explanation of the paramagnetism of nickel salicylalmethyliminate therefore incorporates the assumption that even such a long bond can have an appreciable influence on the magnetic properties of the metal atom. The results of our work also lead to the conclusion that the coordination [illegible] of the metal atoms exist in the form of very elongated octahedrons [illegible] our data, the long metal–oxygen intermolecular bonds do not lead to [illegible] changes in the magnetic properties of the substance.

It seems that problems such as those considered above can at [illegible] time be solved conclusively only by means of structure analysis. However, there are various experimental difficulties in the way of structural investigations of crystals of internal complex compounds. One such difficulty is that it is very often difficult to obtain internal complex compounds in the form of fairly large and well-formed single crystals. This difficulty may be surmounted by the use of structural electron diffraction. In the present investigation we applied this method for the first time to establish the structure of internal complex compounds. Structure types were established by means of geometrical analysis based on the principle of closest molecular packing in crystals [9]; this method gives fairly rapid information on the general features of the [illegible] molecular structure of complex compounds.

This paper is the first communication on a series of [illegible]-diffraction [illegible] of the crystals of internal complex compounds. The following questions were considered in the communication:

a) determination of the structure types of crystals of [illegible] and nickel complex compounds,

b) isostructural compounds in the copper and nickel [illegible]

c) relationship between the crystal structure and the [illegible] compounds; an extensive range of compounds with various ligands was studied;

d) structure of the coordination polyhedron [illegible] intermolecular interaction in crystals of internal complex compounds of copper.

Experimental Methods and Results

The nickel (II) and copper (Cu) complexes of salicylal[illegible]imine (II) and 4-methylsalicylalimine (III)

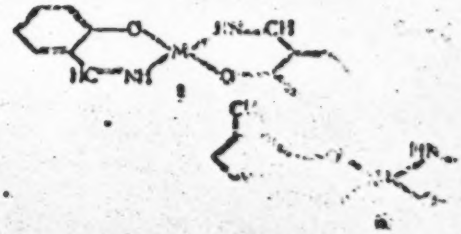

were investigated by electron diffraction. Reports of structural investigations of complexes of (I) have appeared in the literature previously [3, 10, 11]; complexes of (II) and (III) were studied for the first time by us. The substances used in the investigation were provided by L. A. Kazitsina, L. L. Polstyanko, and V. V. Zelentsov (Chemical Faculty of the Moscow State University). The nickel complexes are yellow or yellow-orange, and the copper complexes are green. All the substances studied are soluble in dichloroethane and chloroform, less soluble in benzene and methyl alcohol, highly soluble in pyridine, and insoluble in ligroine and water. The specimens were prepared by evaporation of solutions and the photographs were obtained by transmission. The lattice constants were calculated from the formulas given by Vainshtein [12]. Ammonium chloride or paraffin were used as standards. Point diffraction patterns and direct and "oblique" photographs from the textures were obtained for all six substances. None of these compounds had any tendency to form disordered polycrystals on the support.

All the crystals studied are monoclinic and the respective pairs are isostructural; the lattice constants of the copper and nickel compounds, given in Table 1*, are very close. The densities calculated from our data are close to the values usually found for compounds of this class. The space groups were determined from the systematic extinctions of the reflections. In the cases of II Ni, IICu, IIINi and III Cu the point patterns and direct photographs of the texture contained weak or very weak reflections which were forbidden by the space group; this may be attributed to the dynamic character of the scattering. Our data for the space groups and lattice constants of I Ni and I Cu are in good agreement with earlier data (see Table 1). The similarity of the lattice constants and the identity of the space groups indicate that all the compounds have similar crystal structure.

TABLE 1. Lattice Constants and Symmetry of the Crystals Studied

Substance	a, Å	b, Å	c, Å	β	Unit cell volume, Å³	Number of molecules in cell	Density(calculated), g/cc	Packing density factor	Space group	Literature
I Cu	11.81	5.87	8.09	95°31′	557	2	1.69	0.71	$P2_1/c$	[10]
I Ni	12.96	5.84	8.05	94°33′	607	2	1.68	0.71	$P2_1/c$	[3]
	12.90*	5.85	8.12	95°30′*	610	2	1.67	0.71	$P2_1/c$	[10]
	12.96	5.83	8.11	94°30′	611	2	1.66	0.71	$P2_1/c$	[11]
II Ni	12.93±0.03	5.45±0.01	8.09±0.02	95°57′±5′	566	2	1.77	0.765	$P2_1/c$	Our results
IICu	13.1±0.3	5.39±0.01	8.07±0.02	96°30′±30′	563	2	1.81	0.755	$P2_1/c$	
III Ni	31.6±0.6	5.05±0.01	7.73±0.02	94°35′±10′	1232	4	1.52	0.71	$P2_1/c$	

* Calculated by us from data for another apparatus.

Since the only possible twofold position in the $p\,2_1/c$ space group is at the center of symmetry, we can conclude even from data on symmetry and the number of molecules in the unit cell that the molecules of II Ni and II Cu, like the molecules of I Ni and I Cu, have trans configuration and the bonds formed by the metal atom in the molecule lie in one plane. In the cases of III Ni and III Cu such preliminary data are insufficient for determining the molecular configuration, as the number of molecules in the unit cell is greater than two.

The electron-diffraction data for I Ni and II Ni were used for constructing Patterson projections (the intensities were estimated visually by the multiple-exposure method).

The geometrical analysis was performed with the Kitaigorodskii structure finder [9] with the aid of molecular models made from "elgin" and then coated with collodion. The packings found with the models are illustrated by the photographs in Fig. 2. The models of planar molecules were constructed on the basis of interatomic distances and valence angles found by x-ray structural analysis of nickel salicylaldoximate [13]; in addition, the values given by Kitaigorodskii [9] for interatomic distances and intermolecular radii were used. The results of geometrical analysis with the structure finder were refined by calculation of intermolecular distances with small variations of the molecular rotation angles found; the molecular form established by x-ray investigation of I Ni [11] was used in this refinement.

The packing density factors k are given in Table 1. The value of 0.71 found for I Ni and III Ni is close to the average value of k for molecular crystals. The value of 0.765 calculated for II Ni corresponds to the greatest of the known values of k [9].

*In addition to the modification the constants of which are given in Table 1, another type of structure was detected by electron diffraction in the Cu(II) complex. As the second modification of Cu(II) was observed when the specimen had been prepared from chloroform solution, it is likely that its crystals contain the solvent.

Nickel salicylaliminate (I Ni). In these crystals, as in the crystals of the analogous copper complex I Cu, the metal atoms occupy a twofold position at the centers of symmetry with the coordinates 000,0 ½ ½. Geometrical analysis of crystals of I Cu, isostructural with I Ni, was first performed by Stackelberg [3] on the basis of x-ray diffraction

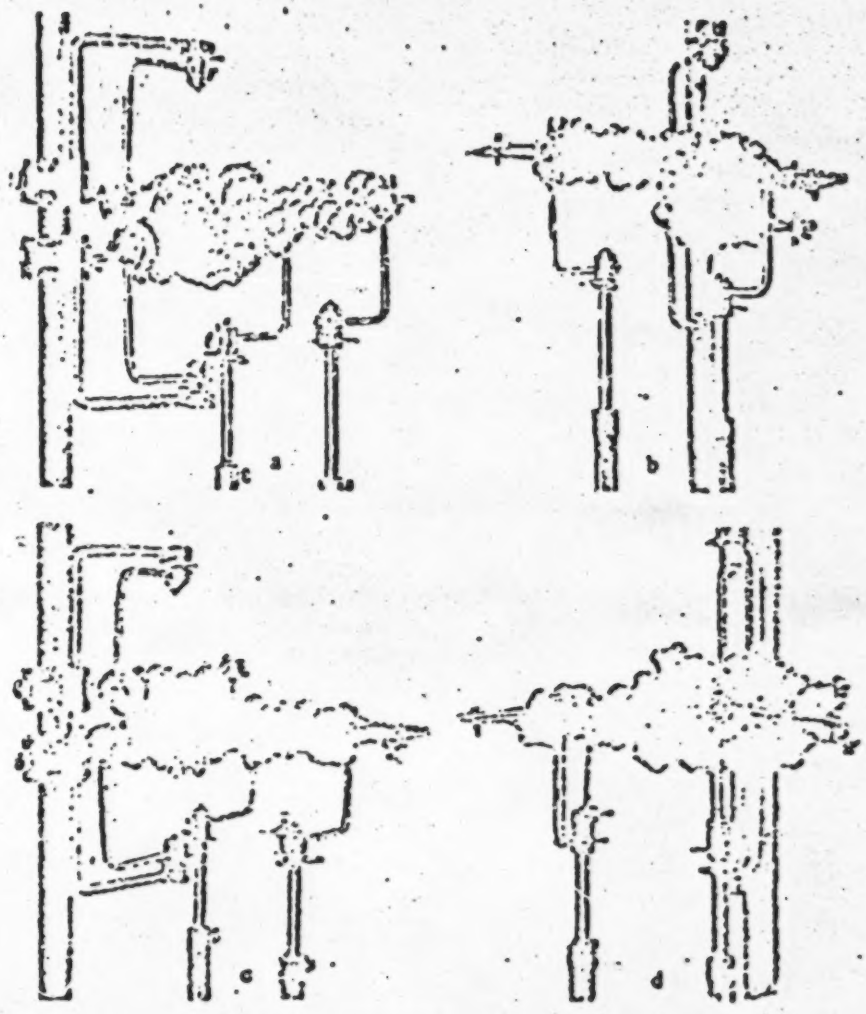

Fig. 2. Packing of molecular models in the structure finder: a and b) nickel salicylaliminate; c and d) nickel 4-methylsalicylaliminate.

data. The general principle of molecular packing was established in his investigation. In particular, it was shown that the molecules, oriented approximately along the x axis by their longest axis, form layers of the 2_1t type in Kitaigorodskii's classification (Fig. 3); these layers are parallel to the Oyz plane. Superposition of these layers in the direction of the x axis gives the period a. However, Stackelberg confined himself to purely qualitative conclusions. While noting that the long axis of the molecule is at a certain angle to the x axis, he does not give even an approximate value for this angle.

The direction of the long axis of the I Ni molecule approximately coincides with the direction of the Ni—C_4 bond (Fig. 4), henceforth termed merely the axis of the molecule. Our geometrical analysis shows that this axis cannot deviate to any significant extent from the xOz plane.

This is to be expected, because rotation of the axis of the molecule the Ni atom of which is at the vertex of the cell (molecule 1) relatively to the xOz plane would cause rotation of the symmetrically bonded molecule with its center at 0½½ (molecule 2), and the latter rotation would be in the opposite direction. This position of the molecules

would decrease significantly the packing density within the layers parallel to the Oyz plane. At the same time, rotation of the axis of the molecule in the xOz plane about the y axis does not lead to a sharp disturbance of the layer packing because in this case the axes of the symmetrically bonded molecules remain parallel after rotation. Therefore, with the molecular axis in the xOz plane, the crystal structure of I Ni can be characterized by two angles: γ_2 between the molecular axis and the z axis, and β_2 between the molecular plane and the xOz plane. The angles between the coordinate axes and the perpendicular to the molecular plane are denoted by α_1, β_1 and γ_1; the angles between the coordinate axes and the molecular plane are given the symbols α_2, β_2 and γ_2. Only three of these six angles are independent; however, the angles α_1, β_1, γ_1 and γ_2 were measured in the structure finder and the angle β_2 was assumed to be 90°. To make measurements and calculations easier, the x axis was replaced by the x' axis, perpendicular to the Oyz plane (conversion to an orthogonal coordinate system). The results are given in Table 2; the angles are measured to an accuracy of 1-2°.

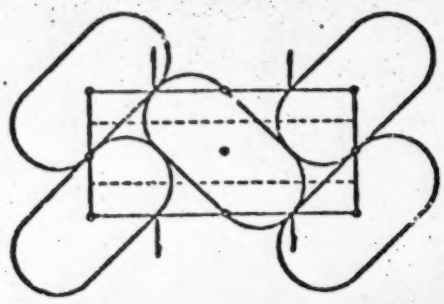

Fig. 3. Packing of molecules in the 2_1 layer.

These values were used for finding the equation of the molecular plane (in normal form, relative to the orthogonal coordinate system):

(1)

With an approximate estimate of the error associated with a priori assumption of the molecular shape, it may be assumed that the atomic coordinates are estimated to an accuracy of 0.1-0.2 A from (1) and the given molecular model. However, such calculations give two series of coordinates, differing in absolute values of x and z and with y coordinates differing in sign. These two series correspond to two possible positions of the molecule in the given plane with the direction of the molecular axis unchanged, i.e., the molecule in a certain position A and the molecule rotated about its axis through 180° from this position (position B). These two structures differ in the character and magnitude of the intermolecular contacts, but are very similar in the configuration of the molecules and

TABLE 2. Angles Characterizing Orientation of the Molecular Planes

Substance	α_1°	β_1°	γ_1°	α_2°	β_2°	γ_2°
I Ni						
our data	71	61	119	29	90	70
data of [11]	70.9	61.0	118.8	29.1	93.6	70.1
II Ni	67	60	121.5	30	90	60

their inclination to coordinate axes. It should be noted that if the molecule had symmetry mmm structures A and B would be identical. The reason for the difference between structures A and B is that the molecule has lower symmetry, namely 2/m. These structures should differ somewhat with regard to favorable packing conditions; however, in view of the fact that the form of the I Ni molecule, when enclosed in a "fur coat" of van der Waals radii, is in the first approximation close to an ellipsoid, these differences are small. It may be postulated theoretically that one of the structures A and B is realized in nature or that these forms represent two modifications which may differ somewhat by their lattice constants. The formation of structures in which some of the molecules occupy position A and others position B (statistical AB structure) is not excluded. However, calculations based on the experimentally determined parameters show that the intermolecular distances are more logical in one of the variants. The more probable structure is A, where the oxygen atom of the molecule with center at 000 has three positive coordinates. The P(Ovw) Patterson projection confirmed the geometrical analysis, but it does not indicate that structure A is preferable, because both possible packing variants (A and B) can be "written into" the system of peaks present in the projections.

The foregoing represents the state of the present investigation at the time of publication of Stewart and Lingafelter's paper [11], which gives an account of a complete x-ray diffraction study of the I Ni structure. The atomic coordinates and electron density projections given by these authors correspond to structure A. They do not discuss the possible existence of structure B or of the statistical structure AB. We used the data in [11] for calculating the angle characterizing orientation of the molecule; the values found are in good agreement with our results (Table 2).

Stewart and Lingafelter do no. give the intermolecular distances calculated with the H atoms taken into account although the coordinates of these atoms are given in their paper. Nevertheless, such analysis is of interest. We found from the data in [11] that the distances between the molecules in the layer are somewhat shortened; the H_3 atom of molecule 2 "climbs" to some extent onto molecule 1 ($H_3 \ldots C_4 = 2.64$ A, $H_3 \ldots C_3$ and $H_3 \ldots C_2 = 2.70$ A, and the sum of the H and C intermolecular radii is 2.89 A). The distances between the molecular layers exceed the sum of the van der Waals radii ($H \ldots H = 2.34$ A); the shortest distance from molecule 1 to one of the molecules of the neighboring layer is $H_3 \ldots H_6 = 2.36$ A; to the other molecule, it is $H_4 \ldots H_6 = 2.52$ A.

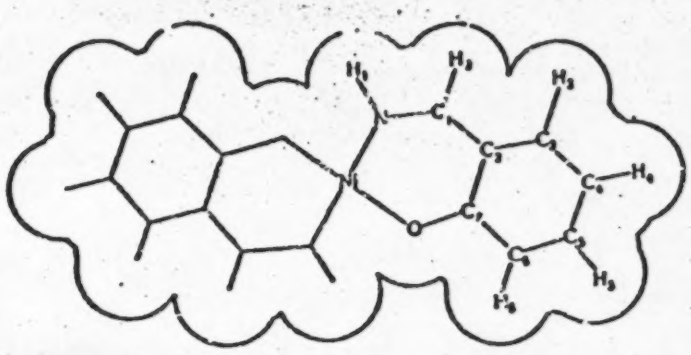

Fig. 4. Model of nickel salicylaliminate molecule.

A characteristic feature of the I Ni structure is that an O atom of a neighboring molecule is located at a distance of 3.85 A from the Ni atom, so that the Ni atom is at the center of a very elongated octahedron. Stewart and Lingafelter consider that this distance is too great to allow for the existence of a bond. However, in view of the rectangular form of this octahedron (its edges are 4.15, 4.20; 4.34 and 4.39 A) and the somewhat anomalous closeness of molecules 1 and 2 to which the Ni and O atoms belong, the existence of a certain, even if weak, additional interaction should not be rejected without proof. It is possible that formation of structure A is associated with the energy gain as the result of such interaction, because such octahedrons do not exist in the B and AB structures.

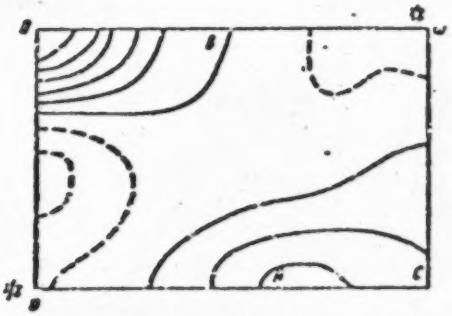

Fig. 5. P(Oyw) projection for nickel 5-bromosalicylaliminate.

Nickel 5-bromosalicylaliminate (II Ni). In the crystals of this compound the Ni atoms also occupy special twofold positions at the centers of symmetry. The similarity between the lattice constants of these two nickel complexes indicates that their structures are very similar. At the same time, the decrease of constant b with c unchanged and with the same positions of the Ni atoms indicates that the molecular packing in the layer should be closer in the case of II Ni. This is consistent with the high value of the packing density factor.

All the symbols used in the geometrical analysis of II Ni are analogous to those used for I Ni. The only exception is that the molecular axis in this case was taken to pass through the bromine atom. It may be pointed out that if the molecular axis had been chosen in the Ni–C_4 direction, as in the case of I Ni, the result would not have been affected significantly, as these directions are very similar. It was also assumed in the case of II Ni that the molecular axis lies in the xOz plane ($\beta_2 = 90°$).

The increase of the constant a (by 2.35 A) over the value for the corresponding constant of I Ni is quite natural because introduction of large Br atoms lengthens the molecule. However, even this increase is not enough to allow the molecules to pack in the unit cell with the same angle γ_2 as in the case of I Ni. This angle decreases to 60°. Therefore in the case of II Ni the molecular layers parallel to the Oyz plane are more "oblique". At the same time the decrease of b leads to a somewhat smaller value of the angle β_2 which is a measure of the inclination of the molecule to the xOz plane. The angles determining the position of the molecule in the cell are given in Table 2. In this case only the angles β_2 and γ_2 were measured in the structure finder, and all the other angles were calculated from them.

Both sides of the molecular layers consist, in their turn, of layers of Br atoms which repeat the centered motif of the Ni atoms in the Oyz plane. The layers are superposed so that each Br atom of one layer fits into the depression between three Br atoms of another layer. It is important to note that with the axis direction chosen for I Ni the monoclinic angle in this case is not 96° as given in Table 1, but 84°.

Calculations of the intermolecular distances showed that in this case too structure A (all three coordinates of the O atom are positive) is clearly more logical than structure B. The distances between the Br atoms of different

layers are 3.7 A, which is close to the sum of the van der Waals radii; in this case there is a small contraction, close to the experimental error. At the same time the intermolecular distance in the layer are considerably shortened ($H_6 \ldots C_1$ = 2.3, $H_4 \ldots C_7$ = 2.4, $H_2 \ldots C_4$ = 2.5, $H_6 \ldots C_5$ = 2.5, $H_4 \ldots C_3$ = 2.7, $H_2 \ldots C_6$ = 2.7, $H_6 \ldots N$ = 2.2 A). This shortening (more considerable than in I Ni) in this case also is manifested by the fact that molecule 2 "climbs" onto molecule 1, while the distances between the molecules translationally bonded along the y axis are close to normal ($C_1 \ldots C_6$ = 3.35 A). Attempts to find a packing variant with less shortening of the intermolecular distances for the given lattice constants were unsuccessful. As in the case of I Ni, the explanation of this compaction of the molecules in the layer parallel to Oyz may be sought in the formation of Ni...O intermolecular bonds. The length of these bonds is 3.5$_4$ A. The extended octahedron which results has fairly regular form; its edges are 3.8; 3.8; 4.1; 4.1 A.

As II Ni showed a strong tendency to form single crystals on the support, we did not succeed in obtaining diagrams from textures without azimuthal orientation. In view of the low accuracy in estimates of the reflection intensities in such patterns, it was difficult to expect anything from the Patterson projection beyond confirmation in principle that the geometrical analysis is correct. The P(Oyz) projection contains, in addition to a trivial maximum at the coordinate origin, a very strong A peak (Fig. 5); the elongated form of the A and zero peaks suggests the existence of B and C peaks hidden in the slopes of the first two maxima. With the atomic coordinate $z_{Br} \approx 3.1$ A, found by geometrical analysis, the independent region of the projection should in the first instance contain peaks with the coordinates 0, 0.23; 0.5, 0.5; 9.5, 0.27, due to Br—Br vectors. It may be assumed that Fig. 5 is not at variance with this.

Nickel 4-methylsalicylaliminate (III Ni). In contrast to the two substances described above, this compound gives crystals with four molecules in the unit cell. Nevertheless, the closeness of constants b and c to the corresponding constants of the structures described above, while a is almost doubled, suggests that in this case also the structure type does not differ significantly from that found for I Ni and II Ni. This is possible if the Ni atoms are situated in two twofold special positions at the centers of symmetry, i.e., if they occupy positions with coordinates: (a) 000, $\frac{1}{2}\frac{1}{2}$ 0 and (d) $\frac{1}{2}$ 0 $\frac{1}{2}$, 0 $\frac{1}{2}$ $\frac{1}{2}$. It follows that molecules of III Ni, like the molecules of the other compounds investigated in the present work, have a planar arrangement of the metal-atom bonds and trans- configuration.

A consequence of the change of the glide direction of the plane of symmetry is that in this structure molecules 1 and 2 are symmetrically independent. At the same time, the nature of the molecular packing in the layer should remain unchanged. The difference between the layers of this structure and the layers in I Ni and II Ni may lie in different angles between molecules 1 and 2. Using the second alternative, we found with the aid of the structure finder a molecular packing in the layer which appears quite logical.

The superposition of layers in this structure differs from the packing motif of the layers in the two structures described above. In the present instance two layers are superposed so that a symmetry plane with gliding along the x axis is formed. The period a results from the superposition not of one but of two symmetrically bound layers. Apparently the monoclinic angle in this case, as in the case of II Ni, with the axes chosen is actually 79.5° and not 100.5°.

The proposed structure accounts for the presence of extinctions at h = 2 n among the hol reflections, and for the low intensity of the l = 2 n reflections.

Exact geometrical analysis of these crystal structures is greatly complicated by the presence of two independent systems of molecules and the indefinite positions of the H atoms of the methyl groups; therefore such analysis was not performed. It can only be stated that the angle β_1 is almost unchanged in comparison with I Ni, while angle γ_2 is increased considerably. The oxygen atom of molecule 2 is so located that in this case a bond with the Ni atom of molecule 1 (structure 2 is also probably formed. Therefore in these crystals too the Ni atoms are at the centers of elongated octahedrons. The possibility of structure B does not arise in this case because of the considerable deviation of the molecular form from mmm symmetry.

Discussion of Results

Klemm and Raddatz [14] reported the preparation of two diamagnetic modifications of I Ni: an unstable yellow-green and a stable orange-red form; the trans configuration is ascribed to the former, and the cis configuration to the latter. Our results do not confirm these data: our yellow-orange stable form of I Ni undoubtedly has trans configuration. The literature does not contain a single definite proof of the existence of trans configuration in planar four-coordinated internal complexes, apart from cases in which the structure of the molecule is such that the trans form cannot exist (for example, the molecule of copper salicylalethylenediaminate). All the complexes studied by us also have planar trans structure.

Octahedral nickel complexes are usually paramagnetic. The diamagnetism of I Ni has been repeatedly confirmed in the literature [15, 16, 17]. II Ni and III Ni are also diamagnetic [18]. Nevertheless, the results of our investigation give reason to believe that owing to intermolecular interaction the copper and nickel atoms in these complexes have coordination polyhedrons in the form of very elongated octahedrons. Apparently in this case the length of the metal—oxygen intermolecular bond is too great (over 3.5 A) to have a significant influence on the magnetic properties of the metal atom. Nevertheless, it is this bond which appears to be the cause of anomalously close packing of the molecules in the layer, which is especially prominent in II Ni and II Cu. It is interesting to note that in the crystals of these two compounds there are, in addition to regions of overlapping of the van der Waals spheres, considerable vacant spaces between the Br atoms.

As the molecules of I Ni, I Cu, II Ni, II Cu are close to ellipsoidal in form, we considered the possibility of polymorphism due to rotation of these molecules about their axes. However, the corresponding modifications were not found. A possible cause of the stabilization of only one of the possible modifications is formation of intermolecular metal—oxygen bonds. Such polymorphism appears possible in the crystallization of substances the molecules of which have mmm pseudosymmetry, in absence of specific intermolecular interactions.

LITERATURE CITED

1. L. Godicky, R. Rundle, Acta crystallogr., 6, 487 (1953).
2. P. M. Zorkii, M. A. Porai-Koshits, Dokl. AN SSSR, 138, 2, 355 (1961).
3. M. Stackelberg, Z. anorgan. Chem. 253, 136 (1947.)
4. G. J. Bullen, Nature, 177, 537 (1956).
5. F. K. C. Lyle, B. Morosin, E. C. Lingafelter, Acta crystallogr., 12, 938 (1959).
6. E. Fraston, R. Zanetti, R. Radi, S. Bezzi, G. Giacometti, J. Inorg. and Nucl. Chem., 8, 452 (1958).
7. E. Frasson, R. Bardi, S. Bezzi, Acta crystallogr., 12, 201 (1959).
8. C. M. Harris, S. L. Lenzer, R. L. Martin, Austral J. Chem., 11, 3, 331 (1958).
9. A. I. Kitaigorodskii, Organic Chemical Crystallography [in Russian] (Izd. AN SSSR, Moscow, 1955).
10. S. H. Simonsen, C. E. Pfluger, Acta crystallogr., 10, 471 (1957).
11. J. M. Stewart, E. C. Lingafelter, Acta crystallogr., 12, 812 (1959).
12. B. K. Vainshtein, Structure Determination by Electron Diffraction [in Russian] (Izd. AN SSSR, Moscow, 1956).
13. L. Merritt, C. Guare, A. Lessor, Acta Crystallogr., 9, 253 (1956).
14. W. Klemm, K.-H. Raddatz, Z. anorgan. und allgem. Chem., 250 207 (1942).
15. J.-N. Tyson, S. C. Adams, J. Amer. Chem. Soc., 62, 1228 (1910).
16. H.-S. Frenck, M.-Z. Magel, E. Sheffield, J. Amer. Chem. Soc., 64, 1924 (1942).
17. J.-B. Willis, D.-P. Mellor, J. Amer. Chem. Soc., 69, 1237 (1947).
18. V. V. Zelentsov, L. A. Savich, V. B. Evdokimov, Nauchn. dokl. vyssh. shkoly. Khimiya i khim. tekhnol., 4, 672 (1959).

All abbreviations of periodicals in the above bibliography are letter-by-letter transliterations of the abbreviations as given in the original Russian journal. *Some or all of this periodical literature may well be available in English translation.* A complete list of the cover-to-cover English translations appears at the back of this issue.

CUBIC PHASES OF VANADIUM CARBIDES

S. I. Alyamovskii, P. V. Gel'd, and I. I. Matveenko

Institute of Chemistry, Ural Branch of the Academy of Sciences USSR, Sverdlovsk
Translated from Zhurnal Strukturnoi Khimii, Vol. 2, No. 4,
pp. 445-448, July-August 1961
Original article submitted August 2, 1960

The data of Gurevich and Ormont [1] on the existence of two higher cubic carbides, δ and ε, in addition to the hexagonal γ phase in the V–C system were confirmed. The concentration regions of stability of the δ phase ($VC_{0.63}$–$VC_{0.79}$) and the ε phase ($VC_{0.79}$–$VC_{0.92}$) were determined more precisely. It is suggested that ε carbides of the composition $VC_{>0.92}$ are unstable. Cubic vanadium carbides are shown to be defective in the carbon sublattice. It is also suggested that in high-carbon phases there is also a slight degree of defectiveness in the vanadium sublattice.

There have been numerous studies of the phase diagram and the structural characteristics of the phase components of the V–C system; a detailed review and critical analysis is given in the paper by Gurevich and Ormont [1]. Without discussing earlier investigations, we shall note only the most significant results in the papers [1,2].

According to Schonberg [2], two carbide phases, V_2C and VC, exist in the V–C system in addition to the solid solution of carbon in vanadium. The lower carbide V_2C, characterized by a hexagonal unit cell, has a fairly wide homogeneity region (from $VC_{0.37}$ to $VC_{0.53}$); the lattice constants vary with composition from $a = 2.875$; $c = 4.538$ kX($VC_{0.37}$) to $a = 2.900$; $c = 4.503$ kX. The lattice constant of the higher carbide with a structure of the NaCl type rises steadily in the one-phase region ($VC_{0.75}$–$VC_{0.93}$) from $a = 4.128$ to 4.174 kX. According to a number of investigators [3,4] Schonberg's data on the structural properties of vanadium carbides are fairly reliable and can be used for construction of the phase diagram of the V–C system.

However, Gurevich and Ormont [1] cast doubts on Schonberg's data with regard to high-carbon products. Their careful investigations showed, in good agreement with Schonberg's data, that the solubility of carbon in metallic vanadium does not exceed 1 at. % (α phase), while the lower hexagonal carbide (γ phase) is stable in the composition range from $VC_{0.43}$ ($a = 2.970$; $c = 4.546$ kX) to $VC_{0.53}$ ($a = 2.894$; $c = 4.572$ kX). With regard to the higher carbide, it was found that, despite the data of all earlier authors (including Schonberg), two cubic phases (δ and ε), continuous with each other, exist in the V–C system. The δ phase is stable in the concentration range from $VC_{0.63}$ ($a = 4.113$ kX) to $VC_{0.93}$ ($a = 4.130$ kX). The homogeneity limits of the ε phase are wider: from $VC_{0.93}$ ($a = 4.150$ kX) to $VC_{0.96}$ ($a = 4.160$ kX). The transition from the δ to the ε phase is accompanied by an abrupt change of lattice constant (~0.020 kX) while the composition remains almost unchanged.

Thus, there are considerable contradictions with regard to the stability region, the number of cubic phases, and the dependence of their lattice constants on composition. The nature of these phases with respect to formation of their crystal lattices is not clear either. In the first approximation it may be assumed that samples of the cubic phase of composition $VC_{<0.88}$ have vacant sites in the carbon sublattice, as was pointed out by Maurer et al. [5]. However, comparison of the x-ray and experimental densities given in [1, 5, 6] give rise to doubts concerning the reliability of the suggestions in [5], since the pycnometric densities are found to be about 5-10% lower than the x-ray values.

All these facts prompted an additional investigation, the results of which are given in this communication.

Starting Materials and Methods of Investigation

Carbide samples of different compositions were synthesized by sintering of briquetted mixtures of powdered vanadium hydride with spectroscopically pure graphite in a vacuum high-frequency induction furnace at 1600-1750°. Vanadium hydride was prepared from metal made by reduction with carbon or calcium. The metal shavings were hydrogenated for 2 hours at $p_{H_2} = 1$ atm and 850°. The lattice constant of the original metal was 3.020 kX, indicating a low oxygen content (<0.01 at. %) [7]; this is also confirmed by the high plasticity of the material. The carbides were sintered for 40-70 hours, and rebriquetted two or three times during the process. The samples were cooled in the

furnace for about 30 minutes. X-ray diffraction tests were performed after each operation. Constancy of the lattice periods and sharpness of the lines in the x-ray patterns were taken as the criteria of equilibrium in the system.

The x-ray investigation was performed with CrK_α radiation in a Debye camera 143.3 mm in diameter. The error in the determination of the lattice constant did not exceed 0.001 kX. The densities of the samples were measured by the vacuum-pycnometeric method with kerosene and decalin as the liquids. The error in the density determinations was about 0.7%.

The vanadium content of the carbides was determined volumetrically, while total and free carbon were determined by the gravimetric method. The accuracy of determination of x in the formula VC_x was about 0.02. Analysis of the samples showed that the oxygen content was less than should correspond to the oxycarbide $VC_x = O_{0.03}$.

Results of the Investigation.

Since the results of earlier investigations of the properties of the lower carbide are in fair agreement, the main object of the present investigation was to study cubic carbides. The total number of samples synthesized was 17, containing from 10.93 to 25.73% of carbon by weight ($VC_{0.52}$–$VC_{1.47}$). The results obtained in x-ray diffraction studies of these samples are given in Table 1 and in the figure.

In agreement with the data of earlier workers, the sample with the empirical composition $VC_{0.52}$ consisted of two phases. It contained a hexagonal V_2C phase with lattice constants $a = 2.901$; $c = 4.570$, and the cubic δ carbide with $a = 4.117$ kX, in good agreement with [1].

TABLE 1. Lattice Constants, X-ray Densities d_x, and Pycnometric Densities d_{meas}, of Cubic Vanadium Carbides

Empirical formula	Phase composition	Lattice constant a, kX	d_x, g/cc	d_{meas}, g/cc	$\frac{d_x - d_{meas}}{d_x} \cdot 100$	Empirical formula	Phase composition	Lattice constant a, kX	d_x, g/cc	d_{meas}, g/cc	$\frac{d_x - d_{meas}}{d_x} 100$
		δ 4,117				$VC_{0.87}$	»	4,146	5,61	—	—
$VC_{0.52}$	γ + δ	γ $\begin{cases} a = 2,901 \\ c = 4,570 \end{cases}$	—	—	—	$VC_{0.91}$	»	4,150	5,60	5,57	0,5
$VC_{0.63}$	δ	4,119	5,55	5,59	0,7	$VC_{0.93}$	»	4,153	5,61	5,58	0,5
$VC_{0.67}$	»	4,123	5,58	5,56	0,4	$VC_{0.93}$	»	4,155	5,61	5,57	0,7
$VC_{0.72}$	»	4,129	5,59	5,60	0,2	$VC_{0.96}$	»	4,155	5,64	—	—
$VC_{0.76}$	»	4,129	5,63	5,56	1,2	$VC_{0.98}$	»	4,156	5,66	5,58	1,4
$VC_{0.78}$	»	4,130	5,65	5,59	1,3	$VC_{0.98}$	»	4,157	5,68	5,59	1,6
$VC_{0.80}$	»	4,133	5,66	5,55	1,8	$VC_{1.02}$	ε + C	4,157	—	5,43	—
$VC_{0.78}$	ε	4,146	5,59	5,57	0,4	$VC_{1.47}$	»	4,159	—	4,94	—

The one-phase cubic carbides were represented by 14 samples with compositions ranging from $VC_{0.63}$ to $VC_{0.98}$. At high carbon contents free graphite was detected in the samples. The figure shows that, contrarily to [2], the dependence of the lattice constant of cubic carbides on concentration is complex in character. In particular, there is an abrupt change of lattice constant (by about 0.013 kX) at compositions near $VC_{0.72-0.80}$. This can probably be regarded as an indication that one (δ) cubic phase of vanadium carbide is stable in the $VC_{0.63}$–$VC_{0.78}$ range, whereas in the $VC_{0.78}$–$VC_{0.98}$ range the stable phase is the (δ′) phase.

Comparison of these results with the data in [1] reveals a certain similarity only with respect to the variation ranges of the constants for the δ phase (4.117–4.133 kX) and δ′ phase (4.146–4.153 kX). On the other hand, the concentration ranges in which the cubic phases are stable differ considerably from those in [1]. This applies especially to the δ phase which, according to [1], is homogeneous in the $VC_{0.63}$–$VC_{0.83}$ composition range, whereas according to our determinations its homogeneity range is $VC_{0.63}$–$VC_{0.78}$. It is possible that the difference between the extents of the stability regions of the cubic carbides is due to some extent to the presence of oxygen in the samples studied in [1].

Schonberg's data [2] disagree entirely both with the results of Gurevich and Ormont [1] and with the characteristics of the δ and ε phases detailed above. It must be specially emphasized that cubic phases with $a_0 > 4.16$ kX were not obtained either by us or by Gurevich and Ormont [1], whereas Schonberg gives a very high value of the lattice constant for the carbide $VC_{0.75}$ (4.174 kX). This gives rise to doubts whether his samples were equilibrium in character.

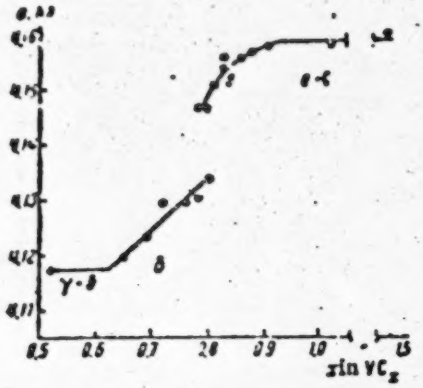

Effects of composition on the lattice constants of cubic vanadium carbides.

It must be pointed out that, according to our data, the concentration limit of the stability region of the ε phase corresponds to $VC_{0.93}$. It is likely that a carbide with a higher carbon content can also be formed, but it apparently decomposes during cooling, similarly to NbC [8]. The following observations support this view. The lattice constant of the carbide $VC_{1.47}$ was 4.159 kX, which is somewhat greater than the constant for the ε phase in the sample $VC_{1.02}$ (4.157 kX). Despite repeated heating of the $VC_{1.47}$ sample, we were unable to obtain x-ray patterns with sharp lines from it at large angles. The hypothesis that the sample was highly disperse was not confirmed, as x-ray patterns taken without rotation indicate that it has coarsely crystalline structure. Evidently the diffuse nature of the lines was due to decomposition of the carbide, so that the sample actually contained a range of carbides differing in composition.

The abrupt change (~0.013 kX) of the lattice constant at the stability boundary of the δ and ε phases is analogous to that described earlier, not only for the V–C system [1] but also for the following systems: V–O [1,9], Pd–H [10], $SrCl_2$–$ThCl_4$ [11]. The cause of this variation of a with concentration is not quite clear and requires further investigation. It may be due to the presence of vanadium ions of different valences and the existence of critical conditions for their spatial distribution.

Comparison of the pycnometric ($d_{meas.}$) and x-ray (d_x) densities is of certain interest in relation to the construction of the crystal lattice of cubic vanadium carbides. The x-ray densities were calculated on the assumption that vacant sites exist only in the lattice points of the carbon sublattice. It is clear from Table 1 that the x-ray density of the δ and ε phases alters very little with composition (by less than 2%). The fluctuations of the pycnometric density are even smaller (<1%). The following fact is noteworthy. The experimental and calculated densities of the δ and ε phases with the minimum carbon content are fairly close; the difference between them is about 0.5%. On the other hand, the differences between $d_{meas.}$ and d_x are twice or three times as large (up to 1.8%) for the cubic phases near the upper stability limit (for example, $VC_{0.75}$ and $VC_{0.93}$).

TABLE 2. Densities of Certain Oxycarbide Samples Containing the ε phase

Empirical formula	Lattice constant, kX	Presence of free carbon	Pycnometric density, g/cc
$VC_{0.87}O_{0.13}$	4,157	yes	5,18
$VC_{0.96}O_{0.09}$	4,157	»	5,20
$VC_{1.21}O_{0.02}$	4,157	»	5,00
$VC_{0.91}O_{0.02}$	4,157	no	5,58
$eVC_{0.9}$	4,146	»	5,57

This apparently indicates, on the one hand, that models of cubic phases with defects in the carbon sublattice are fairly close to reality, and on the other, that there is some likelihood of a certain degree of defectiveness in the vanadium sublattice, increasing with the carbon concentration.

It should be pointed out that the above data on the densities of carbides are not in satisfactory agreement with the data of other authors. For example, according to [5,6] the x-ray density of the ε phase is about 5-10% higher

than the experimental value. A similar conclusion follows from [1]. Here, for example, for the composition $VC_{0.88}O_{0.08}$ d = 5.65 and $d_{meas.}$ = 5.21 g/cc, and for the composition $VC_{0.86}O_{0.13}$ d_x = 5.78 and $d_{meas.}$ = 5.20 g/cc. On the other hand, the pycnometric and x-ray densities of the δ phase are in good agreement with each other.

The considerable discrepancies in estimates of the densities of the δ phase are undoubtedly due to the fact that the equilibrium state of the system and the presence of free carbon in it were not always controlled satisfactorily. In presence of free carbon it is natural to expect that $d_x \gg d_{meas.}$. This is illustrated by the results obtained for certain oxycarbide δ phases obtained by reduction of V_2O_3 with graphite. Table 2 shows that samples containing free carbon had appreciably lower densities than single-phase samples. On the other hand, the densities of single-phase oxycarbides are in good agreement with the carbide characteristics discussed above. Moreover, they are fairly close to the values reported in [1]. Therefore the model given above for the structure of cubic vanadium carbide is probable and consistent with the experimental data described.

LITERATURE CITED

1. M. A. Gurevich, B. F. Ormont, Zh. neorgan. khimii, 2, 1560, 2581 (1957); 3, 403 (1958).
2. N. Schonberg, Acta Chem. scand., 8, 624 (1954).
3. G. V. Samsonov, Ya. S. Umanskii, Solid Compounds of Refractory Metals [in Russian] (Metallurgizdat, Moscow, 1957) p. 123.
4. W. Rostoker, Metallurgy of Vanadium [Russian translation] (Izd. inostr. lit., Moscow, 1959) p. 54.
5. E. Maurer, T. Doring, W. Pulewka, Archiv Eisenhuttenwesen, 13, 337 (1940).
6. R. Becker, F. Ebert, Z. Phys., 31, 268 (1925).
7. M. A. Gurevich, B. F. Ormont, Fizika metallov i metallovedenie, 4, 112 (1957).
8. G. Brauer, R. Lesser, Z. Metallkunde, 50, 8 (1959).
9. E. Vol'f, S. S. Toikachev, L. L. Kozhina, Vestn. Leningrad univ., ser. fiz.-khim., 2, 10, 87 (1959).
10. A. R. Ubbelohde, Proc. Roy. Soc., B[illegible] 305 (1937).
11. G. Brauer, O. Muller, Z. anorgan allgem. Chem., 295, 218 (1958).

All abbreviations of periodicals in the above bibliography are letter-by-letter transliterations of the abbreviations as given in the original Russian journal. *Some or all of this periodical literature may well be available in English translation.* A complete list of the cover-to-cover English translations appears at the back of this issue.

DEETHERIFICATION OF MAGNESIUM BROMIDE TRIETHERATE

G. V. Ravich and I. F. Manucharova

N. S. Kurnakov Institute of General and Inorganic Chemistry, Academy of Sciences USSR
Translated from Zhurnal Strukturnoi Khimii, Vol. 2, No. 4
pp. 449-451, July-August 1961
Original article submitted June 9, 1960

The progressive loss of ether from magnesium bromide triethcrate was studied by a combination of phase-analysis methods. The stepwise character of the deetherification process was demonstrated by means of thermographic, thermogravimetric, and gas-volumetric analysis. This result is interpreted as the consequence of different bond strengths between the three different ether molecules and magnesium bromide triethcrate.

The microstructures of the solid etherate phases are also given. Deetherification is considered by analogy with dehydration.

Whereas dehydration has been studied and described in the literature very extensively, deetherification (removal of ether from compounds) has hardly been studied at all by such sensitive methods of phase analysis as the differential thermal, thermogravimetric, gas-volumetric , and other methods. At the same time, removal of nonaqueous solvents by the action of heat on compounds of the most diverse structures is becoming of considerable interest in connection with the extraction of inorganic substances by means of organic solvents. Moreover, studies of etherates supplement the general views on the bond strength of ether in crystalline solvate structures.

We studied the consecutive liberation of three ether molecules from magnesium bromide triethcrate with the aid of deetherification curves. The etherates of magnesium bromide, first synthesized at the beginning of this century by Menshutkin [1], who pointed out the analogy between the behavior and structure of hydrates and etherates, were later studied by Evans and Rowley [2,3]. These workers showed that the tri-, di-, or monoetherate of magnesium bromide crystallizes out of ethereal solution, dependent on the temperature.

In our investigation we used a multiple form of differential thermal analysis, involving the recording of heating curves simultaneously with weight changes, or of similar thermograms in conjunction with measurement of the volumes of ether liberated. These determinations, performed with N. S. Kurnakov's pyrometer, balances of various design (torsion, McBain's, the Sartorius "Elektron-1"), and G. G. Tsurinov's automatic gas buret, were supplemented by microphotographs of the external appearance of the crystals, taken in polarized light.

Magnesium bromide was synthesized in ethereal solution by the well-known methods [1,2]. Etherates were crystallized out of the ethereal solution of magnesium bromide under conditions excluding the entry of moisture into the solution. In accordance with the crystallization temperature, we obtained the triethcrate (t_{cr} = −10 to 0°), diethcrate (t_{cr} = 15-20°), or monoetherate (t_{cr} = 30°) of magnesium bromide. The compositions of the etherates were confirmed by determinations of H, C, and Mg by chemical analysis.

Magnesium bromide triethcrate crystallizes in spherulite form (Fig. 1a). Crystals of magnesium bromide diethcrate are shown in Fig. 1b. Optical crystallographic investigations showed that crystals of $MgBr_2 \cdot 2(C_2H_5)_2O$ are biaxial, positive, and belong to the triclinic system. Magnesium bromide monoetherate crystallizes in the form of needles or elongated plates (Fig. 1c), which also belong to the triclinic system.

In contrast to the tri- and diethcrate the solubility of magnesium bromide monoetherate in diethyl ether decreases with rise of temperature. This enabled us to distinguish between the diethcrate and monoetherate when crystals of both phases were present in ethereal solution; we were able to photograph these two phases present in ethereal solution; simultaneously (Fig. 1d). At the given temperature one of these phases was metastable (the laminar crystals are the diethcrate, and the needles are the monoetherate).

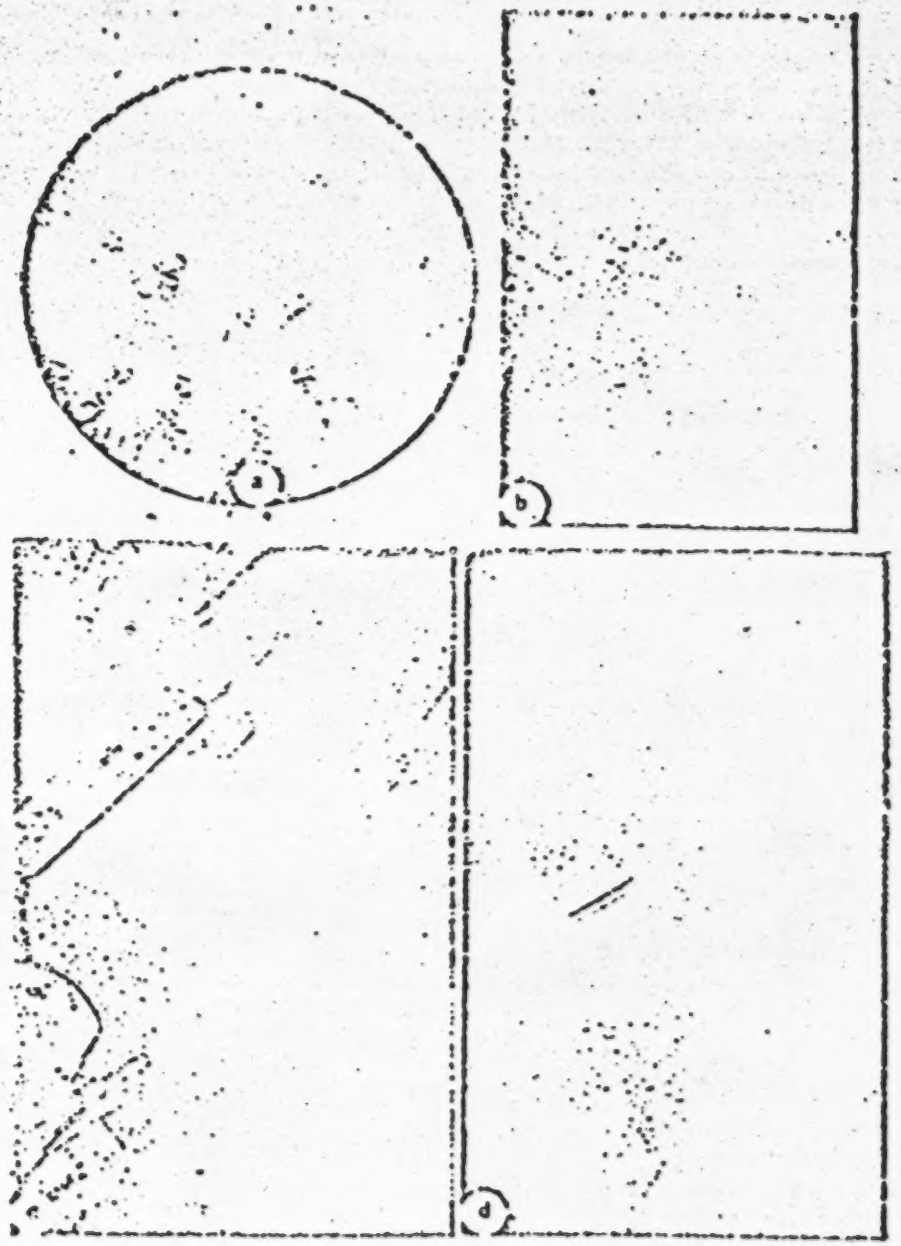

Fig. 1. Outer appearance of magnesium bromide etherate crystals in polarized light, 80×: a) Trietherate, b) monoetherate, c) dietherate + monoetherate.

The heating curve of magnesium bromide triethcrate (Fig. 2) shows three distinct endothermic effects: I at 13-27°, II at 40-49°, III at 61-68°, and IV at 117-127°. The reproducibility of these curves is quite good.

The curve representing the change of weight as the result of liberation of ether from magnesium bromide triethcrate is shown in Fig. 3. The thermogravimetric curve (polytherm) has three characteristic and well-defined steps, all of exactly the same height, corresponding to the loss of the first, second, and third ether molecules at the following temperatures: 12-27°, 38-68° and 118-123° (corresponding to effects I, II, III, and IV on the differential curve in Fig. 2). The probable explanation of the discrepancy between the amount of ether liberated over each temperature range and the theoretical amount (16.3% as against the theoretical value of 22.2%) is that magnesium bromide etherates, like magnesium bromide itself, are extremely hygroscopic and absorb a certain amount of moisture from the air. This is confirmed by the fact that the discrepancy decrease when the experiment is conducted in a current of nitrogen (with a McBain quartz balance).

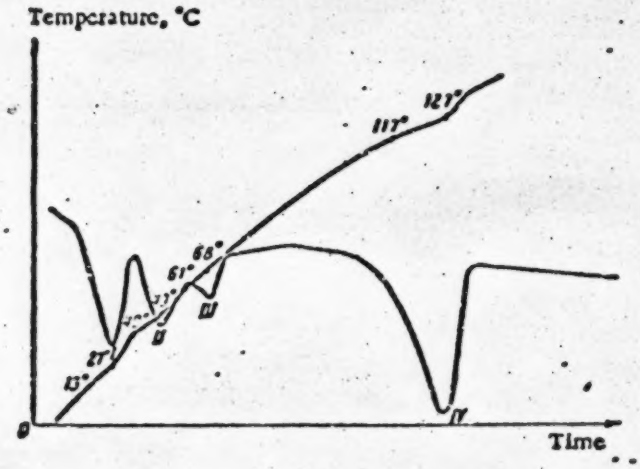

Fig. 2

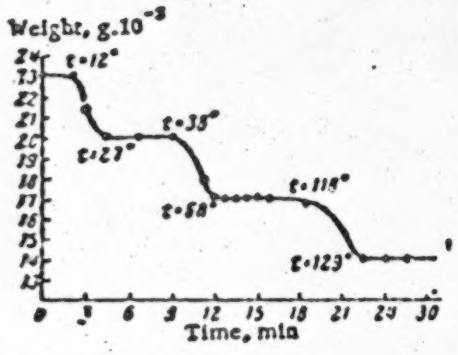

Fig. 3

The following points were of interest.

1. An explanation of the nature of the two endothermic effects at 49 and 68° (Fig. 2), corresponding to the liberation of the second ether molecule.

2. Differences between the bonding strengths ether in the etherates of magnesium bromide, giving rise to stepwise deetherification.

In the former case we were able to show that in the range of ether liberation by magnesium bromide dietherate (49-68°) there is, in addition to the two endothermic effects, a weak exothermic effect "a" preceding the second endothermic effect (see curves 1 and 2 in Fig. 4.). On the other hand, highly sensitive photographic recording with the Sartorius "Elektron 1" automatic balance (sensitivity 10^{-9} g) revealed a certain inflection in the thermogravimetric curve in the 48-58° range; this could also be detected with the torsion balance (see curve 3, Fig. 4). This result led to the suggestion that ether is liberated stepwise in the conversion of diethcrate into monoetherate. This is consistent with the character of the differential curve on the thermogram of magnesium bromide dietherate (Fig. 4) if it is assumed that liberation of the second ether molecule is associated with a certain simultaneous rearrangement of the crystal lattice, accompanied by evolution of heat.

It is evident that the first ether molecule, which is liberated from the triethcrate below the boiling point of ether, is weakly bonded, so that the stability of the triethcrate is extremely low. The bonding of ether in the diethcrate is much more stable and apparently ether cannot be liberated without rearrangement of the crystal lattice (at 48-58°).

Fig. 4.

Finally one cannot fail to notice the extreme stability of the ether bond in the monoetherate, as the latter is stable up to 118 ° (the decomposition is complete at 128°). It is possible that the ether molecule in the monoetherate is in the form of an internal complex; we are at present investigating this by direct x-ray diffraction methods.

LITERATURE CITED

1. B. N. Menshutkin. Zh. Russk. fiz.-khim. obsh., 35, 610 (1903).
2. W. V. Evans, H. H. Rowley. J. Amer. Chem. Soc., 52, 3523 (1930).
3. H. H. Rowley. J. Amer. Chem. Soc., 58, 8, 1337 (1936).

All abbreviations of periodicals in the above bibliography are letter-by-letter transliterations of the abbreviations as given in the original Russian journal. *Some or all of this periodical literature may well be available in English translation.* A complete list of the cover-to-cover English translations appears at the back of this issue.

APPROXIMATE CALCULATION OF THE π-ELECTRON ENERGY OF AROMATIC CONDENSED MOLECULES BY HUCKEL'S VARIANT OF THE MO LCAO METHOD

N. F. Stepanov and V. M. Tatevskii

M. V. Lomonosov Moscow State University

Translated from Zhurnal Strukturnoi Khimii, Vol. 2, No. 4,
pp. 452-455, July-August 1961
Original article submitted April 5, 1960

On the basis of [3], an approximate formula is derived for calculating the π-electron energy W_π of condensed aromatic molecules. The results of calculations with this formula agree to within 1% with the exact values of W_π.

The calculation of the π-electron energy W_π for condensed aromatic hydrocarbons, even with the simplest variant of the MO method (the Huckel variant), is a very difficult one, since in this calculation all the eigenvalues of matrices of high order must be obtained. In the calculations for W_π by this method, however, only the sum of the first N/2 eigenvalues occurs (N is the order of the matrix). Several authors (see, for example [1, 2]) have therefore attempted to calculate this energy directly - starting only with the structure of the molecule. These methods are either directly or indirectly based on a postulate of the phenomenological theory of the relation between properties and structure. According to this postulate, the energy of any molecule of some series of molecules can be obtained as the sum of partial quantities, each obtained from a separate local structural element of the molecule, the properties of which are considered as constant for the whole series. Unfortunately, all these attempts are of an empirical character, i.e., in the calculation of the energies W_π for the series of molecules the above mentioned partial quantities occur, and these quantities are subsequently used for the calculation of the energy of other molecules.

In [3] we pointed out that the validity of this postulate for the Huckel variant of the MO process can be obtained with sufficient accuracy from a consideration of the structure of the matrix A of the permanent equation. It was established that W_π could be obtained from the trace of the matrix $|A|$ with eigenvalues $x_m = |\lambda_m|$, where the λ_m are the eigenvalues of A, which can be obtained in the form of a series in powers of polynomials of A or as a polynomial in A. An approximation to $|A|$ can therefore also be obtained as a polynomial in A, for example by terminating the series at the kth term. In order to obtain a numerical formula for W_π it is therefore convenient to use the following method: write the polynomial $p_k(A)$ of the kth degree with coefficients a_i, and vary the values of $\Delta_k^2 = \sum_m [|\lambda_m| - P_k(\lambda_m)]^2$. Since neither the values of λ_m nor their distribution are known, a rougher method is used, namely the minimizing of the function $\Delta_k^2 = \int_{-t}^{t} [|x| - P_k(x)]^2 dx$, where $[-t, t]$ is an interval containing λ_m. If we now represent the traces of the matrices A^n in the resulting polynomial in terms of types of relations, we obtain a numerical formula for calculating W_π. If we limit ourselves to a polynomial P_{10} of the tenth degree, then we must use the types of relation obtained by taking into account the second environment. These types of relation are the following (m_{ij} is the number of relations of a given type):

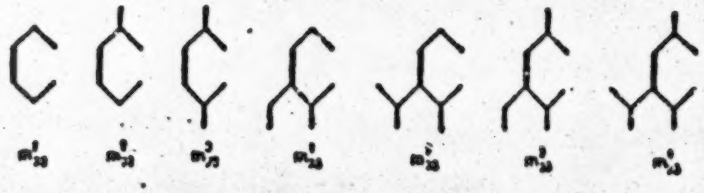

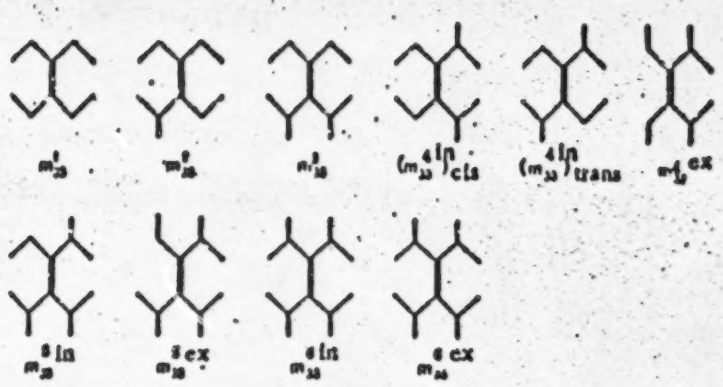

Here "in" represents an internal bond, i.e., a bond belonging to two rings simultaneously; "ex" is an external bond, belonging to one ring only. The total number of bond types is 17. It can be shown that of the 17 values of m^f_{ij} only 13 are independent. Therefore, using P_{13} for finding $|A|$, we obtain in the most general form (W_π in β units):

$W_\pi = 1.33512\, m^1_{33} + (1.30346 + c_1)\, m^2_{33} + (1.29227 + 2c_1)\, m^1_{33} + (1.16455 - c_1 + c_2)\, m^1_{33} + (1.14736 - |c_1| + |2c_2| + c_4)\, m^2_{33} + (1.13456 + c_2)\, m^3_{33} + (1.12176 + 2c_2 + c_4)\, m^4_{33} + (1.12583 - 4c_2)\, m^1_{33} + (1.10023 - 2c_2 - c_3)\, m^2_{33} + (1.07463 - 2c_2)\, m^5_{33} + (1.08340 - 2c_4)\, (m^{4in}_{33})_{cis} + (1.07901 - 2c_3) \times (m^{4in}_{33})_{trans} + (1.07506 - 2c_3 - 2c_4)\, m^{5ex}_{33} + (1.06218 - c_3)\, m^{6in}_{33} + (1.05036 - c_3 - c_4)\, m^{6ex}_{33} + 1.04974\, m^{6in}_{33} + 1.02915\, m^{6ex}_{33}$.

Here c_1, c_2, c_3, and c_4 are arbitrary constants; W_π does not depend on them. For example, with $c_1 = 0.2333$ $c_2 = 1.02176$, $c_3 = 0.2225$ and $c_4 = -0.00427$ we have $W_\pi = 1.33512\, m^1_{33} + 1.33039\, m^2_{33} + 1.34013\, m^3_{33} + 1.16238\, m^4_{33} + 1.16371\, m^5_{33} + 1.15632\, m^6_{33} + 1.16406\, m^{4in}_{33} + 1.03879\, m^1_{33} + 1.03443\, m^2_{33} + 1.03111\, m^3_{33} + 1.03083 (m^{4in}_{33})_{cis} + 1.03445 (m^{4in}_{33})_{trans} + 1.03593\, m^{5in}_{33} + 1.03690\, m^{6in}_{33} + 1.03235\, m^{6ex}_{33} + 1.04974\, m^{6in}_{33} + 1.02915\, m^{6ex}_{33}$.

It follows from this expression that the values of c_1, c_2, c_3, and c_4 may be so chosen that the difference between the coefficients of m^f_{ij} within the limits of each bond type, with the first environment m_{ij} taken into account, is quite small. Therefore by suitable choice of values for c_1, c_2, c_3, and c_4 (for example, from the minimum root mean square deviation of the coefficients of the m^f_{ij} bond types from the average coefficient for the given m_{ij} type) it is possible to obtain from the expression for W_π in the terms of m_{ij} bond types only; values of W_π calculated from this expression should differ very little from the values found from formula (2). In this way we find*:

$$W_\pi = 1{,}336\, m_{22} + 1{,}160\, m_{23} + 1{,}038\, m_{33}. \qquad (3)$$

and the deviations between the values given by formulas (2) and (3) do not exceed 1.1%.

The results of calculations from formulas (2) and (3) are given in the table. The seventh column gives exact values of W_π calculated by a number of authors from the eigenvalues of the matrices A. It is seen that for the hydrocarbons listed in the table the accuracy of the calculation is at least 1% by formula (2), and at least 1.2% by formula (3). The greatest deviations are found for the acene series.

*It is interesting to note that in [1] the following formula was obtained by calculation of the coefficients by the method of least squares from W_π for a series of hydrocarbons: $W_\pi = 1.333\, m_{22} + 1.115\, m_{23} + 1.07\, m_{33}$.

Hydrocarbon	Calculated from (2)	Error, %	Calculated from (3)	Error, %	Exact value	Literature
Benzene C_6H_6	8,012	0,15	8,02	0,2	8,000	[4]
Naphthalene $C_{10}H_8$	13,693	0,07	13,69	0,1	13,683	[5]
Anthracene $C_{14}H_{10}$	19,357	0,24	19,37	0,3	19,311	[5]
Phenanthrene $C_{14}H_{10}$	19,430	0,10	19,43	0,1	19,448	[5]
Pyrene $C_{16}H_{10}$	22,487	0,08	22,49	0,0	22,505	[5]
Naphthacene $C_{18}H_{12}$	25,021	0,36	25,05	0,5	24,911	[5]
Benzanthracene $C_{18}H_{12}$	25,099	0,01	25,10	0,0	25,101	[5]
3,4-Benzophenanthrene $C_{18}H_{12}$	25,151	0,14	25,16	0,1	25,187	[10]
Chrysene $C_{18}H_{12}$	25,172	0,08	25,16	0,1	25,192	[10]
Triphenylene $C_{18}H_{12}$	25,225	0,20	25,21	0,3	25,275	[15]
1,2-Benzopyrene $C_{20}H_{12}$	28,221	0,00	28,22	0,0	28,222	[15]
4,5-Benzopyrene $C_{20}H_{12}$	28,291	0,16	28,27	0,2	28,330	[7, 15]
Perylene $C_{20}H_{12}$	28,273	0,03	28,27	0,1	28,25	[2]
Pentacene $C_{22}H_{14}$	30,685	0,36	30,73	0,8	30,544	[5]
1,2-Benzonaphthracene $C_{22}H_{14}$	30,763	0,12	30,78	0,2	30,726	[15]
Pentaphene $C_{22}H_{14}$	30,767	0,01	30,78	0,1	30,764	[8]
2,3-Benzochrysene $C_{22}H_{14}$	30,841	0,01	30,84	0,0	30,839	[15]
1,2-Benzotetraphene $C_{22}H_{14}$	30,820	0,05	30,84	0,0	30,841	[15]
1,2,5,6-Dibenzoanthracene $C_{22}H_{14}$	30,841	0,13	30,84	0,1	30,859	[8]
1,2,7,8-Dibenzoanthracene $C_{22}H_{14}$	30,841	0,12	30,84	0,1	30,879	[8]
1,2,3,4-Dibenzoanthracene $C_{22}H_{14}$	30,808	0,15	30,84	0,2	30,842	[8]
3,4,5,6-Dibenzophenanthrene $C_{22}H_{14}$	30,826	0,19	30,84	0,2	30,890	[9, 15]
1,2,9,10-Dibenzophenanthrene $C_{22}H_{14}$	30,950	0,16	30,95	0,2	30,900	[15]
3,4-Benzochrysene $C_{22}H_{14}$	30,805	0,15	30,83	0,2	30,939	[15]
Picene $C_{22}H_{14}$	30,914	0,10	30,89	0,2	30,953	[8]
1,1-Benzoperylene $C_{22}H_{12}$	31,374	0,15	31,33	0,3	31,425	[15]
Anthanthrene $C_{22}H_{12}$	31,274	0,07	31,27	0,1	31,253	[15]
1,2,7,8-Dibenzopyrene $C_{24}H_{14}$	33,065	0,00	33,06	0,0	33,065	[7, 15]
Cetrene $C_{26}H_{16}$	33,845	0,37	33,96	0,4	33,708	[15]
1,2,6,7-Dibenzopyrene $C_{24}H_{14}$	33,055	0,08	33,06	0,0	33,028	[15]
Naphtho-(1',2',3,4)-pyrene $C_{24}H_{14}$	33,067	0,03	33,06	0,1	33,087	[15]
2,3,4,5-Dibenzopyrene $C_{24}H_{14}$	34,008	0,07	34,01	0,1	34,020	[7, 15]
Coronene $C_{24}H_{12}$	34,498	0,21	34,39	0,5	34,572	[5]
Hexacene $C_{26}H_{16}$	26,329	0,34	26,41	0,7	26,150	[10]
1,2,1',2'-Anthranthracene $C_{28}H_{16}$	26,509	0,07	26,53	0,2	26,484	[7, 15]
1,2,7,8-Dibenzonaphthacene $C_{26}H_{16}$	26,504	0,04	26,53	0,0	26,517	[15]
1,2,3,4,5,6-Tribenzanthracene $C_{32}H_{18}$	26,630	0,29	26,52	0,5	26,715	[15]
1,2,7,8-Dibenzochrysene $C_{26}H_{16}$	26,731	0,17	26,72	0,2	26,765	[11, 15]
2,3,8,9-Dibenzoperylene $C_{28}H_{16}$	30,750	0,06	30,74	0,1	30,769	[15]
Anthraceno-(1',2',1,2)-tetracene $C_{34}H_{18}$	42,213	0,05	42,25	0,0	42,236	[15]
1,2,3,4,5,6,7,8-Tetrabenzanthracene $C_{34}H_{18}$	42,529	0,25	42,41	0,3	42,343	[11]
1,2,7,8-Dibenzanthrene $C_{30}H_{18}$	42,748	0,02	42,74	0,0	42,741	[15]
1,12,5,6,7,8-Tribenzoperylene $C_{38}H_{18}$	42,812	0,03	42,80	0,0	42,819	[15]
Chalcacene $C_{32}H_{16}$	42,698	0,1	42,85	0,0	42,84	[12]
Ovalene $C_{32}H_{14}$	46,411	0,19	46,39	0,1	46,499	[5, 13]
Circumanthracene $C_{40}H_{18}$	58,367	0,05	58,21	0,3	58,370	[13]

Infinite structures (W_∞ per atom)

Polyacene 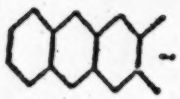	1,416	0,93	1,42	1,2	1,403	[14]
Polyphene 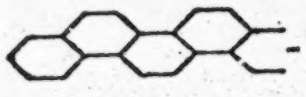	1,436	0,07	1,43	0,2	1,437	[14]

Hydrocarbon	Calculated from (7)	Error, %	Calculated from (5)	Error, %	Exact value	Literature
Polynaphthylene	1,461	0,00	1,46	0,0	1,461	[14]
Graphite lattice 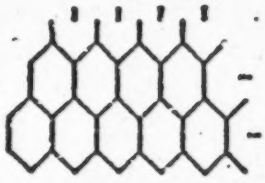	1,575	0,07	1,56	1,2	1,576	[14]

LITERATURE CITED

1. V. M. Tatevskii. Zh. fiz. khimii, 25, 211 (1951).
2. A. L. Green. J. Chem. Soc., 1836 (1956).
3. N. F. Stepanov, V. M. Tatevskii, Zh. struk. khimii, 2, 205 (1961).
4. E. Huckel, Z. Electrochem., 33, 782 (1937).
5. N. S. Ham, K. Ruedenberg, J. Chem. Phys., 29, 1199 (1958).
6. G. Berthier, C. A. Coulson, H. H. Greenwood, A. Pullman, Compt. rend. Acad. sci., 226, 1996 (1948).
7. O. Chalvet, J. Poitier, Compt. rend. Acad. sci., 240, 1760 (1955).
8. G. Baldock, G. Berthier, A. Pullman, Compt. rend. Acad. sci., 223, 931 (1949).
9. F. Senet, An. Real soc. espan. fis. y quim., B50, 337 (1954).
10. R. D. Brown, Trans. Faraday Soc., 46, 1013 (1950).
11. M. A. Hernaez, Zarza, An. Real. soc. espan. fis. y quim., B51, 305 (1955).
12. C. A. Coulson, G. S. Rushbrooke, Proc. Roy. Soc. Edinburg, A62, 336 (1948).
13. J. Baudet, B. Pullman, Compt. rend. Acad. sci., 244, 777 (1957).
14. C. A. Coulson, G. S. Rushbrooke, Proc. Roy. Soc. Edinburgh, A62, 350 (1948).
15. G. G. Hall, Trans. Faraday Soc., 53, 574 (1957).

All abbreviations of periodicals in the above bibliography are letter-by-letter transliterations of the abbreviations as given in the original Russian journal. *Some or all of this periodical literature may well be available in English translation.* A complete list of the cover-to-cover English translations appears at the back of this issue.

DETERMINATION OF THE DEGREE OF IONIC CHARACTER (IONICITY) OF BONDS IN MOLECULES AND RADICALS II

V. I. Durakov and S. S. Batsanov

Institute of Inorganic Chemistry, Siberian Division, Academy of Sciences of the USSR

Translated from Zhurnal Strukturnoi Khimii, Vol. 2, No. 4,
pp. 456-461, July-August 1961
Original article submitted June 17, 1960

The method proposed in communication I for calculation of bond ionicities in molecules has been refined by consideration of the interaction of closed electron shells. The range of substances has been extended by the availability of new overlap integrals. The method has been extended to free radicals, for which bond ionicities and electronegativity values have been determined. Variations of bond lengths in the transition from molecules to radicals are discussed.

In the first communication we gave an account of a method for theoretical determination of bond ionicities in molecules by means of overlap integrals [1]. The method involved a comparison of the sum of the overlap integrals for a real bond AB with that of a hypothetical purely covalent bond AB with length equal to the sum of the covalent radii, for which i = 0. This method gives the effective charges on the partners of the chemical bond.

Our values ionicity i were found to be connected as follows with the electronegativity difference Δx between the respective atoms:

$$i = 1 - \exp[-0{,}22(\Delta x)^2].$$

However because of the limited number of tabulated integral values available, we were not able to perform the calculations for a large number of molecules, and therefore further verification of the above equation was required. We have now received overlap integrals from the Library of Congress, USA, whereby the applications of the method can be extended.

Bond Ionicities in Molecules

Table 1 gives the effective bond charges in a number of molecules composed of elements in periods II-V of the periodic table. Bond ionicities were calculated by means of the formula:

$$i = 1 - \frac{\sum A_j S_j - \frac{1}{2}\sum A_{j'}(S_{j'})^2 + \frac{0{,}82}{n}\sum S_k}{\sum A_j S_j - \frac{1}{2}\sum A_{j'}(S_{j'})^2 + \frac{0{,}82}{n}\sum S_k}, \qquad (1)$$

where $A_j = 1$ for S_{ss}, $A_j = 1{,}732$ for S_{sp}, S_{ps}, S_{pp} and $A_k = 0{,}82$ for $S_{\pi\pi}$. In this formula summation for j and k accounts for the bonding electrons, and summation for j' accounts for repelling electrons. The coefficients A in the sums represent the "specific electron density" of a given type of integral. The coefficient 1/n represents the ratio of the number of free orbitals to the number of isolated electron pairs. In contrast to the earlier calculation, in cases where the bond ionicity is of the order of 70% and over (for example, KF, KCl, etc., we take into account the interaction of the potassium 3po shell with the 2po and 3po halogen shells. Thus, interaction of the two outer electron shells of the atoms of the ionic molecule is taken into account in the calculation because the outer shell of the corresponding anion is virtually complete and its interaction with the lower electrons may be neglected. For this reason the ionicities given here differ by a few percent from the values given earlier. In the case of hydrides the calculations are unchanged, and therefore they are not given here. The ionicities of diatomic molecules depend in a regular manner on the electronegativity difference between the corresponding atoms. Figure 1 shows the graphical relationship between electronegativity and ionicity of diatomic molecules, inclusive of the hydride molecules given in Table 2 of [1]. The curve is represented by the equation:

$$i = 1 - \exp[-0{,}21(\Delta x)^2]. \qquad (2)$$

TABLE 1.

Molecule	R°_{meas}, Å	$r^{\circ\circ}_{k}$, Å	$\theta^{\circ\circ\circ}_{meas}$	$a^{\circ\circ\circ\circ}$	Degree of double-bond character, %	Real bond									Reference bond						L, %
						i	P	S_j	i	P	$S^{'}_{k/n}$	i	P	S_{jr}	P	$S^{'}_{j}$	P	$S^{'}_{k/n}$	P	$S^{'}_{jr}$	
LiF	1,53	2,04				−0,000	4,70	0,000				−0,430	6,65	0,081	0,27	0,201			0,02	0,020	72
LiCl	1,97	2,32				−0,5	[illegible]	0,167				−0,320	7,08	0,120	5,98	0,356			8,51	0,076	55
LiBr *****	2,14	2,46				−0,5	7	0,180							6,29	0,403					53
LiI	2,37	2,65				−0,4	[illegible]	0,251				−0,270	7,95	1,120	6,34	0,506			9,07	0,088	40
NaF	2,09	2,50				0,566	6,29	0,042				0,566	8,32	0,080	7,11	0,190			9,39	0,060	85
NaCl	2,48	2,58				0,420	6,48	0,131				−0,380	8,44	0,159	6,65	0,348			9,12	0,050	64
NaBr	2,61	2,72				−0,471	6,95	0,139				−0,302	7,87	0,245	7,16	0,381			8,11	0,213	66
NaJ	2,87	2,90				−0,443	7,14	0,182				−0,267	8,14	0,250	7,15	0,413			8,29	0,161	60
KF	2,55	2,74				0,625	7,71	0,013				0,555	8,05	0,052	8,29	0,142			8,65	0,137	32
KCl	2,76	3,02				0,540	6,91	0,030				0,466	7,23	0,155	7,51	0,297			8,91	0,249	50
BeF_2	1,40	1,68	180°	$\sqrt{1/2}$		−0,451	4,73	0,210				−0,140	6,02	0,160	5,46	0,430			7,8[illegible]	[illegible]	[illegible]
$BeCl_2$	1,75	1,96	180°	$\sqrt{1/2}$		−0,352	4,93	0,410				−0,020	6,59	0,120	5,40	0,540			[illegible]	0,084	[illegible]
$BeBr_2$ *****	1,91	2,10	180°	$\sqrt{1/2}$		−0,320	5,47	0,415				−0,020	7,22		6,01	0,493				[illegible]	16
BeI_2	2,10	2,29	180°	$\sqrt{1/2}$		−0,320	5,71	0,470				0,020	7,64	0,110	6,22	0,490				0,080	8
MgF_2	1,77	2,10	180°	$\sqrt{1/2}$		0,465	5,91	0,130				−0,280	7,12	0,201	6,87	0,320			[illegible]	0,080	66
$MgCl_2$	2,18	2,38	180°	$\sqrt{1/2}$		−0,343	6,15	0,350				−0,180	7,54	0,195	6,65	0,510			[illegible]	0,120	34
BF_3	1,29	1,45	120°	$\sqrt{1/3}$	31	0,333	4,76	0,200	0,333	4,76	0,057	0,000	6,34	0,080	5,34	0,420	5,34	0,043	7,13	0,050	28
BCl_3	1,74	1,81	120°	$\sqrt{1/3}$	31	−0,220	5,18	0,470	0,220	5,48	0,067	0,120	7,62	0,130	5,70	0,490	5,70	0,057	7,93	0,000	4
BBr_3	1,87	1,91	120°	$\sqrt{1/3}$	33	−0,225	5,93	0,506	0,225	5,93	0,068	0,147	8,22		6,05	0,505	7,05	0,057	—	—	0
$B(CH_3)_3$	1,56	1,61	120°	$\sqrt{1/3}$	—	0,111	4,31	0,530	—	—	—	0,111	8,62	0,005	4,45	0,538	—	—	8,90	0,005	1
$B(OCH_3)_3$	1,38	1,45	120°	$\sqrt{1/3}$	26	0,273	4,66	0,351	0,273	4,66	0,088	0,067	6,36	0,088	4,90	0,462	4,90	0,058	6,68	0,108	20
CF_4	1,36	1,38	109°28'	1/2	16	0,231	5,13	0,340	0,231	5,43	0,032	0,110	7,52	0,040	5,51	0,390	5,51	0,030	7,63	0,040	25
CCl_4	1,77	1,72	109°28'	1/2	17	−0,111	6,00	0,440	−0,111	6,00	0,035	0,230	8,84	0,050	5,95	0,460	5,95	0,017	8,59	0,010	5
CBr_4	1,912	1,86	109°28'	1/2	24	−0,117	6,75	0,427	0,117	6,75	0,033	0,225	9,73	—	6,47	0,451	6,47	0,035	9,32	—	4
SiF_4	1,54	1,76	109°28'	1/2	25	0,300	5,80	0,200	0,300	5,80	0,035	0,110	6,80	0,180	6,62	0,350	6,62	0,025	7,78	0,095	34

*Measured bond length. **Sum of covalent radii. ***Valence angle. ****Hybridization coefficient, calculated from the formula $= \frac{\cos\delta}{\cos\theta - 1}$.
*****Without repulsion.

TABLE 1 (continued)

Molecule	R meas, Å	∠ meas, deg	∠ calc, deg	Real bond								Reference bond						
				s_j	p	t	s_k/s_m	μ	s_j'	p	s_j'	p	s_k'/s_m'	μ'	s_j'	p	s_k'/s_m'	μ'
PF_3	1.54	98°	98°	0.250	6.11	0.238	0.010	6.11	0.250	6.03	0.250	6.03	0.027	6.25	0.193	6.25	0.027	6.25
NH_3	1.37	107°8'	107°8'	0.250	5.89	0.141	0.033	5.89	0.250	5.89	0.320	5.89	0.037	5.89	0.320	5.89	0.037	5.89
AsF_3	1.72	102°	102°	0.250	7.01	0.209	0.026	7.01	0.250	7.01	0.298	7.31	0.031	7.31	0.302	7.31	0.031	7.31
OF_2	1.41	103°	103°	0.250	6.50	0.070	0.053	6.50	0.250	6.50	0.250	6.76	0.052	6.76	0.210	6.76	0.052	6.76
OCl_2	1.69	110°8'	110°8'	0.250	6.87	0.051	0.013	6.87	0.153	6.50	0.239	6.50	0.055	6.50	0.225	6.50	0.055	6.50
FCl	1.63	98°	98°	0.250	7.14	0.120	0.070	7.14	0.170	6.61	0.239	6.61	0.102	6.61	0.215	6.61	0.102	6.61
FBr	1.762	1.63	1.63	0.250	7.75	0.117	0.073	7.75	0.176	7.29	0.306	7.29	0.068	7.29	0.249	7.29	0.068	7.29

Molecule	R meas, Å	∠ meas, deg	r … *	Sum of covalent radii, Å	Real bond								Reference bond						
					s_j	p	t	s_k/s_m	μ	s_j'	p	s_j'	p	s_k'/s_m'	μ'	s_j'	p	s_k'/s_m'	μ'
PF_3	1.54	98°	0.17	1.75	0.250	6.11	0.238	0.010	6.11	0.250	6.03	0.250	6.03	0.027	6.25	0.193	6.25	0.027	6.25
NH_3	1.37	107°8'	0.17	1.30	0.250	5.89	0.141	0.033	5.89	0.250	5.89	0.320	5.89	0.037	5.89	0.320	5.89	0.037	5.89
AsF_3	1.72	102°	0.17	1.80	0.250	7.01	0.209	0.026	7.01	0.250	7.01	0.298	7.31	0.031	7.31	0.302	7.31	0.031	7.31
OF_2	1.41	103°	0.15	1.25	0.250	6.50	0.070	0.053	6.50	0.250	6.50	0.250	6.76	0.052	6.76	0.210	6.76	0.052	6.76
OCl_2	1.69	110°8'	0.250	1.50	0.250	6.87	0.051	0.013	6.87	0.153	6.50	0.239	6.50	0.055	6.50	0.225	6.50	0.055	6.50
FCl	1.63	98°		1.51	0.250	7.14	0.120	0.070	7.14	0.170	6.61	0.239	6.61	0.102	6.61	0.215	6.61	0.102	6.61
FBr	1.762	1.63		1.65	0.250	7.75	0.117	0.073	7.75	0.176	7.29	0.306	7.29	0.068	7.29	0.249	7.29	0.068	7.29

Molecule	Bond length, Å	Valence angle	Sum of covalent radii, Å	Bond ionicities, %
PF_3	1.54	98°	1.75	22
NH_3	1.37	107°8'	1.30	15
AsF_3	1.72	102°	1.80	23
OF_2	1.41	103°	1.25	25
OCl_2	1.69	110°8'	1.50	15
FCl	1.63		1.51	21
FBr	1.762		1.65	22

*Measured bond length. **Sum of covalent radii. *** Valence angle. **** Hybridization coefficient, calculated from the formula $\bullet = \frac{\cos\theta}{\cos\theta - 1}$.
***** Without repulsion.

Comparison of this equation with the equation given in [1] shows that further refinement did not alter the functional relationship but merely altered the coefficient by 0.01. We consider that any further improvement of the formula for calculation of ionicity, by taking into account various additional interactions, is pointless because of the inaccuracy in the experimental determination of electronegativity. It can be easily shown that with a maximum experimental error of 0.2 for the electronegativity difference the uncertainty in the ionicity values is about 5%, whereas a change of the coefficient by 0.02 gives an average uncertainty of about 3% in the ionicity values.

Bond Ionicities in Free Radicals

We also determined bond ionicities in free diatomic radicals from experimental interatomic distances [2,3]. Equation (1) was used for the calculation. The reference scale consisted of the overlap integrals of hypothetical purely covalent bonds, with the specific character of free radicals taken into account, namely, that the bond multiplicity in radicals is greater than in the corresponding molecules because in radicals the ratio of the number of free orbitals to the number of isolated electron pairs is 1. The type of hybridization in free radicals generally differs from that in molecules. Whereas in molecules hybridization is energetically justified in most cases, in diatomic free radicals promotion of other electrons in the formation of one chemical bond is energetically disadvantageous. This is confirmed by the difference between the bond dissociation energies in molecules and radicals; for example, the bond dissociation energy in the CH radical is 80 kcal, and in the CH_4 molecule it is 101 kcal. Digonal hybridization is taken into account only for radicals of the second group of the periodic table, because in these cases bond formation is accompanied by splitting of s-electron pairs. The calculated bond ionicities in radicals are given in Table 2. It should be pointed out that the lengths of the reference bonds were taken to be the same for analogous molecules and radicals because they are determined by the constant values of the covalent radii.

Comparison of Molecules and Radicals

Bond ionicities in radicals and the corresponding molecules are compared in Table 3. It is seen that bond ionicities are higher in hydride radicals and lower in halide radicals than in the corresponding molecules. We attribute this difference to the higher electronegativity of multivalent atoms in free radicals. For example, the electronegativity of carbon is 2.6, that of hydrogen is 2.15, the difference is 0.45, and the corresponding bond ionicity is 5% [4]. In the CH radical the ionicity is 28% which implies an increase of the electronegativity difference. This cannot be caused by changes in electronegativities of univalent atoms, the valence state of which in radicals does not differ essentially from the state in molecules. The increase may be due to a change of the electronegativity of carbon, which changes its valence in the transition from the molecule to the radical. The increased electronegativity difference of the CH radical (Δx_{CH}) may be due either to an increase or to a sharp decrease of the electronegativity of carbon (x_C). The latter possibility is excluded, since the bond ionicity decreases in the CF_4–CF and CCl_4–CCl, transitions. It follows that the increase of Δx_{CH} is due to an increase of the electronegativity of carbon. This conclusion is confirmed by independent determinations of the electronegativities of free radicals from the ionization potentials [5].

Using (2) for I as derived above, we can calculate the electronegativities of free radicals. Substituting into (2) the ionicity values from Tables 1 and 2, we can find the electronegativities of multivalent atoms in molecules and radicals. The electronegativity differences for the same atoms in molecules and radicals are given in Table 4.

TABLE 2.

Radical	R_{meas}, Å	Σr_k, Å	Real bond									Reference bond						Δ, %
			t	P	S_j	t	P	S_k	t	P	S_{jr}	P	S_j^0	P	S_k^0	P	S_{jr}^0	
BeH	1,353	1,33	0,012	2,51	0,804							2,48	0,811					1
MgH	1,741	1,75	0,030	3,19	0,719							3,22	0,733					2
SrH	2,158	2,28	0,168	3,49	0,508							3,69	0,660					23
CdH	1,779	1,80	0,043	3,51	0,628							3,55	0,673					7
BH	1,213	1,21	—0,130	2,68	0,903	0,411	2,10	0,422				2,63	0,558	2,00	0,681			20
AlH	1,658	1,63	—0,077	3,37	0,550	0,400	2,50	0,367				3,34	0,357	2,57	0,620			3
CH	1,12	1,14	0,228	2,78	0,438	0,529	2,25	0,319				2,83	0,526	2,20	0,627			25
SiH	1,52	1,51	—0,161	3,42	0,516	0,469	2,79	0,217				3,47	0,562	2,74	0,587			23
NH	1,048	1,11	—0,322	2,89	0,397	0,592	2,40	0,247				3,09	0,511	2,57	0,563			34
PH	1,423	1,47	—0,231	3,52	0,517	0,521	2,84	0,419				3,61	0,534	2,92	0,557			10
OH	0,980	1,11	—0,389	3,00	0,345	0,640	2,55	0,196				3,43	0,464	2,91	0,488			37
SH	1,35	1,41	—0,240	3,60	0,486	0,568	2,96	0,300				3,75	0,520	3,09	0,526			15
BeF	1,365	1,68	—0,454	4,61	0,569	0,454	4,61	0,166	—0,143	5,87	0,111	5,68	0,379	5,68	0,189	7,22	0,047	31
MgF	1,76	2,10	0,465	5,87	0,171	0,465	5,87	0,101	0,292	6,66	0,231	7,05	0,311	7,05	0,080	8,00	0,080	61
BF	1,27	1,50	0,333	4,68	0,231	0,333	4,68	0,181	0,333	4,68	0,338	4,79	0,327	4,79	0,185	4,79	0,331	26
BCl	1,719	1,69	—0,220	5,41	0,317	0,220	5,41	0,200	—0,220	5,41	0,359	5,23	0,335	5,23	0,214	5,23	0,369	2
AlCl*	2,14₂	2,26	0,269	6,48	0,295				0,269	6,48		6,84	0,352			6,84		16
AlBr	2,298	2,40	—0,274	7,00	0,329				—0,274	7,00	0,330	7,31	0,362			7,31	0,290	12
CF	1,271	1,24	0,231	5,07	0,273	0,231	5,07	0,155	0,231	5,07	0,208	4,95	0,321	4,95	0,169	4,95	0,309	14
CaF	2,02	2,48	0,543	6,43	0,150				0,437	7,17	0,302	7,83	0,237	7,83		8,25	0,142	54

* Without repulsion.

This regular increase of the electronegativity of a multivalent atom when a free radical is formed accounts for the change of interatomic distance in the transition from a molecule to a radical. The length of a bond increases with increase of its ionicity (under otherwise constant conditions). Therefore if the electronegativity of a multivalent element E in a molecule is greater than the electronegativity of a univalent element A, then in the $EA_n \rightarrow EA$ transition the electronegativity difference and hence the bond ionicity must increase, leading to an increase of the interatomic distance (for example, R_{OH} is 0.957 A in H_2O and 0.930 A in OH; R_{NH} is 1.014 A in NH_3 and 1.018 A in NH). If $x_E > x_A$, then the electronegativity difference and interatomic distance decrease in the $EA_n \rightarrow EA$ transition: R_{BeF} is 1.40 A in BeF_2 and 1.355 A in BeF; R_{CF} is 1.36 A in CF_4 and 1.271 A in CF.

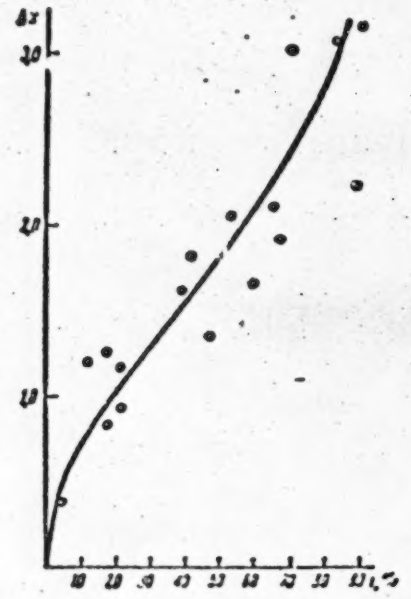

Bond ionicity i in diatomic molecules as a function of the electronegativity difference Δx.

TABLE 3. Comparison of Bond Ionicities in Molecules and Radicals.

Molecule	BH$_3$	CH$_4$	NH$_3$	PH$_3$	H$_2$O	H$_2$S	BeF$_2$	MgF$_2$	BF$_3$	BCl$_3$	CF$_4$
i, %	1	5	17	5	27	6	49	66	28	4	25
Radical	**BH**	**CH**	**NH**	**PH**	**OH**	**SH**	**BeF**	**MgF**	**BF**	**BCl**	**CF**
i, %	20	28	34	10	37	15	44	60	20	2	14

TABLE 4. Increase in the Electronegativities of Multivalent Atoms in the Molecule–Radical Transition.

Molecule→radical $x_{rad} - x_{mol}$	BH$_3$ → BH 0.83	CH$_4$ → CH 0.99	NH$_3$ → NH 1.19	PH$_3$ → PH 0.22	H$_2$O → OH 0.25	H$_2$S → HS 0.36
Molecule→radical $x_{rad} - x_{mol}$	BeF$_2$ → BeF 0,14	MgF$_2$ → MgF 0,22	BF$_3$ → BF 0,05	BCl$_3$ → BCl 0,11	CF$_4$ → CF 0,33	

SUMMARY

1. The method developed earlier for calculating bond ionicities in molecules with the aid of overlap integrals has been improved. The ionicities of a number of molecules formed by elements of periods I-V in the periodic table have been calculated.

2. The method was used for calculating ionicities in diatomic free radicals.

3. The difference between bond ionicities in molecules and the corresponding free radicals is interpreted in terms of the higher electronegativity of multivalent elements in free radicals.

4. Differences between interatomic distances in molecules and corresponding radicals are discussed in relation to the higher electronegativity of atoms in free radicals.

LITERATURE CITED

1. S. S. Batsanov, V. I. Durakov, Zh. strukt. khimii, 1, 3, 353 (1960).
2. T. L. Cottrell, Strengths of Chemical Bonds (Russian translation) (Izd. inostr. lit., Moscow, 1956).
3. L. E. Sutton, Tables of interatomic distances and configuration in molecules and ions. The Chemical Society, London, 1958.

4. L. Pauling, Nature of the Chemical Bond [Russian translation] (Goskhimizdat, Moscow-Leningrad, 1947).
5. G. S. Batsanov, Izv. SO AN SSSR, 1, 68 (1960).

All abbreviations of periodicals in the above bibliography are letter-by-letter transliterations of the abbreviations as given in the original Russian journal. *Some or all of this periodical literature may well be available in English translation.* A complete list of the cover-to-cover English translations appears at the back of this issue.

DETERMINATION OF ELECTRON AFFINITIES OF ELEMENTS

N. N. Maksimova

Lensoviet Technological Institute, Leningrad
Translated from Zhurnal Strukturnoi Khimii, Vol. 2, No. 4,
pp. 462-469, July-August 1961
Original article submitted May 9, 1960

Extrapolation methods for determination of electron affinities are based on graphical relationships for isoelectronic series of elements. Changes of the successive ionization potentials I_w of a given element in relation to the atomic charge w are considered in the paper. An isoelectronic system of this type has the advantage that the atomic nucleus is the same. The relationship $\sqrt{I_w} = f(w)$ is found to be linear. Electron affinities of 66 elements were found by extrapolation of linear plots of this relationship. The relationship is also presented in analytical form. An attempt is made to correlate the course of the straight lines with the electron shell structures and it is shown that their parallel character depends on the number of outer electrons with the same azimuthal quantum number and on the structure of the inner layers of electrons.

Electron affinities of elements can be determined from spectroscopic data [1-6], from measurements of the energy levels of electrons in negative ions by the methods of quantum mechanics [7-9], from the lattice energies of ionic crystals and the Born-Haber cycle [10], and by extrapolation of polarization potentials of isoelectronic series [7, 9, 11-15].

Most widely used are the semiempirical methods [16-20] based on quadratic extrapolation of the ionization potentials of isoelectronic systems, first proposed by Glockler [12]: $I = 1/n^2 (AZ^2 - BZ + C)$. Here Z is the atomic number of the element, A is constant for the given total quantum number n, and B and C vary from one element to another. This equation is applicable only to the elements of the first two periods. For elements of atomic number greater than 18 the relationship is more complex, and Glockler was unable to derive the equation for it. Bates [21], who analyzed the electron affinities found by Glockler and compared them with experimental data, states that quadratic extrapolation leads to low values. However, this discrepancy is not general. For example, in the case of fluorine the electron affinity found experimentally is 3.62 ± 0.03 ev [3], whereas quadratic extrapolation gives 3.94 ev. For oxygen, quadratic extrapolation gives 3.8 ev, while experimental values reported are 2.2 ev [22,23] and 1.48 ± 0.1 ev [24]; in the case of hydrogen the extrapolation method gives 0.76 ev whereas the experimental value is 0.72 ev. Therefore we cannot agree with Bates, who states that the results obtained by quadratic extrapolation must always be regarded as the lower limits of electron affinity.

The extrapolation method proposed by Glocker has been used by Johnson [9], Ginzberg [7], Geltman [16], and Dibrova [25].

To find the ionization potentials I_Z, Johnson derived the following equation:

$$I_Z = \alpha (Z - \sigma)^2 + \gamma + \frac{a_1}{Z - \sigma} + \frac{a_2}{Z - \sigma^2} + R,$$

where α, γ, σ, and a_1, and a_2 are determined from experimental data by extrapolation of the ionization potentials of isoelectronic systems, and R is a correction, usually about 10%. The values of I_Z so found are extrapolated to the negative ion and the electron affinity of the element is found. Johnson's data give good agreement with experimental values of the electron affinities of carbon, chlorine, and fluorine. In the cases of sulfur and nitrogen Johnson's extrapolation gives high results. The value for sulfur is 31% higher than the experimental.

Ginzberg and Miller [7] found ionization potentials from the expression $\Delta I(Z,N) = I(Z+1,N) - I(Z,N)$ where N is the number of electrons in the ion. They were unable to justify their empirical method theoretically, but noted that the values found for electron affinities are in good agreement with experimental data. However, Ginzberg and Miller [7] found a somewhat high value of electron affinity for sulfur, 2.21 ev (the experimental value is 2.07 ev [24]).

Hellman and Mamotenko [18] proposed the linear relationship $\Delta E = \alpha + w$, for ion energy as a function of the charge, although this is initially derived from the equation $\Delta E = \alpha + w + \delta w^2$. They pointed out that omission of δw^2 has little influence on the results.

Dibrova [25] also considered variations of ionization potentials in isoelectronic series of atoms and ions. She stated that this variation conforms to the simple linear equation $I = An(Z-a)$, where n, is the ionization order, a is a shielding constant, and A is a constant. However, the $I = f(Z)$ Moseley curves are distinct parabolas, and a linear relationship between I and Z can be considered only in the approximate sense, and then only if A itself varies in accordance with a quadratic relationship between one element and another.

All these methods are based on extrapolation in isoelectronic series, such as $H^- - F^{7+}$; i.e., ions with the same electronic structure but differing in the structure of the nuclei are always considered. Introduction of various corrections does not fully allow for the influence of changes in the composition of the atomic nuclei on ionization potentials.

If we consider the consecutive ionization potentials of the same atom, we again have an isoelectronic system, but one in which the atomic nucleus remains the same. Extrapolation of the ionization potentials of isoelectronic systems of this type should lead to smaller errors.

At the present time electron affinities are known for only 25 elements. The most reliable data obtained are for F [9], Cl [9], Br [26], I, H [2], O [22-24], C [7], Ag [3]. Numerous investigations have been concerned with the electron affinities of B, N, Al, Si, P, S, O, C, Na. However, the values obtained in different investigations often differ from each other several tenths of the total value. Nevertheless, it has been concluded from values found for electron affinities that negative ions of Be, Mg, He, Ne, and A cannot exist [12]. On the other hand, negative ions of Li, Na, H, K, Rb, Cs are expected to have real existence [11], and this is confirmed by experimental work. However, Windham [28] succeeded in detecting negative helium ions; this result is inconsistent with the electron affinities found for helium [3,27].

For determination of electron affinities, we considered the dependence of the consecutive ionization potentials I_w of various elements on the degree of ionization w. As expected, this dependence is of the quadratic type; therefore the relationship between $\sqrt{I_w}$ and w is linear (Fig. 1). The lines are plotted from the values of four to seven consecutive ionization potentials (for $w = 4-7$). Extrapolation of the straight lines to $w = 0$ gives $\sqrt{I_0}$, and hence $-I_0$, which is the electron affinity (Table 1).

The linear relationship between $\sqrt{I_w}$ is especially distinct for the following elements: F, Cl, Br, I, Ne, A, Kr, Xe, Rh, Ni, Fe, Co, Ru, Pd, Pt, Mn, Re, Tl, Zr, As, Sb, Bi, Cr, Mo, C, S, Te, Se, C, Sn; Ge, Pb, V, Nb, In, Sc, Tl, Ga, Au, Cu, Cd.

For He, Li, Na, K, Rb, Cs, Be, Ca, Ba, Ra, Hg, i.e., elements of the first two groups, the linear relationship is obeyed somewhat less well, and this leads to error in determinations of electron affinities.

Comparison of the calculated and experimental electron affinities shows good agreement for H^-, S^-, F^-, Cl^-, Br^-, I^- (deviation 0-3%). The relative error is 10% for C, 20% for Be, and 16% for O in comparison with Hagstrum's [23] and Metlay's [22] data, and 70% in comparison with Branscomb's data [24]. Of course, only further experimental investigations will decide which of the values is correct, but Hagstrum's value for O coincides with the calculated values given by many authors [21, 28-30].

In view of the lack of experimental values of electron affinity for the other elements, it is impossible to demonstrate convincingly the advantage of the proposed method over other extrapolation methods, but the good agreement between our values and those which have been determined most accurately (for halogens) indicates that our method is of value.

The electron affinities of elements determined from the $\sqrt{I_w} = f(w)$ relationship are in good agreement with values found by various workers by calculation or extrapolation for H^-, Br^-, Cl^-, F^-, S^-, Ge^-, P^-, Si^-, Al^-, Mg^-, Be^- and other elements. It is only for Hg, Ne, A, and K that the values of I_0 differ greatly from literature data [3,7,21,27].

Examination of the straight lines (Fig. 1) shows that lines of the same direction are obtained partially for groups (A, Xe, Kr, and Rn; Si, Ge, and Sn; Cl, Br, and I) and partially for horizontal rows (Nb, Mo, Ru, Rh, and Pd; Tl, Pb, and Bi; Cd, In, and Sr; Sb and Te; Ni, Fe, and Co; K, Ca, and Sc). Such lines are satisfactorily parallel only if the external electron shells of the elements have similar structure. Fe, Co, and Ni give parallel straight lines, probably because they have similar structure of the outer shell and the same 4d layer is completed. Examination of the lines

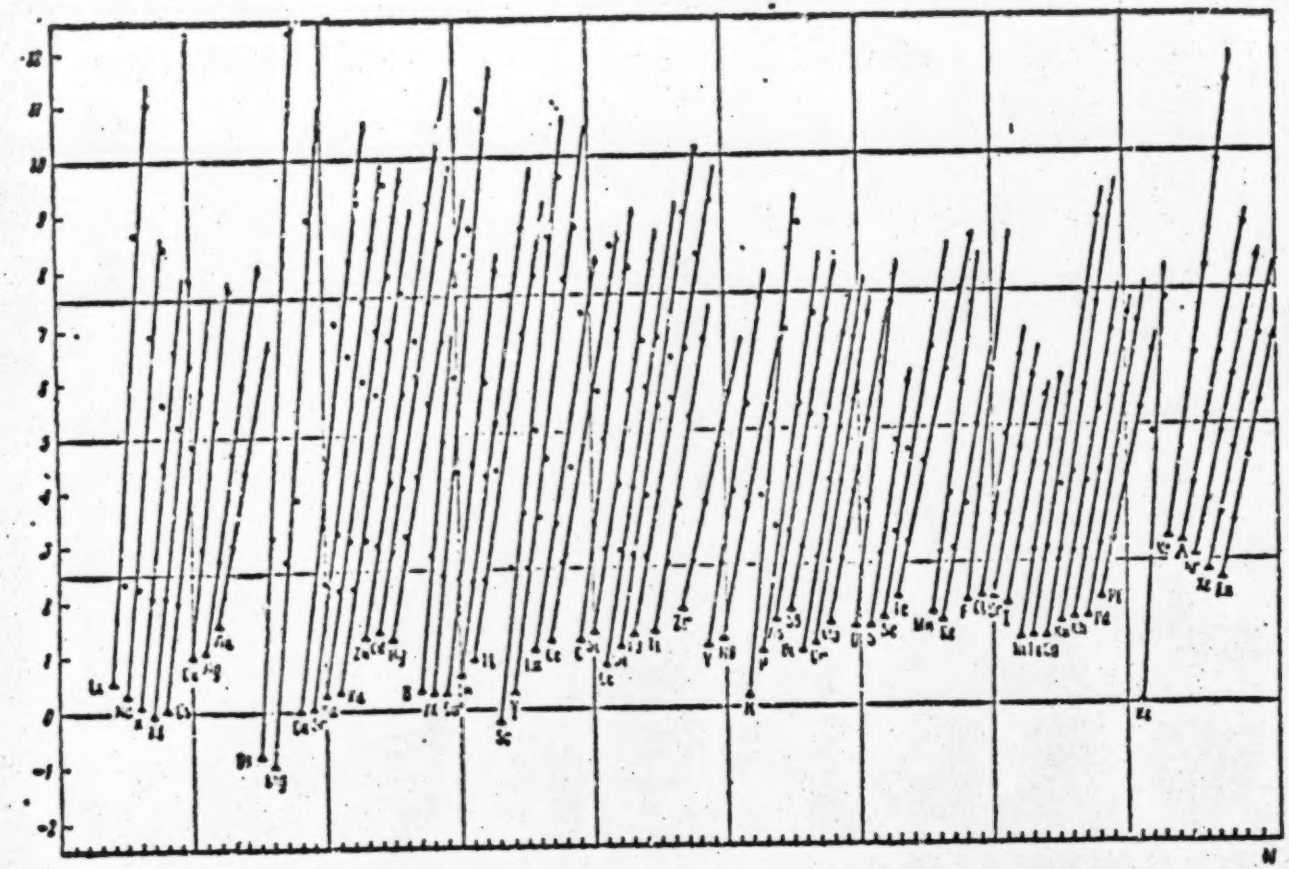

Fig. 1. Variation of the consecutive ionization potentials I_W with the ionic charge W. The triangles represent the values found for I_0. Each abscissa division corresponds to unit W.

TABLE 1.

Element	Data from Fig. 1	Experimental values	Calculated and extrapolated values
H	—	0,72 [2]	0,76 [12], 0,83 [21], 0,73 [27], 0,75 [37]
Li	0,28	—	0,3 [2], 0,34 [12], 0,28 [16], 0,47 [21] 0,38 [27], 0,9 [33], 0,81 [35]
Na	0,08	—	0,08 [12], 0 [21], 0,08 [27], 0,46 [27], 0,81 [32]
K	0,0	—	0,82 [32]
Rb	−0,0	—	—
Cs	0,0	—	—
Cu	0,97	—	0,99 [3]
Ag	1,08	—	1,1 [3]
Au	2,58	—	2,4 [3]
Be	−0,725	−0,6 [20]	−0,8 [12,21]
Mg	−0,9	—	0,91 [12, 21, 27]
Ca	0,0	—	—
Sr	0,01	—	—
Ba	0,16	—	—
Ra	0,16	—	—
Zn	1,82	—	2,17 [7]
Cd	2,1	—	—
Hg	1,89	—	—
B	0,16	> 0 [9]	0,82 [9], 0,1 [12], 0,2 [21], −0,1 [27], −0,13 [33]
Al	0,09	> 0 [9]	0,43 [7], 1,19 [9], 0,15 [12], 0,2 [21], 0,7 [21], 0,5 [27]
Ga	0,09	—	0,18 ± 0,04 [7]
In	0,42	—	0,2 [7]
Tl	1,9	—	—
Sc	−0,01	—	—
Y	0,123	—	—
La	1,1	—	—
Ce	1,56	—	—
Th	1,96	—	—
Zr	3,24	—	—
C	1,44	1,2 [2], 1,6 [7], 1,13 [9], 1,75 [23] 1,2 [38]	1,59 [7], 1,21 [9], 1,37 [12], 1,7 [13], 1,3 [21], 0,91 [24], 1,7 [33] 1,63 [7], 0,6 [12], 1,7 [21], 2,7 [27]
Si	1,82	—	—
Ge	0,56	—	—
Sn	1,1	—	—
Pb	1,56	—	—
V	1,1	—	—
Nb	1,56	—	—
N	0,01	< 0 [7]	0,54 [9], 0,01 [12], −0,5 [17], −0,72, [33]
P	1,0	> 0 [9]	0,75 [7], 1,33 [9], 0,15 [12], 1,1 [21], 0,57 [27]
As	3,43	—	—
Sb	3,43	—	—
Bi	0,9	—	> 0,7 [20]
Cr	1,2	—	—
Mo	2,25	—	—
O	2,56	2,2 [22], [23], 1,48 [24]	2,33 [2], 2,7 [3], 1,4 [9], 3,8 [12], 1,55 [18], 2,2 [21], 1,24 [27], 2,2 [28, 29], 2 [30], 1,13 [33], 1,05 [34], 1,044 [36], 2,35 [39]
S	2,02	2,07 [24]	2,5 [2], 2,25 [7], 2,06 [12], 1,5 [21], 2,17 [27], 2,79 [9]
Se	2,41	> 1,7 [20]	2,2 [7]

TABLE 1 (continued).

Element	Data from Fig. 1	Experimental values	Calculated and extrapolated values
Te	3,42	—	—
Mn	2,73	—	—
Re	2,25	—	—
F	3,62	3,5 [6]. 3,624-0,09 [9], 3,5 [26]	2,0 [1], 4,1 [2], 3,91 [12], 2,9 [27], 3,41 [31]
Cl	3,79	3,82 [6]. 3,824-0,006 [9] [26]	3,78 [2], 3,7 [12], 4,2 [21], 3,54 [31]
Br	3,09	3,6 [6,26]	3,54 [2]
I	3,43	3,3 [6], 3,16 [18], 3,3 [26]	3,12 [2], 3,22 [18]
Fe	1,56	—	—
Ru	2,25	—	—
Co	1,44	—	—
Rh	2,47	—	—
Ni	1,37	—	—
Pd	2,4	—	—
Pt	3,69	—	—
He	0	—	0,0 [3], —0,53 [27]
Ne	9,0	—	—1,2 [21], 3,9 [27]
A	8,4	—	—1,0 [3]
Kr	6,92	—	—
Xe	5,78	—	—
Rn	4,98	—	—

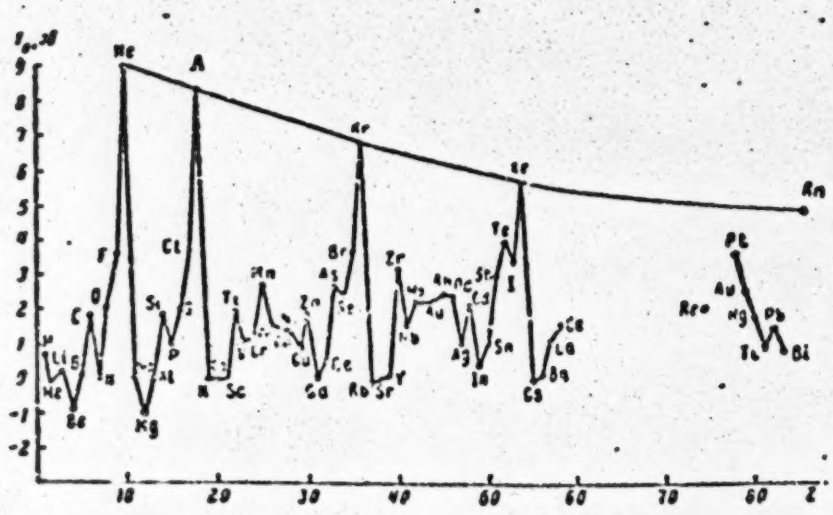

Fig. 2. Variation of the zero ionization potential I_0 with atomic number.

for Nb, Mo, Ru, Rh, Pd leads to a similar conclusion. However, the slope of the lines for these five elements differs from the slope of the lines for Fe, Co, and Ni. The probable explanation is that elements of the iron group have two electrons at the outer s sublevel, whereas elements of the Nb–Rh series have one. The same number of electrons at the outer sublevel with the same azimuthal quantum number l leads to parallel straight lines for the inert gases. For Si, Ge, and Sn, for Co and Zn, and for Sr, and Ba. It should be noted that the slope of the Be and Mg lines is different. It seems that the lighter the elements, the greater influence of the deeper electronic layers on the course of the lines. With increase of the number of electron shells in the atom the parallel effect becomes more pronounced, and the influence of the number of deeper electrons is lost. For the elements of the ninth series (Tl, Pb, Bi) the slope of the lines is not influenced even by the different numbers of 6p electrons.

Table 2 contains values of the constants A and B in the equation $\sqrt{I_w} = A + Bw$ calculated for the straight lines for certain elements. The variation of B shows that the slope of the $\sqrt{I_w} = f(w)$ lines is determined by the quantum numbers. For this reason, for example, the value of B for Zr is not the same as for Co and Fe.

TABLE 2. Values of the Constants A and B in the Equation $\sqrt{I_w} = A + B$ for a Number of Elements ($A = \sqrt{I_0}$)

Element	A	B	Element	A	B	Element	A	B	Element	A	B
Cu	0,98	1,7	I	1,85	1,25	Sb	1,85	1,1	Ni	1,17	1,59
Zn	1,35	1,6	Fe	1,2	1,55	Mo	1,5	1,2	No	3,0	1,65
Tl	1,0	1,48	Ru	1,5	1,26	O	1,6	2,1	A	2,9	1,17
Zr	1,8	0,95	Co	1,2	1,53	Te	1,85	1,17	Kr	2,63	1,12
V	1,05	1,45	Rh	1,6	1,33	F	1,9	2,0	Xe	2,4	1,08
Nb	1,25	1,22	Pd	1,55	1,35	Cl	1,95	1,45	Rn	2,23	1,08
As	1,85	1,3	Pt	1,92	1,12	Br	1,92	1,35			

Equations for groups of elements can be written on the basis of the calculated values of A and B. It is also possible to find missing values of I_w (for example, $I_1 \approx 2.47$ ev for Nb). Examinations of the values found for I_0 indicates that the existence of the negative ions Be-, Mg-, Rb-, Sc-, He- is impossible and that the probability of existence of K-, Cs-, Ca-, Sr- is low.. After the values of I_0 had been determined they were plotted against the atomic numbers of the elements (Fig. 2); the result shows a well-defined periodicity in variations of I_0 (i.e. of electron affinity with the sign reversed).

LITERATURE CITED

1. Atomic Energy Levels. Circular 467, 1949, 1. National Bureau of Standards, Washington.
2. Landolt-Bornstein, Atom und Molekular-physik, Teil. 1: Atome und Ionen, S. 211, Berlin, 1950.
3. Chemist's Reference Book (in Russian) (Goskhimizdat, Moscow-Leningrad (1951) Vol. 1.
4. H. Oldenberg, Phys. Rev., 43, 531 (1933).
5. V. F. Dukel'skii, Dokl. An SSSR, 105, 5, 955 (1955).
6. L. Bakulina, N. Ionov, Dokl. AN SSSR, 116, 1, 41 (1957); 105, 4, 680 (1955).
7. A. Ginsberg, J. Miller, J. Inorgan. Nucl. Chem., 7, 351 (1958).
8. G. Bethe, Z. Phys., 57, 815 (1929).
9. F. Johnson, Nature, 183, 4656, 244 (1959).
10. J. Mayer, Phys., 75, 19 (1932).
11. J. M[illegible], 75, 748 (1932).
12. C. Gl[illegible]ys. Rev., 48, 111 (1934).
13. H. Mass[illegible], Negative Ions, London, 1950.
14. Ta You-wu, Phil. Mag., 22, 837 (1936).
15. H. Fritchard, J. Chem. Phys., 22, 1936 (1954).
16. S. Geltman, J. Chem. Phys., 25, 4, 782 (1956).
17. B. Mobelwitsch, Proc. Phys. Soc., A67, 25 (1954).
18. H. Heilman, M. Mamotenko, Acta Physicochimica, URSS, 7, 1, 127 (1937).
19. L. Szasz, Acta Physic. Acad. Sci hung. (in English), 6, 2, 207 (1956).
20. N. Buchel'nikova, Uspekhi fiz. n., 1, 351 (1958).
21. D. Bates, B. Mobelwitsch, Proc. Phys. Soc., A 68, 540 (1955).
22. M. Melloy, G. Kimball, J. Chem. Phys., 16, 774 (1948).
23. H. Hagstrum, [illegible] mod. Phys., 23, 185 (1951); J. Chem. Phys., 23, 1178 (1951).
24. L. Kerwecomb, S. Smith, Phys. Rev., 88, 4, 1127 (1955); 111, 2, 504 (1958); J. Chem. Phys., 25, 3, 599 (1956); J. Res. Nat. Bur. Standards, 55, 3, 165 (1955).
25. A. Dibrov, [illegible] AN SSSR. Ser. fiz., 19, 1, 10 (1955).
26. P. Windham, P. Joseph [illegible]nman, Phys. Rev., 103, 4, 1103 (1958).
27. H. Pritchard, Chem. F[illegible]. 529 (1953).
28. R. Lozier, Phys. Rev., 46, 268 (1934).

29. H. Bacher, Phys. Rev., 46, 918 (1931).
30. G. Hansen, Phys. Rev., 48, 467 (1935).
31. H. Skinner, H. Pritchard, J. Chem. Phys., 22, 11, 1936 (1954).
32. R. Gaspar, B. Molnar, Acta Phys. Acad. Sci. hung. 5, 1, 75, (1955).
33. Ta You-wu, Phys. Rev., 100, 1195 (1955).
34. H. Schuler, W. Bingel, Z. Naturforsch., 10a 3, 250 (1955).
35. F. Holcien, Nature, 183, 4555, 173 (1959).
36. H. Schmeising, D. Morris, Nature, 181, 4607, 469 (1958).
37. T. Aray, T. Onishi, J. Chem. Phys., 26, 1, 70 (1957).
38. R. Honig, J. Chem. Phys., 22, 126 (1954).
39. J. Margrave, J. Chem. Phys., 22, 11, 1937 (1954).

All abbreviations of periodicals in the above bibliography are letter-by-letter transliterations of the abbreviations as given in the original Russian journal. *Some or all of this periodical literature may well be available in English translation.* A complete list of the cover-to-cover English translations appears at the back of this issue.

INTERNAL ROTATION IN PROPANE AND n-BUTANE

N. P. Borisova and M. V. Vol'kenshtein

Institute of High Polymers, Academy of Sciences USSR, Leningrad
Translated from Zhurnal Strukturnoi Khimii, Vol. 2, No. 4,
pp. 469-475, July-August 1961
Original article submitted July 4, 1960

The potentials given in the preceding paper [21] were used for calculating the steric contribution to the potential barrier to internal rotation in propane, and the energy of internal rotation in n-butane in relation to three angles of internal rotation. It is shown that rotational isomerization of n-butane may occur by-passing the high barrier, and that the energy difference between rotational isomers of n-butane depends both on the steric effect and on the effect of bond orientation. The main contribution of the "steric" energy difference between rotational isomers is made by interaction of methyl-group carbons with hydrogen atoms nearest to each other in these groups. The angle corresponding to the minimum energy for the coiled isomer must be somewhat less than 120°.

INTRODUCTION

Internal rotation about single bonds is not free, and this is the cause of rotational isomerism. The nature of the restricting potential has been the subject of numerous investigations, but the question cannot be regarded as finally solved.

Several authors consider restriction in ethane and its substituted derivatives to be due to steric (van der Waals) repulsion of nonbonded atoms [1-6]. We shall show that in fact this factor is not of primary significance.

In another group of papers [7-10] electrostatic (multipole) repulsion of the electron shells of the bonds is considered.

This interaction should probably be taken into account, especially in the case of polar bonds, but it is not the main cause of the restriction. Evidence for this is provided, in particular, by the fact that replacement of an H atom by an F atom in ethane does not result in any appreciable change of the value of the potential barrier of internal rotation [11].

Disturbance of the axial symmetry of the C–C bond by the perturbing influence of attached groups has been considered in [11] and [12]. It was shown that this effect cannot restrict internal rotation to any appreciable extent.

Attempts [12-15] were made to explain restriction by the fact that the C–C bond is partially double as the result of hyperconjugation. However, the effect was not calculated systematically; moreover, restriction can be interpreted without it.

Finally, there have been several investigations of the influence of exchange repulsion of the bond orbitals on internal rotation in molecules [12,17-19]. With the ordinary sp^3 hybridization of the electrons of the carbon atom the interaction energy is independent of the angle of internal rotation [17]. Dependence of this type appears if an "admixture" of the d and f states is taken into account [12,18]. However, G. and F. Harris [19] showed that the internal rotation barrier cannot be explained in terms of this effect. Taking the excited covalent structures of the H--C--C--H six-electron system into account and using the sp^3 carbon orbitals and the s hydrogen orbitals, these authors obtained a value for the barrier in ethane which was roughly double the experimental value. The barrier should probably decrease if the d and f state are taken into account. Further details concerning calculations of the restricting potential are given in [20].

The internal rotation potential for substituted ethanes can be represented by the expression

$$U(\varphi) = \frac{U_0}{2}(1 - \cos 3\varphi) + \sum_{i,k} U_{i,k}(r_{i,k}), \qquad (1)$$

where φ is the angle of rotation about the C–C bond, relative to the trans configuration of ethane; the term U_0 includes interaction of the $C_i \cdots C'_k$, $C_i \cdots C'_4$, $C'_k \cdots C_4$, $C_i \cdots Y'_k$, $C_i \cdots Y'_k$, $C'_k \cdots X_i$, $C_4 \cdots X_i$, electron clouds (i, k = 1, 2, 3; see Fig. 1); $U_{ik}(r_{ik})$ is the energy of $X_i \cdots Y_k$, $X_i \cdots Y_k$ interaction. Since $U_{ik}(r_{ik})$ also depends on φ, U_0 is not the potential barrier of the $X_1X_2X_3C-CY_1Y_2Y_3$ molecule, and therefore it cannot be found directly from experimental data. For a rigorous quantum-mechanical calculation of U_0 we must consider spin–spin interaction [19] and $X_i - C_i \cdots C'_k - Y'_k$ exchange repulsion [18] with the excited states of the C_i, C_k and X_i, Y'_k taken into account. It seems likely, however, that for $H_3C-CX_1X_2X_3$ molecules U_0 differs little from the value of the potential barrier.

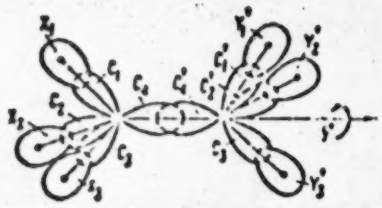

Fig. 1. Schematic representation of a $X_1X_2X_3C-CY_1Y_2Y_3$ molecule.

The first term in (1) characterizes the effect of bond orientation. U_{ik} is obtained additively from the steric and electrostatic interactions of the "attachments" [16]. In hydrocarbons, because of the small dipole moment of the C–H bond, only steric interaction is significant. The form of the potential curve of internal rotation is primarily determined by the bond orientation effect. The steric effect deforms the curve of the "ethane" type [10]. In the case of ethane this effect is independent of φ and (1) reduces to the form

$$U(\varphi) = \frac{U_0}{2}(1 - \cos 3\varphi), \qquad (2)$$

and U_0 is the exact value of the barrier. An equation of type (2) is also valid for $X_3C-CY_1Y_2Y_3$ molecules where the steric factor alters the value of the barrier but not the character of the angular dependence. For molecules of other substituted ethanes (XH_2C-CH_2Y, $XH_2C-CHY_1Y_2$ etc.) the potential does not have the periodic form of (2); in such cases rotational isomerism is observed [20]. It is generally considered that the energy difference ΔU between rotational isomers is determined by interaction of the attached groups [6].

Calculations of these energy differences, based on the concepts discussed above, are given in [6]. Excessively high values of ΔU were obtained for hydrocarbons. We consider that the discrepancy is due, first, to the fact that the "triplet" potential was used for estimating interaction of hydrogen atoms and, second, to the fact that the average value of the methane potential was used for estimation of methyl group interaction. An analysis of these hypotheses is given in the previous paper [21].

The good agreement with experimental data for halogen-substituted ethanes, despite the first of the above errors, is associated with partial compensation of H – – – H and H – – – Hal interactions.

Pitsyn and Sharonov [22] analyzed the various interatomic distances in n-butane and showed that interaction of distant "attachments" must be taken into account. They considered that the most advantageous configurations of the methyl groups are determined by the minimum steric interaction between these groups, corresponding to a rotation of each methyl group through an angle of about 23° relatively to the trans position. In this position interactions of the $H_1,H_2,H_3 \cdots C_4,H_5H_7$ type are responsible for 40% of the energy difference between the coiled and trans isomers, and interactions of the $H_1, H_2, H_3 \cdots H_8, H_9, H_{10}$ type for 20% ΔU. However, the effect of bond orientation is not considered in [22]. Moreover, since their estimates of the contributions to ΔU were based on a consideration of interatomic distances, and the character of the potentials was not taken into account, we consider that their results require verification.

The purpose of the present investigation is an examination of the conditions for internal rotation in molecules of the simple alkanes, propane and n-butane.

Steric Interactions in Propane and Butane

The arrangement of atoms in the propane molecule is shown in Fig. 2. We aim to find the contribution of steric interactions to the energy of internal rotation about the C_1-C_2 bond. These interactions may be classified as follows.

1. Interactions independent of φ_1. It was shown in the preceding paper [2] that $H_1,H_2,H_3 \cdots H_4,H_5$ interactions are virtually independent of the angle φ and therefore have no influence on the barrier. With regard to $H_1,H_2,H_3 \cdots C_3$ interactions, calculations based on the U_{C-H} potential, given in [21], show that this interaction represents attraction at any value of φ. The least energy corresponds to $\varphi = 0$ (the angles are reckoned from the trans position, and the anticlockwise direction is taken as positive).

2. Interactions dependent on φ_1. The $H_6,H_7,H_8 \cdots H_4,H_5,C_1$ interactions are independent of φ. The relative positions of the $H_6,H_7,H_8 \cdots H_4, H_5\,C_2$ atoms are determined by the effect of bond orientation, which gives minimum energy at $\varphi_1 = 0$, i.e., in the trans position. Steric interaction (weak attraction) again corresponds to minimum energy at $\varphi_1 = 0$.

The $H_1, H_2, H_3 \cdots H_6, H_7, H_8$ interactions depend also on φ, and at any angle $\varphi_1 \neq 0$ the effect of bond orientation results in repulsion. If we assume that U_0 for propane is close to U_0 for ethane, i.e., about 3.0 kcal/mole, then 15° rotation about the $C_2 \cdots C_3$ bond corresponds to a repulsion energy of 0.4 kcal/mole. Therefore it may be taken that φ_1 varies within narrow limits. Let us suppose that $15° < \varphi_1 \geq 0$. Calculation shows that with this assumption any value of φ gives attraction, and $\varphi = \varphi_1 = 0$ corresponds to minimum energy. Summation of all the interactions shows that the contribution of steric attraction to the potential barrier of propane is 0.25 kcal/mole.

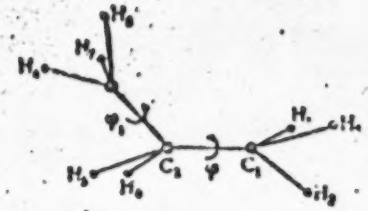

Fig. 2. Rotations in the propane molecule.

It is evident that steric interaction should also result in attraction in the molecules of isobutane and $(CH_3)_2CHCH_3$ and tetramethylmethane $(CH_3)_3C-CH_3$ and the steric contributions to the potential barriers of these molecules are likely to be of the same order of magnitude as in propane. We consider that in any molecules of the XH_2C-CH_3, $X_1X_2HC-CH_3$, $X_1X_2X_3C-CH_3$ types the $X \cdots H$ interactions are small, and this accounts for the similar values of the barrier. In molecules of the XH_2C-CH_2Y type $X-Y$ interactions may be considerable and may introduce substantial contributions into the barrier. The n-butane molecule (Fig. 3) belongs to this type.

Internal rotation in n-butane depends, generally speaking, on the three angles $\varphi_1, \varphi_2, \varphi_3$. As was first pointed out by one of us [23], the barrier in butane should be considerably higher than in ethane, and the $\varphi, \varphi_1, \varphi_3$ rotations must be so correlated that the molecule does not pass through this barrier.

It was shown above that $H_1, H_2, H_3 \cdots H_4, H_5, H_8, H_9, H_{10} \cdots H_6, H_7, H_4, H_5 \cdots H_6, H_7$ interactions are virtually independent of the angles $\varphi, \varphi_1, \varphi_3$. The other interactions are characterized as follows.

1. Interactions independent of φ_1 and φ_3. Calculation based on the potential given in [21] shows that with $0 \leq \varphi \geq 90°$ this interaction corresponds to weak attraction, and with $\varphi > 90°$, to repulsion (see table). The $H_1, H_2 \cdots C_4$ and $H_6, H_7 \cdots C_1$ interactions correspond to attraction at any value of φ; their contributions to the barrier and to ΔU are very small.

2. Interactions dependent on φ_1 (or φ_2). The relative positions of the atoms are determined mainly by the effect of bond orientation and to a lesser extent by steric interaction (attraction). For $H_1, H_2, H_3 \cdots H_4, H_5, C_2$ interaction both effects give an energy minimum at $\varphi_1 = 0$ ($\varphi_2 = 0$), i. e., in the trans position.

The $H_1, H_2, H_3 \cdots C_4$ interactions depend on φ_1 and φ (on φ_2 and φ). With $0 \geq \varphi < 120°$ there is weak attraction which depends little on φ_1. With $180° > \varphi \geq 120°$ the interaction depends on φ_1, but is again very weak. Finally, when $\varphi = 180°$ the effect of φ_1 on the energy is considerable. In the most advantageous position, when $\varphi_1 = 0$, the energy is 0.15 ± 0.05 kcal/mole. When $\varphi_1 \geq 30°$ it increases to 1.0 kcal/mole.

The most advantageous position for $H_1, H_2, H_3 \cdots H_6, H_7$ interactions corresponds to $\varphi_1 = \varphi_2 = 0$. The interaction energy is negative and depends little on φ.

3. Interactions dependent on all three rotation angles. With $0 \geq \varphi < 60°$ attraction which is almost independent of φ_1 and φ_2 corresponds to $H_1 H_2 H_3 \cdots H_8 H_9 H_{10}$ interactions. When $\varphi = 90°$, φ_1 and φ_2 have a slight effect: the energy difference between the least advantageous position $\varphi_1 = \varphi_2 = 60°$ and the most advantageous position $\varphi_1 = \varphi_2 = 0$ is 0.3 kcal/mole. At $\varphi = 120°$ attraction occurs if $75° < \varphi_1, \varphi_2 < 105°$; with other values of φ_1 and φ_2 there is repulsion. Its energy at $\varphi_1 = \varphi_2 = 0$ is 0.4 ± 0.1 kcal/mole. Thus, at $\varphi = 120°$ steric repulsion is superposed on the bond orientation effect. Here the most advantageous values of φ_1 and φ_2 are no longer 0°, but are shifted somewhat in the direction of negative angles ($\varphi_1 = \varphi_2 \approx -10°$). A shift of $\varphi_1 = \varphi_2$ to −5° also occurs with $\varphi = 150°$. When $\varphi = 180°$ there is repulsion with an energy minimum of 1.0 ± 0.2 kcal/mole at $\varphi_1 = \varphi_2 = 0$.

Summation of all the main steric interactions at $\varphi_1 = \varphi_2 = 0°$ (the interaction energy U in kcal/mole) gives the following results (see also Figs. 4 and 5):

φ	$U_{C_1-C_4}$	$U_{H_1-H_8}$	U_{tot}
120°	0.50±0.10	0.40±0.10	0.90±0.20
180°	2.00±0.50	1.00±0.30	3.00±0.50

Calculations show that the energy difference ΔU between rotational isomers and the steric contribution to the potential barrier are determined essentially by only two types of interactions: $C_1 \cdots C_4$ and the nearest hydrogens of the methyl groups (see table). The contributions of the remaining interactions are negligibly small and can therefore be ignored. It follows from the table that these interactions make roughly equal contributions to ΔU; therefore interactions of the I and III orders, and not [illegible] and II orders as stated in [22], are the most important in this respect.

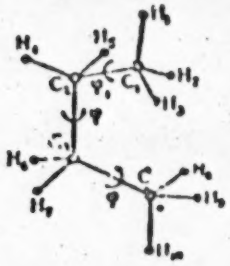

Fig. 3. Rotations in the n-butane molecule.

The dependence of the internal rotation energy on φ with $\varphi_1 = \varphi_3 = 0$ is plotted in Fig. 4. The diagram contains the curve for steric interaction calculated in this paper, the curve corresponding to the bond orientation effect

$$U(\varphi) = \frac{3}{2}(1 - \cos 3\varphi) \text{ kcal/mole}$$

and the curve for the total energy, the sum of the other two. The energy difference for rotational isomers is found to be $\Delta U = 0.9 \pm 0.2$ kcal/mole, which is in good agreement with the experimental value [20]. The steric contribution to the barrier is 3.0 ± 0.8 kcal/mole*.

Figure 5 represents the dependence of U on φ and $\varphi_1 = \varphi_3$. It is seen that as the result of correlation of rotations about the H_3C-CH_2 and H_2C-CH_2 bonds the transition of the molecule from the trans to the coiled position can be effected by the route shown by the dash line, without the surmounting of a high barrier.

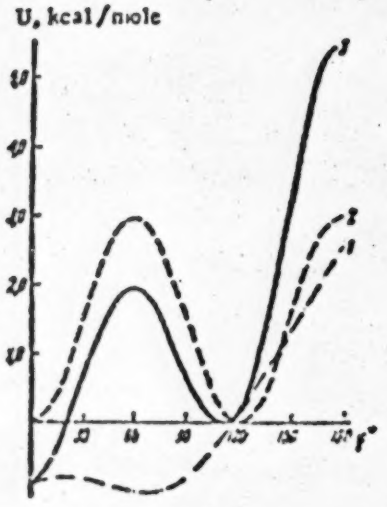

Fig. 4. Dependence of the internal rotation energy of n-butane on φ with $\varphi_1 = \varphi_3 = 0$. Curve 1) Steric interaction; 2) interaction due to the bond orientation effect; 3) total curve.

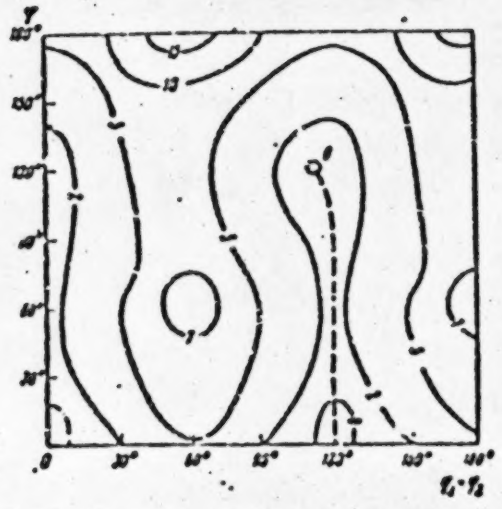

Fig. 5. Dependence of the internal rotation energy (in kcal/mole) of n-butane on φ and $\varphi_1 = \varphi_3$. The dash line represents the course of isomerization.

Rotational Isomers of n-Butane

In addition to the stable trans isomer, n-butane exists as the right and left coiled rotational isomers, but with the angle φ different from 120°. The value of the angle φ_{coll} is given by the minimum of (1):

$$1{,}5U_3 \sin 3\varphi_{min} + \sum_{i,k} \frac{\partial U'_{ik}}{\partial r_{ik}} \left(\frac{\partial r_{ik}}{\partial \varphi}\right)_{\varphi=\varphi_{min}} = 0. \qquad (3)$$

It can be shown that (3) is satisfied when $\varphi_{min} < 120°$. The shift from $\varphi_{min} = 120°$ is determined by the magnitude of U_3. It is evident that when $\varphi = 120°$ the energy difference between rotational isomers is determined not only by

*No reliable experimental data are available on the internal rotation barrier in n-butane. However, the experimental value, in kcal/mole, of the potential barrier in the $(CH_3)_3C-C(CH_3)_3$ molecule is in fair agreement with our value of 12 kcal/mole, which indicates that steric interaction of methyl groups makes a considerable contribution to the barrier of the $(CH_3)_3C-C(CH_3)_3$ molecule, and therefore of n-butane.

th· steric but also by the orientational factors,

$$\Delta U = \frac{U_0}{2}(1 - \cos 3\varphi) + \Delta U_{steric}. \quad (4)$$

We wish to find φ_{min} from conditions (3) and (4), starting with the experimental value $\Delta U = 0.9 \pm 0.4$ kcal/mole and ΔU_{steric} based on the preceding calculations (See Fig. 1). Varying U_0 within reasonable limits, we find $\varphi_{min} = 106°$ with $U_0 = 3.5 \pm 1.0$ kcal/mole. In this case $\Delta U = 0.7 \pm 0.2$ mole. The steric and orientational contributions to ΔU are 0.25 ± 0.05 and 0.45 ± 0.15 kcal/mole respectively. Varying φ between 106 and 120°, we find that even with $\varphi = 110°$ we have to assume $U_0 > 5$ kcal/mole to obtain sensible values of ΔU; however, this value seems too high. If we take $\varphi = 120°$, then $\Delta U = U_{steric} = 0.9 \pm 0.2$ kcal/mole. Therefore, for simplicity in calculations involving ΔU only, we may confine ourselves to steric interaction only, although in reality the energy difference between rotational isomers cannot be ascribed solely to the steric effect, but, like the potential barrier, it also depends on the bond orientation effect. All the foregoing is applicable to calculations of steric effects in hydrocarbons of both low and high molecular weight.

Calculation Error

The relative calculation error, associated with the choice of the U_{C-C} potential and determined by inaccuracy of the parameters, is about 10-20% in the region of $r/3.3 \text{ A} \geq 0.85$, and somewhat greater in the $r/3.3 \text{ A} < 0.80$ region. We shall assume that the errors associated with the U_{H-H} and U_{C-H} potentials are of the same order. The use of these potentials with distances $r_{C-C}/3.3 \text{ A} > 0.85$, $r_{H-H}/2.4 \text{ A} > 0.75$, $r_{C-H}/2.85 \text{ A} > 0.75$ results in relatively small errors (of the order of 0.02 kcal/mole in the attraction region; of the order of 0.20 kcal/mole with repulsion not in excess of 1 kcal/mole. As these are just the distances used in estimates of energy differences of rotational isomers, it is quite legitimate to use these potentials for quantitative estimations. In calculations of the steric contribution to the barrier these potentials should be used with caution, because of the large error (of the order of 1 kcal/mole); therefore such calculations are to be regarded as semiquantitative.

It must be emphasized that we assumed the valence angles to be tetrahedral in all cases. In reality they may differ appreciably from 109° 28'; the electron-diffraction value of the C–C–C valence angle in n-butane is 112° [24].

Therefore one should not attach special importance to our value of $\varphi_{min} = 106°$ or be surprised at its disagreement with the experimental value $\varphi_{min} = 117 \pm 5°$ (more probably 117°–8° = 109°) [21]. However, this cannot influence the general inferences regarding the energy differences of rotational isomers.

We thank T. M. Birshtein and O. B. Ptitsyn for valuable discussions.

LITERATURE CITED

1. H. Eyring, J. Amer. Chem. Soc., 54, 3191 (1932).
2. J. Aston, J. Chem. Phys., 12, 336 (1944).
3. F. French, R. Rasmussen, J. Chem. Phys., 14, 339 (1946).
4. S. Midzushima, Structure of Molecules and Internal Rotation [Russian translation] (Izd. inostr. lit., Moscow, 1957).
5. K. Howlett, J. Chem. Soc., 4353 (1957).
6. E. Mason, M. Kreevoy, J. Amer. Chem. Soc., 77, 5808 (1955); 79, 4851 (1957).
7. J. W. Smith, Sci. Progr., 43, 660 (1955).
8. L. J. Oosterhoff, Disc. Faraday Soc., 10, 79 (1951).
9. E. Lassettre, L. Dean, J. Chem. Phys., 17, 317 (1949).
10. Au Chin-Tang, J. Chin. Chem. Soc., 18, 123 (1951); 19, 33 (1952); Sci. Sinica, 3, 279 (1954).
11. E. B. Wilson, Proc. Nat. Acad. Sci U. S. A., 43, 816 (1957).
12. E. Gorin, J. Walter, H. Eyring, J. Amer. Chem. Soc., 61, 1876 (1939).
13. A. Eucken, K. Schafer, Naturwiss. 8, 122, (1939).
14. K. Pitzer, J. Hollenberg, J. Amer. Chem. Soc., 76, 1493 (1954).
15. H. Eyring, G. Stewart, R. Smith, Proc. Nat. Acad. Sci. U. S. A., 44, 259 (1958)
16. E. B. Wilson, Advances Chem. Phys., II, 367 (1959).
17. W. Penney, Proc. Roy. Soc., A144, 166 (1934).
18. L. Pauling, Proc. Nat. Acad. Sci. U. S. A., 44, 211 (1958).
19. G. Harris, F. Harris, J. Chem. Phys., 31, 1450 (1959).
20. M. V. Vol'kenshtein, Configuration Statistics of Polymer Chains [in Russian] (Izd. AN SSSR, Moscow, 1959).
21. N. P. Borisova, M. V. Vol'kenshtein, Zh. strukt. khimii, 2, 3, 316 (1961).
22. O. B. Ptitsyn and Yu. A. Shatonov, Zh. tekhn. fiziki, 27, 2741 (1957).

23. M. V. Vol'kenshtein, Dokl. AN SSSR, 49, 511 (1945).
24. K. Kuchitsu, Bull. Chem. Soc. Japan, 32, 748 (1959); R. Bonham, L. Bartell, J. Amer. Chem. Soc., 81, 3491 (1959).

All abbreviations of periodicals in the above bibliography are letter-by-letter transliterations of the abbreviations as given in the original Russian journal. *Some or all of this periodical literature may well be available in English translation.* A complete list of the cover-to-cover English translations appears at the back of this issue.

BRIEF COMMUNICATIONS

ELECTRON-DIFFRACTION STUDY OF THE FERROCENE MOLECULE

P. A. Akishin, N. G. Rambidi, and T. N. Bredikhina

M. V. Lomonosov Moscow State University

Translated from Zhurnal Strukturnoi Khimii, Vol. 2, No. 4,
p. 476, July-August 1961
Original article submitted December 14, 1960

Systematic studies of the molecular structure of electron-unsaturated compounds are being conducted in the Laboratory of Electron-Diffraction Molecular Studies of the Chemical Faculty, Moscow State University. This brief communication gives the preliminary results of a study of the geometry of the ferrocene molecule in the vapor state.

The "sandwich" structure of the ferrocene molecule has been reliably established, both by x-ray diffraction studies of crystals [1-4] and by electron-diffraction studies of ferrocene vapor [5]. The purpose of our investigation was refinement of the geometrical parameters of the ferrocene molecule and of the nature of the relative motion of the cyclopentadienyl groups.

Nine series of electron-diffraction patterns with two plates in each series, were obtained and studied. A refined technique was used for interpretation of the experimental sector-microphotometric scattering intensity. The following parameters were found for the ferrocene molecule:

$$r(C-H) = 1.12 \pm 0.02 \text{ Å};$$
$$r(C-C) = 1.42 \pm 0.01 \text{ Å};$$
$$r(Fe-C) = 2.07 \pm 0.01 \text{ Å}.$$

Analysis of the experimental results indicates free rotation of the cyclopentadienyl groups about the axis perpendicular to the ring plane. These results are in agreement with the data reported by Seibold and Sutton [5]. A detailed account of the results and of the refined technique for interpretation of the electron-diffraction patterns will be published in the near future.

LITERATURE CITED

1. E. O. Fischer, W. Pfab, Z. Naturforsch., 7b, 377 (1952).
2. P. Eiland, R. Pepinsky, J. Amer. Chem. Soc., 74, 4971 (1952).
3. J. D. Dunitz, L. E. Orgel, A. Rich, Acta crystallogr., 9, 373 (1956).
4. Yu. T. Struchkov, Zh. obshch. Khimii, 27, 2039 (1957).
5. E. A. Seibold, L. E. Sutton, J. Chem. Phys., 23, 1967 (1955).

All abbreviations of periodicals in the above bibliography are letter-by-letter transliterations of the abbreviations as given in the original Russian journal. *Some or all of this periodical literature may well be available in English translation.* A complete list of the cover-to-cover English translations appears at the back of this issue.

THE TWO-STRUCTURE MODEL OF WATER

A. Ye. Namiot

All-Union Petroleum Gas Scientific Research Institute
Translated from Zhurnal Strukturnoi Khimii, Vol. 2, No. 4,
pp. 476-477, July-August 1961
Original article submitted April 12, 1961

Recently certain investigators have used a two-structure model of water for explaining various properties of water and aqueous solutions [1-4]. It is assumed in the two-structure model of water that liquid water contains two structures at equilibrium: the first which reproduces, within the limits of short-range order, the ice lattice (structure 1); and a second, denser structure (structure 2). Different authors define the second structure in different ways. Hall [1] considers that the second structure corresponds to closest packing of the water molecules. Grotheim and Krogh-Moe [2] takes the second structure to be water in the hypothetical state of a "normal" liquid. It has already been noted [3] that the earlier concept introduced by Samoilov [5,6] according to whom some of the molecules in liquid water are in places corresponding to cavities in the ice lattice is the physical basis for identification of the second, close-packed, water structure.

We shall show that the ratio between the number of water molecules in the first and second structures, calculated with Hall's data from the difference between the free energies of the two structures [1], and used by other authors [3,4], is almost the same at 0° as the calculated value based on Samoilov's theory.

We assume that the density of structure 1 is equal to the density of ice at 0°. Regarding structure 2 as the ice lattice in which all the cavities are filled with water molecules, we find that the density of this structure is 1.5 times the density of ice. In the ice structure each cavity is enclosed by six of its nearest molecules at distances of 2.84 A from its center. At the same time each molecule is the nearest neighbor of three cavities. Therefore the number of molecules is double the number of cavities in the ice structure, and when all the cavities have been filled with molecules (structure 2) the number of molecules per unit volume and hence the density increases by a factor of 1.5.

From the expression for molar volume of water as the sum of the molar volumes of the constituent structures we find the mole fraction N_1 of structure 1:

$$\frac{18.02}{0.9998} = N_1 \frac{18.02}{0.9168} + (1 - N_1) \frac{18.02}{0.9168 \cdot 1.5}$$

The numerical values in the equation represent the molecular weight of water and the densities of water and ice at 0°. The value found, $N_1 = 0.75$ is very close to the value $N_1 = 0.72$ calculated from Hall's data.

LITERATURE CITED

1. L. Hall, Phys. Rev., 73, 775 (1948).
2. K. Grotheim, J. Krogh-Moe, Acta chem. scand; 8, 1193 (1954).
3. I. G. Mikhailov, Yu. P. Syrnikov, Zh. strukt. khimii, 1, 12 (1960).
4. A. Yu. Namiot, Zh. strukt. khimii, 2, 4, 405 (1961).
5. O. Ya. Samoilov, Zh. fiz. khimii, 20, 12, 1411 (1946).
6. O. Ya. Samoilov, Structure of Aqueous Electrolyte Solutions and Ion Hydration [in Russian] (Izd. AN SSSR, Moscow (1957).

CRYSTAL STRUCTURE OF DIPHENYLTRICHLOROSTIBINE

T. N. Polynova and M. A. Poral-Koshits

M. V. Lomonosov Moscow State University

Translated from Zhurnal Strukturnoi Khimii, Vol. 2, No. 4,
pp. 477–478, July-August 1961
Original article submitted September 12, 1960

Crystals of $(C_6H_5)_2SbCl_3$, obtained by the double diazonium salt method [1], are in the form of plates and belong to rhombodipyramidal type of symmetry. Simple forms are developed: pinacoid {010}, rhombic prism {110}, and rhombic bipyramid {111}. The ratio $a:1:c = 1.641:1:0.883$ was found from x-ray oscillation patterns and powder diagrams: $c = 17.94$, $b = 9.71$, $c = 8.56$ A ($\pm$ 0.02 A) $\rho_{meas} = 1.62$ g/cc, $\rho_{calc} = 1.72$ g/cc, $N = 4$. The axial ratio from x-ray data is: $a:1:c = 1.85:1:0.884$. Space group Pbcn.

The positions of the Sb atoms were found from Patterson projections on the XY and YZ plane. The positions of the Cl atoms were determined by the minimalization method. Electron density projections on the same plane were used for confirmation. The following values were obtained for the atomic coordinates:

	x	y	z
Sb	0,250	0,473	0,750
Cl_I	0,176	0,473	0,000
Cl_{II}	0,323	0,473	0,500
Cl_{III}	0,250	0,723	0,750

The positions of the C atoms were determined by geometrical analysis with Kitaigorodskii's structure finder [2]. The slopes of the phenyl-group planes such that the molecules are packed in the cell without appreciable strain were found. On this basis the coordinates of the C atoms were found in the first approximation:

	x	y	z		x	y	z
C_1	0,33$_9$	0,26$_1$	0,36$_6$	C_7	0,12$_1$	0,42$_5$	0,51$_3$
C_2	0,35$_9$	0,20$_6$	0,81$_9$	C_8	0,06$_3$	0,31$_9$	0,43$_5$
C_3	0,41$_5$	0,15$_3$	0,89$_3$	C_9	0,0[illegible]$_4$	0,21$_6$	0,48$_3$
C_4	0,45$_3$	0,21$_6$	0,01$_7$	C_{10}	0,10$_4$	0,[illegible]$_3$	0,63$_3$
C_5	0,43$_6$	0,35$_6$	0,07$_7$	C_{11}	0,09$_3$	0,15$_4$	0,60$_3$
C_6	0,38$_3$	0,42$_5$	0,95$_7$	C_{12}	0,14$_3$	0,20$_6$	0,68$_6$

The $(C_6H_5)_2SbCl_3$ molecule has the configuration of a trigonal bipyramid, like $(CH_3)_2SbCl_3$ [3], $(ClCH=CH)_3SbCl_2$ [4] and $(C_6H_5)_3SbCl_2$ [5]. The phenyl groups lie in the equatorial plane of the bipyramid, occupying two vertices of a triangle with an Sb atom in its center, and one of the Cl atoms (III) at the third vertex. The other two (axial) Cl atoms (I and II) occupy the remaining vertices of the trigonal bipyramid. The Sb–Cl distances are unequal: 2.52 A for Cl_I and Cl_{III}, and 2.43 A for Cl_{III}. The nonequivalence of the Sb–Cl bonds should evidently influence the chemical properties of $(C_6H_5)_2SbCl_3$. Apparently, by analogy with compounds of the R_3PX_2 type [6], the two axial Cl atoms in diphenyltrichlorostibine have greater mobility than the third (equatorial) chlorine.

It is intended to determine the atomic coordinates more precisely by calculations based on the electron density projections with C atoms taken into account, and also with the aid of difference series.

LITERATURE CITED

1. O. A. Reutov, O. A. Pritsyna, Izv. AN SSSR, Otd. khim.n., 1, 93 (1952).
2. A. I. Kitaigorodskii, Izv. AN SSSR, Otd. khim. n., 6, 587 (1946).
3. A. F. Wells, Z. Krystallogr., A99, 367 (1938).
4. Yu. T. Struchkov, T. L. Khotsyanova, Dokl. AN SSSR, 91, 3, 565 (1953).
5. T. N. Polynova, M. A. Poral-Koshits, Zh. strukt. khimii, 1, 2, 159 (1960).
6. Gennadyi, M. Kosolapoff, Organophosphorus Compounds, 61, New York, 1960.

THE STRUCTURE OF BENZOFUROXANE

G. A. Gol'der Z. V. Todres-Selektor, and S. V. Bogdanov

L. Ya. Karpov Physicochemical Scientific Research Institute
K. E. Voroshilov State Scientific Research Institute of Organic Intermediates and Dyes
Translated from Zhurnal Strukturnoi Khimii, Vol. 2, No. 4,
478-479, July-August 1961
Original article submitted August 18, 1960

The chemical properties of benzofuroxane may be represented by means of formula (I), but the absence of substitutional isomers of benzofuroxane derivatives [1] and the formation of only one compound in the synthesis of naphtho-α,β-furoxane or pyridofuroxane [2,3] suggest the possible structural formulas (II, III).

The existing literature data are inadequate [4] for definite choice of one of these structures.

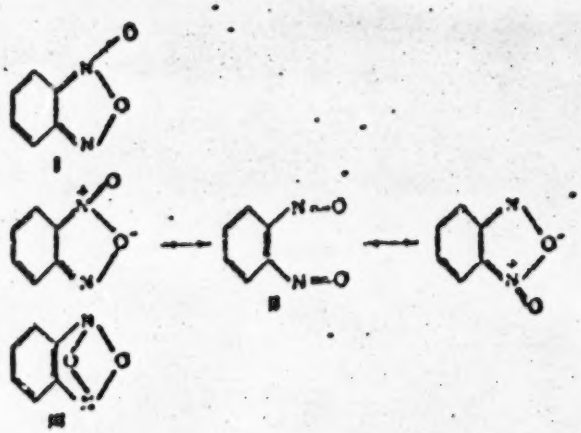

In the present communication an attempt is made, without recourse to very laborious complete x-ray structural analysis, to deduce the molecular structure of benzofuroxane from x-ray diffraction measurements and geometrical analysis of the molecular packing in the unit cell.

Single crystals of benzofuroxane (m.p. 70-71°), suitable for x-ray work, were obtained by slow evaporation of an aqueous solution of the compound at room temperature. The slightly yellowish transparent crystals are unstable in air; therefore they had to be sealed in Pyrex capillaries. Goniometric measurements and Laue patterns taken along the three principal crystallographic axes showed that the crystal belongs to the C_{2h} Laue class. Oscillation x-ray patterns and x-ray goniometric scanning of the zero layer lines gave the following unit cell constants: $a = 13.90$, $b = 7.56$, $c = 6.32$ A, $\beta = 111°$. From the interference extinctions, the benzofuroxane crystal can be assigned to the $C_{2h}^3 = C2/m$ or $C_2^3 = C2$ or $C_s^3 = Cm$, space groups. Goniometric measurements of well-formed crystals suggest the existence of a center of symmetry; i.e., the crystal may be assigned to the $C_{2h}^3 = C2/m$ group. This suggestion was confirmed by measurements of the piezo effect (not detected) and by analysis of Patterson projections in the [010] and [100] directions. The pycnometric density of the crystal is 1.45 g/cc, which defines the number of molecules in the unit cell as $Z = 4$; the x-ray density calculated from the constants given above is 1.44 g/cc. The presence of four molecules in the unit cell of a crystal belonging to the $C_{2h}^3 = C2/m$ space group required that the molecules should be in special positions, and this, in its turn, indicates the presence of either a plane of symmetry of a twofold axis of symmetry in the molecule. This condition definitely excludes structure with oxygen outside the nucleus, which would not have these structural elements.

The structure of benzofurazane

was determined earlier [5], and the following cell constants were found for it: a = 13.46, b = 6.85, c = 3.00 A, β = 115° 46', Z = 2, space group $C_s^1 = Pa$; planar molecule. If benzofuroxane exists in the form of the n-oxy isomer (II), its molecule must be planar, like that of benzofurazane. The cell constants of benzofuroxane show that it does not have the short axis present in benzofurazane (c = 3.00 A). This may to some extent indicate that the benzofuroxane molecule is nonplanar. Analysis of the molecular packing in the unit cell and of the intermolecular contacts indicates that formula III is to be preferred. However, a final decision about the structure of the benzofuroxane molecule can be made only on the basis of a complete x-ray structural analysis, which is being conducted at the present time.

LITERATURE CITED

1. A. Green F. Row. J. Chem. Soc., 897 (1913).
2. M. Forster, H. Fierz. J. Chem. Soc., 91, 1943 (1903).
3. J. Boyer, R. Reinisch, M. Danzig, G. Stoner, F. Sahhar, J. Amer. Chem. Soc., 77, 5688 (1955); J. Boyer, W. Schoen, J. Amer. Chem. Soc., 78, 423 (1956).
4. J. Kaufman, J. Pelard. Chem. Rev., 59, 429 (1959).
5. V. Luzzati, Acta crystallogr., 4, 193 (1951).

All abbreviations of periodicals in the above bibliography are letter-by-letter transliterations of the abbreviations as given in the original Russian journal. *Some or all of this periodical literature may well be available in English translation.* A complete list of the cover-to-cover English translations appears at the back of this issue.

INTERMOLECULAR INTERACTION OF CHLORINE AND IODINE WITH CERTAIN ORGANIC COMPOUNDS

Yu. G. Borod'ko and Ya. K. Syrkin

M. V. Lomonosov Institute of Fine Chemical Technology

Translated from Zhurnal Strukturnoi Khimii, Vol. 2, No. 4, pp. 480-483, July-August 1961
Original article submitted April 28, 1961

Molecules of I_2, Br_2, and Cl_2 form molecular complexes both with polar and nonpolar compounds which can serve as electron donors [1]. This may be due on the one hand, to the presence of low antibonding orbitals in I_2, Br_2, and Cl_2 [2] and, on the other, to their low polarizability.

We have studied the infrared absorption spectra of a number of molecular complexes of I_2 and Cl_2. The UR-10 spectrometer was used for experiments.

Colling and D'Or were the first to observe that benzene saturated with gaseous chlorine exhibits absorption at about 526 cm^{-1}, which should be attributed to the chlorine molecule [3]. It was of interest to study the interaction of chlorine with a number of substituted benzenes differing in their donor power. Figure 1 shows absorption by chlorine in benzotrichloride, benzene, toluene, and p-xylene. Spectra of freshly prepared solutions were determined at 10-15°. It must be pointed out that after some time a narrow absorption band appears at 550 cm^{-1} in the spectrum of the solution, and its intensity increases with time. This is due to slow chlorination of the solvent molecules. The reaction of chlorine with the solvent is most noticeable in the case of p-xylene (Fig. 1).

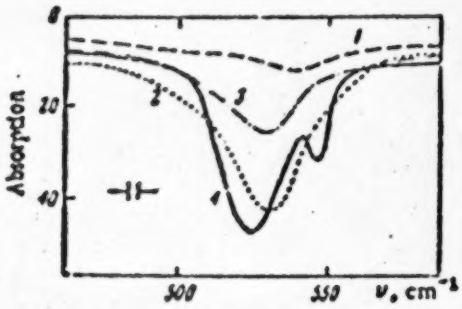

Fig. 1. Absorption spectra of chlorine in 1) benzotrichloride (ν_{max} = 540 cm^{-1}); 2) benzene (ν_{max} = 530 cm^{-1}); 3) toluene (ν_{max} = 527 cm^{-1}). d = 0.2-0.5 mm, h = 5 cm^{-1}, t = 10-15°.

It was shown by Mulliken [2,4] that the interaction is of the donor-acceptor type and the interaction energy depends on the overlap integral of the molecular orbitals of benzene and chlorine $S = \int \varphi_g \varphi_a d\tau$ where φ_g is the highest completed π orbital of the donor (benzene), and φ_a is the lowest free antibonding orbital of the acceptor (chlorine). Mulliken postulates that the acceptor orbital of chlorine is $\sigma_u(3p_z)$. This led him to conclude that the most probable structure of the complex is such that the halogen molecule is symmetrically situated in a plane parallel to the benzene ring, as this ensures maximum overlapping of the chosen orbitals [2,4]. With this geometry of the complex the chlorine molecule has a center of symmetry and its vibration is inactive in the infrared spectrum. However, it was found experimentally that I_2, and Br_2, and Cl_2 exhibit strong absorption in benzene solution [3,5] and in solutions in benzene derivatives (Fig. 1). As the result of formation of molecular complexes of chlorine with benzene and its substituted compounds the chlorine atoms in the molecule become nonequivalent and therefore the dipole moment and the derivative $d\mu/dr$ are not zero and the Cl–Cl vibration is active in the infrared spectrum. Such strong polarization of chlorine can apparently be induced by the formation of a complex in which the chlorine molecule lies along the C_6 axis of symmetry, perpendicular to the plane of the benzene molecule

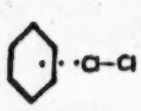

Evidence of this is provided by x-ray diffraction studies of the structure of crystalline Br_2–benzene and Cl_2–benzene compounds [6]. However, according to Mulliken this configuration of the complex should be the least advantageous [2,4]. The occurrence of infrared absorption in the Cl_2 molecule shows that the symmetry and form of the molecular orbitals of chlorine in the complex are different from those of the isolated molecule and apparently the overlap integral reaches a considerable value with this configuration. It is also possible that other filled benzene orbitals are utilized [7]. The vibration frequency of gaseous chlorine is 557.5 cm^{-1} [8]. When chlorine is dissolved in benzene or its derivatives this frequency is lower; the higher the electron density in the ring and the lower the ionization potential

of the solvent molecules, the greater is this lowering. For example, $\nu = 624$ cm^{-1} in p-xylene and 610 cm^{-1} in benzotrichloride. The higer the electron density in the ring, the greater is the shift of ν Cl–Cl and the higher is the stability of the molecular complexes.

The C=C double bond may be the electron donor. Smyth [9] observed a strong increase of polarization above the additive value in the system cyclohexene–iodine. The polarization of iodine in the vapor state is 31 cm^3. In dilute benzene solution it rises to 39 cm^3, and in cyclohexene to 66 cm^3. We studied the infrared absorption spectra of freshly prepared dilute solutions. A new band at 1624 cm^{-1} appears in the spectrum; this should probably be assigned to vibration of the cyclohexene double bond in the molecular compound of cyclohexene and iodine:

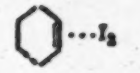

The decrease of the vibration frequency of the C=C bond from 1650 to 1624 cm^{-1} is probably due to the formation of a π complex (Fig. 2). It is known that I_2, Br_2, and Cl_2 also react with polar molecules containing nitrogen or oxygen atoms which may act as donors by virtue of their unshared electron pairs. Donor–acceptor interaction induces considerable displacement of electrons and leads to the appearance of a dipole moment in halogens. Interaction of induced dipoles, which is associated with the high polarizability of iodine, bromine, and chlorine molecules arises in the complex.

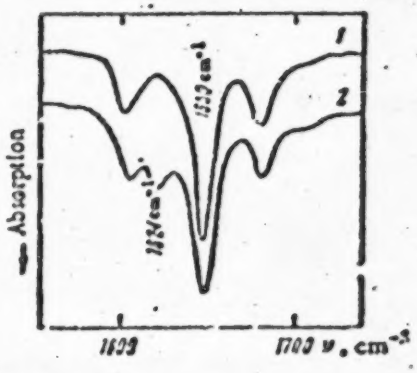

Fig. 2. Absorption spectra of: 1) individual cyclohexane in CCl_4; 2) the system cyclohexene + I_2 in CCl_4.

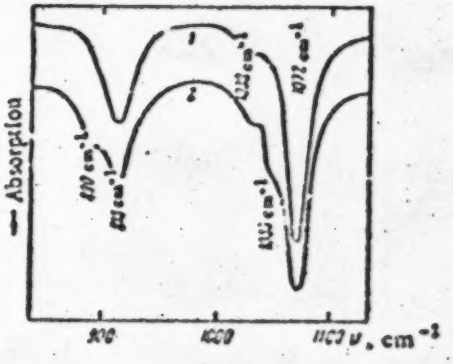

Fig. 3. Absorption spectra of 1) individual tetrahydrofuran in CCl_4; 2) the system tetrahydrofuran + I_2 in CCl_4.

Splitting of the 915 and 1072 cm^{-1} bands, which correspond respectively to symmetrical and antisymmetrical valence vibrations of the group [10], is observed in the spectrum of the tetrahydrofuran–iodine system. The new bands at approximately 899 and 1053 cm^{-1} (Fig. 3) correspond to vibrations of the 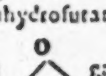 group of tetrahydrofuran in the molecular complex

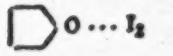

The conditions for interaction of iodine with tetrahydrofuran are most favorable with orientation of the I_2 molecule along the bisector of the valence angle [11]:

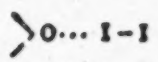

Evidence in favor of this structure of the complex is provided, for example, by the appreciable increase of polarization in the system diethyl ether–iodine ($\Delta P = 40$ cm^3) [12]. Interaction in the system tropone–iodine is probably of the same character:

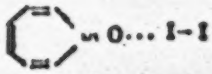

New bands with frequencies of 1571 and 1631 cm^{-1} (Fig. 4) appear in the spectrum of this system. The intensity of the new bands increases with the iodine concentration in solution, while that of the carbonyl band at 1599 cm^{-1} [13] and of the 1644 cm^{-1} band decreases. Lowering of temperature has a similar effect. These data indicate the formation of a molecular complex of tropone and iodine, with the interaction apparently localized at the oxygen atom. The dependence of the integral intensity of the carbonyl band on temperature in the 4-60° range was used for estimating the entropy, enthalpy, and free energy of formation of the molecular complex; the values found were: $\Delta H = -6.6$ kcal/mole, $\Delta S = -16.5$ eu, $\Delta F = -1.7$ kcal/mole. Earlier we had shown that resonance interaction occurs between the vibrational levels with frequencies of 1599 and 1644 cm^{-1} [13]. This accounts for the splitting of the 1644 cm^{-1} band into two components, the intensities of which reproduce the changes of the 1571 and 1599 cm^{-1} carbonyl bands. At a given temperature an equilibrium exists in solution between isolated tropone and iodine molecules and tropone–iodine complexes. Whereas in the case of free tropone (in tetrachloroethylene solution) the resonating vibration frequency of the carbonyl group is decreased to 1571 cm^{-1}, and this leads to a lowering of the frequency of the vibration resonating with it to 1631 cm^{-1}. In the infrared spectrum of a dilute solution (Fig. 4) the two absorption bands are superposed. The system of resonance levels for free tropone and tropone in the complex may be schematically represented as follows [14]:

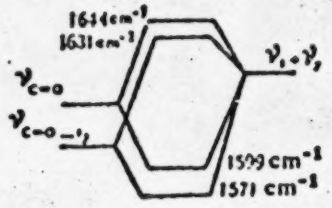

Change of temperature leads to displacement of equilibrium in the system

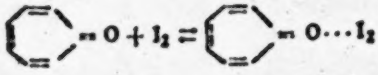

which influences the relative intensity of the 1599 and 1571 cm^{-1} carbonyl bands and this, in presence of Fermi resonance, affects the relative intensity of the 1644 and 1631 cm^{-1} bands. The existence of two frequencies is apparently characteristic of the carbonyl group conjugated with the tropone ring, and is observed for a number of known substituted tropones (frequencies in cm^{-1}):

Tropone	1635	1590	[13]
2,3-benzotropone	1644	1610	[15]
4,5-benzotropone	1633	1599	[16]
2,3,4,5-dibenzotropone	1645	1595	[17]
3,2-(1',2'-naphtha)tropone	1642	1590	[18]
4,5-(2',3'-naphtha)tropone	1634	1600	[17]

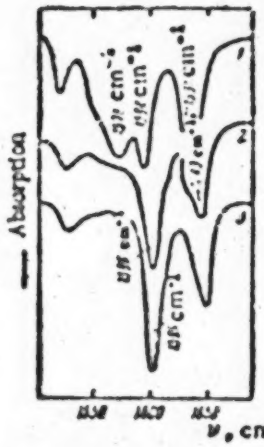

Fig. 4. Infrared absorption spectrum of the system tropone–iodine in tetrachloroethylene solution. $c_{I_2} = 8.10^{-2}$ M, $c_{tr} = 2.8 \cdot 10^{-2}$ M, t = +25°, h = 6 cm^{-1}; 2) same, at t = +60°; 3) absorption by individual tropone in tetrachloroethylene, $c_{tr} = 2.8 \cdot 10^{-2}$ M, t = +60°.

LITERATURE CITED

1. L. L. Andrews, Chem. Rev., 54, 713 (1954); S. P. McGlynn, Chem. Rev. 58, 1113 (1958).
2. R. S. Mulliken, J. Amer. Chem. Soc., 74, 811 (1952).
3. J. Collin, L. D'Or, J. Chem. Phys., 23, 397 (1955).
4. R. S. Mulliken, J. Chem. Phys., 19, 514 (1951).
5. E. P. Tyler, R. Mulliken, J. Amer. Chem. Soc., 81, 4, 823 (1959); W. Person, R. Ericson, R. Bucles, J. Chem., Phys. 27, 1211 (1957).

6. O. Hassel, K. Strømme, Acta chem. scand., 12, 8, 1146 (1958); 13, 9 1781 (1959).
7. S. Aono, Progr. Theoret. Phys., 22, 3, 313 (1959).
8. P. Stammreich, D. Sala, R. Forneris, Anais. Acad. brasileira cienc., 25, 4, 375 (1956).
9. C. P. Smyth, Dielectric behavior and structure, N. Y., 1955.
10. G. M. Barrow, S. Searles, J. Amer. Chem. Soc., 75, 1175 (1953).
11. O. Hassel, I. Havoslen, Acta chem. scand., 8, 5, 873 (1954); O. Hassel, K. Stromme, Acta chem. scand., 13, 9, 1775 (1958).
12. V. M. Kazakova, Ya. K. Syrkin, Izv. AN SSSR, Otd. khim.n., 6, 673 (1958).
13. Yu. B. Borod'ko, Ya. K. Syrkin, Dokl. AN SSSR, 134, 5, 1127 (1960).
14. Yu. G. Borod'ko, Ya. K. Syrkin, Optika i spektroskopiya (in the press).
15. G. L. Buchanan, J. Chem. Soc., 1069 (1954); 1610 (1956).
16. H. H. Rennhard, E. Heilbronner, A. Eschenmoser, Chem. Ind., 415 (1955); W. Simon, E. Heilbronner, A. Eschenmoser, Helv. chim. Acta 40, 957 (1957).
17. G. Naville, H. Strauss, E. Heilbronner, Helv. Chim. Acta, 43, 1221 (1960).
18. M. Josien, N. Fuson, J. Lebas, T. Gregory, J. Chem. Phys., 21, 331 (1953).

All abbreviations of periodicals in the above bibliography are letter-by-letter transliterations of the abbreviations as given in the original Russian journal. *Some or all of this periodical literature may well be available in English translation.* A complete list of the cover-to-cover English translations appears at the back of this issue.

REVIEW

NUCLEAR MAGNETIC RESONANCE AND THE HYDRATION OF IONS IN AQUEOUS SOLUTIONS

V. A. Shcherbakov

Khlopin Radium Institute, Academy of Sciences of the USSR
Translated from Zhurnal Strukturnoi Khimii Vol. 2, No. 4,
pp. 481-517, July-August 1961
Original article submitted January 5, 1961

The review deals with the main results from magnetic-resonance studies on hydration and structure for aqueous solutions of electrolytes. Particular attention is given to self-diffusion in water, to interactions between ion and water, and to exchange between the closest water molecules and others further away. The advantages of magnetic-resonance methods in physical chemistry are pointed out.

The number of direct magnetic-resonance studies on hydration is fairly small as yet, but lately there has been a marked increase in the volume of work published. Some studies of nuclear relaxation in water and solutions do not fall fully within this field, because these had as object not hydration proper but some features of magnetic resonance. All the same, many papers on resonance in aqueous and other solutions throw light on ion hydration and the structures to be found in aqueous solutions of electrolytes.

Physical chemists have begun to show much interest in magnetic-resonance techniques; the physicist working in this field requires a good understanding of the problems of physical chemistry. The result is the appearance of many joint papers, which are very often concerned with free radicals. This applies even to some purely physical studies, in which the nature of the objects is of particular importance.

Magnetic-resonance methods are especially valuable for use with water and aqueous solutions; such objects were among the first to be examined by Zavoiskii, who discovered electron resonance in 1944 [1]. Bloch's group [2] discovered nuclear magnetic resonance (NMR) on these same objects in 1946 (Purcell's group made the same discovery simultaneously). The study of proton resonance in aqueous solutions by Bloembergen et al.[3] laid the basis for the theory of nuclear relaxation for liquids. Magnetic-resonance techniques have always been closely associated with chemical problems on account of their exceptional sensitivity to the state of the particles.

The theory of hydration (the principal division of the theory of solutions) covers numerous problems, many of which can be elucidated by means of NMR. This may be seen merely by counting the number of references to hydration problems in Samiolov's book [4]. Some of the more important ones are 1) structure of the molecule for water in its various states, 2) self-diffusion in water, 3) structures of hydrated crystals, 4) coordination numbers for water, 5) energy aspects of water-molecule exchange, 6) ion-water interactions, and 7) structures of aqueous solutions.

I shall indicate how some of these problems have been examined by means of NMR, and, in order to make the subject readily intelligible to most chemists, I give first a brief survey of the principles and of some of the methods. The interaction between ion and water is important to interpretations of NMR results, so I deal also with the principles of the hydration theory, for which I draw on Samoilov's [4] treatment.

Spin Resonance

Magnetic (spin) resonance is the selective absorption of a radio-frequency quantum by a spin system placed in a steady magnetic field. The vector $\underline{u}$ of a spin in this field H_0 can take up only certain definite positions, each of which corresponds to a certain energy level (Fig. 1). A quantum $h\nu_0$ is absorbed from the radiofrequency field H_1, which is perpendicular to H_0; this absorption can occur only when the quantum energy equals the energy difference between levels. That difference is determined by H_0, by $\underline{u}$, and by the g-factor (the last is analogous to the Lande factor in atomic spectroscopy):

$$h\nu_0 = g\beta H_0 = g\beta H, \qquad (1)$$

in which ν_0 is the nuclear magneton and I is the nuclear spin.

The effect is one of resonance and may be described from the viewpoint of classical mechanics as follows. The moment $\underline{\mu}$ of a particle in a field H_0 rotates [5] around the direction of that field at the Larmor precession frequency $\omega_L = 2\pi\nu_0$. A rotating external field $H_1 (H_1 \ll H_0)$ at right angles to the main field causes the vector to pass periodically from one precession cone to the other (Fig. 1); the energy associated with the precession also changes periodically. The energy levels of Fig. 1 belong to the various possible positions of the moment in H_0 [6].

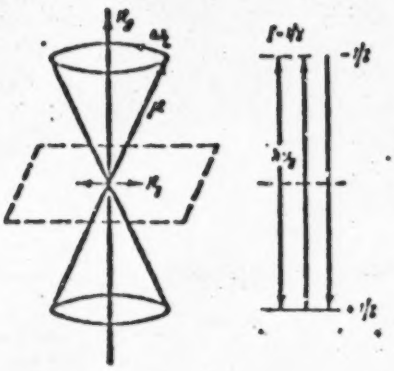

Fig. 1.

The effect is called electron spin resonance (ESR) if it is associated with electron spins and nuclear magnetic resonance (NMR) if it is associated with nuclear spins. The frequencies of these two resonances differ by about three orders of magnitude no matter what H_0.

The NMR is observed from the reaction on the circuit that produces H_1. The simplest device for observing NMR is as follows. The coil of a tuned circuit contains the specimen and lies in H_0; the circuit magnification falls when absorption occurs, and so the voltage drops. The resonance is observed by modulating H_0 at a low frequency and with an amplitude of a few gauss, the mean field being the one producing resonance. The NMR signal then appears twice during a cycle of the modulating frequency; the high-frequency voltage is rectified, the low-frequency component is amplified, and the output operates an oscilloscope synchronized with the field modulation.

The NMR process may also be treated as follows [6-8]. The spins are randomly oriented in space when H_0 is zero, so the resultant magnetization M is zero. A finite H_0 produces the Larmor precession around the direction z of the field. This precession is associated with an isotropic spin distribution; the spin system does not come to thermal equilibrium with the rest of the system as soon as H_0 is applied, because the energy of the spin system is thereby altered. All the energy levels remain equally populated; the distribution corresponding to the temperature T of the medium is reached only after a certain period. Interactions between particles can cause the spin system to take up the lowest energy state (that in which its magnetization vector lies along the positive direction of z). The result is a small (but finite) excess population in the lowest level, and this excess is responsible for the absorption. If the two populations are equal, the number of upward transitions equals the number of downward ones, so absorption and emission are absent. The excess is 0.0001% for protons at room temperature (relative to the population of one level) in a field of 5000 oersted. The macroscopic axial magnetization M_z varies in accordance with the spin-lattice (axial) relaxation time T_1, which is the time needed for the spin system to come to equilibrium with the lattice, by which is understood the body of matter (in any state) containing the relevant nuclear species.

Now M_z is given as a function of time $\underline{t}$ by

$$M_z = M_0 (1 - e^{-t/T_1}) \tag{2}$$

or

$$\frac{dM_z}{dt} = -\frac{M_z - M_0}{T_1}. \tag{2a}$$

Here M_0 is the equilibrium magnetization at temperature T and is

$$M_0 = N\mu \cdot \frac{\mu H_0}{kT} \cdot \frac{I+1}{3I} \tag{3}$$

in which N is the number of relevant nuclei per unit volume and $N\mu$ is the magnetization that would occur if thermal motion did not interfere. The energy exchange between the lattice and the spin system may be described more clearly in terms of the temperature T_s of that system:

$$M_z = N\mu \cdot \frac{\mu H_0}{kT_s} \cdot \frac{I+1}{3I}. \tag{4}$$

Now (4) implies that T_s is infinite when H_0 is applied but falls to T when $M_z = M_0$. Energy passes from the spin system to the lattice, or conversely when the field is removed.

An alternating field $H_1 (H_1 \ll H_0)$ perpendicular to H_0 produces a rotating transverse magnetization $M_{x,y}$, so we have a second relaxation time T_2, which is the spin-spin (transverse) relaxation time and which is dependent on exchange

within the spin system. Again, T_2 is determined by (2a), but with $M_0 = 0$. It is found that T_1 and T_2 range between 10 and 10^{-6} sec.

Theory of Nuclear Relaxation

Bloembergen et al. [3] worked out this theory on the basis of elementary magnetic dipoles, whose interactions determine T_1 and T_2. If all the nuclei are of the same type, if thermal agitation is absent, and if H_0 is exactly the same at all points in the specimen, then Mz is constant and $M_{x,y}$ would persist indefinitely if all nuclei had the same ν_0, but H_0 is altered locally by the z-component of the fields of adjacent nuclei, so the various nuclei differ in Larmor frequency (the NMR line is broadened). The local field is governed by the magnetic moments and distances of adjacent nuclei; it is commonly about one oersted. This field destroys the phase relations that initially exist between the individual magnetic moments, so $M_{x,y}$ vanishes the less the value given by (2a) for T_2, the phase memory (a component of T_2) [3]. The contribution from dipole-dipole interactions depends essentially on the mean time one dipole spends in the neighborhood of another; this time is governed by the thermal motion and is a very important feature of spin-spin interactions, which alter when restrictions on thermal agitation are removed.

The thermal agitation makes T_1 finite; this time is inversely proportional to the probability of transitions between the levels caused by H_ℓ. Now H_ℓ is associated with the forward and rotational motions of adjacent nuclei and so is a rapidly varying function of time; it may be treated as magnetic noise having a continuous Fourier spectrum. Only that part of the spectrum which lies near the proper value can affect the transitions that determine T_1. The spectrum has the form [6,7]

$$S(\omega) \propto \tau_c / (1 + \omega^2 \tau_c^2). \tag{5}$$

in which the correlation time τ_c is constant and to a first approximation is η/T (η being the viscosity); it is of the order of the time needed by a molecule to turn through 1 radian or to travel a distance comparable with its own size. Then $S(\omega)$ is almost constant if $\omega\tau_c \ll 1$ but dies away rapidly at higher frequencies if $\omega\tau_c \gg 1$ (Fig. 2). The spectrum is broad, and the intensity near ν_0 is small, if η/T (i.e., τ_c) is small, so T_1 is large, and $T_1 \propto 1/\tau_c$. The upper limit of the Brownian-noise spectrum lies below ν_0 if η/T is large, so $S(\omega)$ is very small near ν_0, and T_1 is again large ($T_1 \propto \tau_c$). There is a certain η/T for which $S(\omega)$ is maximal near ν_0 if $\omega\tau_c \approx 1$; the transitions reduce $M_{x,y}$ so the finiteness of T_1 affects T_2. These two related [3] as follows:

$$1/T_2 = (2\pi)^2 (1/T_2') + (1/2T_1). \tag{6}$$

This dipole-dipole theory of relaxation thus indicates that $T_1 = T_2$ (both being of the order of a second) if η/T is very small the two decrease (to about 10^{-3} sec) as η/T increases, but further increase in η/T causes the T_2 for liquids to lie at small or medium values, with T_1/T_2 not unity. (The ratio is only 10^{-5} to 10^{-6} sec for solids [6,7].)

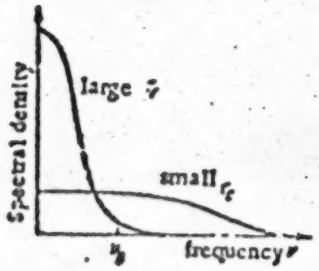

Fig. 2.

Theoretical Calculation of T_1 for Pure Water

Results here are of special interest as having a bearing on the molecular interactions in water [6]. Each proton in a water molecule has the other proton as a near neighbor; the contribution of intramolecular interactions to $1/T$ is

$$1/T_{1,\mathrm{I}} = 2U_{\mathrm{I}} = \frac{3\gamma^4\hbar^2}{10 b_0^6}\left(\frac{\tau_c}{1+4\pi^2\nu_0^2\tau_c^2} + \frac{2\tau_c}{1+16\pi^2\nu_0^2\tau_c^2}\right). \tag{7}$$

(This applies to the H–H interaction in a molecule treated as rigid; the H–H direction is assumed to have no preferred orientation.) The symbols are U the transition probability, γ the gyromagnetic ratio, and b_0 the distance between the protons. The τ_c is one-third of τ_0, the Debye correlation time encountered in the theory of polar liquids $\tau_D = 8.1 \cdot 10^{-12}$ sec for water at 20°, so $\tau_c = 2.7 \cdot 10^{-12}$ sec.; the period of vibration of a water molecule about its equilibrium position is calculated [4] as 1.4×10^{-12} sec). This gives us $1/T_{1,\mathrm{I}}$ as 0.12 sec^{-1} for $b_0 = 1.5$ A.

The interactions between molecules give rise to the other part of T_1; now the fluctuations in H_ℓ are governed mainly by the forward motion, so we must calculate τ_{cj} for a nucleus lying at point I and acted on by molecules in a shell between radii r and r + dr. As τ_{cj} we take the time needed to displace nucleus j a distance r relative to nucleus I. This motion may be described in terms of the diffusion coefficient, which the Stokes-Einstein relation gives as $D = kT/6\pi a\eta$ for a spherical molecule of radius a (k is Boltzman's constant). Then the theory of Brownian motion gives us that

$$\tau_{cj} = r^2/12D = \pi\eta r^3 a/24T. \tag{8}$$

Then the intermolecular (Brownian contribution to $1/T_1$ is

$$1/T_{1,b} = 9\pi^2\gamma^4\hbar^2\eta N/10kT. \qquad (9)$$

Now T_1 for pure water is determined mainly by the intermolecular component; the net T_1 is approximately [6,10]

$$1/T_1 = 1/T_{1,b} + 1/T_{1,i} \approx \frac{3}{10}\gamma^4\hbar^2\left(\frac{3\tau_c}{b_2^6} + \frac{\pi N}{a^3}\right). \qquad (10)$$

For 20° (9) gives us $1/T_{1,b}$ as 0.08 sec^{-1}, so $1/T_1 = 0.20\ sec^{-1}$ or $T_1 = 5$ sec. The calculated τ_{cj} is not accurate; the error in T_1 may be as much as 100%. The measured T_1 for pure water is 3.5 sec [9], which agrees quite well with the theory. These and other results indicate that the theory [3] is generally correct; Anderson and Arnold [11] have confirmed the dipole-dipole mechanism by means of mixtures of light and heavy water. The above theory indicates that T_1 for the protons increases with the deuterium content, which is found to be so.

The Spin-Echo Method and Self-Diffusion in Water

Hahn's [12] spin-echo method has proved exceptionally important as a means of measuring nuclear relaxation times; a modified form is described by Carr and Purcell [13,14]. The method differs from the ordinary one of observing NMR signals in that H_1 is applied as pulses instead of continuously. This H_1 rotates around H_0 and has the resonance frequency; the first pulse is of duration such that it transfers the moments to the equatorial plane. For this reason it is called the 90° pulse. The nuclear moments then undergo free precession in the equatorial plane. But H_0 always varies from point to point (inhomogeneity can be introduced artificially if necessary), so the set of moments gradually loses phase coherence. A second pulse of double the duration (the 180° pulse) is applied after a time t; this alters the precession in a way such that phase coherence is restored at time $2t$. The resulting signal is called the echo.*

This NMR technique enables one to measure relaxation times in absolute terms; it also provides a means of studying self-diffusion. The latter feature is especially valuable, because no special label is needed; the phase or direction of the nucleus is used instead. (Purcell remarks that it is difficult to conceive of a label having less effect on the properties of the material.) The method is used to study self-diffusion as follows. Phase coherence is lost in the inhomogeneous field but is restored by the 180° pulse; that pulse is less effective if during the time t the molecule has moved to another point in the field as a result of diffusion. The result is a spin-echo signal that dies away as $\exp(-k^2)$ instead of as $\exp(-kt)$. Carr and Purcell replace the 90° and 180° pair (Method A) by a pulse train (one 90° and a series of 180°; Method B); this method enables one to eliminate much of the effect of self-diffusion.

The theory shows that the spin-echo method can be applied to self diffusion in certain liquids [14]. In this way Carr and Purcell measured D for water at 25° as $(2.5 \pm 0.3) \times 10^{-5}$ cm^2/sec (the limits are those of the maximum error), a result that agrees well with other measurements [4]. The method, if applicable, gives the most accurate value for D, because the label is extremely specific.

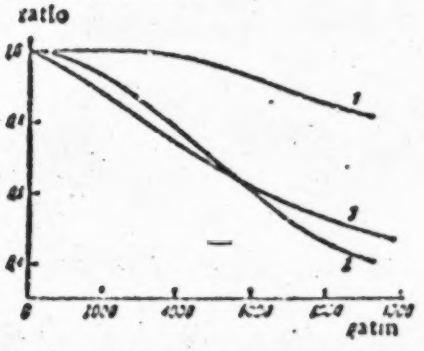

Fig. 3. Dependence on pressure P (atm) at 28.8° of 1) $T_1(P)/T_1(1)$ [$T_1(1)$ is the relaxation time at 1 atm]; 2) $D(P)/D(1)$; 3) $\eta(1)/\eta(P)$.

Benedek and Purcell [10] have used the echo method to measure T_2 and D for various liquids at pressures up to 10,000 atm. Figure 3 gives the results for gas-free twice-distilled water further purified by ion exchange; if we put (10) in the more general form

$$1/T_1 = (\alpha + \beta N)\eta/T, \qquad (10a)$$

in which α and β are constants that do not depend on T and P, we see from Fig. 3 that T_1 is not proportional to $1/\eta$. The discrepancies become even larger if allowance is made for the change in N. Similar effects are found for liquids not free from gas [10] (n-hexane, n-pentane, toluene, ethyl iodide, methyl iodide; the values for the gas-free liquids agree well with those given here [15]. Bridgman's results for η [16] enable us to verify the Stokes-Einstein formula for D and η; Fig. 3 shows that the normalized curves for D and $1/\eta$ are in good agreement for water, although the results do not fit (10a). The explanation [10] is that the assumptions made in reducing the formula for calculating τ_c

$$\tau_c = \tau_D/3 = 4\pi\eta r^3/3kT, \qquad (11)$$

are not justified because they relate the correlation time for orientation to the macroscopic viscosity, and hence with D, via

* If the moments are considered as sprinters, the first pulse is the starting gun; after a certain time the runners are spread out along the track (loss of phase coherence). The 180° pulse is then a second start, at which all runners turn in their tracks and run in the reverse direction with the same speed; they all arrive at the start together [6,12]. The analogy is incomplete, for the runners turn around, whereas the nuclei continue to precess in the same sense. We might say that the second start (the 180° pulse) lets the runners go in the reverse order (if the order would have been C, B, A at the finish, it is reversed to A, B, C immediately after the second start) whereupon they run as before and arrive together at the end (echo signal).

the Stokes-Einstein formula which would make that time proportional to the time required for a change of velocity. The assumptions are reasonably justified for high temperatures, but the free space within the liquid is reduced by pressure, which affects mainly the translational motion; the rotational motion is not much affected, so τ_c varies less than (11) would indicate.* This means that the $T_{1,t}$ part of T_1 does not fall so rapidly as the other part. Now this first part is larger than the second one, so T_1 is larger than the theoretical value. This shows that loss of free space hinders migration rather than rotation; the effect is related to the mechanism of self-diffusion in the case of water, because there is no need for a hole to appear [4] in order to permit sideways transfer.

TABLE 1

T, °C	$D \times 10^5$, cm²/sec (7%)	T_1, sec (2%)	$\frac{D\eta}{T} \Big/ \left(\frac{D\eta}{T}\right)_{25°}$ (7%)	$\frac{T_1}{D} \Big/ \left(\frac{T_1}{D}\right)_{25°}$ (9%)	$\frac{T_1\eta}{T} \Big/ \left(\frac{T_1\eta}{T}\right)_{25°}$ (2%)
0	0,97	1,59	1,00	1,04	1,03
5	1,16	1,88	0,99	1,02	1,02
10	1,36	2,20	0,98	1,02	1,01
15	1,58	2,55	0,98	1,01	1,00
20	1,85	2,95	0,99	1	1,00
25	2,13	3,37	1	0,98	1
30	2,46	3,82	1,02	0,97	1,00
35	2,79	4,30	1,02	0,96	1,00
40	3,14	4,76	1,03	0,95	0,99
45	3,52	5,27	1,04	0,93	0,98
50	3,94	5,77	1,05	0,91	0,97
55	4,37	6,78	1,06	0,89	0,96
60	4,82	6,81	1,06	0,87	0,95
65	5,30	7,36	1,07	0,86	0,94
70	5,78	7,91	1,07	0,86	0,93
75	6,27	8,49	1,07	0,85	0,92
80	6,81	9,10	0,08	0,84	0,91
85	7,26	0,70	1,07	0,84	0,90
90	7,75	10,30	1,06	0,84	0,89
95	8,20	10,95	1,05	0,84	0,88
100	8,65	11,55	1,03	0,84	0,87

Simpson and Carr [3] have measured D and T_1 for water for the range 0 to 100° (Table 1); their values show that the D obtained from tracer measurements are about 25% too high (see [4] for a review of tracer measurements). It is found [18] that the results also demonstrate the following. If Bloembergen's relaxation theory is correct, if Stokes law for η applies to the rotation time, and if the Stokes-Einstein equation applies for η and D, then we would expect to find that:

$$T_1 \propto D \propto T/\eta \propto e^{-E/RT}$$

[three activation energies, denoted respectively by E_R** , E_D, and E_V (see below), are assumed all equal to E]. The last three columns in Table 1 give $D\eta/T$, T_1/D, and $T_1\eta/T$ (the figures in brackets are the maximum errors). These results are taken [18] to show that the Stokes-Einstein equation applies to pure water, although $T_1\eta/T$ (which is more accurate) clearly fails to reproduce the theoretical relation of T_1 to η, as in [10] (the deviation sets in at about 40°). It is pointed out [18] that this deviation occurs near the minimum in the isobaric thermal capacity and at

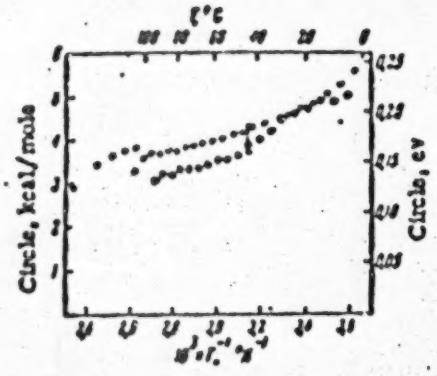

Fig. 4. Circles, E_R for T_1; points, E_V for T/η. The vertical lines indicate the maximal errors.

*Mitchell and Eisner have measured T_1 for benzene, chlorobenzene, and cyclohexane as functions of concentration in carbon disulfide and carbon tetrachloride; they find that the correlation time is proportional to I (the moment of inertia) and m (the reduced mass of the system) rather than to the molecular volume. An empirical formula $\tau_c = 2\eta a_0/mkT$ (in which a_0 is the mean radius of the molecule) describes the results as well [17]

**E_R is an effective activation energy for relaxation-determining processes. The term for the rotational motion is the dominant one in E_R.

the point of inflection in the magnetic susceptibility; the deviation is explained [18] as being caused by differences between the activation energies E_R and E_V (for T_1 and T/η respectively) as functions of temperature. Figure 4 shows the activation energies calculated on this basis.

Douglass and MacColl [19] have confirmed this conclusion [13] about the various methods of measuring D; Fig. 5 gives their spin-echo measurements for H_2O-D_2O mixtures, which agree well with those from the use of O^{17} but differ greatly from those found in other ways from the use of heavy water. This led them to conclude [19] that the molecule diffuses as a whole and that exchange plays no great part.

A later paper [20] gives new results for D as a function of pressure, which show that $E_D = -R[\partial \ln D/\partial(1/T)]_p$ is a function of the temperature T for water but is not so (within the 5% error of experiment) for nitromethane, acetone, benzene, cyclohexane, isopentane, and neopentane. The values for water range for 5 kcal/mole at 0° to 3 kcal/mole at 100°; the activation volume for diffusion, $\Delta V = -RT(\partial \ln D/\partial P)_T$ does not depend on P (of the above liquids, only nitromethane and isopentane show such a dependence). The activation energy for the viscosity, $E_V = R[\partial \ln \eta/\partial(1/T)]_p$ decreases from 4.4 kcal/mole at 0° to 2.9 kcal/mole at 100°. Further, D and η have been calculated [20] on the basis of Longuet-Higgins and Pople's [21] relation of viscosity to thermal conductivity. Here E_D was found from the equations of [21]. The results are in general (not exact) agreement with experiment, except for alcohols.

Motchaune and Uebersfeld [22,23] have made a different use of NMR in self-diffusion measurements. Diffusion makes itself felt in dynamic nuclear polarization; the electron-spin system here was free radicals in carbon, while the nuclear-spin one is a suitable proton-donating liquid e.g., water. Here the diffusion occurs at the interface between solid and liquid; other applications are possible [23].

Chemical Shifts

All the above results relate to protons in water, but relaxation is not the only use of NMR in hydration research. Another very important parameter is ν_0 itself, which is not entirely constant even for a given nuclear species; it varies with the chemical binding of the element. The resonance frequency is governed by the field in the molecule, which is dependent on the reaction of the electrons to H_0. For this reason (1) must be modified to include the screening effect of the electron density ρe, as in

$$h\nu_0 = g\mu_0(1 - \sigma)H_0. \tag{12}$$

Here σ is the magnetic-screening constant. The variation in NMR frequency with the nature of the compound is called the chemical shift. Knight [24] was the first to observe the effect for metals and compounds of phosphorus; Dickenson [25] and Proctor and Yu [26] demonstrated it for liquids containing N^{14} and F^{19}.

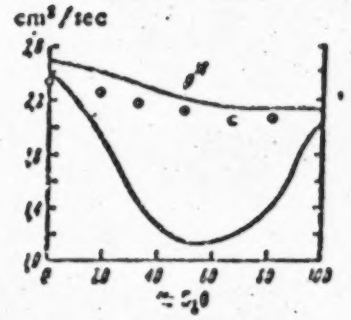

Fig. 5. The points are from [19]; the full lines derive from the use of O^{17} (top) and deuterium (bottom).

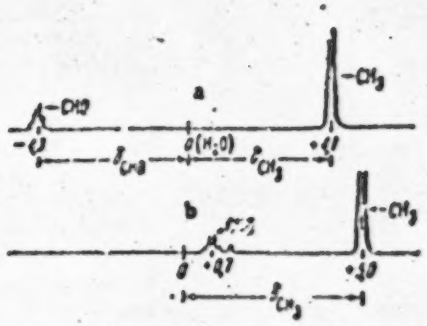

Fig. 6. High-resolution spectra for acetaldehyde a) alone and b) mixed with water.

The electron shells screen the nucleus from H_0 to an extent σ; now ρe varies from one compound to another, i.e., so does the effective screening field $H' = -\sigma H_0$. The screening factor may be derived for an atom having electrons in 1s states by means of Lamb's formula [8,27]:

$$\sigma = \frac{e^2}{3mc^2}\sum_i\left(1/r_i\right) = \frac{4\pi e^2}{3mc^2}\int_0^\infty r\rho_e(r)\,dr, \tag{13}$$

in which e is the charge and m is the mass of an electron, c is the velocity of light, and ρ_e is the electron density at a distance r from the nucleus.

This shows that the screening factor is proportional to the energy of the electrostatic interaction between the nucleus and the electrons. The expression for σ becomes much more complicated if the atom is in a molecule; Ramsey [28] was the first to consider the general case for an isolated molecule. His equation is analogous to Van Vleck's for the molecular diamagnetism [29] and may be put approximately in the form

$$\sigma_{zz} = \frac{e^2}{2mc^2}\int \frac{x^2+y^2}{r^3}\rho_e dr + \frac{e^2\hbar^2}{m^2c^2\Delta E}M(r,\varphi). \qquad (14)$$

Here $\Delta E = E_n - E_0$ is some mean difference between E_n (the energies of all possible excited states) and E_0 (the energy of the ground state); $M(r,\varphi)$ is dependent on the polar coordinates of the electron. The first term in (14) resembles Lamb's formula and becomes exactly that formula when an average is taken with respect to all directions. (The integration is to be carried over the entire molecule, not only over the atom [8].) The second term corresponds to a perturbation in the free rotation of the molecular system; it is very similar to the temperature-independent paramagnetism in van Vleck's formula for the magnetic susceptibility (the high-frequency or polarization paramagnetism, as Dorfman has it [30]). This terms represents the magnetic moment observed in a molecule having an excited state very close to the ground state (the two mix in the presence of an external magnetic field [28]).

This second term (for paramagnetism) is in opposition to the first (diamagnetism) as regards the effect on H_0; the screening factor σ is thus the sum of σ_d and σ_p. The result is a chemical shift δ that is found by experiment as

$$\delta = (H_x - H_c)/H_c \approx \sigma_x - \sigma_c . \qquad (15)$$

in which H_x is the H_0 for the compound and H_c is the H_0 for the calibration (standard) compound (usually water in the case of solutions). The δ range from 10^{-3} to 10^{-5} for most nuclides, but protons give only 10^{-5} or less, so the shift can be difficult to detect. The heavier elements give larger δ; the δ for Pt^{195} is 5%, for example [31].

Figure 6 shows the shifts for acetaldehyde, especially as affected by interaction with water [32]; the detailed structure (quadruplet for CH_3, doublet for CH_2) is caused by spin-spin interaction between the groups. The two sets of lines shift when water is added, because the hydrated form is produced; that for CH_3 shifts more than that for CH_2. This shows that the electron cloud becomes less polarizable near the aldehyde group (the ρ_e becomes close to the ρ_e for water). These effects have been used [32] to calculate the equilibrium constant; the result is in good agreement with those from other methods.

Chemical Shifts in Aqueous Solutions of Electrolytes

The two components of the screening are both present here; the paramagnetic one is important for water, as is shown by the large shift in the vapor state (relative to methane and ammonia) [8,33]. The diamagnetic component appears to dominate the δ for water, because the difference between the liquid and vapor states is 0, -1.59, and 4.53 (all $\times 10^6$) respectively for methane, ammonia, and water.

The electric field of O* polarizes the OH bond in a hydrogen bond OH . . . O* and causes [33] a shift to lower fields, although the paramagnetic contribution from this atom can cause a shift to larger H_0. The hydrogen bond is partly covalent, which hinders any alternation in ρ_e; it also makes the effect difficult to predict until we have a more detailed understanding of hydrogen bonds, and the above general treatment [8] must suffice at present. The effects of hydrogen bonds on chemical shifts are particularly interesting in relation to aqueous solutions, although the presence of solutes makes the results more difficult to interpret. There is no theory of the chemical shift for pure water, so at present we have to rely on empirical relations, of which the one of greatest importance to us is that the formation of a hydrogen bond causes only a negative shift for that proton in question [33]. Table 2 and Fig. 7 illustrate this; they show that inert solvents destroy the structure of water and reduce the number of hydrogen bonds, and in this way they make δ more positive (increase the screening). The hydrogen bonds reduce ρ_e so there is a relative shift of δ towards the negative side. This rule gives us only the sign of the change in δ, but the shifts for solutions (including those of electrolytes) are of much interest, because they are very sensitive to the state of the compounds (particularly of the water).

Shoolery and Alder [34] were the first to make a detailed study of this topic; they found a δ that varies from electrolyte to electrolyte and that increases with the charge and with the reciprocal of the radius of the caption. This behavior is correlated with the state of hydration; the concentration dependence of δ for 1-1 electrolytes is explained in terms of the change in the number of hydrogen bonds. The fall in the number of those bonds causes the

δ for a 1-1 electrolyte to vary little above a certain concentration (e.g., above 6 M for sodium iodide and perchlorate). Polarization of the water molecule is said [31] to be a second cause of changes in the proton frequency for solutions of ionic compounds; this gives a linear concentration dependence for δ (up to 4 M for 1-1 electrolytes and up to 1 M for others). This linearity indicates [31] that only the first layer of water molecules is polarized (any other effect would cause a deviation from linearity), so such deviations (e.g., for zinc and magnesium chlorides) are [31] ascribed to interaction with a second layer or to the formation of ion pairs, which leads to a flattening-off in the response (the ion pairs have less polarizing effect). It may be that linearity is the resultant of ion-pair and hydrogen-bond effects, as for KG and LiCl (compensation). Refractometry confirms this conclusion [31] about ion pairs and δ, so such curves can be used in studies of ion-ion interactions.

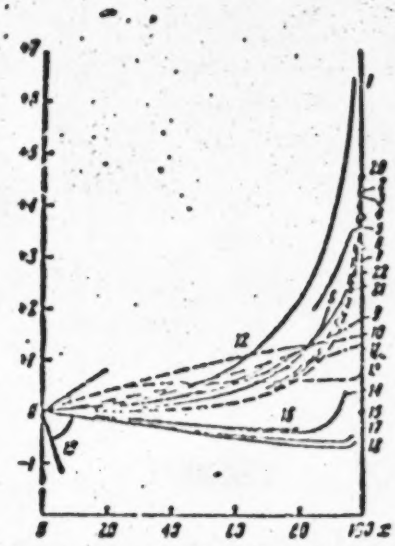

Fig. 7. Chemical shift $(\delta_x - \delta_c) \times 10^6$ in proton NMR for water, alcohols, and acids diluted in solvents (x is the mol. % solvent): 1) acetic acid in acetone; 2) water in benzene; 3) methanol in CCl_4; 4) water in CCl_4; 5) methanol in $CHCl_3$; 6) water in $CHCl_3$; 7) ethanol in C_6H_6; 8) methanol in C_6H_6; 9) water in acetone; 10) methanol in acetone; 11) water in $(CH_3)_2SO$; 12) water in dioxane; 13) methanol in $(CH_3)_2SO$; 14) acetic acid in 1,1-dichloroethane; 15) acetic acid in CCl_4; 16) acetic acid in propyl bromide; 17) acetic acid in CCl_4; 18) acetic acid in cyclohexane; 19) water with strong electrolytes; 20) water vapor; 21) ethanol in CCl_4; 22) t-butanol in CCl_4.

It is possible to distinguish the contributions from the anion and from the cation. As standard it is assumed that $\delta_{ClO_4^-} = -0.85 \pm 0.1$; and δ is calculated from

$$\delta = m(n^+\delta^+ + n^-\delta^-). \qquad (16)$$

in which δ^+ and δ^- are the relative molar shifts caused by cation and anion, n^+ and n^- are the numbers of moles of those ions respectively resulting from dissociation of one mole of the salt, and m is the molarity. Calculations (Table 3) show that the above argument is generally correct, although the precise effects of charge and radius on δ are far from simple, on account of the complicated structure of the fields produced around the protons by the ions and dipoles, not to mention the hydrogen bonds. The relative effects of these two factors may be estimated if we derive some figure for the hydrogen bonds broken by reference to results for the vapor (about 0.4×10^{-7} per bond per mole). If each ion breaks 5-6 bonds, the effect per mole is 2×10^{-7}, which value, used in conjunction with Table 3 [31], gives us the shift caused solely by polarization.

Hertz and Spalthoff [33] have recently made a more detailed study of the NMR shifts for protons in water containing dissolved salts; in general, their results agree with those of [31], but some errors in the latter work give rise to discrepancies. In fact, [31] demands a fuller and more systematic examination*.

The chemical shift is a very important physicochemical quantity and is of very much greater general significance than many other more specific quantities. On this basis Hertz et al. [33] interpret their results as do Shoolery et al. [31], in that they take the linear concentration dependence of δ (Fig. 8) to reflect the dominant effect of the hydration shell around each ion. Curvature, as in [31], is ascribed to a substantial diminution in the free water (to 7-8 molecules per ion). It is considered [33] that the total δ may be represented as δ (dilution) + δ (hydration); the first of these may be taken to a first approximation as unspecific, so the individual effects of ions appear via the second. On the assumption that K^+ and Cl^- have identical forms of hydration, they separate out the contributions from the ions to δ on the basis of results for low concentrations, to which (16) applies strictly. Table 3 illustrates certain general trends. If δ (dilution) is constant, we would expect the total shift to increase monotonically with the ionic radius, but this is observed only for halide ions. The alkali metals give no variation; Na^+ gives the same shift as K^+ although the two differ in hydration [1]. The difference between Mg^{2+} and Ca^{2+} is also unexpected [33]. All the same, the results are as yet too inaccurate for any final conclusions to be drawn. It may be also that δ (hydration) includes a quantity dependent on the free water in the solution; this quantity may be substantial, in which case small effects might be masked.

*The discrepancies between the results in [33] and [31] have the following causes: 1) No correction for the magnetic susceptibility of the solution was used in calculating the molar shifts in [31], 2) the method used in [31] to measure δ was less accurate than that used in [33], and 3) differing assumptions were made in computing the ion contributions to δ. On the whole, the results of [33] are the more accurate.

TABLE 2

Solvent	δ × 10⁶ for:		Solvent	δ × 10⁶ for	
	water	methanol		water	methanol
$CHCl_3$	3.2	3.6	propanol	0.38	-
CCl_4	3.75	4.5	acetone	1.75	1.4
C_6H_6	4.3	2.1	$(CH_3)_2SO$	1.3	0.8
dioxane	1.0	-	electrolytes	−2.2 to +0.5	-
ethanol	0.28	-			

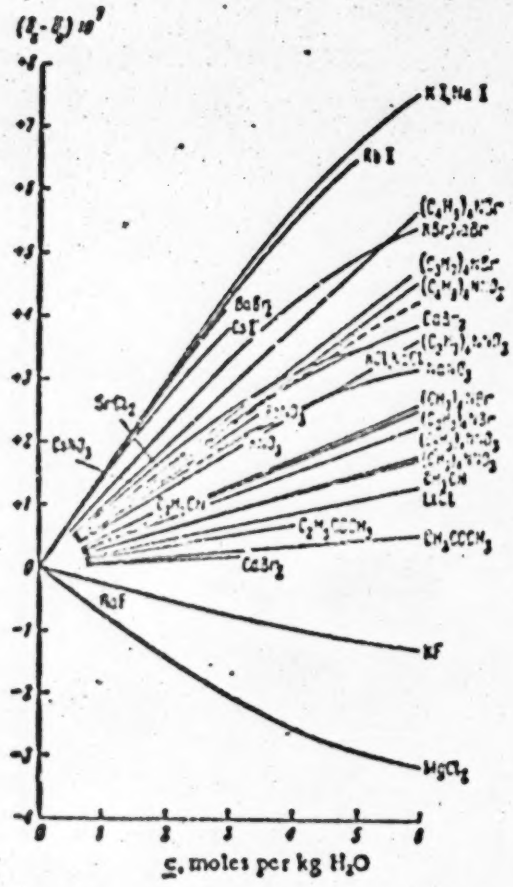

Fig. 8. Broken line: values of δ interpolated between those for liquid water and for water vapor; δ_0, pure water; δ_c, solution of concentration c.

Tetraalkylammonium salts give shift curves that are linear (within the experimental errors) up to the highest concentrations; the $(d\delta/dc)_{c=0}$ (c is the molal concentration) are not additive. For example, the differences for bromides and nitrates having from one to four CH_2 groups (in increasing order) are 1.4, 1.5, 1.9, $1.6 \cdot 10^{-6}$, whereas for inorganic cations the difference is constant at 4.3×10^{-6}. The rise is especially unexpected for tetra-n-butylammonium bromide and nitrate. Some other evidence indicates that hydrocarbon radicals can bind water in solutions; if they give rise to hydrogen bonds, the screening ought to be less, whereas in fact it is greater. An attempt has been made [33] to explain this in terms of a direct interaction between the protons in the water and the electrons in the aliphatic chain; the concentration dependence of the δ for $(C_4H_9)_4NBr$ in methanol indicates that the methyl groups of the one compound do not produce a chemical shift in the other, but that there is a nonlinear shift to the OH group towards the methyl group (towards larger field strengths). This shows that δ for the hydroxyl-group proton can be affected by direct interaction with the protons in the hydrocarbon radicals (at least when these are solvated). The temperature dependence of δ for 1.42 and 3.05 M solutions of $(C_4H_9)_4NBr$ is also remarkable in being the same as for water itself (see Fig. 9). Only the hydroxyl line shows a nonlinear shift to higher fields at higher temperatures for solutions of $(C_4H_9)_4NBr$ in methanol. Line a of Fig. 9 is δ for pure water; curves b and c enable one to compare the experimental results with the published results for the number of hydrogen bonds. Eucken's results [35] and the difference of shift between liquid water and vapor [8] have been used for curve b to calculate δ as a function of temperature (it is assumed that the proton δ becomes the δ for water vapor if the hydrogen bond is broken, although this is not strictly true). Curve c is similar and derives from the data of Haggis et al. [36]; the difference between the measured and calculated curves indicates [33] that the structure of the water is conserved more than Eucken supposes but less than Haggis et al. [36] suppose. Figure 9 shows that the temperature coefficients of the δ for inorganic salts are less than that coefficient for water, which is interpreted [33] as a loss of distinction between free and bound water at high temperatures.

The above discussion covers only the main features of the work of Hertz and Spalthoff, on account of the unsatisfactory state of the theory of chemical shifts; this is especially so for aqueous solutions, for which we need additional results on relaxation times, as has been emphasized [33].

TABLE 3

Ion	δ·10⁶ from [31]	δ·10⁶ from [33]	Ion	δ·10⁶ from [31]	δ·10⁶ from [33]
Li^+	−0,09	−0,22	Zn^{++}	−1,24	—
Na^+	0,57	0,44	La^{+3}	−2,39	—
K^+	0,71	0,44 •	Al^{+3}	−5,19	—
Rb^+	—	0,47	F^-	−1,20	−0,69
Cs^+	—	0,40	Cl^-	0,0₅	0,44 •
Be^{+2}	−4,89	—	Br^-	0,21	0,69
Mg^{+2}	−2,08	−1,65	I^-	0,35	1,06
Ca^{+2}	0,45	−0,50	NO_3^-	0,09	0,26
Sr^{+2}	—	−0,08	ClO_4^-	0,85 •	—
Ba^{+2}	0,23	0,07	SO_4^{-2}	−1,17	—
			PO_4^{-3}	−3,83	—

• assumed

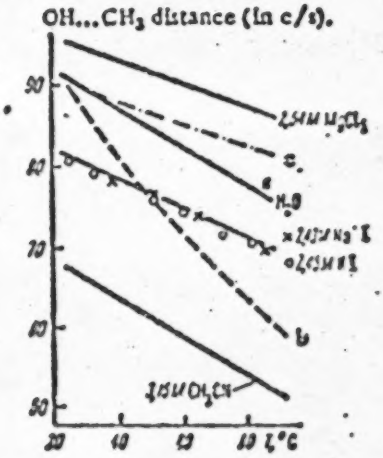

Fig. 9. Shift as between aqueous solutions and pure water as a function of temperature for H_0 = 6007 gauss.

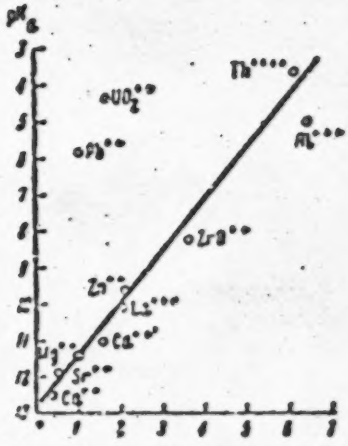

Fig. 10

Axtmann [37] has recorded proton spectra for solutions of nitrates; he found a doubtful correlation (Fig. 10) between δ M (the molar shift) and pK_a for the reaction.

$$M(H_2O)_6^{z+} + H_2O \rightleftarrows H_3O^+ + M(H_2O)_5(OH)^{+(z-1)}.$$

Such ions interact with the water by an ion-dipole mechanism; independent evidence shows that ions which do not obey this relation are bound covalently to the water. On the other hand, some of the deviations (e.g., for Mg^{++}) are to be ascribed to differences in the coordination numbers. Axtmann has proposed to use this correlation as a test for the type of interaction.

Mavel [33] has examined the proton resonance of water dissolved in solvents containing oxygen in their molecules (also in pyridine) and has interpreted the results on the basis [31] discussed above. The dominant process as regards δ is the loss of structure in the water; the main one in pyridine is the formation of complexes (δ as a function of composition has a minimum). Mavel has calculated the part of δ to be ascribed to complexing, and the results are in reasonable agreement as regards the sequence of interaction with organic solvents. He [38] has also measured the equilibrium constant of

n-mer of water + solvent ⇄ complex + monomer.

The degree of association of water was taken as 3.6, although the best form for the curve is obtained if the water is assumed to occur as dimers.

Effects of Exchange on NMR spectra

Acids and bases were among the first solutes to be examined by means of NMR; Gutowsky and Saika [39] were the first to record the proton spectra of solutions of strong acids, while Masuda and Kanda [40] were the first to record spectra for other nuclides in such solutions. The proton spectrum of any inorganic acid (or base) consists of a single line whose chemical shift depends upon the concentration. This result is at first sight surprising, because one would expect the protons to give three lines corresponding to the three states HA, H_2O, and H_3O^+. However, the above discussion related to systems in which exchange was slow or absent, whereas this factor is important for the NMR spectra of acids and bases. The effect may be explained as follows [8, 39, 41]. If the exchange frequency is low, the protons of HA (proportion P_A) give a line at ω_A; the protons of HB (proportion P_B) give a line at ω_B. Figure 11 shows the effects as the rate of exchange between HA and HB increases (from top to bottom). The lines first broaden, then fuse into one whose width is of the order of the chemical shift between HA and HB; finally, we get a fairly narrow line. The width is maximal when $1/\tau' \approx |\omega_A - \omega_B|$ (τ' is the mean time a proton spends in HA or HB). This behavior is explained as follows. The initial broadening results from the restricted time for which a proton has a given precession frequency; if this time is τ', the spectral width is proportional to $1/\tau'$, on account of the uncertainty principle $\Delta E \cdot \Delta t = \hbar$. But $E = \hbar\omega$ and $\Delta t = \tau'$, so we have that $\Delta\omega = 1/\tau'$, in which $\Delta\omega$ is the uncertainty in the angular frequency (the line width).

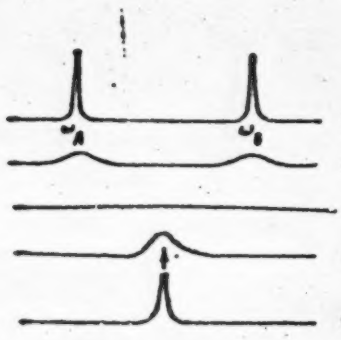

Fig. 11. Variation of NMR spectrum with exchange rate ($P_A = P_B$, strengths arbitrary).

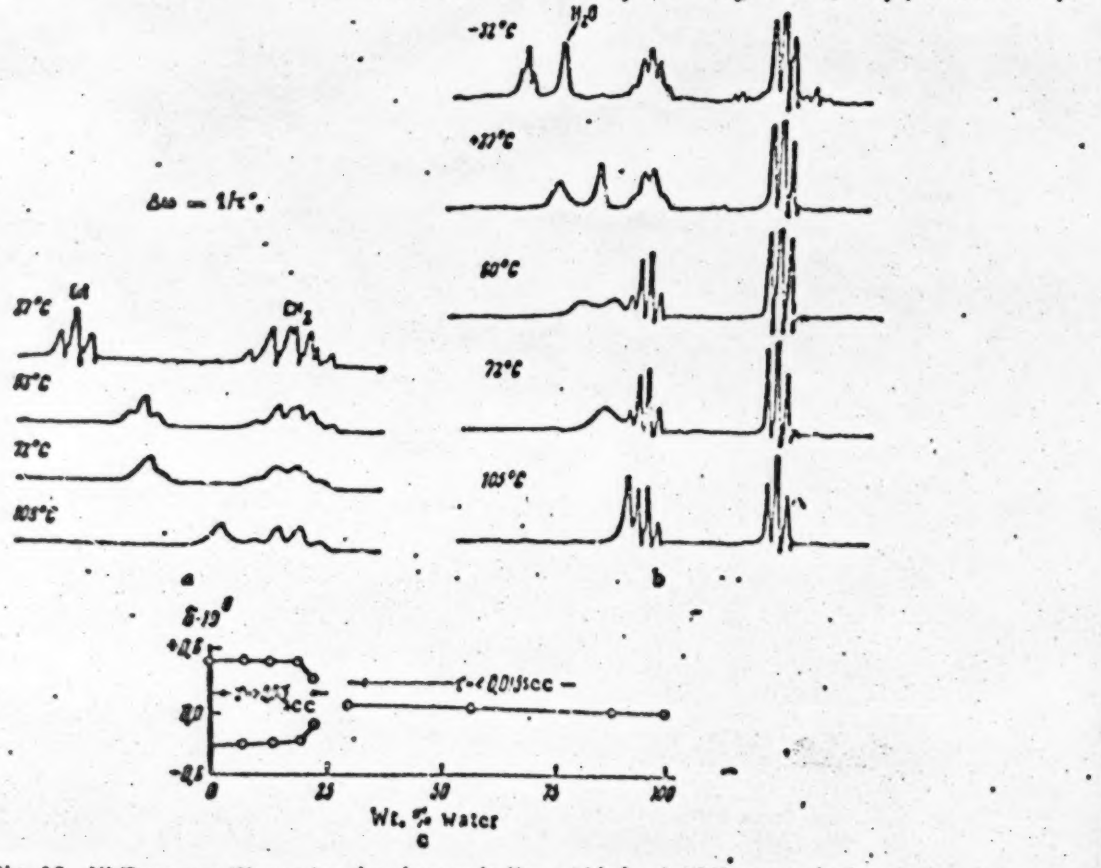

Fig. 12. NMR spectra illustrating the changes in line width for the OH group of ethanol: a) Pure ethanol at several temperatures; b) 2:1 ethanol-water mixture; c) variation of δ for OH in ethanol-water mixtures.

The line does not broaden indefinitely as the exchange rate increases, because the mean time between acts of exchange becomes small when the exchange rate is high, and for $\tau' \ll 1/\delta$ the protons have some effective mean frequency; exchange then causes only small random fluctuations in phase. The higher the exchange rate the smaller these fluctuations, so the sharper the line [41]. (The process is considered quantitatively in [8].)

Any multiplet splitting caused by spin-spin interaction can be used to examine exchange between identical molecules, as for the hydroxyl proton in ethanol (Fig. 12) or methanol. The hydroxyl lines of these compounds have fine-structures resulting from the spin states of CH_3 (methanol) or CH_2 (ethanol), and exchange in general is accompanied by a change in the proton frequency (on account of differences in the spin states). The individual components thereby become broadened at low rates of exchange and fuse into one at high rates. Figure 12 illustrates this effect of the rate of exchange; each component gives an independent estimate of the exchange rate. Arnold [42] has used the effects of HCl on the spectrum of ethanol to calculate the exchange time; similar effects are produced by raising the temperature, and related ones by the addition of water. In the last case the lines of H_2O and OH fuse into one as the water content increases; the signals are no longer separate even for a 1:1 mixture, and δ is independent of the concentration (Fig. 12). The relation

$$\Delta / \Delta_c = \sqrt{1 - \frac{1}{2\pi^2 \tau'^2 (\nu_A - \nu_B)^2}} \qquad (17)$$

gives an exchange time of 7.3×10^{-3} sec for 72° (Δ is the actual distance between the peaks, and $\Delta\tau$ is the same for τ' large). The activation energy is 7.6 kcal/mole.

Mavel has made a detailed study of proton exchange for water-alcohol mixtures [43], from which he deduces the proportions of complexes, free and bound forms, etc. He finds that the degree of molecular association is dependent on the length and branching of the alkyl chains.

If the exchange rate is fairly high, and if the spectrum is as for the middle curves in Fig. 11, then the line width $1/T_2'$ is

$$1/T_2' = P_A/T_{2A} + P_B/T_{2B} + P_A^2 P_B^2 (\tau_A' + \tau_B')(\omega_A - \omega_B)^2. \qquad (18)$$

This effect appears as a fall in T_2 relative to T_1. Meiboom et al.[44] have recorded the effect as a function of pH for water (Fig. 13); they interpret the fall in T_2 relative to T_1 in terms of a relaxation mechanism whose correlation is $\tau_c > 1/\omega_L$. The mechanism for the middle range of pH is supposed to be the formation and breakage of hydrogen bonds by proton migration; this model explains the minimum in T_2 at pH 7. The rapid transfer between $H_3O^+OH^-$ and H_2O is responsible for this minimum in T_2, but this process cannot explain why T_2 remains lower than T_1 at the ends of the range. There is a further mechanism operative in these pH regions (see below).

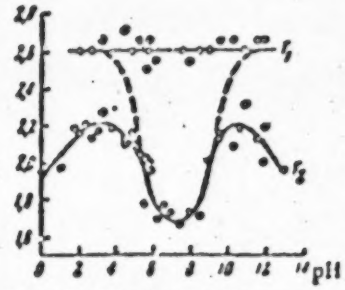

Fig. 13. The broken line represents the T_2 calculated from (18).

Exchange is an important feature of proton resonance for solutions of electrolytes, although its effects might appear to be concealed, because the rate is very high (the rates of formation and rupture of hydrogen bonds are large). A proton in such a bond has a screening that differs from that for a proton not in such a bond; if the correlation time corresponding to the mean life of these two states is small (less than 10^{-2} sec), the resonance will occur at the frequency corresponding to the mean screening for the two states. Any change in temperature or in the concentration of electrolytes or other solutes will cause a change in the proportion of the protons in the bonds; this is responsible for the variations in δ for water with temperature and concentration [8].

On this basis we can explain the NMR spectra of solutions of strong acids; the shift should be proportional to the fraction p of protons that exist in the H_3O^+ state if dissociation is complete: $\delta = p\delta_{H_3O^+}$. This relation generally applies up to $p = 0.2-0.3$, but $\delta_{H_3O^+}$ [8] takes different values (-11.8, -11.1, and -9.2, all $\times 10^{-6}$) for nitric, hydrochloric and perchloric acids respectively. The anion has some effect on the water bound to it, as is also indicated by the deviation from linear concentration dependence for δ. The effect may be explained [39] if allowance is made for incomplete dissociation:

$$\delta = \alpha p \delta_{H_3O^+} + (1 - \alpha) p \delta_{HA}/3. \qquad (19)$$

In this way we may determine α (the degree of dissociation) as well as the dissociation constant K. The δ for nitric acid give K = 22, which agrees well with K = 21 found in Raman spectra. Proton resonance gives K = 38 for perchloric acid. The dibasic acids, e.g., sulfuric [39,45], give a more complicated concentration dependence for δ; the shift for H_3O^+ is -13.1 for sulfuric acid, and the α so found agrees well with that from Raman spectra [45].

Masuda and Kanda have recorded the chemical shifts for N^{14}, Cl^{35}, Br^{81}, and I^{127} as functions of concentration for nitric, hydrochloric, hydrobromic, and hydriodic acids in aqueous solution [40]. In every case the line was single and moved to lower fields at the high concentrations. The results point to the occurrence of ion pairs and undissociated molecules; the trend of the shifts shows that the Cl ion is more heavily screened than the chlorine in hydrochloric acid (the effective electron-density distribution is more spherical for the hydrated ion). The α found for nitric acid from the N^{14} NMR spectra does not agree either with that found from Raman spectra or with that from proton resonance [8,40] (Fig. 14).

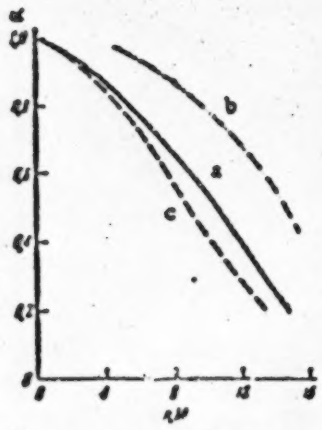

Fig. 14. Relation of α for nitric acid to concentration c: a) from proton resonance; b) from N^{14} resonance; c) from Raman spectra.

Borodin and Skripov [46] have recorded the chemical shift of F^{19} in hydrofluoric acid as a function of concentration. There is rapid exchange between HF, F^-, and HF_2^-, because there is only one line in the spectrum; these species are considered to explain the behavior of δ at low concentrations. The δ_{HF} found for the solutions are less than that for the anhydrous acid, which is explained in terms of heavier screening of the F^{19} in associated forms at high concentrations. The effect should appear for the acceptor atom (H) if the HF–H_2O system is one in which the hydrogen bonding affects the screening of the donor (F).

Utyanskaya et al. [47] have computed the acidity function and the molecular composition for the middle range of concentrations from the NMR results for F^{19} in HF; the results agree well with independent results for Hammett's function, but doubt has been cast [48] on the interpretation given to the chemical shifts.

Hood and Reilly [49] have deduced the temperature coefficients of dissociation for nitric and perchloric acids from proton NMR results. The results for the first acid agree well with those from Raman spectra, but this is not so for the second; they ascribe the discrepancies to differences in the assumptions made in working up the results. For example, no allowance has been made for the change in proton hydration (from $H^+ \cdot 4H_2O$ to $H^+ \cdot 4H_2O$) at high acidities in the case of the NMR results. An appreciable error is also introduced by the assumption that the proton screening for the dilute acid is the same as that for the anhydrous acid, since this assumption forms the basis for calculating α.

Hogfeld [50] has considered the hydration of anion and proton for nitric acid on the basis of NMR and Raman spectra; he finds that the concentration of NO_3^- is maximal when there are 3–4 molecules of water per H^+ (and per NO_3^-), whereas the corresponding value for perchloric and sulfuric acids is about one molecule. Nitric acid is less dissociated than the other two; even when the molar proportion of that acid is 0.40, there are about four water molecules per molecule of dissociated acid, whereas sulfuric acid of this concentration contains almost no free water and no appreciable amount of HSO_4^- (i.e., the latter does not appear until all the water has become bound).

Gutowsky and Saika [39] have recorded the proton-resonance spectra of solutions of NaOH and KOH; the signal moves to lower fields as the concentration increases, the effect being more marked for KOH, which is explained in terms of the larger radius of the cation. The $\delta_{OH^-} = 10 \cdot 10^{-6}$ is found as 10×10^{-6}; the lifetime of OH^- is estimated as not more than 10^{-4} sec. Gutowsky and Fujiwara [51] have found that the spectrum of NH_4OH consists of one narrow line only, which means that the individual proton states have lives of less than a millisecond. If

$$NH_3 + H_2O \rightleftarrows NH_4^+ + OH^-$$

represents the actual process, we should have that $\delta = p\delta_{NH}$ describes the concentration dependence, but this is not found to be so. For this reason they consider that the equilibrium is not based solely on free NH_3 and free H_2O but on strongly interacting molecules connected by hydrogen bonds.

If dissociation is assumed to be complete, we have that H_3O^+ and OH^- proton frequencies about 10×10^{-6} parts higher than the proton frequency of pure water at room temperature [8]. This is surprising, because the ions have opposite signs, and δH^+ (relative to water) is -27×10^{-6} [8]. The explanation proposed [39] is that the bonds in H_3O^+ are 1/3 ionic, but this does not serve to explain the position of the signal for OH^-; allowance must be made for the

environment of the ions. The effect is dependent upon the interaction between the ion and the protons in the surrounding water as well as upon the influence of the ion on the closest protons. The hydration and hydrogen bonding are forms of association that produce large shifts to the low-field side, so the bond type cannot always be deduced from δ alone [8].

Axtmann et al.[54] have recorded the proton shift as a function of nitric acid concentration for solutions containing aluminium nitrate. It is found that the salt reduces α considerably (Fig. 15), and it is supposed that the equilibrium

$$HNO_3 + H_2O \rightleftarrows H_3O^+ + NO_3^-$$

is the main one for acid concentrations below 18 M; α is calculated on this basis. Another assumption made is that the equilibrium constant does not depend on the salt concentration; the salt is supposed to act mainly by binding water to Al^{3+} ions, which causes the equilibrium point to shift to the left. In other words, α is calculated with allowance for the common-ion effect of the salt, for the effective hydration number n of the cation, and for the apparent α. It is very difficult to determine n; use is made [52] of the NMR results for electrolytes. Shoolery and Alder [34] have determined the exchange time (about 8 msec) for the water in the hydration sphere of the Al^{3+} ion on the basis of the proton line width; Broersma [53] gives about the same value on the basis of relaxation measurements, and he also claims that the Al^{3+} ion is surrounded by two or three layers of water molecules in strong solutions. On this account it was assumed [52] that $n > 6$, and an effective n of 10 was used in the calculations. This is equivalent to saying that each ion binds 20-40 molecules of water, of which only four are strongly bound. The good agreement with experiment (Fig. 15) shows that this model is correct.

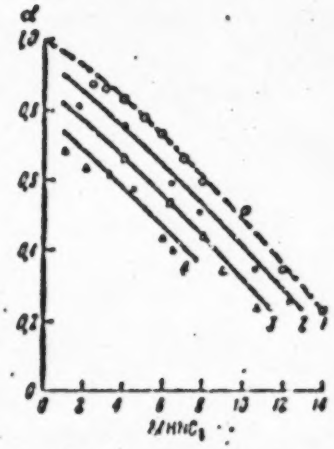

Fig. 15. Degree of dissociation of nitric acid as a function of concentration for solutions containing aluminium nitrate at concentrations (M) of 1) zero; 2) 0.525; 3) 1.05; 4) 1.50. The full lines represent calculations made for n = 10.

Confirmation of the hydration of Al^{3+}, in so far as it affects the degree of dissociation, is obtained from the effects of lithium chloride and nitrate, which reduce α in accordance with the degree of hydration of Li^+. In this way it was also demonstrated that the anion also plays a part in reducing α.

The temperature coefficients for the shifts for aluminium nitrate in water and in aqueous nitric acid are in good agreement with theoretical [34] concepts, particularly as regards the solutions in water. All the same, it did not prove possible [52] to explain why α decreases (not increases) at high temperatures; the fall at 80° is about 20% for 6.32 M HNO_3 that is 1.05 M in $Al(NO_3)_3$.

Mavel [54] has examined solutions of 100% nitric acid in chloroform, methylene chloride, acetic acid, dioxane, etc. The degree of ionization is negligible for these solutions, and the proton-resonance results then give a value (about 0.1) for the dissociation constant of the dimer of the acid.

There are several papers on the chemical shifts for the proton resonances given by solutions of weak acids. Gutowsky and Saika [30] have examined acetic acid dissolved in water or in 1,1-dichloroethane; the latter solvent gives a concentration dependence for δ that points to the existence of a dimer bound by strong hydrogen bonds.

Patterson and Ettinger [55] have examined the CO_2-H_2O system by means of the resonance of C^{13}; carbon dioxide (57.8% C^{13}) was dissolved in solutions of alkali, and these gave spectra consisting of two lines only (those for the dioxide and for the bicarbonate ion; the lines of H_2CO_3 and of the carbonate ion were not seen). The chemical shifts for C^{13} in the acid and in the bicarbonate ion are probably small, and there should be rapid proton exchange between these two species, so the line for H_2CO_3 is probably fused with that of the ion. The spectra are made yet more difficult to interpret by the low concentration of the acid and by the poor sensitivity of the apparatus for C^{13}. The results are in agreement with earlier studies on this system, but they contribute nothing really new to our knowledge, because saturation effects (in the C^{13} signals) and the proton exchange hindered the investigation. At present no reason can be given for the presence of much unhydrated carbon dioxide or for the slowness of the hydration. The mean lifetime of a molecule of CO_2 is about 40 sec; it is hoped that more reliable lifetimes can be measured for CO_2 and H_2CO_3 under more favorable conditions.

Nuclear Relaxation in Solutions

I turn now to researches in which several NMR techniques have been used simultaneously; these are concerned with some more or less quantitative parameters of ion hydration and of solution structures. First of all I consider the theory of nuclear relaxation in solutions. Block et al. [2] some years ago demonstrated that the relaxation time of a solution is reduced by the presence of paramagnetic ions; Bloembergen et al. [3] gave the following explanation for this effect. The magnetic moment of a paramagnetic ion is about 10^3 times the nuclear moment μ, so the fluctuating local fields are strong and the relaxation time is short. The contribution from intramolecular effects becomes much less important than that from intermolecular effects, whose contribution is [3]

$$1/T_1 = \frac{12\pi\gamma^2\eta N_i\mu_N^2}{5kT}, \qquad (20)$$

in which N_i is the number of ions per cm^3 and μ_N is the effective magnetic moment of an ion; $1/T_1$ is directly proportional to N_i and to μ_N^2. The general agreement with experiment is good, although there are certain discrepancies at low concentrations.

Kozyrev and Rivkind [56] have shown that chelation of a paramagnetic ion effects μ_N and T_1 for water protons. The paramagnetic species is responsible for the energy transfer to and from protons, and the ligands screen the ion from the protons; they also increase the distance of closest approach, which weakens the ion-dipole interaction and so increases T_1 [55]. An empirical screening rule applicable to the 3d-elements has been formulated in terms of M, the molecular weight of the complex:

$$M/\mu_N^2 \approx \text{const.} \qquad (21)$$

This rule has been used in deducing the structures of complexes; it is found to apply if the hydration shell is not included as part of the molecular weight, which is explained [56] in terms of rapid exchange of intact water molecules and also of rapid hydrogen exchange between the water bound to the ion and the rest of the solution. The role of pH is not discussed, although this must be substantial, at least for proton exchange; but Rivkind does state that T_1 is very sensitive to the length of the $Me^{n+}-OH_2$ bond, because that length determines the distance of closest approach [57]. For example, results for Cr (III) indicate that Cr^{3+} forms covalent $Cr^{3+}-OH_2$ bonds to its hydration water and that these bonds are 15-20% shorter than the bonds formed by other ions [57].

Rivkind's measurements of T_1 and T_2 for aqueous solutions reveal that the short-range order affects proton relaxation [56]; T_1/T_2 should [3] be 1 for liquids, but this is not always so, the explanation offered being that chelation affects T_1. Rivkind [58] has shown that this anomaly occurs with many paramagnetic ions, from which he concludes that τ_c for the region near an ion is very much larger than would correspond to the random Brownian motion (about 10^{-11} sec) assumed in [3]. The water in the hydration shell is of low mobility, so the relaxation is governed by the more rapid process (electron spin reversal), which is characterized by the electron-spin relaxation time τ_s. This deduction has been confirmed by means of tests on aqueous solutions of glycerol. Rivkind [58] claims that relaxation-time measurements thus provide a powerful means of studying the structures of solutions.

There is a large increase in T_1 when heavy water replaces the ordinary kind [18]; this effect is to be ascribed to the stability of the hydration shell, which reduces the Brownian motion. Rivkind has demonstrated [59] that the exchange rate is altered when deuterons replace protons; the absence of Brownian translational motion in the first two or three hydration layers is quite sufficient to explain the effect [59]. The curve relating T_1 to the deuterium content is distinctive of the ion, which may prove of value in future studies [59].

The results of [59] point to the importance of work on proton resonance for solvents other than water. It is likely that the impermeable layer around a solvated ion will diminish μ_N, with the result that T_1 will be large (on account of the large ion-proton distance). Rivkind has made some measurements on hydrated paramagnetic salts in solution in alcohol and acetone [60]; he finds that T_1 increases with the charge on the ion, which he explains in terms of increase in the size and strength of the solvation shell.

Rivkind [61] has also recorded relaxation times for deuterons, from which he has drawn conclusions about the $Me^{n+}-OH_2$ and $Me^{n+}-OD_2$ bonds. The effects of Mn^{2+} on T_1 and T_2 for deuterons are different from those of other ions (Cu^{2+}, Fe^{3+}, Cr^{3+}), but the effect vanishes when the ion is chelated, because the hydration shell is altered. He considers that the $Mn^{2+}-OH_2$ bond is somewhat covalent, whereas the bond to heavy water is purely ionic, which weakens the magnetic interaction between the Mn^{2+} and the deuterons in the first coordination layer (this is seen as

an anomalous increase in T_1). It remains uncertain why Cr^{3+} does not behave in the same way as Mn^{2+}, because the $Cr^{3+}-OH_2$ bond is also covalent. It may be that exchange of the bound water is important here (that exchange is very slow for Cr^{3+}).

Bloembergen has explained the anomalous T_1/T_2 for Mn^{2+} and Gd^{3+} in terms of a contact interaction between the electrons in the ion and the protons in the water [62, 63]. This interaction has a correlation time very much longer than the dipole one, so T_2 is reduced relative to T_1. This contact interaction is said to occur only when the electron density at the nucleus differs from zero [63]; if this is so, we have the very interesting result that the density of the d-electrons of Mn^{2+} at the protons of the closest water molecules is not zero.

The contact interaction is taken account of in nuclear relaxation partly via τ_s and partly via τ_n (the time spent near the ion by a water molecule or proton).

This again shows that ion-water interactions have major effects on T_1 and T_2; T_2 is governed not only by the dipole-dipole interaction but also by the contact interaction (if any). Kin and Davidsen [64] have confirmed this from the effects of chelation on T_1/T_2 for solutions containing Mn^{2+}. If a hexadentate chelating agent (EDTA) is used (to give MnY^{2-}), or a tetradentate one (nitrilloacetate, to give MnX^-), there is little increase in T_1 but a large increase in T_2; the two become equal and the anomaly is removed. In fact, $T_1/T_2 = 9.5$ at 40 Mc for Mn^{2+}, whereas the values for MnY^{2-} and MnX^- are 1.15 and 1.05 respectively. The ESR spectra indicate a fall in τ_s from $3\cdot10^{-9}$ sec (Mn^{2+}) to $3\cdot10^{-10}$ sec (MnX^-); these ESR results are considered [64] to show that the MnX^- complex contains two water molecules. The response of τ_s to the composition and structure of the solution will now be examined further, as being very important.

The T_1 and T_2 for solutions of paramagnetic ions are determined by dipole-dipole (spin-spin) and contact (spin-exchange) interactions as between nuclei and electrons. The probabilities of the transitions associated with these interactions are additive, and so they make additive contributions to the relaxation times. Solomon's [65] correct expressions for the dipole interaction, used in conjunction with the Curie-Weiss law and the equations for the transition probabilities associated with contact interactions [63, 66], give us the Bloembergen-Solomon [67] relations for T_1 and T_2:

$$1/T_1 = \frac{2S(S+1)\gamma^2g^2\beta^2P}{15k^2}\left[\frac{3\tau_c}{1+\omega_e^2\tau_c^2}+\frac{7\tau_c}{1+\omega_e^2\tau_c^2}\right]+\frac{2S(S+1)A^2P}{3k^2}\left[\frac{\tau_c}{1+\omega_e^2\tau_c^2}\right] \tag{22}$$

$$1/T_2 = \frac{S(S+1)\gamma^2g^2\beta^2P}{15k^2}\left[\tau_c+\frac{13\tau_c}{1+\omega_e^2\tau_c^2}\right]+\frac{S(S+1)A^2P}{3k^2}\left[\tau_c+\frac{\tau_c}{1+\omega_e^2\tau_c^2}\right]. \tag{22a}$$

Here S is electron spin, P is the probability that a proton is in the hydration shell of a paramagnetic ion (P is clearly proportional to the concentration N_I), ω_s is the ESR frequency, A is the exchange-interaction constant (in c/s), and τ_c is the correlation time of the exchange interaction. Expressions (22) and (22a) apply for the normal case $\omega_L \ll \omega_s$; the first term derives from the dipole interaction, the second from the exchange. Further, τ_c is itself composite:

$$1/\tau_c = 1/\tau_e + 1/\tau_h. \tag{23}$$

The characteristic times appearing in (22) and (23) are related to temperature by

$$\tau_e = \tau_e^0 \exp(V_e/RT) \tag{24}$$

$$\tau_h = \tau_h^0 \exp(V_h/RT) \tag{24a}$$

$$\tau_s \approx \tau_s^0 (T - T_0)/T_0. \tag{24b}$$

Here V_e is the activation energy for the molecular motion of the hydrated ion; this motion is principally one of rotation, because translational motion is hindered by the large size of the assembly [67]. But activated translation with the shell can occur [4] and may even be dominant over translation without the shell (e.g., as for Mg^{2+}). (The V_h is the energy of activation for the loss of a proton or water molecule from the shell.)

Bernheim et al. [67] have made spin-echo measurements of T_1 and T_2 as functions of temperature for solutions containing Mn^{2+}, Co^{2+}, and Ni^{2+}; the results fit (24) exactly, and the relaxation in solutions containing Mn^{2+} is governed by exchange interaction as well as by chemical exchange. At low temperatures τ_s determines τ_c, but the value

tends to τ_h at high temperatures, although it is not clear whether proton or water-molecule exchange is the factor that governs τ_h. They [67] suppose, from the fact that $V_h = 8.4$ kcal/mole ($\tau_h = 2.5 \cdot 10^{-9}$ sec), that the exchange is mainly that of protons, because the activation energy for H_2O in the aquocomplexes of Co^{2+} and Cu^{2+} is about three times larger. The V_c of Table 4 were calculated from the straight parts of the experimental curves.

TABLE 4

Salt	Concentration, ion/cm³	V_c kcal/mole
$Cu(NO_3)_2$	$1 \cdot 10^{20}$	2.48
$CuCl_2$	$1 \cdot 10^{20}$	2.64
$CuSO_4$	$0.5 \cdot 10^{20}$	2.67
$CuSO_4$	$1.0 \cdot 10^{20}$	2.74
$CuSO_4$	$2.04 \cdot 10^{20}$	2.78
$CoCl_2$	$3 \cdot 10^{20}$	1.45
$MnCl_2$	$3 \cdot 10^{18}$	5.5
$Gd_2(SO_4)_3$	$3 \cdot 10^{18}$	2.4

It may be that the values obtained for the energies are too high, although they [67] believe that the V_c are compatible with the mechanism that governs the relaxation time. Solutions containing Cr^{3+} have T_1 and T_2 that vary with temperature as for Mn^{2+}, but more rapidly [68, 69]. Here the violet form of $Cr(H_2O)_6^{3+}$ is present, and the results are very much dependent on the extent to which the system has approached thermodynamic equilibrium; that approach is very much slower than the rate of variation of the temperature in the experiments, so the reproducibility is poor. On the whole, the reproducibility is better at low temperatures, because the changes involve only the second hydration layer (the changes in the first layer occur at higher temperatures and are accompanied by hydrolysis and polymerization). The Cr^{3+} ion represents a limiting case, but the properties it displays must occur in other instances, which have so far been overlooked [69].

Laukien and Haeuser [68] have made proton-relaxation measurements on aqueous solutions of paramagnetic ions, including some not considered in [67], namely Fe^{3+}, Ti^{3+}, Fe^{2+}, and VO^{2+}. The results are considered only from the point of view of the changes in τ_s.

Principles of the Theory of Hydration and Exchange of Water of Hydration

The above review of NMR techniques indicates that the various problems are related (exchange, ion-water interactions, structural questions, self-diffusion). The examples are mainly general and concern the theory of hydration as a whole, but some papers contain detailed results on particular aspects. At this point I shall consider some principles of Samoilov's [4] theory of hydration.

First we distinguish between short-range and long-range hydration; in the latter the liquid is polarized by the field of the ion. The short-range hydration represents primarily the effect of the ion on the translational motion of the water molecules; this interaction is very important, because it governs the kinetic parameters of the solution and the mechanisms of many processes. This short-range hydration is no mere binding of a certain amount of water; it is governed by the strength of the interaction with the nearest water molecules, whose number is in some case determined by the structure of water [4]. This form is specified by ΔE, the change in the height of the potential barrier separating adjacent positions of equilibrium for a water molecule. This quantity is directly related to exchange (jumps) of water molecules, i.e., to τ_i/τ (the ratio of the mean lifetime of a water molecule in an equilibrium position immediately adjacent to the ion to the mean lifetime in pure water). Samoilov gives for this the approximate relation

$$\tau_i/\tau = \exp \Delta E/RT. \qquad (25)$$

The exchange frequency is related principally to the short-range hydration, because this hydration is a result of the effects on the translational motion, which is an essential feature of such exchange. The exchange is governed not by the total interaction energy as between particles but by the change in that energy at small separations, so the important feature is any difference in the slopes of the interaction-energy curves near the potential minima (Fig. 16). A large value for H (the energy of the interaction between ion and water molecule) does not necessarily imply slow exchange. For exchange, if H is larger than W (the energy of the interaction between water molecules, H and W being the total energies required to produce infinite separation), the exchange may still be more rapid than that in pure water, because we may have that $\Delta w > \Delta h$, $\Delta E < 0$ ($\tau_i/\tau < 1$). Here Δw and Δh are the changes in the potential energy of a water molecule in the field of another such molecule or of an ion respectively, these changes being those consequent on displacement from the equilibrium position to the top of the potential barrier (Fig. 16). The situation is termed negative hydration to distinguish it from positive hydration, for which $\Delta E > 0$ ($\tau_i/\tau < 1$). In the latter case the motion of the water molecules next to the ion is hindered, whereas in the former case the motion is more free than that in pure water (the exchange becomes more rapid). This shows that τ_i/τ and ΔE are quantities of great in-

terest, but they are difficult to calculate on account of lack of data on Δh and Δw (the first cannot even be estimated on the basis of ion-dipole interactions). It is often difficult or impossible to derive η/T on the basis of transport numbers and self-diffusion measurements, so the NMR results are of particular importance. Some papers cited below illustrate the advantages of the method.

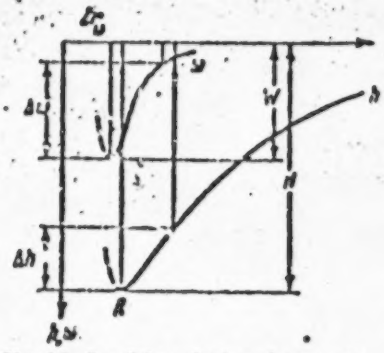

Fig. 16. Possible relations between H, W, Δh, and Δw (after Samoilov [4]).

Broersma [70-72] has considered the relations between the relaxation times of the components, the concentrations, and the relaxation times of the mixtures. The system behaves as though it consists of a single phase (as regards the relaxation time) if the relaxation effects are entirely averaged within a certain period (see [70] on that period); but if such averaging does not occur, the proton-resonance signal is governed by the sum of the contributions from the components, each of which has its own relaxation time. In the intermediate case it is proposed to use a quantity $\int_0^t dt/T_{2v}$ (the amount of relaxation in a time t), in which T_{2v} is the mean relaxation time for the system. Tests on copper sulfate suspended in hexane and dilute solutions of paramagnetic ions show that the amount of relaxation is governed by diffusion and by the contact time of the protons, as the theory predicts. The method of relaxation spectroscopy [70] is based on this observation, and it appears to be very valuable in that it gives information on self-diffusion and hydration for paramagnetic solutions. One important result so obtained is the time for which the water molecules in the paramagnetic field are equal in number to the average value; this time is close to τ_l, and for Cu^{2+} comes out as $6 \cdot 10^{-6}$ sec (for three molecules), or $1.2 \cdot 10^{-6}$ for Fe^{3+} (two molecules) [70]. Apart from Shoolery and Alder's results for Al^{3+}, this represents the first independent determination of a quantity closely related to τ_l.

Broersma has considered the effects of diamagnetic ions on proton relaxation also [71]; he has derived temperature and concentration curves. The experimental results can be explained if allowance is made for hydration and for mutual viscosity (the interaction between the free and bound layers of liquid). For example, the effects of singly charged ions are explainable in terms of a slight reduction in the diffusion rate for free water molecules. Further, τ_h (which is analogous to τ_c in certain ways) can be estimated if the system is treated as consisting of two phases as regards nuclear relaxation. Broersma's theory explains this if allowance is made for diffusion and for the changes in the sizes of the assemblies, so the equations defining the relaxation times contain terms representing the H–H interaction in a free water molecule, the relative motion of the free and bound water, the H–H interaction in a bound water molecule, and the motions of the free water and of the ion. Allowance is also made for rotation and translation of the water of hydration if the ion is paramagnetic. Broersma discusses the effects of hydration on the viscosity of water and demonstrates that the η derived from capillary-flow measurements is only the mean of widely varying values for the local viscosity. He considers that η_h varies widely with the concentration and that it is exponentially related to the activation energy for the escape of a water molecule from the hydration layer; on this basis he explains the differences between the various values of η_h. He gives [71] the η_h for solutions of the chloride and sulfate of Al^{3+} (5 and 60 mμ); these agree well with Shoolery and Alder's [31] values.

A later paper [72] deals in more detail with τ_h in relation to the local relaxation times for the various relaxation phases. It is found that τ_h falls off exponentially with distance, but that T_{2v} increases (at least for paramagnetic ions). The concentration curves are used to distinguish the contributions from the various sources and thence to derive η_h. Further, the effects of ionic radius are used to find τ_h as a function of distance. Values are also given [72] for the ratio of the relaxation times for the hydration shells and for the free water; it is not clear why the values for Li^+, Rb^+, Mg^{2+}, and Ba^{2+} are as small as that for K^+ (numerical estimates are not given in the paper), because these ions differ in hydration. Moreover, it is not stated to which ions the observed change in the ratio of 0.1 [72] (which is almost within the experimental errors) applies. Some of the ions show negative hydration, which makes the topic of particular interest; the effect is treated [72] as indicating loss of order in the system, in which assemblies consisting of several water molecules are preferentially broken up by the ions. This effect appears to be one of negative hydration; the τ_h calculated in [72] are (Table 5) in some cases in good agreement with the τ_l, but large discrepancies also occur, particularly for Cr^{3+} and Co^{3+}, which are known to bind water very firmly. These discrepancies arise in part from errors in the measurements and in part from incorrect assumptions in the theory. An important feature of the latter is the distinction between the time of contact for a proton and the ion and that time for the molecule as a whole. This feature is especially important for neutral and alkaline solutions.

Recently Broersma [73] has examined the hydrodynamic equations for an unbounded medium whose viscosity is a function of the distance from a suspended particle of a given radius. The theory shows that proton resonance may provide a means of measuring the diffusion constant of such particles, which also affects the viscosity of the suspension and the transition to a gel. He [73] discusses in this respect some results (Table 6) for n, the hydration numbers of some diamagnetic ions.

TABLE 5. Parameters for the Exchange of Water Molecules Closest to an Ion

Cation	τ_A, sec [71,75]	$\tau_c^{(1\cdot10^{-3})}$, sec [71,75]*	τ_1 sec [80]	$\tau_1^{(1\cdot10^{-3})}$ sec [81]	τ_2 sec **	τ_2/τ_c
Li^+		0,8(3,0)***		$<1\cdot10^{-3}$	$5,92\cdot10^{-9}$ [4]	3,48
Na^+		0,4(1,5)***			$2,48\cdot10^{-9}$ [4]	1,46
K^+		0,1(0,5)***			$1,10\cdot10^{-9}$ [4]	0,65
NH_4^+		0,03				
Be^{2+}		2,0****		$>1\cdot10^{-4}$		
Mg^{2+}		1,8****		$<1\cdot10^{-3}$	$1,47\cdot10^{-7}$ [4]	
Ca^{2+}		1,0****			$3,67\cdot10^{-9}$ [4]	
Zn^{2+}	$(1+30)\cdot10^{-3}$	2,5****				
Sr^{2+}		0,6****				
Cd^{2+}		1,4****				
Ba^{2+}		0,3****		$\lesssim1\cdot10^{-4}$		
Hg^{2+}		9,5****		$\lesssim1\cdot10^{-3}$		
Al^{3+}	$0,9\cdot10^{-3}$			$\gtrsim1\cdot10^{-3}$	>0,02 [86]	
Ga^{3+}	$(5+60)\cdot10^{-3}$					
Bi^{3+}				$\gtrsim1\cdot10^{-4}$		
Nd^{3+}	$3\cdot10^{-3}$			$\lesssim1\cdot10^{-4}$		
Fe^{3+}	$2\cdot10^{-6}$					
Cu^{2+}	$1,5\cdot10^{-6}$		$1,6\cdot10^{-6}$			
Cr^{3+}	$1,5\cdot10^{-7}$		slowly			
Fe^{2+}	$1,8\cdot10^{-7}$		$9,0\cdot10^{-7}$		<0,02 [86]	
Mn^{2+}	$1\cdot10^{-7}$		$1,0\cdot10^{-7}$			
Gd^{3+}	$0,8\cdot10^{-7}$					
Co^{2+}			$5\cdot10^{-6}$			2,4
Ni^{2+}			$2,5\cdot10^{-5}$		<0,02 [86]	

*$\tau_c^0 = 2,7\cdot10^{-12}$ sec. **$\tau = 1,7\cdot10^{-9}$ sec [4]. ***τ_c^1 for $Mn(NO_3)_2$ [74]. ****τ_c^1/τ_c^0.

Vdovenko and Sheherbakov [74,75] have measured T_1 as a function of concentration for the nitrates of groups I and II; as previously [70], it is found that T_1 is reduced relative to the T_1 of pure water. This effect is described in terms of Δ_M, the change in T_1 for a molar solution (the molar relaxation shift). The Δ_M and radii for the cations of the main subgroup of group II are inversely proportional one to another; this is not so for those of the other subgroup. Similar effects have been reported [74] for the δ_M for the same ions as calculated from Axtmann's results [37]. There is clearly a correlation between Δ_M and δ_M, as was first noted by Kanda for the NMR spectra of Br^{79} and Br^{81} [76]. The reduction in T_1 is considered [74] to be a consequence of the increase in τ_c resulting from hydration for the main subgroup; in the other subgroup of group II there is a superimposed effect from the covalent $Me^{n+}-OH_2$ bonds (these ions have a larger effect on T_1). Various results [77,78] support this deduction, which is applicable also to T_1 for solutions of uranyl salts [79].

Vdovenko and Sheherbakov [74] have calculated τ_c^1/τ_c^0 for the various ions (τ_c^0 is τ_c for pure water; τ_c^1 is the same for the solution) on the basis of Solomon's [65] equation

$$1/T_1 = 1/T_2 = \frac{3h^2\gamma^2\tau_c}{2b^6}, \qquad (26)$$

which is assumed to be applicable. Further, the change in T_1 is ascribed mainly to τ_c (the H–H distance b is assumed not to change appreciably. It is considered [74] that τ_c^1/τ_c^0 is proportional to τ_1/τ. The T_1 for alkali-metal cations and for halide anions for which the τ_1/τ are known [75] support this conclusion, since τ_c^1/τ_c^0 is almost exactly the same as τ_1/τ. But a full survey [80,81] indicates that the regularity observed in [74] is only a particular case; the rule is not applicable to Be^{2+} (Table 5). As previously [70-72], we must point out that proton-resonance results, although valuable, are subject to certain limitations as regards water-molecule exchange.

Comparison of (20) with (22) on the basis of Broersma's results shows that the μ_N of (20) (the magnetic moment deduced from the proton T_1) is in fact a very complicated quantity that in general differs from μ_s, as Conger and Selwood's [82] results show. There is no direct relation between μ_s and μ_N, especially for the lanthanides; the variation of μ_N with the composition of the solution is not accidental. Rivkind [77] has shown that μ_s remains constant while μ_N varies widely (it falls almost to zero and then rises again as covalent bonds are formed in the complexes). It may be that the μ_N for solutions free from chelating agents may throw some light on ion hydration; (20) and (22) show that μ_N specifies the effect of the paramagnetic ion on proton relaxation in the solvent. This means that it is related to τ_h (for water-molecule exchange). The effects of τ_h appear at low concentrations if the exchange rate is high; in this region we find certain deviations from (20), which Broersma [70] has shown to be caused by the effects of τ_h on the relaxation time. The hydration shell ceases to be permeable to protons if the frequency of proton (or water-molecule) exchange becomes comparable with the frequency of Brownian collision between the protons and the ions. Rivkind's concept of permeability [57] remains applicable at high ionic strengths when the contribution from the hydration shell is small; but the contribution from that shell may be large at high concentrations if the ion is paramagnetic, and this can occur even though the water is firmly bound (as for Cr^{3+}). The μ_N for Cr^{3+} and Gd^{3+} are notable here; the rise in μ_N (which makes μ_N/μ_s about 1.4 [82]) may be caused by the covalent bonds from ion to water.

TABLE 6

Ion	n from			
	proton resonance (±40%) [73]	conduction	diffusion	[4]
Li^+	5	7	2.5	3.8
Na^+	3	5	1.0	3.7
K^+	1	—	0.6	3.8
Mg^{2+}	6	12	—	3.8
Zn^{2+}	12	12	—	—
Al^{3+}	16	—	—	—
Cl^-	2	—	0.2	4.4
OH^-	4	—	—	—
SO_4^{2-}	5	—	—	—

Confirmation of this comes from Shulman and Wyluda's work [83] on the chemical shift for O^{17} in water containing Gd^{3+}; here δ is a linear function of concentration and is $1.2 \cdot 10^{-3}$ for a solution 2 M in $GdCl_3$. The T_2 for O^{17} in pure water is 0.2 sec; T_1 and T_2 depend on the Gd^{3+} concentration, and T_1 may be three orders of magnitude larger than T_2. The shift may be caused by contact interaction in the hydration shell, because the water in this shell is bound to the Gd^{3+} via the 4f-electrons. If we assume (as in [83]) that this ion is coordinated to nine water molecules, the interaction corresponds to 0.02 unpaired electron per oxygen atom, so an alternative explanation of this effect of Gd^{3+} on O^{17} is electron transfer from the oxygen to the ion (products Gd^{2+} and H_2O^+). Orgel [84] comes to this conclusion in his comments on [83].

The use of O^{17} NMR is a very promising technique in hydration studies; this method gave the first direct estimates of the mean lifetimes of water molecules in hydration shells [85], and these are free from the uncertainties associated with proton-resonance results. Connick and Poulson [80] have used the broadening of the O^{17} lines for solutions of paramagnetic ions (Cr^{3+}, Mn^{2+}, Fe^{3+}, Co^{2+}, and Ni^{2+}) for the same purpose; the results show that Cr^{3+} in $CrCl_3$ has the least effect on the relaxation of O^{17}. This is to be explained in terms of the fixed binding, which is allowed for in calculations on the rate of exchange of the water molecules. The line width gives only a lower limit to the exchange rate, because data are lacking for T_2. The formula used is

$$1/T_2 = (1/T_2)_p + (1/T_2)_d \qquad (27)$$

in which the first term arises from the presence of O^{17} near the paramagnetic ion and the second from the diamagnetic environment. For example, the $(1/T_2)_p$ for a $4 \cdot 10^{-3}$ M solution of Fe(III) is $2 \cdot 10^{-3}$ sec. If now Fe^{3+} binds six water molecules, the upper limit to the lifetime of a water molecule in the first coordination sphere is $2 \cdot 10^{-3} \times 6 \times 4 \cdot 10^{-3} / 55.5 = 9 \cdot 10^{-7}$ sec (55.5 is the molarity of water). This corresponds to a lower limit of $1.1 \cdot 10^6$ M^{-1} sec^{-1} for the rate constant of

$$Fe(H_2O)^{3+} + H_2O^* \rightleftarrows Fe(H_2O^*)^{3+} + H_2O.$$

The lower limit for the rate constant of the reaction in which all six water molecules are exchanged is $1.6 \cdot 10^6 \times 6/55.5 = 1.2 \cdot 10^5$ M^{-1} sec^{-1}; comparison with the constants for the chloride and thiocyanate complexes of Fe^{3+} (1.9×10^{-2} and $3.3 \cdot 10^2$ [30]) shows that the exchange rate for water is high, which may be [80] a consequence of the molecular size or of the activation energy. Table 5 gives calculated results for the other ions. Connick and Poulson's results provide an experimental confirmation of earlier deductions about the short-range hydration of ions [4, 85].

Jackson et al.[81] have supposed that the $Me^{n+}-OH_2$ interaction is strong enough to produce a chemical shift for O^{17}; this has been found to be so [82, 83], and the first paper gives a very good picture of the interaction between solvent and solute.

A shift of 1.3 gauss was found for $H_0 = 10{,}000$ gauss for a solution of $[(NH_3)_5Co(OH_2)]^{3+}$ whose half-exchange time for water (as measured isotopically) was 28 hr; this was so for the fluoride and for the chloride. The shift was 1.0 gauss for alkaline solutions, the difference probably being the result of withdrawal of the hydrogen from water bound in the ion. The position of the free-water signal (standard) was not affected, but Co(II) perchlorate produced a shift of −3.3 gauss; this shift (negative) is a consequence of the paramagnetism of Co^{2+}, for the same salt also shifted the signal from the water in $[(NH_3)_5Co(OH_2)]^{3+}$. It is supposed [82] that the last effect is caused by interaction of the complex with the Co^{2+}, which gives rise to a binuclear complex such as $[(NH_3)_5Co\,O\,\overset{H}{}\,Co(OH_2)_6]^{5+}$. Studies were also made of the nitrates and perchlorates of H^+, Li^+, Be^{2+}, Mg^{2+}, Ba^{2+}, Sn^{2+}, Hg^{2+}, Al^{3+}, Ga^{3+}, and Bi^{3+}; in every case there was a signal from the oxygen in the water and another from the oxygen in the anion, but signals from the free and bound water were not detected in [81]. The shift produced by Co^{2+} was therefore used as a means of separating these signals, because the free-water signal is shifted measurably, whereas that from the bound oxygen is shifted little or not at all. In this way studies were made on the water of hydration in solutions containing Be^{2+}, Al^{3+}, and Ga^{3+}; it was found (as predicted from Gutowsky and Saika's theory [30]) that the exchange time for water bound to these ions is more than 0.1 msec. This agrees well with results from isotope exchange (the half-exchange time for Al^{3+} is given [86] as 0.05 sec) and with the NMR results discussed above (Table 5). The water was not highly enriched in O^{17}, so n could not be determined precisely [81] (rough values for n are 4 for Be^{2+} and 6 for Al^{3+} and Ga^{3+}).

The special feature of studies of the first coordination sphere is that it is necessary to measure the exchange of intact solvent molecules (e. g., as for H_2O) rather than the exchange of component parts (protons or hydroxyl). Such measurements are not easy by any method, including NMR, as we have seen for proton resonance. If the rates of exchange of the parts are found to be similar or identical, we may say that the rate of exchange of the intact molecule is known; but if there is a wide divergence in the rates, the rate of exchange of the intact molecule will probably be determined by the rate for the part most closely bound to the ion. The work of Pearson et al.[37] is of interest here; proton resonance was used to examine exchange in solutions of paramagnetic ions in water, methanol, and ethanol. The line widths were measured; for dilute solutions, these depend on $(1/T)_p$, the rate of relaxation in the proton spins of solvent molecules bound to the ion, $1/\tau_p$, the rate of exchange for those molecules, and $(1/T_2)_d$, the rate of relaxation for protons in free solvent molecules:

$$1/T_2 = (1/T_2)_d + p/[(T_2)_p + \tau_p].$$

If now $1/T_2$ is almost independent of adjustable factors (e. g., pH) that affect the exchange, and if temperature changes have no great effect, then $1/T_2$ is governed by $(T_2)_p$. In the converse case, the line width is governed by exchange, i. e., $\tau_p = \tau_h$. That is, we can distinguish between relaxation mechanisms (if the activation energies are fairly large), which was the guiding principle used in [87].

The organic hydrogeneous solvents (e. g., CH_3OH and C_2H_5OH) have measurable τ_m for exchange of molecules when the τ_p for the groups (e. g., CH_3 and OH, if the latter is observable) are similar or equal. Exchange of molecules can then be distinguished from exchange of parts; the results for methanol (Table 7) show that Ni^{2+}, Cu^{2+}, and probably Fe^{3+} have $1/\tau_p$ that represent the exchange rate for methanol molecules, have measured as $1/T_2$. The line width is determined by $(1/T_2)_p$ for the other ions. The same situation occurs with water; the NMR results for protons and O^{17} give different values for τ_p, which is in agreement with measurements of T_2 as a function of temperature for some of these ions [67]. This shows that the τ_l as measured by means of proton resonance are similar to the true τ_l but not equal to them. The oxygen is bound more directly than the protons to the ion, so the NMR results for O^{17} give the true τ_l.

The $1/\tau_p$ for the alcohols are less than the $1/\tau_p$ for water; this is a little surprising, because the water is more strongly coordinated by the ions [87]. It is probable that the large ΔE for the alcohols hinder the exchange; the rate of exchange of ethanol is generally larger than the rate for methanol (Cr^{3+} and Co^{2+} excepted). Results have been

given [87] for the rates of hydrogen exchange for a variety of coordination compounds of Cr^{3+}; exchange mechanisms and temperature coefficients are discussed.*

This above feature detracts somewhat from the value of results obtained from NMR studies of only one type of nucleus in the solvent (e. g., protons). The point is particularly important if the interaction between solvent and ion is strong (as for the paramagnetic ions considered by Pearson et al.[87], for example). The requirement is less stringent (proton resonance may suffice) if the interaction is weak, as the results [70-75] for the alkali-metal cations show; the NMR results for protons and O^{17} agree mutually fairly well and also with the calculated τ_1/r [4]. The O^{17} NMR results alone are not sufficient criterion for the correctness of the proton results; important evidence can be obtained from the effects of factors that affect the states of the molecules. Proton resonance is also technically simple and can give very good results for negative hydration.

TABLE 7. Values of

Ion	Methanol		Ethanol			Water		Ion	Methanol		Ethanol			Water	
	K_{OH}	K_{CH_3}	K_{OH}	K_{CH_2}	K_{CH_3}	K_H	K^*		K_{OH}	K_{CH_3}	K_{OH}	K_{CH_2}	K_{CH_3}	K_H	K^*
Cr^{3+}	9,9	31	18	47	59	1	low	Ni^{2+}	40	45	10	45	52	16	2,5
Fe^{3+}	5,0	10	6,7	20	27	0,5	0,09	Cu^{2+}	10	10	5,2	12	43	12,5	0,16
Mn^{2+}	4,0	5,6	9,5	4,5	7,1	0,2	0,01	Ce^{3+}	400	120	—	—	—	125	—
Co^{2+}	9,9	58	83	520	660	20	0,5	Gd^{3+}	0,83	4,7	0,77	5,8	7,7	1,0	—

The above section on NMR and exchange of solvated molecules has not only surveyed new results on hydration but has also demonstrated that Samoilov's hydration theory [4] is correct. In fact, if the exchange of a coordinated water molecule were governed solely by the total interaction energies, the rate of exchange would be extremely small; calculations show that even for Li^+ the τ_1 would be many hours ([88], p. 30).

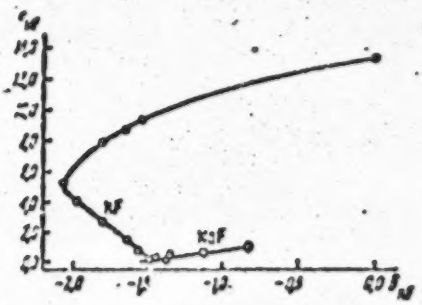

Fig. 17.

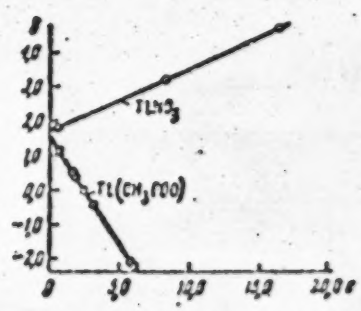

Fig. 18.

*Meiboom's [89] note (on the mechanism of proton relaxation in pure water) is of interest in relation to the NMR results for O^{17}. We have seen [42] that T_2 for protons is less than T_1 at the ends of the pH range. This fact cannot be explained in terms of the mechanism of hydrogen exchange, but allowance for the spin-spin interaction between protons and O^{17} gives the correct result; the difference between T_1 and T_2 is proportional to the O^{17} concentration in the water, which confirms that this interaction with O^{17} does occur. The amount of O^{17} in ordinary water (0.04%) is sufficient to make T_1 distinct from T_2. A more detailed examination of this topic might give fresh evidence on the structure of water. While this review was in preparation there appeared a paper on proton transfer in water [S. Meiboom, J. Chem. Phys., 34, 375 (1961)]; these NMR results for protons and O^{17} are in excellent agreement, and they give direct determinations of the rate constants of the exchange reactions

$$H_2O + H_3O^+ \xrightarrow{k_1} H_3O^+ + H_2O$$

$$H_2O + HO^- \xrightarrow{k_2} HO^- + H_2O$$

$k_1 = (10.6 \pm 4) \cdot 10^9$ and $k_2 = (3.8 \pm 1.5) \cdot 10^9$ l/mol·sec.

NMR results for species other than protons and O^{17} are of interest in relation to exchange studies for water of hydration. For example, Wertz [90] has recorded the NMR spectra of Cl^{35} in solutions containing various paramagnetic ions.

Wertz compared the μ_N for the 3d-elements with respect to protons and Cl^{35}; in general, μ_N shows the same general trend as μ_s for protons (Fe^{2+} and Mn^{2+}, Cr^{3+}, Cu^{2+}, Ni^{2+}, Co^{2+}, and Ti^{3+}), but the sequence has Cr^{3+}, Co^{2+}, and Ni^{2+} at the end for Cl^{35} (these ions interact very strongly with the water). The μ_N are governed by the distance of closest approach, by the contact time, and by the surroundings of the ion; Wertz [90] explains the results in terms of screening by water molecules, which is related to the exchange rate for water. The exchange is rapid for Mn^{2+} and Cu^{2+} (which have major effects on Cl^{35}) but is slow for Cr^{3+} and Co^{2+} (which have little effect on Cl^{35}). It is concluded [90] that the sequence of activation energies for exchange can be deduced in this way.

Screening of F^{19} is observed for strong solutions of fluorine compounds; this effect may be used to examine interactions at high concentrations. Carrington and Hines [91] have found that the resonance of F^{19} is extraordinarily sensitive to the solvent, to temperature, to concentration, and to various electrolytes; the addition of acetone, n-propanol, ethanol, ethylene glycol, or methanol to 0.4-M potassium fluoride causes a shift to higher fields that is a linear function of the molar proportion of the organic compound. Iodide, bromide, chloride, and carbonate shift the F^{19} frequency in the reverse sense (so does rise in temperature). These effects can be given a general explanation in terms of hydrogen bonding; methanol displaces water readily gives weak hydrogen bonds, and the screening increases, whereas formamide binds the F^- ion more strongly than water does, so the screening is reduced. It is believed that δ for fluorine can thus give evidence on the steric hinderance that occurs when an organic compound displaces water of hydration. Carrington and Hines consider that there is no distinction between the rupture of hydrogen bonds by cations and instantaneous association in the region of the fluoride ion if the solutions are very strong, so it is difficult to draw conclusions about the formation of ion pairs at such concentrations.

Connick and Poulson have found that the fluoride complexes of Al^{3+} show a chemical shift for F^{19} that is dependent on the other electrolytes present [92]; a special study [93] of solutions containing AlF^{2+} and AlF_2^+, and of solutions containing potassium and sodium fluorides, has shown that these other fluorides produce noticeable differences in the behavior of δ as a function of concentration (Fig. 17). The mechanism of this effect on δ is not clear, because KF gives a minimum on the curve (the derivative of δ changes sign at low concentrations). A proposed explanation [93] is that δ is affected by differences in the ion pairs; the ion of sodium gives a pair by direct contact with F^-, whereas K^+ is separated from F^- by a layer of water molecules at low concentrations. This special form of association is lost as the KF concentration increases, and so δ shows the reverse trend. However, no interpretation is given to the notable feature that the type of hydration of the ion affects the sign of the chemical shift for fluorine.

Gutowsky and McGarvey [91] have used the NMR spectrum of Tl^{203} in a study of the effects of concentration and nature of anion (Fig. 18). A model that gives a satisfactory general explanation of the results is one in which the interaction is intermediate between that in a covalent bond (chemical exchange) and that for pure Coulomb forces (allowance for polarization). The time of association for ions in solution can be very small, so it is assumed [91] that the ion pairs formed in strong solutions are not simply undissociated molecules. Association is treated as a sticky collision; then, if electron-exchange interactions occur only during the time of association, the diamagnetic screening that occurs during the rest of the time will be the screening for the free ion; this ion gives no electron exchange, and so gives rise to a paramagnetic contribution to the chemical shift. Experiment (Fig. 18) shows that δ is proportional to the numbers of the anions and water molecules that surround a thallium ion. The model indicates that the direction of the shift depends on the balance between the Tl^+-OH_2 and Tl^+-anion interactions. Figure 18 shows that the $Tl^+-CH_3COO^-$ interaction is stronger than the Tl^+-OH_2 one; the reverse is true for the nitrate. This explanation fits in naturally with the known chemical properties of the ions. The concentration-dependence curves for δ for Tl^{3+} and Tl^+ (as nitrates) are explicable in terms of electron exchange in which the 6d-orbitals take part, as is possible if we assume that the differing modes of filling for the 6s-orbitals (in the case of Tl^{3+}, this involves the formation of a mononitrate ion) have no great effect on the solvent and on the interaction of the anion with the 6p-orbitals of the cation. The final conclusion is that the effect can occur for a variety of ions but may sometimes be too small to be observable. For example, the δ for Cs^{133} as a function of CsCl concentration show a behavior similar to that for Tl^+, although they are much smaller (on account of the differences between the electron shells of the ions). These results show that ions in solution cannot be treated in the same way as free ions, as is often done.*

*Hertz [Z. Elektrochem. 65, 30 (1961); see also Z. Elektrochem. 61, 53 (1960)] has measured the rates of exchange for Br^- and I^- in aqueous solutions of the bromides and iodides of zinc, cadmium, and mercury on the basis of the NMR line widths of $Br^{79,81}$ and I^{127}. He gives a very interesting comparison of the rate constants for exchange with the dissociation constants for the various complexes.

Structures of Solutions

Direct NMR studies of solution structures are based primarily on line shapes; deductions may also be drawn from chemical shifts and theoretical predictions, but such methods are at present troublesome and laborious [95, 96]. The first method is of use (apart from instances considered above) mainly when the nucleus has an electrical quadrupole moment Q. All nuclei having spins of 1 or more have such moments; Q is a measure of the deviation from sphericity, and $Q > 0$ means elongation along the spin direction, with $Q < 0$ meaning compression along that direction. The moment interacts with the outside world via any inhomogeneity in the electric field at the nucleus; this inhomogeneity is very much dependent on the structure. (Fedin and Semin [97] have reviewed this topic.) The quadrupole interaction broadens the NMR signal; the motion of the molecule in a liquid generates a fluctuating field inhomogeneity, and so the line may become too broad to be observable. The hydration shells are responsible for much of the broadening shown by solutions. It is very difficult to calculate the field gradient for a crystal, let alone for a liquid, so there are few papers on the use of quadrupole resonance in solutions. The main place is taken by the work of Wertz and Jardetzky [98-100], which gives rise to some general conclusions about the immediate environments of the Na^+ and Cl^- ions. For example, the line width for Na^+ does not vary from 0.1 M up to saturation for salts formed with the anions F^-, S_2^-, NO_3^-, SO_4^{2-}, and $Fe(CN)_6^{3-}$; changes are found for the iodide, perchlorate, thiocyanate, and hydroxide at concentrations above 6 M. The phosphates (PO_4^{3-} and $P_2O_7^{2-}$) give broad lines even for 1-2 M solutions, though. This line broadening (loss of signal amplitude) for Na^{23} is caused by the quadrupole interaction, which reflects the deviation from spherical symmetry in the field [98]. The loss of amplitude may be caused in part by a reduction in the number of atoms in the [illegible] ionic state; there is insufficient water for complete hydration at high concentrations, so the distribution around the nucleus becomes unsymmetrical and the NMR line of Na^{23} becomes broader.

The line width of Cl^{35} in HCl and $HClO_4$ increases with concentration, which is also explained [98,99] in terms of ion pairs (e. g., $H_3O^+ClO_4^-$). The NMR signal is broadened to vanishing point as the interaction becomes stronger; the line is very broad for a solution 0.02 M in $CdCl_2$ and 3 M in NaCl (relative to the Cl^{35} line for pure NaCl), and the width is a linear function of the cadmium chloride concentration. This may be considered as evidence for rapid exchange of chlorine, the number of exchangeable nuclei being greater than the number of bound ones. Lanthanum chloride gives a line width that increases rapidly with concentration; the amplitude points to the existence of anionic and cationic complexes.*

Valiev and Khabibulin have computed T_1 for I^{127} in solution as diamagnetic ions and have compared the results with the experimental values [101, 102]. It is assumed that I^- forms no stable complexes or associations with the solvent, so the solvent molecules can move and rotate freely. This should be correct for halide salts generally in aqueous solutions; the water molecules closest to the ion then form a random array, and the dipoles all together produce at the nucleus a certain field gradient that acts on Q and so alters the spin levels. Ito and Yamagato have used the iodides of sodium and potassium to show that T_1 for I^{127} varies with temperature in the same way as η/T, in accordance with the expression [101] for T_1. All the same, KI gives very little variation of T_1 with concentration, whereas the sodium salt gives a large variation, which may be the result of the change of η with concentration. Numerical estimates for the T_1 of I^{127} in dilute aqueous solutions disagree widely with the measured values; Valiev et al [101] explain this in terms of the negative hydration of I^-. Now the spin relaxation is caused mainly by the motion of the closest water molecules, so T_1 should be calculated from the local (not macroscopic) viscosity. Thus the hydration can be deduced from the calculated and measured T_1 for ions having nuclear quadrupole moments.**

*Chesnut [J. Chem. Phys. 33, 1234 (1960)] has measured $\delta(Cl^{35})$ for solutions of $CoCl_2$ and finds that the NMR signal shifts to lower H_0 when the concentration of Co^{2+} or Cl^- is increased. This indicates that hydration plays a major part in the formation of complexes; the observed δ point to contact interaction in the chloride complexes of Co^{2+}.

**Hertz has measured the line widths ΔH for the NMR signals from $Br^{79,81}$ and I^{127} as functions of concentration for aqueous solutions of the bromides and iodides of various alkali-metal and alkaline-earth elements [H. G. Hertz, Z. Elektrochem. 65, 20 (1961)]. The results confirm his theoretical expression for ΔH and enable him to determine $\underline{a}'$, the effective distance between cation and anion in the solution. There is no conflict between the $\underline{a}'$ found for strongly hydrated ions by means of NMR and by means of activity coefficients (the first are slightly lower, because the minimal $\underline{a}'$ were calculated). The two sets of $\underline{a}'$ do not agree, in general, if the ions show negative hydration.

Kozyrev and Rivkind's work [56-6*] has shown that the proton T_1 can be used in studies of complexes formed by paramagnetic ions. Vdovenko and Shcherbakov [103] have applied the method to the nonmagnetic ions chromate, dichromate, and permanganate.

Very interesting results have come from ESR and electron-spin-relaxation studies on paramagnetic solutions. The structure of the complex affects the ESR spectrum via the electric fields; these features of ESR are very sensitive to the structure of the environment of the ion, which makes ESR a valuable technique.

The ESR results for aqueous solutions of Ti^{3+}, Co^{2+}, Cr^{3+}, and Cu^{2+} show that the complexes are not tetrahedral [104]; this is shown also by other results. The theoretical calculations agree with experiment for Cu^{2+}, which shows that complexes of CuA_6^{2+} type have a bipyramid structure somewhat elongated along the fourfold axis [104]. Kozyrev [105] has found that this elongation can occur along any of the coordinate axes, and that the transition from one state to another involves a potential barrier whose height is about 1000 cm^{-1} for the hydrate (transition time about 10^{-11} sec). The electron density of the ion varies with the same frequency. The frequency falls as the complex becomes stronger, more massive, or of lower symmetry. The Cr^{3+} ion exists in aqueous solution in the form $Cr(H_2O)_6^{3+}$ (violet modification), which has a somewhat distorted tetrahedral structure [104]. The symmetry of the electric field near the ion is basically cubic, but with a certain degree of lower symmetry, which is introduced largely by the second coordination sphere. This sphere is fairly stable for Cu^{2+} solutions in organic solvents, as has been demonstrated recently [106]. The ESR line widths given by solutions containing $[Cr(OH_2)_5A_2]^{2+}$ indicate that the octahedron is very much distorted. The aquocomplexes of Mn^{2+} have almost purely cubic symmetry at low concentrations (solutions in organic solvents give strongly axial electric fields at the ion) [104]. The τ_s for Mn^{2+} is a function of the anion (at high concentrations) and of the general ionic strength [107]; it is supposed that the structure of the complex is similar to that of the crystalline hydrate* if the solution is sufficiently strong, so the nearest neighbors of the cation include anions as well as water molecules. This serves to explain why τ_s is dependent on the anion. The anions are ejected by water at lower concentrations, so the symmetry rises (at about 0.25 M for Mn^{2+}). It is believed that anions start to enter the complexes at about 0.5 M and that the uptake is complete at 3.5 M (sulfate) or above 5 M (chloride) for Mn^{2+}. This is precisely the range in which the anion has the greatest effect on τ_s. Values are quoted for the parameters of the internal electric field as functions of concentration; these serve as a measure of the changes in the structure. The field increases linearly with the concentration for the chloride, sulfate, and nitrate of Mn^{2+}, although the slope is dependent on the anion and decreases in the above order.**

This review does not deal fully with all the problems listed in the introduction but this does not mean that NMR cannot assist in solving these problems. For example, it may be combined with x ray, neutron-diffraction, and other methods in studies on crystalline hydrates, adsorbed water, etc. Recently Kume [100] published an interesting proton-resonance study of the structure of ice, for example. Lack of space has prevented me from examining all of these topics, but it is not an exaggeration to say that most of the topics considered here are of major importance to the physical chemistry of solutions.

I am indebted to Professor V. M. Vdovenko and Dr. F. L. Skripov for very valuable discussions on this review, and also to Yu. V. Gurikov and V. B. Kolokol'tsov for advice and suggestions.

*Wang I-Ch'iu has measured $\delta(F)$ for the fluorides of potassium and ammonium and finds that the concentration dependence causes $\delta(F)$ to tend to the value for the solid salts. The tendency appears at 3-4 M, which indicates that the environment of the F^- ion in the solution resembles that in the solid if the concentration is high [108].

**A detailed study has been made [N. Bloembergen and L. Morgan, J. Chem. Phys. 34, 842 (1961)] of the effects of τ_s on T_1 and T_2 for protons; it is considered that the τ_s for ions formed by elements are governed mainly by distortion in the hydrated complexes caused by collisions with water molecules. Measurements have been made of τ_v (the vibration time for H_2O in the complexes) and of V_v (the activation energy for this motion). The values for Mn^{2+} are $\tau_v = 2.8 \cdot 10^{-12}$ sec at 21°C (the calculations given in the paper give $\tau_v = 2.4 \cdot 10^{-12}$ sec), $V_v = 3.9$ kcal/mole ($U_h = 81$ kcal/mole (U_h is given as 8.4 kcal/mole by [67]); those for V^{2+} are $\tau_v = 1.60 \cdot 10^{-12}$ sec (calculated $\tau_v = 1.4 \cdot 10^{-12}$ sec) and $V_v = 2.6$ kcal/mole; and finally, the τ_v for Cr^{3+} (violet) and Gd^{3+} lie in the region of 2.5 to 20 $\times 10^{-11}$ sec, in agreement with [105]. Studies have also been made on Cu^{2+}, Ni^{2+}, Co^{2+}, and Fe^{2+}; the resulting parameters (e.g., τ_v) for the aquocomplexes are comparable with those for the crystals.

LITERATURE CITED

1. E. K. Zavoiskii, Dissertation for doctorate, Institute of Physics, Academy of Sciences of the USSR; Zh. Eksperim. i Teor. Fiz. 15, 253 (1945).
2. F. Bloch, W. Hansen, and M. E. Packard, Phys. Rev. 69, 127 (1946).
3. N. Bloembergen, E. M. Purcell, and R. V. Pound, Phys. Rev. 73, 679 (1948).
4. O. Ya. Samoilov, Structures of Aqueous Solutions of Electrolytes and Hydration of Ions [in Russian] (Izd. AN SSSR, Moscow, 1957).
5. E. V Shpol'skii, Atomic Physics [in Russian] (Moscow, GITTL, 1951).
6. E. R. Andrew, Nuclear Magnetic Resonance [Russian translation] (Izd. Inost. Lit., Moscow, 1957).
7. H. Kopfermann, Nuclear Moments [Russian translation] (Izd. Inost. Lit., Moscow, 1960).
8. J. A. Pople, W. J. Shneider, and H. J. Bernheim, High Resolution Nuclear Magnetic Resonance (N. Y., 1959).
9. G. Chiarotti and L. Giulotto, Phys. Rev. 93, 124 (1954).
10. G. B. Benedek and E. M. Purcell, J. Chem. Phys. 22, 2003 (1954).
11. W. A. Anderson and J. T. Anderson, Phys. Rev. 101, 511 (1956).
12. E. L. Hahn, Phys. Rev. 80, 580 (1950); Phys. Today 6, 41, 4 (1953).
13. H. Y. Carr and E. M. Purcell, Phys. Rev. 94, 630 (1954).
14. E. M. Purcell, J. phys. et radium 15, 785 (1954).
15. A. W. Nolle and P. P. Mahedroo, J. Chem. Phys. 33, 863 (1960).
16. P. W. Bridgman, The Physics of High Pressures (London, 1949).
17. R. W. Mitchell and M. E. Eisner, J. Chem. Phys. 33, 86 (1960).
18. J. H. Simpson and H. Y. Carr, Phys. Rev. 11, 1201 (1958).
19. D. Douglass and D. W. McCall, J. Chem. Phys. 31, 569 (1959).
20. P. W. McCall, D. C. Douglass, and E. W. Anderson, J. Chem. Phys. 30, 1556 (1960).
21. H. C. Longuet-Higgins and J. A. Pople, J. Chem. Phys. 25, 884 (1956).
22. J. L. Motchaune and J. Uebersfeld, Compt. rend. 251, 73 (1960).
23. J. L. Motchaune and J. Uebersfeld, J. phys. et radium 21, 194 (1960).
24. W. D. Knight, Phys. Rev. 76, 1259 (1949).
25. W. C. Dickinson, Phys. Rev. 77, 736; 80, 563 (1950).
26. W. G. Proctor and F. C. Yu, Phys. Rev. 78, 471; 717 (1950).
27. W. E. Lamb, Phys. Rev. 60, 817 (1941).
28. N. F. Ramsey, Phys. Rev. 78, 699 (1950).
29. J. H. Van Vleck, Electric and Magnetic Susceptibilities, Oxford Univ. Press (1932).
30. Ya. G. Dorfman, Magnetic Properties and the Structure of Matter [in Russian] (GITTL, Moscow, 1955).
31. T. J. Powland, Phys. and Chem. Solids 7, 95 (1958).
32. E. Lambardi and P. B. Soco, J. Chem. Phys. 32, 635 (1960).
33. H. G. Hertz and W. Spalthoff, Z. Electrochem. 63, 1096 (1959).
34. J. N. Shoolery and B. J. Alder, J. Chem. Phys. 23, 805 (1955).
35. A. Eucken, Z. Electrochem. angew. Phys. Chem. 52, 255 (1948).
36. G. H. Haggis, J. B. Hasted, and T. J. Buchanan, J. Chem. Phys. 20, 1452 (1952).
37. R. K. Axtmann, J. Chem. Phys. 30, 340 (1959).
38. M. G. Mavel, Compt. rend. 248, 1505 (1959).
39. H. S. Gutowsky and A. Saika, J. Chem. Phys. 21, 1688 (1953).
40. G. Masuda and T. Kaada, J. Phys. Soc. Japan 8, 492 (1953); 9, 82 (1954).
41. S. Meiboom, Z. Electrochem. 64, 50 (1960).
42. J. T. Arnold, Phys. Rev. 102, 136 (1956).
43. M. G. Mavel, J. phys. et radium 21, 731 (1960).
44. S. Meiboom, Z. Luz, and D. Gill, J. Chem. Phys. 27, 1410 (1957).
45. G. C. Hood, O. Redlich, and C. A. Reilly, J. Chem. Phys. 22, 2067 (1954).
46. P. M. Borodin and F. I. Skripov, Izv. Vyssh. Uchieb. Zav., Radiofizika 1, 37 (1958).
47. E. Z. Utyanskaya, G. U. Stepanyants, M. I. Vlasik, and N. M. Chernov, Dokl. AN SSSR 131, 1095 (1959).
48. Wang I-Ch'iu and F. I. Skripov, Dokl. AN SSSR 136, 58 (1961).
49. G. C. Hood and C. A. Reilly, J. Chem. Phys. 32, 127 (1960).
50. E. Hogfeld, Nature 185, 760 (1960).
51. H. S. Gutowsky and S. Fujiwara, J. Chem. Phys. 22, 1782 (1954).
52. R. K. Axtmann, W. E. Shuler, and R. B. Murray, J. Phys. Chem. 64, 57 (1960).

83. J. Broersma, J. Chem. Phys. 24, 659 (1956).
84. M. G. Mavel, Compt. rend. 250, 3473 (1960).
85. A. Patterson and R. Fuoss, Z. Electrochem. 64, 93 (1960).
86. B. M. Kozyrev and A. I. Rivkind, Zh. Eksperim. i Teor. Fiz. 27, 69 (1954).
87. A. I. Rivkind, Zh. Neorg. Khimii 2, 1262 (1957).
88. A. I. Rivkind, Dokl. AN SSSR 102, 1107 (1955).
89. A. I. Rivkind, Dokl. AN SSSR 112, 290 (1957).
90. A. I. Rivkind, Dokl. AN SSSR 117, 416 (1957).
91. A. I. Rivkind, Zh. Eksperim. i Teor. Fiz. 34, 1007 (1958).
92. N. Bloembergen, J. Chem. Phys. 27, 572 (1957).
93. T. R. Khutsishvili, Usp. Fiz. Nauk 71, 9 (1960).
94. J. Kin and N. Davidson, J. Chem. Phys. 29, 787 (1958).
95. I. Solomon, Phys. Rev. 99, 559 (1955).
96. I. Solomon and N. Bloembergen, J. Chem. Phys. 25, 261 (1956).
97. R. A. Bernheim, T. H. Brown, H. S. Gutowsky, and D. E. Woessner, J. Chem. Phys. 30, 950 (1959).
98. G. Lauklen and R. Hausser, Z. Physik. 153, 301 (1959).
99. T. H. Brown, R. Y. Bernheim, and H. S. Gutowsky, J. Chem. Phys. 33, 1593 (1960).
100. S. Broersma, J. Chem. Phys. 24, 153 (1956).
101. S. Broersma, J. Chem. Phys. 24, 661 (1956).
102. S. Broersma, J. Chem. Phys. 27, 481 (1957).
103. S. Broersma, J. Chem. Phys. 28, 1158 (1958).
104. V. M. Vdovenko and V. A. Shcherbakov, Zh. Strukt. Khimii 1, 28 (1960).
105. V. M. Vdovenko and V. A. Shcherbakov, Zh. Strukt. Khimii 1, 122 (1960).
106. T. Kanda, J. Phys. Soc. Japan 10, 85 (1955).
107. A. I. Rivkind, Zh. Neorg. Khimii 4, 1291 (1959).
108. E. Scrocco and O. Salvetti, Gazz. chim. ital 81, 1003 (1954).
109. V. M. Vdovenko and V. A. Shcherbakov, Zh. Strukt. Khimii 1, 268 (1960).
110. R. E. Connick and R. E. Poulton, J. Chem. Phys. 30, 759 (1959).
111. J. A. Jackson, J. F. Lemons, and H. Taube, J. Chem. Phys. 32, 553 (1960).
112. R. L. Conger and P. W. Selwood, J. Chem. Phys. 20, 353 (1952).
113. R. G. Shulman and B. J. Wyluda, J. Chem. Phys. 29, 335 (1959).
114. L. E. Orgel, J. Chem. Phys. 30, 1617 (1959).
115. O. Ya. Samoilov, Zh. Fiz. Khimii 33, 2031 (1959).
116. H. W. Baldwin and H. Taube, J. Chem. Phys. 33, 206 (1960).
117. R. G. Pearson, J. Palmer, M. M. Anderson, and A. L. Allred, Z. Electrochem. 64, 110 (1960).
118. K. P. Mishchenko and A. M. Sukhotin, Zh. Fiz. Khimii 27, 26 (1953).
119. S. Meiboom, Bull. Amer. Phys. Soc. 5, 176 (1960).
120. J. E. Wertz, J. Chem. Phys. 24, 484 (1956).
121. A. Carrington and T. Hines, J. Chem. Phys. 28, 727 (1958).
122. R. E. Connick and R. E. Poulton, J. Amer. Chem. Soc. 79, 5153 (1957).
123. R. E. Connick and R. E. Poulton, J. Phys. Chem. 62, 1002 (1958).
124. H. S. Gutowsky and B. R. McGarvey, Phys. Rev. 91, 81 (1953).
125. P. E. O'Reilly, J. Chem. Phys. 32, 1007 (1960).
126. L. V. Aleksandrov, Usp. Khimii 29, 1138 (1960).
127. G. K. Semin and E. I. Fedin, Zh. Strukt. Khimii 1, 252 (1960).
128. J. E. Wertz and O. Jardetzky, J. Chem. Phys. 25, 357 (1956).
129. J. E. Wertz, J. Chem. Phys. 27, 51 (1957).
130. O. Jardetzky and J. E. Wertz, J. Amer. Chem. Soc. 82, 318 (1960).
131. K. A. Valiev and B. M. Khabibulin, Summaries of Papers at the 3rd Conference on Spectroscopy [in Russian] (1960).
132. J. Ito and Y. Yamagato, J. Phys. Soc. Japan 13, 1182 (1958).
133. V. M. Vdovenko and V. A. Shcherbakov, Zh. Strukt. Khimii 1, 500 (1960).
134. V. I. Avvakumov, N. S. Garif'yanov, B. M. Kozyrev, and P. G. Tishkov, Zh. Eksperim. i Teor. Fiz. 37, 1564 (1959).

105. B. M. Kozyrev, Disc. Faraday Soc. 19, 135 (1955).
106. B. M. Kozyrev and A. I. Pivkina, Dokl. Akad. Nauk SSSR 127, 1011 (1959).
107. P. G. Tishkov, Zh. Eksperim. i Teor. Fiz. 36, 1337 (1959); P. G. Tishkov and G. P. Vishnevskaya, Zh. Eksperim. i Teor. Fiz. 38, 335 (1960).
108. Wang I-Ch'iu, Zh. Strukt. Khimii 2, 367 (1961).
109. K. Kuno, J. Phys. Soc. Japan 15, 1493 (1960).

All abbreviations of periodicals in the above bibliography are letter-by-letter transliterations of the abbreviations as given in the original Russian journal. *Some or all of this periodical literature may well be available in English translation.* A complete list of the cover-to-cover English translations appears at the back of this issue.

CURRENT EVENTS

SECOND CONFERENCE ON THE USE OF ELECTRONIC COMPUTERS IN STRUCTURE ANALYSIS OF CRYSTALS

V. F. Dvoryankin

Translated from Zhurnal Strukturnoi Khimii, Vol. 2, No. 4, p. 518, July-August, 1961

The Second Conference on the Use of Electronic Computers in Structure Analysis of Crystals, convened by the N. S. Kurnakov Institute of General and Inorganic Chemistry of the Academy of Sciences USSR, the Institute of Crystallography of the Academy of Sciences USSR, and the Computer Center of the Moscow State University (VTs MGU), was held in Moscow from April 17 to April 19, 1961.

During the six years since the First Conference the work on programming of problems of crystal structure analysis and the use of electronic computers for their solution has increased considerably. Work on programming of problems of crystal structure analysis is now being successfully conducted in the computer centers of the Moscow State University, the Siberian Division of the Academy of Sciences USSR (VTs SO AN SSSR), and other institutions.

About 20 papers were presented at the conference. They can be subdivided into four large groups: 1) programming of direct methods; 2) programming of routine methods for interpretation of crystal structures; 3) programming of methods for refining crystal structures (the methods of differential synthesis and of least squares); 4) papers on specialized computers for solving problems of the structure analysis of crystals.

The paper by M. A. Porai-Koshits and B. M. Shchedrin dealt with the main trends in the work of the structure analysis group of VTs MGU. A. N. Saltykov presented a paper on the principal trends and formulation of problems of structure analysis for solution by the large computer in the VTs SO AN SSSR.

In recent years direct methods have been intensively developed for structure analysis of crystals. It is therefore not surprising that most of the papers were concerned with programming of various direct methods. A. F. Skaritskaya (VTs SO AN SSSR) gave a paper on a program for determination of the signs of structure amplitudes with the aid of the Harker–Kasper fundamental inequalities. The main part of the program also revealed sign relationships which were usually omitted with "manual" use of the method. The paper by A. V. Tovbis (VTs MGU) contained a program for the Strela-4 machine for determination of the signs of structure amplitudes by a direct statistical method.

V. I. Rodin (VTs MGU) reported on programs for superposition methods of interpretation of crystal structures and on the use of electronic computers with these methods. A paper by S. V. Borisov (Institute of Inorganic Chemistry, SO AN SSSR) and V. D. Kudrin (VTs SO AN SSSR) dealt with presentation of the problem of determination of structure models by minimalization of the Patterson function for solution in an electronic computer, and gave details of some parts of the program. L. I. Efimenkova (VTs MGU) described the program for computation of weighted projections.

The paper by F. A. Bruentsov (Institute of Inorganic Chemistry, SO AN SSSR) on programs for calculations of electron densities with a larger computer dealt with the problem of reducing the information fed into the computer by presentation of the atomic factor curve in the form of a power polynomial or as an exponential function. N.G.Rambidi reviewed the VTs MGU programs for processing of experimental data on gas electron diffraction. T. S. Kamenskaya (VTs MGU) discussed the use of the large computer for the method of differential synthesis.

Models of specialized computers and devices for structure analysis were considered in papers by V. I. Vlasenko (L. Ya. Karpov Physicochemical Institute) and also by A. M. Zaezdnyi (Leningrad Institute of Electrical Engineering) in a paper on a model of the "Sintez" digital computer.

The conference adopted a resolution on problems of coordination of work on programming of problems of crystal structure analysis, and on questions of organization. The next (Third) Conference on the Use of Electronic Computers in Structure Analysis of Crystals is to be held in Novosibirsk in April 1963.

BIBLIOGRAPHY

INTERNATIONAL UNION OF CRYSTALLOGRAPHY

COMMISSION ON CRYSTAL STRUCTURE DATA

LIST OF 1957 PUBLICATIONS CONTAINING NEW DATA ON CRYSTAL STRUCTURES

Translated from Zhurnal Strukturnoi Khimii, Vol. 2, No. 4,
pp. 519-528, July-August, 1961

A. Metals

1. Agarwala R. P. and Sinha A. P. B., Cr. str. of Ni_3Se_2, Z. anorg. Chem. 289, 203.
2. Ageev N. V., Gureva N. L., and Markovich K. P., Phase transformns. in Cr-rich Cr–Mo–Fe alloys, Izv. AN SSSR, otd. tekhn. n., 4, 23.
3. Ageev N. V. and Samsonov V. P., X-ray investn. of cr. str. of TlSi and TlGe, Dokl. AN SSSR 112, 853.
4. Aggarwal P. S. and Goswami A., New phase str. of Mo. Proc. Phys. Soc. Lond. 70B, 703.
5. Anderko K., Strukturelle Unters. in d. Systt. Tl–Ga u. Tl–In, Naturwissenschaften 44, 88.
6. Anderko K. P., Kilmek E. J., Levinson D. W., and Rostoker W., Constn. studies on syst. Mg–Zn. Trans. Am. Soc. Metals 49, 778.
7. Anderko K. P., Sagel K., and Zwicker U., Hex. Ordnungsphasen ind. Systt. Tl–Al u. Tl–In. Z. Metallk. 48, 57.
8. Andresen A., McReynolds A. W., Nelkin M., Rosenbluth M., and Whittemore W., N. Investn. of opt. vibration levels in Zr hydride, Phys. Rev. 103, 1092.
9. Argent B. B. and Wakeman D. W., Lat. pars. of alpha solid solns. of Cu–Zn–Ge a. Cu–Zn–Ga alloys, J. Inst. Metals 85, 413.
10. Arlya S. M., Kolbina E. M., and Apukina M. S., Chem. of compds. of variable compn. VII. The Co–Te system and enthalpy of formn. of Co tellurides. Zh. neorg. khim. 2, 23.
11. Arkharov V. I., Berenova L. P., and Magat L. M., Acceleration of aging of Al_6–Mg alloys under influence of small addns. of Ag and Zn. (Causes of influence of small addns. on kinetics of alloy aging. III). Fiz. met. i metalloved. 5, 516.
12. Arkharov V. I. and Borisov B. S., Mechanism of oxidn. of magnetite, Dokl. AN SSSR 114, 293.
13. Arkharov V. I. and Borisov B. S., Texture in iron scale. IX. E. diffrn. investn. of texture in hematite layer at different stages of iron oxidn. in air, Fiz. met. i metalloved. 4, 76.
14. Arkharov V. I. and Bulychev D. K., Effect of high pressure on decompn. of ferrous oxide, Dokl. AN SSSR 113, 791.
15. Arkharov V. I. and Esin V. O., Mechanism of reaction diffusion in the systs. Cu–Se, Cu–Te, Ag–Se, and Ag–Te, Fiz. met. i metalloved. 5, 245.
16. Arkharov V. I., Mar'evich V. P., Reinhold M., and Simonova M. I., Texture in iron scale. XI. Investn. of scale formed by oxidn. of Fe in CO_2, Fiz. met. i metalloved. 5, 251.
17. Arkharov V. I. and Simonova M. I., Texture in iron scale. X. Texture in wuestite scale, Fiz. met. i metalloved. 4, 278.
18. Arkharov V. I. and Vangengeim S. D., X-ray investn. of intergranular internal adsorption in Ag-based alloys, Fiz. met. i metalloved. 4, 439.
19. Aronsson B., Cr. str. of Mo_5SiB_2. XVI Congrès International de Chimie Pure et Appliquée (Paris, 1957) p. 211.
20. Aronsson B. and Lundström T., Investns. on ε-FeCrSi, Acta Chem. Scand. 11, 365.
21. Atoji M., Gschneidner K. A., Rundle R. E., Daane A., and Spedding F. H., Str. of La-dicarbide a. sesquicarbide by X-ray a. n. diffrn. Program. a. Abstracts 12th Pittsburgh Diffrn. Conf., 6-8 Nov. 1957, 59.
22. Austin A. E. and Doig J. R., Str. of trans. phase omega in Ti–Cr alloys, J. Metals 9, 27.
23. Avghatorho C., Etude radiocristallogr. de l'hydruration de Ce. Essai d'interpretn. etendu au La. Compt. rend. 244, 1766, 2438.
24. Bagaryatskii Yu. A., Cr. str. of metastable phase formed in annealing of Cu–Sn alloys with 21-27 % Sn, Kristallografiya 2, 283.

25. Bagaryatskii Yu. A. and Tyapkin Yu. D., Mechanism of str. transformns. in aging Ni-based alloys, Kristallografiya 2, 419.
26. Bagaryatskii Yu. A. and Tyapkin Yu. D., Interaction of diffusion and lat. rearrangement processes in decompn. of supersaturated solid solns. in alloys, Dokl. AN SSSR 115, 1111.
27. Ballufft R. W. and Simmons R. O., Low-temp. therm. expan. of Cu, Bull. Am. Phys. Soc. 2, 137.
28. Bally D. and Maris C., La dissociation de certains alliages Cu–Ni–Fe (etude a l'aide de r. X). Acta Cryst. 10, 772 (Abstracts of papers delivered at 4th General Assembly a. Internat. Congr. I.U.C.), Montreal, July 1957*.
29. Banerjee B. C. and Goswami A., Influence of impurities on str. of electrodeposited Ni, J. Sci. Ind. Res. 16B, 141.
30. Bardelle J., Recherches sur le mecanisme d'oxydation de cr. uniques de Fe a haute temp. et . . a basse pression d'oxygene, Publ. sci. et tech. ministere air (France), 327.
31. Barret C. S., Str. of Hg at low temps, Acta Cryst. 10, 58.
32. Barson F., Legvold S., and Spedding F. H., Therm. expan. of rare earth mets., Phys. Rev. 105, 418.
33. Bastien P. and Stora G., Decompn. de l'austenite en phase α sous l'effet des contraintes latentes dans les aciers inoxydables du type 18–8, Compt. rend. 244, 2613.
34. Batchelder F. W. von and Raeuchle R. F., Str. of new series of MBe_{12} compds., Acta Cryst., 10, 648.
35. Batchelder F. W. von and Raeuchle R. F., Str. of new series of MBe_{12} compds. from elements in grs. V-A, VI-A a. VII-A, Acta Cryst. 10, 705 (Abstracts. . .).
36. Batchelder F. W. von and Raeuchle R. F., Tetrag. MBe_{12} str. of Ag, Pd, Pt a. Au, Program a. Abstracts 15th Pittsburgh Diffrn. Conf., 6-8 Nov. 1957, 47.
37. Batenin V. V. and Sharov B. V., X-ray study of U in relation to growth effect on irradiation, At. energiya 3, 261.
38. Beattie H. J., jr. and Hagel W. C., Intermet. compds. in Ti-hardened alloys, J. Metals 9, 45; 911.
39. Beattie H. J., jr. and Versnyder F. L., Influence of Mo on phase relnshs. of high temp. alloy, Trans. Am. Soc. Metals 49, 883.
40. Bell R. E. and Herfert R. E., Prepn. a. char. of new cr. form of Mo disulfide, J. Am. Chem. Soc. 79, 3351.
41. Bergman G., Waugh J. L. T., and Pauling L., Cr. str. of met. phase $Mg_{32}(Al,Zn)_{49}$, Acta Cryst. 10, 254.
42. Berkowitz A. E., Donahoe F. J., Franklin A. D., and Stelja R. P., Phase transformns in Fe–Pt alloys near compn. Fe_3Pt, Acta Met. 5, 1.
43. Bigelow W. C., Amy J. A., and Brockway L. O., Effect of high-temp. aging on development of minor phases in age-hardening Ni-base alloy, J. Metals 9, 44.
44. Bland J. A., Str. geometry of trans. met. alloys $MnAl_6$, Mn_4Al_{11}, a. WAl_4, Acta Cryst. 10, 770; (Abstracts...).
45. Blok N. L., Kozlova M. N., Lashko N. F., and Shpunt K. Ya., Ni_3B compd. in Ni–B alloys, Dokl. AN SSSR 113, 811.
46. Bohm H. and Lohberg K., Uber einige Uberstr.-phase v. CsCl–Typ im Syst. Ti–Mo–Al, Metall. 11, 904.
47. Borie B., X-ray diffrn. effects of at. size in alloys, Acta Cryst. 10, 89.
48. Boyko E. R., Str. of δ-phase in U–Zr syst., Acta Cryst. 10, 712.
49. Brocklehurst R. E., Goode J. M., and Vassamillet L. F., Coef. of expan. of Po, J. Chem. Phys. 27, 985.
50. Brown P. J., Str. of α(V–Al), Acta Cryst. 10, 133.
51. Bublik A. L., E. diffrn. investn. of str. of thin Sn films, Kristallografiya 2, 249.
52. Bublik A. L. and Buntar' A. G., Detn. of atomic density distribn. in liquid Al and Bi at various temps. from e. diffrn. data, Fiz. met. i metalloved. 5, 53.
53. Bublik A. L. and Buntar' A. G., Detn. of radial distribn. function of atoms in liquid met. alloy from e. diffrn. data, Kristallografiya 2, 255.
54. Buckle C. and Manenc J., Mise en evidence pour un alliage Ni–Ti, d'un stade de precipitation suivi d'un stade a phase trans., au cours de vieillissements isothermes, Compt. rend. 244, 1643.
55. Buckle C. and Pouligner J., Identn. et etude du "phenomene de bordure claire" dans les alliages Ni–Cr et Ni–Cr–Co a durcissement str. "Journees metallurg. d'automne, 1957. Avant-programme et res. communic," Paris, Soc. Fr. Metall., 66.
56. Buhl O. and Schuler C., Feldelectronenmikr. Beob. d. allotropen Umwandl. v. Co, Z. Metallk. 48, 116.
57. Bulnov N. N., Podrezov L. I., and Komarova M. F., Investn. of decompn. in Ni–Be alloy, Izv. AN SSSR, ser. fiz. 21, 1220.
58. Bulow H., El.-beug.-aufnahmen v. neuart. Zn–Bi–Legier., Z. phys. 148, 321.
59. Butcher B. R., β→α phase change in pure U., J. Nuclear Energy 4, 273.
60. Bychkov Yu. F., Rozanov A. N., and Skorov D. M., Certain props. of Zr–Nb alloys, At. energiya 2, 146.
61. Cagnet M. and Moreau J., Sur la resorption des lacunes du protoxyde de Fe au cours de l' oxydation du Fe aux temps. elevees, Compt. rend. 244, 2. 3.

62. Calvert L. D., Dunmore H. S., Kuhl L. V., and Tse R. S., Cr. strs. of AgCa a. Ag_4Ca, Acta Cryst. 10, 775 (Abstracts, . . .).
63. Castellitz L., Barrett C. S., and Massalski T. B., Lat. pars. of coldworked Cu–Zn–Ga alloys, Acta Cryst. 10, 716.
64. Catterall J. A., Electronic str. of PU–U alloys, Phil. Mag. 2, 491.
65. Chatterjee S. N., Variation in lat. const. in thin films of Au, Indian J. Phys. 31, 110.
66. Cherkashin E. E., Gladishevs'kii E. I., and Krip'yakevich P. I., Alloys of trans. mets. with Be, Si, Ge, and Sn, Dopovidi ta povidomlennya, L'viv univ. 7, 3, 180 (Ukr.).
67. Cherkashin E. E., Krip'yakevich P. I., and Frankevich D. P., Ternary solid soln. in Cu–Mg–Cd syst, Dopovidi URSR 1, 33 (Ukr.; Russ. and Eng. summaries).
68. Chiotti P., Klepfer H. H., and Gill K. J., U–Zn syst., J. Metals 9, 51.
69. Chornii V. G., Study of decompn. processes in supersaturated solid soln. of Ni–Cr–Ti–Al, Dopovidi AN URSR 4, 362 (Ukr. Russ. and Eng. summaries).
70. Chornii V. G., Fine cr. str. of binary Ni alloys, Ukr. fiz. zh. 2, 2 (suppl.), 73 (Ukr.).
71. Christian J. W. and Spreadborough J., Stacking faults a. dislocns. in Cu–Al a. Co–Ni alloys, Proc. Phys. Soc. Lond. 70B, 1151.
72. Clark J. B. and Rhines F. N., Al–Mg equilibrium diagram, J. Metals 9, 6.
73. Clark J. B. and Rhines F. N., Central region of Mg–Zn phase diagram, J. Metals 9, 425.
74. Covington E. J. and Montgomery D. J., Lat. const. of separated Li isotopes, J. Chem. Phys. 27, 1030.
75. Dahms H. and Sauerwald F., Uber d. Verhalten v. Re zu Al, Naturwissenschaften 44, 260.
76. Darby J. B. and Beck P. A., Sigma-phase in certain ternary systs. with V, J. Metals 9, 69.
77. Dimitriev V. A., Pzhevskaya E. V., and Khristoforov V. A., Str. of electropolished copper, Izv. Kazansk fil. AN SSSR, ser. khim. n. 4, 115.
78. Domagala R. F., Levinson E. W., and McPherson D. J., Transformn. kinetics a. mech. props. of Zr–Mo alloys, J. Metals 9, 1191.
79. Donnay G., Donnay J. D. H., and Kullerud G., Cr. a. twin str. of digenite Cu_9S_5, Acta Cryst. 10, 764 (Abstracts, . . .).
80. Dos D. K. and Pitman D. T., Prepn. a. diffn. data of Sn–Al alloys, J. Metals 9, 1175.
81. Dudkin L. D. and Abrokosov N. Kh., Investn. of the influence of Ni on props. of the semiconductor compd. $CoSb_3$, Zh. neorg. khim. 2, 212.
82. Emel'yanov V. S., Godin Yu. G., and Evstikhin A. A., Investn. of the Zr–Ta syst., At. energiya 2, 42.
83. Ence E. and Margolin H., Compds. in Ti-rich region of Ti–Al syst., J. Metals 9, 484.
84. Epel'baum V. A. and Gurevich M. A., Investn. of phase diagram of the Zr–B syst. I. Formation of a solid soln. of B in Zr, Zh. fiz. khim. 31, 708.
85. Epel'baum V. A., Sevast'yanov N. G., Gurevich M. A., Ormont B. F., and Zadanov G. S., Phases formed in the Cr–B syst. I. Formation of "β-Cr" under influence of small additions of B, Zh. neorg. khim. 2, 1848.
86. Esslinger P. and Schubert K., Zur Systematik d. Str.-familie d. NiAs. I. Verbreit. d. Strr. d. NiAs–Familie, Z. Metallik., 48, 126.
87. Evans D., Early aging effects in Cu–1.76% Be single crs. Proc., Conf. Ind. Appl. X-ray Anal., 6th, Denver, p. 143.
88. Evans D. A. and Jack K. H., Interstitial alloys with str. of β-Mn, Acta Cryst. 10, 799 (Abstracts, . .).
89. Evans D. A. and Jack K. H., γ→β phase transformn. in Mo–N syst., Acta Cryst. 10, 833 (Abstracts, . .).
90. Falvre R. and Piarrelli L., Contribn. a l'etude du diagramme Au–Cu autour de la compn. equiatomique, Bull. soc. chim. France 6, 754.
91. Ferro R., Cr. strs. of Th bismuthides, Acta Cryst. 10, 476.
92. Flinn R. A., Wallace W. E., and Craig R. S., Volume-temp. relnshs. in Mg–Cd alloys. I. Therm. expansivities in order-disorder rang-. II. Kinetics of order-disorder transformn. in $MgCd_3$, J. Phys. Chem. 61, 231; 236.
93. Fruchart R. and Michel A., Un nouveau borure de nickel Ni_3B de meme str. que la cementite, Compt. rend. 245, 171.
94. Frisch A. J., Jr., Cr. str. polymorphism a. twinning of acanthite (Ag_2S), Acta Cryst. 10, 764 (Abstracts, . .).
95. Fujiwara K., On period of out-of-step of ord. alloys with antiphase domain str., J. Phys. Soc. Japan 12, 7.
96. Gal'perin E. L. and Terminasov Yu. S., Change of cr. str. of steel during cold and thermal treatments, Kristallografiya 2, 519.
97. Gal'perin E. L. and Terminasov Yu. S., State of C in annealed silicon steel, Kristallografiya 2, 693.
98. Gelchenko V. V. and Smirnov A. A., Investn. of interat. interactions in interstitial alloys by scatting. method, Dopovidi AN URSR 5, 470 (Ukr.; Russ. and Eng. summaries).

99. Geller S., Comments on Pauling's paper on effective met. radii for use in β-W str., Acta Cryst. 10, 380.
100. Gladyshevskii E. I., Mutual solubility of e. compds. in alloys of Ag with Cd and Zn, Dopovidi ta povidomlenlya, L'viv univ. 7, 3, 190.
101. Gladyshevskii E. I. and Kripyakevich P. I., Cr. str. of the compds. $MoBe_{12}$, WBe_{12}, and $TaBe_{12}$, Kristallografiya 2, 742.
102. Glazov V. M., Mirgalovskaya M. S., and Petrakova L. A., New semiconductor matls. with chalcopyrite str., Izv. AN SSSR, otd. tekhn. n., 10, 68.
103. Goldenstein A. W., Rostoker W., Schonberger F., and Gutzeit G., Str. of chem. deposited Ni, J. Electrochem. Soc. 101, 101.
104. Goldhoff R. M. and Spretnall J. W., Distribn. of B in gamma Fe grains, J. Metals 9, 1278.
105. Goldschmidt H. J., New intmd. phases in Fe–Nb syst. Research (London) 10, 28.
106. Goldschmidt H. J., Occurrence of β-Mn str. in trans. met. alloys, a. some observns. on χ-phase equilibria, Acta Cryst. 10, 769 (Abstracts. . .).
107. Goldschmidt H. J., High-temp. X-ray study on high speed steel. I. Lat. expan. of matrix a. carbide. II. Transformns. during tempering a. some considerations on martensite-type reactions, J. Iron Steel Inst. (London) 186, 68; 79.
108. Golubkov V. M., Il'ina V. A., Kritskaya V. K., Kurdyumov G. V., and Perkas M. S., Study of phys. factors detng. hardening of alloyed iron, Fiz. met. i metalloved. 5, 465.
109. Goodman C. H. L., New gr. of compds. with diamond-type (chalcopyrite) str., Nature 179, 828.
110. Gorum A. E., Cr. strs. of PuAs, PuTe, PuP a. PuOSe, Acta Cryst. 10, 144.
111. Graham J. and Raynor G. V., In-rich In–Mg a. In–Li alloys, Phil. Mag. 2, 1354.
112. Gridnev V. N. and Trefilov V. I., Relatn. between cr. lat. pars. of austenite and temp. of start of martensite transforma. in Fe–C alloys, Dokl. AN SSSR 115, 60.
113. Grigor'ev A. T., Sokolovskaya E. M., and Pyatnitskii V. N., Transformns. in solid state in alloys of the Cu–Zn syst. in the region of the α-solid soln., Zh. neorg. khim. 2, 1547.
114. Grønvold F. and Rost E., Cr. str. of $PdSe_2$ a. PdS_2, Acta Cryst. 10, 329.
115. Gulkova N. V., Levina E. I., and Tolomasov V. A., Investn. of carbide phases in annealed carbon steel, Fiz. met. i metalloved. 4, 509; 5, 178.
116. Gurevich M. A. and Ormont B. F., Identity period of lat. of pure met. V and influence of O on change of period, Fiz. met. i metalloved. 4, 112.
117. Gurevich M. A. and Ormont B. F., Investn. of phase compn., str., and homogeneity boundaries of phases in the V–C–O syst. I. The V–C syst. II. Investn. of V–O syst. (lower oxides of V), Zh. neorg. khim. 2, 1506; 2531.
118. Gurova L. N., At. scattering of x-rays in Cu–Zn alloys, Dokl. AN SSSR 113, 567.
119. Gurova L. N. and Ovechkin D. I., Investn. of Cr-rich Cr–Si alloys, Izv. AN SSSR, otd. tekhn. n., 6, 27.
120. Haasen P., Twinning in In antimonide, J. Metals 9, 30.
121. Hahn H., Uber d. Beeinfluss. d. Str. ternarer u. quaternarer Phasen bzw. Verbindd. durch d. Wahl geeigneter Komponenten. Uber d. Str. v. Mischkristallen d. InAs mit InSe, In_2Se_3 u. InTe, Naturwiss. 44, 534.
122. Hahn H. and Frank G., Zur Kr.-str. d. In_2Se_3, Naturwiss. 44, 533.
123. Hahn H. and Harder B., Unterss. uber ternare Chalkogenide. IX. Uber d. Str. d. $CuTi_2S_4$, Z. anorg. Chem. 288, 257.
124. Hahn H. and Harder B., Zur Kr.-str. d. Ti Sulfide, Z. anorg. Chem. 288, 241.
125. Hahn H., Harder B., Mutschke U., and Ness P., Zur Kr.-str. einiger Verbindd. u. Phasen d. Syst. Zr–S, Z. anorg. Chem. 292, 82.
126. Hahn H. and Lorent C., de, Unterss. uber ternare Chalkogenide. XII. Uber ternare Chalkogenide d. Cr mit einwertigem Cu u. Ag, Z. anorg. Chem. 290, 68.
127. Hahn H. and Mutschke U., Unterss. uber ternare Chalkogenide. XI. Versuche zur Darst. v. Thioperowskiten, Z. anorg. Chem. 288, 269.
128. Hahn H. and Ness P., Zur Str. d. im Syst. Zr–Te auftretenden Phasen, Naturwiss. 44, 534.
129. Hahn H. and Ness P., Zur Str. d. im Syst. Zr–Se auftretenden Phasen, Naturwiss. 44, 534.
130. Hann H. and Ness P., Zur Frage d. Existenz. v. Subchalkogenidphasen d. Ti, Naturwiss. 44, 581.
131. Hall E., La str. des alliages Ag–Mn–Al et leurs props. magn. "Journees metallurg. d'automne, 1957. Avant-programme et res. communic." Paris, Soc. Fr. Metall., 67.
132. Hall E. O., Twinning in Co, Acta Met. 5, 110.
133. Hall E. O. and Crangle J., X-ray investn. of reported high-temp. allotropy of Ru, Acta Cryst. 10, 240.
134. Halteman E. K., Cr. str. of U_3Mo, Acta Cryst. 10, 166.

135. Hardie D. and Perkins R. H., Solid-soln. hardening of Al a. Mg, J. Inst. Met. 85, 449.
136. Harris W. W., Gall F. L., and Gwathmey A. T., Str. of oxide films formed on smooth faces in single cr. of Cu, Acta Met. 5, 674.
137. Hatt B. A., Roberts J. A., and Williams G. I., Occurrence of meta-stable omega phase in Zr alloys, Nature 180, 1406.
138. Hayase K. and Harada T., Rela. entre la compn. chim., la str. cr. et le magnetisme de la pyrrhotine. Etude des props. de la pyrrhotine, V. J. Mining Inst. Japan 73, 486.
139. Heidenreich R. D. and Nesbitt E. A., Stacking disorders in Ni base magn. alloys, Phys. Rev. 105, 1678.
140. Hendus H., Dawihl W., and Bartsch G., Teilchengrosse u. Gitterverzerrung v. W u. W-karbidpulvern, Z. Metallk. 47, 615.
141. Herbstein F. H., Note on str. of evapd. Ag deposits prepared at high temps., Proc. Phys. Soc. London 70B, 251.
142. Heumann T. and Knlepmeyer M., A_3-B Phasen v. Typ Cu_5Ca u. Lavesphasen in d. Systt. Sr mit Pd, Pt, Rh u. Ir., Z. anorg. Chem. 290, 191.
143. Heyding R. D. and Calvert L. D., Arsenides of trans. mets. I. Arsenides of Fe a. Co. II. Ni arsenides, Canad. J. Chem. 35, 449; 1205.
144. Hinnuber J. and Kinna W., Uber d. Loslichk. v. W-karbid in Ti-karbid., Tech. Mitt. Krupp. 15, 155.
145. Hirabayashi M. and Ogawa S., On superstr. of ord. alloy Cu_3Pd. II. X-ray diffrn. study, J. Phys. Soc. Japan 12, 259.
146. Honjo G. and Miyake S., E. diffrn. str. anal. of some inorg. substances, Acta Cryst. 10, 860 (Abstracts. . .).
147. Hornbogen E., Segmuller A., and Wassermann G., Martensit. Umwandl. bei d. Verform. v. abgeschrecktem β_1-Messing., Z. Metallk. 48, 379.
148. Ignatov D. V., E. diffrn. investn. of phase changes in thin films of mets. and oxides, Kristallografiya 2, 484.
149. Il'ina V. A., Kritskaya Y. K., Kurdyumov V. G., Osip'yan Yu. A., and Stellerskaya T. I., Study of the dependence of bond forces on the state of crs. in mets. and solid solns., Fiz. met. i metalloved. 4, 417.
150. Jack K. H. and Wachtel M. M., Char. a. cr. str. of Cs antimonide, photoelectr. surface material, Proc. Roy. Soc., Ser. A, 239, 46.
151. Jack K. H. and Wachtel M. M., Str. of photoelectr. Cs antimonide. Temp. fs. in cub. crs., Acta Cryst. 10, 775 (Abstracts. . .).
152. Juza R., Puff H., and Wagenknecht K., Zur Kenntnis d. Syst. Mn-N, Z. Elektrochem. 61, 801.
153. Juza R. and Opheff W., Uber Phosphid Sulfid- u. Arsenid/Selenid-Mischkristalle, Angew. Chem. 69, 96.
154. Juza R. and Opheff W., Darst. u. Eigg. d. Verbb. Li_7VP_4 u. Li_7VAs_4, Z. anorg. Chem. 292, 65.
155. Karlikov D. M., X-ray investn. of short-range order in Cd amalgams, Ukr. fiz. zh. 2, 3 (suppl.), 43 (Ukr.; Eng. and Russ. summaries).
156. Kato N., Study of lat. distortion by x-ray diffrn. technique, Acta Met. 5, 237.
157. Katz G., Kohn J. A., and Broder J. D., Crystallogr. data for Sn monophosphide, Acta Cryst. 10, 607.
158. Kaufmann A., Cullity B., and Eitutanes G., U-Si alloys, J. Metals 9, 23.
159. Kempter C. P., Krikorian N. H., and McGuire J. C., Cr. str. of Yt-nitride, J. Phys. Chem. 61, 1237.
160. Khandros L. G., Change of fine cr. str. of Superinvar in the $\gamma-\alpha$ transformn., Sb. nauchn. rabot Inst. metallofiz. AN SSSR 8, 121.
161. Klepfer H. H., Chars. of solid state transformns. in U. Iowa State Coll. J. Sci. 32, 205.
162. Knapton A. G., Mo-Re syst., Bull. Inst. Metals 3, 161.
163. Knodler H., D. strukturelle Zusammenhang zwischen γ- u. ε-phase im Syst. Cu-Zn, Acta Cryst. 10, 86.
164. Kohanovska A., Possibility of studying distribn. of lattice defects in crystallites by means of x-rays of different wave lengths, Czechoslov. J. Phys. 7, 169.
165. Kogan L. I. and Engin R. I., Redistribn. of C in transformn. of austenite in the middle region, Fiz. met. i metalloved. 4, 300.
166. Kohn J. A. and Katz G., Crystallogr. of AlB_{10} a. AlB_{12}. Program a. Abstracts, 15th Pittsburgh Diffrn. Conf., 6-8 Nov. 1957, 36.
167. Kolm C., Kulin S. A., and Averbach B. L., Studies on gr. III-V intermet. compds., Phys. Rev. 108, 965.
168. Komar A. P. and Shrednik V. N., The $\alpha \rightleftarrows \beta$ transformn. of Zr from observns. with aid of e. projector, Fiz. met. i metalloved. 5, 452.
169. Komura Y., Shoemaker D. P., and Shoemaker C. B., Cr. str. of R phase, Mo-Co-Cr, Acta Cryst. 10, 774 (Abstracts. . .).
170. Konig H., Hex. Ag, Physik. Verhandl., 8, 210.
171. Kornilov I. I. and Bulberg N. B., Phase diagram of the ternary syst. Ni-Cr-W, Tr. Inst. metallurgii AN SSSR 1, 132; Zh. neorg. khim., 2, 860.

172. Kornilov I. I. and Matveeva N. M., Phase transformns. in the Fe–Cr–V syst., Zh. neorg. khim. 2, 355.
173. Kornilov I. I., Snetkov A. Ya., and Tikov F. M., Study of the solubility of Ti and phase compn. of alloys in the quinary Ni–Cr–W–Al–Ti syst., Zh. neorg. khim. 2, 103.
174. Kost W. L., Finnie L. N., Searcy A. W., Cr. strs. of monosilicides of Os, Ir a. Ru, J. Phys. Chem. 61, 1541.
175. Koster W. and Haug K., D. Dreistoffsyst. Ti–V–Zn, Z. Metallk. 48, 327.
176. Koster W. and Sampaio A., D. Dreistoffsyst. Ti–Ag–Al, Z. Metallk. 48, 331.
177. Kouer W. and Spemer F., D. Dreistoffsyst. Co–Ni–V, Z. Metallk. 48, 510.
178. Kotovich V. A. and Frank-Kamenetskii V. A., Standard x-ray patterns of certain selenides, tellurides, arsenides, and sulfides of Cu, Ag, Zn, Cd, Ga, In, Uch. zap. Leningr. Univ. 215, 136.
179. Krebs H. and Ludwig T. D., Str. d. Polyphosphids $IIgP_5P_{11}$, Angew. Chem. 69, 718.
180. Krip'yakevich P. I. and Gladishevs'kii E. I., X-ray str. investns. of Cr–Be alloys with high Be contents, Dopovidi ta povidomlenlya, L'viv. Univ. 7, 3, 183 (Ukr.).
181. Kuo K., Researches on carbides in alloy steels, Jernkontor. Ann. 141, 206.
182. Kuriyama M., Kohra K., and Takagi S., E. diffrn. study of polish layers of Au, I. J. Phys. Soc. Japan 12, 151.
183. Kurov G. A., Semiletov S. A., and Pinsker Z. G., Electrical properties and real str. of single-cr. Ge films obtained by evapn. in vacuum, Kristallografiya 2, 59.
184. Kusumoto K., Ohta M., and Konishi N., Etudes aux r. X sur le processus de precipitation des alliages Al–Ag–Mg, J. Japan. Inst. Metals (Sendai) 21, 561.
185. Kuz'min R. N., Zhdanov G. S., and Zhuravlev N. N., Metallographic and x-ray investns. of alloys in the Sb–Ir syst., Kristallografiya 2, 48.
186. Lacombe P., Rebillard A., and Calais D., Influence de traitements therm. en phase γ sur l'apparition desous-strs. dans U., Compt. rend. 244, 1367.
187. Langeron J. P. and Lehr P., Etude de la transformn. α → β du Zr, "Journees metallurg. d'automne, 1957. Avant-programme et res. communic." Paris, Soc. Fr. Metall. 63.
188. Larach S., Shrader R. E., and Stocker C. F., Anomalous variation of band gap with compn. in Zn sulfo- a. seleno-tellurides, Phys. Rev. 103, 587.
189. Larson A. C., Cromer D. T., and Stambaugh C. K., Cr. str. of $PuAl_3$, Acta Cryst. 10, 443.
190. Lashko O. S., Str. of liquid Bi–Sn alloy, Dopovidi AN URSR 1, 30 (Ukr.; russ. and Engl. summaries).
191. Lashko A. S., X-ray investn. of the str. of liquid Sn–Zn alloy, Sb. nauchn. rabot Inst. metallofiz. AN USSR 8, 132.
192. Leont'ev B. A., Palatnik L. S., and Spektor Ya. L., Investn. of kinetics of stepwise transformn. of supercooled austenite, Fiz. met. i metalloved. 5, 301.
193. Lerioman R. M. and Bulnov N. N., E. micr. and e. diffrn. investn. of aging of Al–Ag alloys, Fiz. met. i metalloved. 5, 279.
194. Lieberman D. S., Read T. A., and Wechsler M. S., Graphical anal. of diffusionless phase changes-cub. to twinned orthoh. transformn., J. Appl. Phys. 28, 532.
195. Lin S. T. and Kaufmann A. R., Magn. props. of UMn_2, Phys. Rev. 108, 1171.
196. Liu Yi-Huan and Hsu Chen-Chia, Investn. of Ag–Au–Zn alloys with 50 at.% Zn, Acta Phys. Sinica 13, 403.
197. Lyashchenko B. G., Litvin D. F., Puzei I. M., and Abov Yu. G., N. diffrn. investn. of Fe–Ni alloys of the Permalloy class, Kristallografiya 2, 64.
198. Lyudkovskaya B. G. and Sarychev B. L., X-ray str. investn. of iron oxidized by steam at high temps., Tr. gos. n.-i. i proektnogo inst. azotnoi promyshlennosti 3, 259.
199. Llewellyn J. P. and Smith T., Therm. expan. of Fe ditelluride, Proc. Phys. Soc. Lond. 70B, 1113.
200. Lloyd L. T., Discussion on "X-ray diffrn. determn. of coefs. of expan. of α-U," J. Metals 9, 532.
201. Lotgering F. K. and Gorter E. W., Solid solns. between ferromagn. a. antiferromagn. compds. with NiAs str. Phys. Chem. Solids 3, 238.
202. Lu S. S. and Chang T., Cr. str. changes in phase of Al–Cu–Ni alloys, Scientia Sinica 6, 431; Acta Phys. Sinica 13, 150 (Chinese; Engl. summary).
203. Lu S. S. and Chang T., Syst. str. changes in single-phase field-extra-ordinary phenomenon observed in Al–Cu–Ni alloys, Sci. Record (Peking) 1, 41.
204. Lutts A. and Lambot H., Etude de la precipitation dans les alliages du type "almasilium", Rev. met. 54, 775.
205. Mabarro F. R. N., Axial ratio of Zn, a. of eta a. epsilon brasses, Phil. Mag. 2, 716.
206. Mack G., Rontgenprazisionsunterss. an Ge-Zinkristallen u. an legierten Ge–In–pn-Ubergangen, Angew. Chem. 69, 489.
207. MacKenzie J. K. and Bowles J. S., Crystallogr. of martensite transformns. IV. Body-centered cub. to orthoh. transformns., Acta Met. 5, 137.

208. Manenc J., Dispositif permettant l'etude aux r. X par deflexion de la diffusion au voisinage des noeuds du reseau reciproque, Acta Cryst. 10, 259.
209. Manenc J., Etude aux r. X de l'evolution str. d'un alliage Ni–Cr type 80-20 modifie, Rev. met. 54, 161.
210. Manenc J., Precipitation de la phase Ni_3Al dans un alliage a 7,8% de Al, Rev. met. 54, 867.
211. Marburger R. E. and Neuluchter A. W., Precipitated phases a. their distribn. in Al–Si–Cd alloy, Bull. Am. Phys. Soc. 2, 123.
212. Marion P. G., Haines H. R., Pearce J. H. and Waldron M. B., Pu–Fe syst., J. Inst. Met. 86, 166.
213. Margolin H. and Bunshah R. F., Discussion of "Phase transformns. in Ti-rich alloys of Ni a. Ti", J. Metals 9, 524.
214. Marion F. and Faivre F., Etude radiocristallogr. des carbures de revenu de la martensite. "Journees metallurg. d'automne, 1957. Avant-programme et res. communic." Paris, Soc. Fr. Metall., 69.
215. Massalski T. B., Lat. sps. of close-packed hex. Au–In, Au–Cd, a. Au–Hg alloys, Acta Met. 5, 541.
216. Massalski T. B. and Barrett C. S., Strain induced transformn in β-brass, J. Metals 9, 455.
217. Masson D. B. and Barrett C. S., Effect of deformn. a. low temps. on strs. of AgCd a. AuZn, J. Metals 9, 7.
218. Matthias B. T. and Corenzwit E., Superconducting alkaline earth compds., Phys. Rev. 107, 1558.
219. McHargue C. J., Yakel H. L., Jr., and Jetter K., Allotropic modifns. of met. Cc, Acta Cryst. 10, 832 (Abstracts. . .).
220. Meneghetti D. and Sidhu S. S., Magn. strs. in Cu–Mg alloys, Phys. Rev. 105, 130.
221. Michell D. and Haig F. D., Investn. of annealing of deformed Ni powder by X-ray a. stored energy measrts., Phil. Mag. 2, 15.
222. Mingazin T. A., Investn. of the Bi–Rb syst., Uch. zap. Turkm. univ. 11, 231.
223. Mirgalovskaya N. S., Matkova L. N., and Kornova E. M., The syst. Mg–Al–Mn, Tr. Inst. metallurgii AN SSSR 2, 139.
224. Mitra G. B. and Mitra S. K., Trunelsen's rule a. therm. expan. of mets., Nature 179, 1295.
225. Miyazawa H. and Sugaike S., Phase trans. of In_2Se_3, J. Phys. Soc. Japan 12, 312.
226. Moore A. and Raynor G. V., Superlat. strs. a. their relnsh. to constn. diagram in Mg–Cd syst., Acta Met. 5, 601.
227. Mueller M. H., Knott H. V., and Heaton LeR., Hex. phase found in certain Z. a. Ti alloys, Program a. Abstracts, 15th Pittsburgh Diffrn. Conf., 6-8 Nov. 1957, 46.
228. Muller E. W., Study of at. str. of met. surfaces in field ion micr., J. Appl. Phys. 28, 1.
229. Muller H. K. F. and Hendus H. D., Atomverteil. im flussigen Sb, Z. Naturf. 12A, 102.
230. Munster A. and Sagel K., Rontgenograph. Best. d. Nahordn. in Al–Zn-Legier., Metall 11, 963.
231. Nagakura S., Study of met. carbides by e. diffrn. I. Formn. a. decompn. of Ni_3C, J. Phys. Soc. Japan 12, 482.
232. Nakayama T., Etude diffractometriques X sur l'oxydation, a haute temp. des alliages Fe–Al. I. Sur les couches resistant a l'oxydation, J. Japan. Inst. Metals 21, 716 (Jap.).
233. Neshpor V. S. and Samsonov V. G., New borides of rare-earth elements, Dopovidi AN URSR 5, 478 (Ukr.; Russ. and Engl. summaries).
234. Nevitt M. V. and Downey J. W., Sigma phases containing Os a. Ir., J. Metals 9, 1072.
235. Newkirk J. B., Mechanism of precipitation in Cu—2,5% Fe alloy, J. Metals 9, 1214.
236. Newton C. J. and Vacher H. C., X-ray study of textural stresses in two-phase alloys, Bull. Am. Phys. Soc. 2, 202.
237. Nicholson M. E., Solubility of B in Fe_3C a. variation of saturation magnetization, Curie temp. a. lat. par. of $Fe_3(C,B)$ with compn., J. Metals 9, 1.
238. Niwa K. and Shimaoka G., E. diffrn. study of flake graphite extracted from molten pig iron, J. Metals 9, part II, 430.
239. Noakes J. E., Turner A. H., and Arajnan R. A., Anomalous behavior of soln. of Ti in Fe, Acta Cryst. 10, 770 (Abstracts. . .).
240. Novikov I. I. and Dautova L. I., Investn. of the copper corner of the Cu–Ni–Si syst., Zh. neorg. khim. 2, 2766.
241. Novikova O. A. and Rudnitskii A. A., Investn. of the Ag–Pt syst., Zh. neorg. khim. 2, 1840.
242. Nowotny H., Dimakopoulou E., and Kudielka H., Untersu. in d. Dreistoffsyst. Mo–Si–B, W–Si–B u. im Syst. VSi_2–$TaSi_2$, Mh. Chem. 88, 180.
243. Obrowski W. E., δ-Phase im Syst. Ru–W, Naturwissenschaften 44, 581.
244. Ogawa S., Mizuno J., Watanabe D., and Fujita F. E., On twin str. of Ni films electrodeposited on single crs. of Cu, J. Phys. Soc. Japan 12, 999.
245. Ogawa S. and Watanabe D., Str. anal. of ord. alloys with long period, Acta Cryst. 10, 860 (Abstracts. . .).
246. Ogawa S., Watanabe D., Takeuchi Y., and Kawanishi R., Etudy sur l'oxydation a l'air du Ti et de ses alliages, J. Japan. Inst. Metals 21, 410 (Jap.).

247. Otte H. M., Fermn. of stacking faults in austenite a. its reln. to martensite, Acta Met. 8, 614.
248. Otte H. M. and Read T. A., Habit planes of martensite in Cr–C steel, J. Metals 9, 412.
249. Pagnelli M. and Negare E. Dalle, Esame al micr. elettronica del riprecipitato indurente in una lega binaria Al–50%Cu, Alluminio 26, 51 (Ital.).
250. Parthe E., Contrions to Nowotny phases, Powder Met. Bull., 8, 23; Acta Cryst. 10, 768 (Abstracts, . .).
251. Paskin A. and Weiss R. J., Short-range order in partially ord. Cu_3Au, J. Appl. Phys. 28, 146.
252. Pauling L., Set of effective met. radii for use in compds. with B-W str., Acta Cryst. 10, 374.
253. Pauling L., Use of at. radii in discussion of interat. distances a. lat. consts. of crs., Acta Cryst. 10, 685.
254. Pearson W. B. and R'mek D. M., Constn. of Ni–Ga alloys in region 0–35 at.%Ga, Canad. J. Phys. 35, 1228.
255. Pearson W. B. and Thompson L. T., Lat. sps. of Ni solid solns., Canad. J. Phys. 35, 349.
256. Pelah I., Eisenhauer C. M., Hughes D. J., and Palevsky H., Detection of opt. lat. vibrations in Ge a. ZrH by scatrg. of cold neutrons, Phys. Rev. 103, 1091.
257. Perkas M. D. and Shamov A. E., Study of the solubility of carbides in γ-Fe by meas. of the width of the interference line, Tr. Kuibyshevsk. Inzh.-stroit. Inst. 4, 177.
258. Philip T. V. and Beck P. A., CsCl-type ord. strs. in binary alloys. of trans. elements, J. Metals 9, 1269.
259. Picon M. and Flahaut J., Sur la caracterisation phys. des carbures de Mn, Compt. rend. 245, 534.
260. Pietrowsky P. and Frink E. P., Constn. diagram for alloy syst. Ti–Sn, Trans. Am. Soc. Metals 49, 339.
261. Pinsker Z. G. and Kaverin S. V., E. diffrn. investn. of nitrides and carbides of trans. mets., Kristallografiya 2, 386.
262. Pinsker Z. G. and Kaverin S. V., Troitskaya N. V., E. diffrn. investn. of Mo nitrides, Kristallografiya 2, 179.
263. Pinsker Z. G. and Skobel'tsyna N. A., E. diffrn. investn. of decompn. of supersatd. solid solns. in the Al–Cu and Ag–Cu systs., Kristallografiya 2, 618.
264. Pluiquellec J., Azon P., and Bastien P., Localisation de l'hydrogene dans le reseau du Fe α, Compt. rend. 244, 1195.
265. Poole D. M., Williamson G. K., and Marples J. A. C., Preliminary investn. of Pu–Th syst., J. Inst. Met. 86, 172.
266. Popper P. and Ruddlesden S. N., Str. of nitrides of Si a. Ce, Nature 17, 1129.
267. Puzei I. M., Superstr. and effect of temp. on the energy of magn. anisotropy in Ni–Fe alloys, Izv. AN SSSR, ser. fiz. 21, 1094.
268. Radchenko I. V., Str. of liquid mets., Usp. fiz. n. 61, 249.
269. Raub E., D. Os–Cr Legierr, Z. Metallk. 43, 53.
270. Raub E. and Mate W., D. Ru–Cr Legierr, Z. Metallk. 49, 444.
271. Ray A. E. and Smith J. F., Compn. variation in α-phase compd. of V–Al syst., Acta Cryst. 10, 604.
272. Raynor G. V. and Graham J., Experiments on syst. In–Sn, Research (London) 10, 369; 371.
273. Raynor G. V. and Ward B. J., Al-rich alloys of quaternary syst. Al–Fe–Cu–Ni, J. Inst. Metals 86, 135.
274. Reimer L., Zur Str. v. PbTe-Aufdampfschichten, Naturwissenschaften 44, 416.
275. Richter H. and Gommel G., Str. d. gefällten amorphen As bei verschied. Tempp., Z. Naturf. 12, 906.
276. Richter H. and Herre F., D. Atomverteil. in festem amorphem u. flussigem Se, Naturwiss. 44, 31.
277. Roberts B. W. and Swalin R. A., Concerning order-disorder trans. in Ni–Cr syst., J. Metals 9, 845.
278. Roche N. de, Zur Kenntnis d. Syst. Ga–Ge, Z. Metallk. 43, 59.
279. Rode V. E., Kinetics of superstr. transformn. of Fe_3Al alloy, Izv. AN SSSR, ser. fiz. 21, 1234.
280. Romanow W. J., Crystallogr. angles for Mn-bismuthide, J. Metals 9, 1284.
281. Rudman P. S. and Averbach B. L., X-ray determn. of order a. at. sizes in Co–Pt solid solns., Acta Met. 5, 65.
282. Rudnitskii A. A., Phys. props. of Ru., Zh. neorg. khim. 2, 2758.
283. Rundqvist S., Cr. str. of BP XVI Congres International de Chimie Pure et Appliquee, Paris, 1957, 162.
284. Sailer H. A., Rough F. A., Bauer A. A., and Doig J. R., Constn. of deltaphase alloys of syst. U–Zr–Ti, J. Metals 9, 878.
285. Samsonov V. P., Cr. strs. of Ti silicides and germanides. Author's abstract, tech. sci. cand. diss. (in Russian) (Inst. of Metallurgy USSR, Moscow).
286. Samsonov G. V., Intermediate stages in reactions of formn. of Ti, Zr, V, Nb, and Ta carbides, Ukr. khim. zh. 23, 287.
287. Samsonov G. V., Phases of the W–B syst., Dokl. AN SSSR 113, 1299.
288. Samsonov G. V. and Popova N. M., Prepn. and some chars. of Th sulfides, Zh. obshch. khim. 27, 3.
289. Samsonov G. V. and Umanskii Ya. S., Hard compds. of refractory mets. (in Russian) (Metallurgizdat, Moscow) 388 pp.
290. Savitskii E. M., and Burkhanov E. S., Phase diagrams of Ti–La and Ti–Ce alloys, Zh. neorg. khim. 2, 2609.
291. Scheil E. and Saftig E. D., Einfluss v. Spannungen auf d. Gitterkonst. d. Austenits, Archiv. Eisenhuttenw. 28, 49.

292. Schubert K., Über einige Beziehh. zwischen Kr.-str. III. Einachsige D.bn. v. Kr.-strr. bei Erhöh. d. El.-konzentrat., Z. Naturf. 12A, 310.
293. Schubert K., Breimer H., Burkhardt W., Gunzel E., Haufler R., Lukas H. L., Vetter H., Wegst J., and Wilkens M., Einige strukturelle Ergebnisse an met. Phasen. II. Naturwiss. 7, 229.
294. Schubert K., Burkhardt W., Gunzel E., Wegst J., and Wilkens M., Some cr. strs. in alloys of Au with B-subgr. mets., Acta Cryst. 10, 776; (Abstracts. . .).
295. Schubert K. and Esslinger P., Zur Systematik d. Strukturfamilie d. NiAs. II. Deut. einiger struktureller Erscheln auf Grund v. Ordnungskorrelationsvorschlägen, Z. Metallk. 48, 193.
296. Schwartz M. and Muldawer L., X-ray determns. of Debye temps. in alloy β-AuZn, Bull. Am. Phys. Soc. 2, 213.
297. Sebilleau F., Achromatisme en rayonnement X. Application a l'etude des raies de diffm. de la soln. solide Al–Cu a 4% au cours du durcissement str. Off Nation. et Rech. Aeronaut. Public. Fr., 87.
298. Selitskii Ya. P., Ord. process in Fe_3Al alloy, Fiz. met. i metalloved. 4, 191.
299. Semiletov S. A. and Rozsival M., E. diffm. investn. of InSb films, Kristallografiya 2, 287.
300. Servi I. S., Stern M., and Webb W. W., Autoradiographic a. metallographic evidence for met. second phase in high-purity Zn, J. Metals 9, 12.
301. Shaw S. W. K. and Quarrell A. G., Formn. of carbides in low-carbon, Cr–V steels at 700°C, J. Iron Steel Inst. (London) 185, 10.
302. Sherrill F. A., Wittels M. C., and Blewitt T. H., X-ray determn. of conjugate deformn. twins in Cu, J. Appl. Phys. 28, 526.
303. Shimaoka G., Str. of surface films on molten mets. IV. Oxide film of Bi. V. Oxide film of Cd, J. Chem. Soc. Japan 78, 175; 178 (Jap.).
304. Shinoda G. and Amano Y., Phenomenes de durcissement par recuit aux joints de grains du laiton α, J. Japan. Inst. Metals (Sendai) 21, 59 (Jap.).
305. Shishakov N. A., Anomalous str. of Fe crs. formed at initial stage of condensation from vapor., Fiz. met. i metalloved. 5, 169.
306. Shoemaker D. P., Shoemaker C. B., and Wilson F. C., Cr. str. of P phase Mo–Ni–Cr. II. Refint. of para. a. discussion of at. coordn., Acta Cryst. 10, 1.
307. Silcock J. M., Discussion on "Intmd. phase in U–Zr syst.," J. Metals 9, 521.
308. Simmons R. O. and Balluffi R. W., Low temp. therm. expan. of Cu., Phys. Rev. 108, 278.
309. Skrishevs'kii A. F., Str. of molten alloys of the Au–Sn syst., Ukr. fiz. zh. 2, 263 (Ukr.; Russ. and Engl. summaries).
310. Skrishevs'kii A. F., Karlikov D. M., and Karlikova D. P., Str. of liquid Hg, Ukr. fiz. zh. 2, 2 (suppl.), 49 (Ukr.; Russ. and Engl. summaries).
311. Skryshevskii A. F., X-ray investn. of short-range order in certain liquid alloys, St. nauchn. rabot Inst. metallofiz. AN USSR 3, 187.
312. Smallman R. E. and Westmacott K. H., Stacking faults in face-centered cub. mets. a. alloys, Phil. Mag. 2, 669.
313. Smith E. and Guard E. W., Investn. of Ni-rich portion of syst. Ni–Zr, J. Metals 9, 1189.
314. Smith J. F. and Bailey D. M., Str. of $ZrGe_2$, $HfSi_2$ a. $HfGe_2$, Acta Cryst.
315. Smith J. F. and Ray A. E., Str. of V_4Al_{23}, Acta Cryst. 10, 169.
316. Smith J. H. and Street Dr. R., Resistivity a. magnetoresistance of Au_2Mn, Proc. Phys. Soc. Lond. 70B, 1089.
317. Speeding F. H., Daane A. H., and Herrmann K. W., Electr. resistivities a. phase transformns. of La, Ce, Pr, a. Nd, J. Metals 9, 895.
318. Spektor E. Z., X-ray investn. of metl strs. Sb, fiz.-khim. osnovy proizvodstva stali (Physicochemical Principles of Steel Production) [in Russian] (Inv. AN SSSR, Moscow, p. 257, Discussion on p. 332).
319. Strock L. W., Anisotropic ZnS crs. with three-layer stacking, Acta Cryst. 10, 310 (Abstracts. . .).
320. Strock L. W. and Brophy V. A., Single crs. of Zn sulfide with 6-a. 18-layer polytype str., Bull. Geol. Soc. Am. 68, 1801.
321. Strukov L. N. and Gel'd P. V., Transformns. in alloys containing lebolite, Tr. Ural'sk. politekhn. inst. 72, 149.
322. Strum W. J. and Wechsler M. S., Density a. resistivity changes in Au–Cd upon quenching, J. Appl. Phys. 28, 1509.
323. Svechnikov V. N. and Sinelin A. K., Phase diagram of Fe–As, Sb, nauchn. rabot Inst. metallofiz. AN USSR 8, 51.
324. Swalin R. A., Orientation relnshs. involved in formn. of α-W_2C on W, Acta Cryst. 10, 473.
325. Swanson H. E., Gilfrich N. T., Cook M. I., and Stinchfield R., Standard X-ray diffm. powder pats., Nat. Bur. Standards, Rep. 5308, 17; 42.
326. Swanson H. E., Gilfrich N. T., Cook M. I., Stinchfield R., and Parks P., Standard X-ray diffm. powder pats., Nat. Bur. Standards, Rep. 5402, 39.

327. Sze Shih-Yuen, Mise en ordre et diffusion de lacunes dans $AuCu_3$, Acta Phys. Sinica 13, 245 (Chinese).
328. Takahashi N. and Mihama K., Etude par microdiffrn. et micr. e. de la transformn. des alliages Al–Cu due au chauffage dans le vide, Acta Met. 5, 159.
329. Takeyama T. and Koda S., Preferred precipitation on disloca. lines in Al alloy, Nature 179, 777.
330. Taoka T. and Sakata S., Crystallogr. orientations of low-angle boundaries in Ni–Mn single crs., Acta Met. 5, 236.
331. Tatarinova L. L., E. diffrn. investn. of amorphous Sb sulfide, Kristallografiya 2, 260.
332. Taylor J. L., Preliminary investn. of Ti–Ce syst., J. Metals 9, 94.
333. Taylor A. and Jones R. M., X-ray a. magn. investn. of Fe-rich Fe–Al alloys, Acta Cryst. 10, 771 (Abstracts...).
334. Teitel R. J., U–Pb syst., J. Inst. Met. 85, 409.
335. Teitel R. J., U–Bi syst., J. Metals 9, 131.
336. Tideswell N. W., Kruse F. H., and McCullough J. D., Cr. str. of Sb_2Se_3, Acta Cryst. 10, 99.
337. Tiedema T. J., Bouman J., and Burgers W. G., Precipitation in Au–Pt alloys, Acta Met. 5, 310.
338. Toman K., Str. of Guinier-Preston zones. II. Room-temp. ageing of Al–Cu alloy, Acta Cryst. 10, 187.
339. Toypenets E. S. and Sin'kovskaya G. N., Dilatometric and x-ray str. analyses of steels, Tr. Donetsk. industr. Inst. 19, 59.
340. Trillat J. J. and Mihama K., Etude par micr. et diffrn. e., des couches d'alliage etain-fer sur le fer blanc, Metaux (Corrosion-Indus.) 32, 102.
341. Trillat J. J., Tertian L., and Britton S. C., Etude par diffrn. et micr. e., de films d'oxydation naturels ou artificiels formes sur de l'etain pur et sur du fer etame, Metaux (Corrosion-Indus.). 32, 475.
342. Trillat J. J., Tertian L., and Lecomte C., Etude par diffrn. e. de la nitruration du Ni, Compt. rend. 244, 596.
343. Trillat J. J., Tertian L., Terao N., Etude par diffrn. e. de la nitruration du Ni, Bull. soc. chim. France 7, 866.
344. Trillat J. J., Tertian L., Terao N., and Lacomte C., Sur l'action de N sur Ni, Bull. soc. chim. France 2, 215.
345. Trzebiatowskii W., Lukaszewicz K., and Weglowski St., Cr. str. of Ba tetratitanate a. two Zr arsenides, Acta Cryst. 10, 792 (Abstracts...).
346. Vangengeim E. D., Influence of temp. on interer. internal adsorption in binary Ag-based alloys, Fiz. met. i metalloved. 5, 174.
347. Ventriglia U., Sudi strutturali sugli arseniuri di Co. Period. Miner. 26, 345.
348. Vickers W., Further contribn. to crystallogr. angles for Bi a. Sb., J. Metals 9, 827.
349. Vucht J. H. N. van, Some data about syst. Ce–Th, Philips Research Repts. 12, 351.
350. Vucht J. H. N. van, Beitrag zur Kenntnis d. Syst. Ce–Al, Z. Metallk. 48, 253.
351. Wadsley A. D., Partial order in nonstoichiometric phase $Ti_{2+x}S_4 (0.2 < x < 1)$, Acta Cryst. 10, 715.
352. Wagner C., Etude par. r. X des defauts d'empilage dans les met. cub. a faces centrees, "Journees metallurg. d'automne, 1957. Avant-programme et res. communic." Paris, Soc. Fr. Metall., 64.
353. Wagner C. N. J., Stacking faults by low-temp. cold work in Cu a. alpha brass, Acta Met. 5, 427.
354. Wagner C. N. J., X-ray study of low-temp. cold work in Ag a. Al, Acta Met. 5, 477.
355. Watanabe D., Cr. str. oford. alloy Au_2Mn, Acta Cryst. 10, 483.
356. Waterstrat R. M. and Kasper J. S., X-ray diffrn. study of sigma phase in syst. Re–Cr, Ru–Cr a. Os–Cr, J. Metals 9, 872.
357. Wei C. T., X-ray study of plastic deformn. in Zn single crs., Acta Met. 5, 435.
358. Wei C. T., Parthasarathi M. N., and Beck P. A., X-ray study of polygonization in Cu single crs., J. Appl. Phys. 23, 874.
359. Weiner R. T., Freeth W. E., and Raynor G. V., Lat. sps. a. melting points in Th–Ce syst., J. Inst. Met. 86, 185.
360. Weiss V. and Klier E. P., X-ray satellite line str. of ferrite for CrK radn., J. Metals 9, 41.
361. Weller W., Zur Diffusion v. Sb. in Ag, Ann. Phys. 20, 42.
362. Werner F. E., Averbach B. L., and Cohen M., Tempering of Fe–C martensite crs., Trans. Am. Soc. Metals 49, 823.
363. Weston N. E. and Shoemaker D. P., Cr. strs. of three phases in Na–Pb syst., Acta Cryst. 10, 775 (Abstracts...).
364. Weston N. E. and Shoemaker D. P., Further comment on Na_4Pb_{23}, J. Phys. Chem. 61, 1448; 1687.
365. Wet J. F. de., New met. layer str., Nature 180, 1412.
366. Weyerer H., Verfeiner. d. Auswerteverf. fur d. Prazisionsbest. v. Git-konstt. kub. Kristalle nach d. Pulvermethode, Z. Krist. 109, 338.
367. Whelan M. J. and Hirsch P. B., E. diffrn. from crs. containing stacking faults, I; II, Phil. Mag. 2, 1121; 1303.
368. Wilde R. F. and Grant N. J., Aging in complex commercial Ni–Cr alloys hardened with Ti a. Al, J. Metals 9, 865.
369. Wilkens M. and Schubert K., Uber einige met. Ordnungsphasen mit grosser Periode, Z. Metallk. 48, 550.
370. Williams B. E., E. micr. a. diffrn. studies of 7% Cr–Mo steels, Brit. J. Appl. Phys. 8, 241.

371. Williams R. O., Nature of Ni–Cr syst., J. Metals 9, 1257.
372. Wilson W. D., Austin A. E., and Schwartz C. M., Solid solubility of U in Th, a. allotropic transformn. of Th–U alloys, J. Metals 9, 55.
373. Wolfson M. R., Phase relnshs. of Ca–Li syst., Trans. Am. Soc. Metals 49, 704.
374. Woolley J. C. and Smith B. A., Solid solns. in GaAs–InAs syst., Proc. Phys. Soc. Lond. 76B, 153.
375. Worsham J. E., Jr., Wilkinson M. K., and Shull C. G., N.-diffrn. observns. on Pd–H, a. Pd–D systs., J. Phys. Chem. Solids 3, 303.
376. Yokoyama T., Etudes experimentales sur la formn. d. supersreseaux dans les alliages FeCo. Force thermoelectrometrice, dilatation et recherches aux r. X., J. Japan. Inst. Metals (Sendai) 21, 321 (Jap.).
377. Young F. W. Jr. and Cabrera N., Partial polygonization in impure Cu crs., J. Appl. Phys. 29, 787.
378. Zachariasen W. H. and Ellinger F., Cr. str. of α-Pu met., J. Chem. Phys. 27, 811; Acta Cryst 10, 776 (Abstracts. . .).
379. Zakharova M. I. and Stetsenko P. N., I. Study of magn. props. and str. of Fe alloy with 27% V. II. Phase transformn. in Fe–V alloys, Vestn. Mosk. Univ., ser. mat., mekh., astr., fiz., khim. 12, 47; 53.
380. Zalkin A., Cr. str. of $Li_{22}Pb_5$, Acta Cryst. 10, 791 (Abstracts. . .).
381. Zalkin A. and Ramsey W. J., Intermet. compds. between Li a. Pb. III. β'–β trans. in LiPb, J. Phys. Chem. 61, 1413.
382. Zhdanov G. S., Zhuravlev N. N., Stepanova A. A., and Umanskii M. M., Cr. chem. of met. hexaborides, Kristallografiya 2, 280.
383. Zhuravlev N. N., Str. of superconductors. X. Therm. micr. and x-ray investn. of Bi–Pd syst., Zh. eksp. i teor. fiz. 32, 1305.
384. Zhuravlev N. N. and Kertes L., Str. of superconductors. XXI. Investn. of alloys of Bi with Pt, Ru, Os, and Ir, Zh. eksp. i teor. fiz. 32, 1313.
385. Zima G. E., Some high temp. oxidation chars. of Ni with Cr additions, Trans. Am. Soc. Metals 49, 924.
386. Zvereva N. P., Sulfides of La, Dokl. AN SSSR 113, 333.

All abbreviations of periodicals in the above bibliography are letter-by-letter transliterations of the abbreviations as given in the original Russian journal. *Some or all of this periodical literature may well be available in English translation.* A complete list of the cover-to-cover English translations appears at the back of this issue.

SIGNIFICANCE OF ABBREVIATIONS MOST FREQUENTLY ENCOUNTERED IN SOVIET PERIODICALS

FIAN	Phys. Inst. Acad. Sci. USSR
GDI	Water Power Inst.
GITI	State Sci.-Tech. Press
GITTL	State Tech. and Theor. Lit. Press
GONTI	State United Sci.-Tech. Press
Gosenergoizdat	State Power Press
Gorkhimizdat	State Chem. Press
GOST	All-Union State Standard
GTTI	State Tech. and Theor. Lit. Press
IL	Foreign Lit. Press
ISN (Izd. Sov. Nauk)	Soviet Science Press
Izd. AN SSSR	Acad. Sci. USSR Press
Izd. MGU	Moscow State Univ. Press
LEIIZhT	Leningrad Power Inst. of Railroad Engineering
LET	Leningrad Elec. Engr. School
LETI	Leningrad Electrotechnical Inst.
LETIIZhT	Leningrad Electrical Engineering Research Inst. of Railroad Engr.
Mashgiz	State Sci.-Tech. Press for Machine Construction Lit.
MEP	Ministry of Electrical Industry
MES	Ministry of Electrical Power Plants
MESEP	Ministry of Electrical Power Plants and the Electrical Industry
MGU	Moscow State Univ.
MKhTI	Moscow Inst. Chem. Tech.
MOPI	Moscow Regional Pedagogical Inst.
MSP	Ministry of Industrial Construction
NII ZVUKSZAPIOI	Scientific Research Inst. of Sound Recording
NIKFI	Sci. Inst. of Moden Motion Picture Photography
ONTI	United Sci.- Tech. Press
OTI	Division of Technical Information
OTN	Div. Tech. Sci.
Stroiizdat	Construction Press
TCE	Association of Power Engineers
TsKTI	Central Research Inst. for Boilers and Turbines
TsNIEL	Central Scientific Research Elec. Engr. Lab.
TsNIEL-MES	Central Scientific Research Elec. Engr. Lab.-Ministry of Electric Power Plants
TsVTI	Central Office of Economic Information
UF	Ural Branch
VIESKh	All-Union Inst. of Rural Elec. Power Stations
VNIIM	All-Union Scientific Research Inst. of Metrology
VNIIZhDT	All-Union Scientific Research Inst. of Railroad Engineering
VTI	All-Union Thermotech. Inst.
VZEI	All-Union Power Correspondence Inst.

NOTE: Abbreviations not on this list and not explained in the translation have been transliterated, no further information about their significance being available to us. -Publisher.